AGARD-LS-184

AGARD

ADVISORY GROUP FOR AEROSPACE RESEARCH & DEVELOPMENT
7 RUE ANCELLE 92200 NEUILLY SUR SEINE FRANCE

AGARD LECTURE SERIES 184

Advances in Fibre-Optic Technology in Communications and for Guidance and Control

(Techniques de Pointe en Matière de Fibres Optiques dans le Domaine des Communications et pour le Guidage et le Pilotage)

This material in this publication was assembled to support a Lecture Series under the joint sponsorship of the Electromagnetic Wave Propagation Panel and the Guidance and Control Panel of AGARD and the Consultant and Exchange Programme of AGARD presented on 18th—19th May 1992 in Rome, Italy, 21st—22nd May 1992 in Leiden, The Netherlands and 26th—27th May 1992 in Monterey, United States.

NORTH ATLANTIC TREATY ORGANIZATION

Published May 1992

Distribution and Availability on Back Cover

40th Anniversary Year

AGARD

ADVISORY GROUP FOR AEROSPACE RESEARCH & DEVELOPMENT

7 RUE ANCELLE 92200 NEUILLY SUR SEINE FRANCE

AGARD LI

Advanc
in Con
and for

(Technique
dans le Dor
le Guidage

This material
joint sponsor
and Control
presented on
Leiden, The

er the
ance
f AGARD
.

N
C

The Mission of AGARD

According to its Charter, the mission of AGARD is to bring together the leading personalities of the NATO nations in the fields of science and technology relating to aerospace for the following purposes:

- Recommending effective ways for the member nations to use their research and development capabilities for the common benefit of the NATO community;
- Providing scientific and technical advice and assistance to the Military Committee in the field of aerospace research and development (with particular regard to its military application);
- Continuously stimulating advances in the aerospace sciences relevant to strengthening the common defence posture;
- Improving the co-operation among member nations in aerospace research and development;
- Exchange of scientific and technical information;
- Providing assistance to member nations for the purpose of increasing their scientific and technical potential;
- Rendering scientific and technical assistance, as requested, to other NATO bodies and to member nations in connection with research and development problems in the aerospace field.

The highest authority within AGARD is the National Delegates Board consisting of officially appointed senior representatives from each member nation. The mission of AGARD is carried out through the Panels which are composed of experts appointed by the National Delegates, the Consultant and Exchange Programme and the Aerospace Applications Studies Programme. The results of AGARD work are reported to the member nations and the NATO Authorities through the AGARD series of publications of which this is one.

Participation in AGARD activities is by invitation only and is normally limited to citizens of the NATO nations.

Published May 1992

ISBN 92-835-0673-1

Printed by Specialised Printing Services Limited
40 Chigwell Lane, Loughton, Essex IG10 3TZ

Preface

In the last thirty years, optics has been an inexhaustible source of new ideas for applications in the field of advanced technology, in particular, in the field of telecommunications.

We have witnessed a continuous transfer of knowledge from research laboratories and universities to more application-oriented institutions and to industry.

This very healthy process requires a constant upgrading of the cultural background of the people involved since the topics are often quite sophisticated and, in order to understand them, it is necessary to become familiar with new concepts and mathematical techniques.

It is, therefore, hardly necessary to underline the usefulness of bringing together a group of experts who can hopefully convey to the attendees of this Lecture Series enough information to keep them abreast of the most recent advances in fibre-optic telecommunications.

Although the choice of subjects is necessarily limited, and obviously biased by the particular fields of expertise of the organizers, the aim has been to provide as wide as possible a view of the present state-of-the-art, keeping in mind both the application-oriented developments and the more advanced research lines.

The expectation and the hope is that the lecturers will be able to convey to the attendees not only a collection of facts and figures, but also the feeling of what are the new significant directions in fibre optics and some of the excitement associated with advanced research.

Bruno Crosignani
Co-Director of the Lecture Series

The second day of this Lecture Series will focus on practical applications of fibre optics in aerospace. Following the considerable technology development for telecommunications, fibre optics has found novel uses in the field of sensing, where it brings, in particular, electromagnetic immunity since the remote sensor head can be made completely passive.

The first lecture will describe the numerous systems that have now been studied for 15 years to apply optical fibre to the sensing of various measurements.

The second lecture will concentrate on the new exciting field of smart structures where optical fibres are embedded inside composite materials to perform non-invasive remote sensing of fundamental parameters such as stress, damage, temperature and structural integrity. These techniques appear essential for optimization of the structures of future aerospace systems.

The third lecture will be dedicated to the specific problem of rotation sensing for inertial guidance. This subject is now a leading domain of fibre-optic sensing. It has been a driving force for this technology and it is a very good example of the high potential of these techniques. Due to its solid-state configuration, the fibre optic gyroscope is now considered as an essential inertial technique of the 90s and several companies are starting industrial production.

Finally, the last lecture will return to telecommunication applications to emphasize the specific problems of data buses in aerospace systems.

Hervé Arditty
Co-Director of the Lecture Series

Abstract

Fibre-optics is progressively changing from the research stage to the field of application. However, new possibilities are emerging, which will probably bring a new revolution in the field of telecommunications, such as coherent transmission, new transmission material transparent to mid-infrared radiation, active fibres and soliton propagation.

Fibre-optics is gaining increasing importance in tactical missile and aircraft guidance and control. This has been driven by the commercial development of fibre optic cable and related components over the last ten years. The requirements for military guidance and control applications are highly demanding for the characteristics of the fibres and the necessary related components (transmitters, receivers, connectors etc.).

The Lecture Series will bring together a group of speakers with both theoretical and practical experience in the areas of communications and guidance and control. The Lecture Series will introduce fibre optics technology to scientists and engineers who are now in the field as well as enhance the knowledge of those already working in the area.

This Lecture Series, sponsored jointly by the Electromagnetic Wave Propagation Panel and the Guidance and Control Panel of AGARD, has been implemented by the Consultant and Exchange Programme.

Abrégé

Les fibres optiques passent progressivement du domaine de la recherche à celui des applications concrètes. De nouvelles possibilités se dessinent qui promettent de révolutionner les télécommunications, telles que la transmission cohérente, les nouveaux supports de transmission transparents aux rayonnements infra-rouges, les fibres actives et la propagation soliton.

Les fibres optiques prennent de plus en plus d'importance dans le guidage et le pilotage des avions et des missiles tactiques. Ce phénomène s'explique, principalement par le développement commmerical du câble à fibres optiques et des composants connexes au cours des dix dernières années. Les spécifications des applications militaires dans le domaine du guidage et du pilotage sont très rigoureuses en ce qui concerne les caractéristiques des fibres et les composants connexes nécessaires. (émetteurs, récepteurs, connecteurs etc...)

Ce cycle de conférences rassemble une équipe de conférenciers ayant de l'expérience théorique et pratique dans les domaines des télécommunications et du guidage et pilotage. Le cycle de conférences servira d'introduction aux technologies des fibres optiques pour les scientifiques et les ingénieurs pour qui ce domaine est nouveau et complétera les connaissances de ceux qui y travaillent déjà.

Ce cycle de conférences est présenté conjointement par les Panels AGARD de Propagation des Ondes Electromagnétiques (EPP) et du Guidage et Pilotage (GCP) et organisé dans le cadre du programme des Consultants et des Echanges.

List of Authors/Speakers

Lecture Series Co-Directors:

Mr H. Arditty
Photonetics
52, Avenue de l'Europe
B.P. 39
78160 Marly-le-Roi
France

Prof. B. Crosignani
Universita di Fisica
Universita "La Sapienza"
Piazzale A. Moro 2
00185 Rome
Italy

SPEAKERS

Prof. B. Culshaw
Opto-Electronics Group
University of Strathclyde
Royal College Building
204 George Street
Glasgow G1 1XW
United Kingdom

Dr G. De Marchis
Fondazione Ugo Bordoni
Via Baldassare Castiglione 59
00144 Roma
Italy

Dr P. Gardiner
Director, Smart Structures
Research Institute
Opto-Electronics Group
University of Strathclyde
Royal College Building
204 George Street
Glasgow G1 1XW
United Kingdom

Dr H. Hodara
Tetra-Tech Inc.
9645 Scranton Road
Suite 200
San Diego, CA 92121
United States

Dr H. Lefèvre
Photonetics
52, Avenue de l'Europe
B.P. 39
78160 Marly-le-Roi
France

Dr N. Lewis
Litton Poly-Scientific Division
1213 North Main Street
Blacksburg, VA 24060
United States

Mr E. Miles
Tetra-Tech Inc.
9645 Scranton Road
Suite 200
San Diego, CA 92121
United States

Dr D. Payne
University of Southampton
Southampton S09 5NH
United Kingdom

Dr E. Udd
McDonnell Douglas Electronic
Systems Company
Manager, Fiber Optic
1801 E. St. Andrew Place
P O Box 35020
Santa Ana, CA 92705-6520
United States

Prof. K. Vahala
128-95 California Institute
of Technology
Pasadena, CA 91125
United States

Contents

Semiconductor lasers and fiber lasers for fiber-optic telecommunications

Kerry J. Vahala, Namkyoo Park, Jay Dawson, and Steve Sanders
California Institute of Technology
Mail Stop 128-95
Pasadena, California 91125

Summary

The performance characteristics of state-of-the-art semiconductor lasers for fiber telecommunication systems are reviewed. Modulation speed, intensity noise, single-frequency line width, and tunability are addressed. In addition, recent results concerning the same characteristics in single-frequency, tunable, fiber lasers are reviewed and compared with the semiconductor laser.

I. Introduction

Semiconductor lasers have now found their way into several large commercial markets. Brightness, diffraction-limited spot size, power efficiency, reliability, and cost per component are the overriding concerns in most of these applications. This includes laser printers, compact disc players, and their use as solid-state laser pump sources. A sole exception is their application to fiber optic telecommunication systems. Research and product-development activities in this area continue to set impressive device performance records concerning spectral purity, tunability, modulation speed, and relative intensity noise levels. As a result of this effort commercial semiconductor lasers are nearly ideal in terms of their physical properties. Their intensity noise spectra and short-term frequency stability are governed almost exclusively by quantum mechanical effects. The tuning range in monolithic devices has recently been extended to encompass most of the available semiconductor gain band width and direct modulation speed has entered the millimeter-wave band.

In parallel with the above developments which emphasize their use as sources and local oscillators, the rapid development of traveling-wave optical-fiber amplifiers based on the rare-earth impurity erbium has created a new role in fiber systems for the semiconductor laser. As early as 1964 Koester and Snitzer demonstrated the first traveling wave amplifier as well as fiber laser based on neodymium doped glass (1). It was not until 1985, however, that experiments by researchers at Southhampton University ignited new and sustained interest in rare-earth doped fibers (in particular, erbium-doped fibers) as a viable and practical amplification medium (2). Central to the success of these remarkable amplifiers has been the ability to efficiently pump erbium-doped fiber at wavelengths attainable with semiconductor lasers. In particular, 1480 nm pump sources were first available as a slight modification of proven 1500 nm technology, and later strained quantum-well active-layer technology was perfected for pumping at the more efficient 980 nm absorption band (3). This new strained-layer technology can also be applied to pumping of other potentially important rare-earth doped systems. Specifically, 1017 nm strained-layer devices have been used to pump praeseodymium-doped fiber which has demonstrated amplification in the important low-dispersion 1.3 micrometer fiber communications window (4).

In addition to new system opportunities that have resulted from erbium-doped fiber amplifiers (EDFA's), the availability of a new and highly reliable amplifying medium has stimulated work on a new class of laser oscillators that employ EDFA's. Early examples of oscillation by erbium fiber amplification were simple Fabry-Perot resonator devices in which oscillation (sometimes unintentional) resulted from feedback supplied by cleaved fiber facets (5). More recently, impressive performance in terms of spectral purity, tunability, and intensity noise levels have been demonstrated in more sophisticated geometries (6,7,8). Thus, rather paradoxically, the semiconductor laser has assisted in the development of a potential competitor for its more traditional telecommunication applications.

In this paper we will review the state-of-the-art performance characteristics of semiconductor lasers and fiber lasers. The underlying physics governing field fluctuations, tunability, and modulation speed will be discussed and recent measurements will be presented. A comparison between these two very different technologies as concerns their application to fiber systems will be made. Finally, the discussion of semiconductor lasers will focus only on single frequency monolithic devices.

II. Semiconductor lasers: *Direct modulation*

Owing to their small size, large gain, and ability to be excited by an electrical current, semiconductor lasers have the ability to be modulated at very high rates. This gives them an enormous advantage over any other source technology for application to fiber optic systems. Direct modulation speed in a semiconductor laser is limited by both chip parasitic effects as well as the basic physics of electron-hole stimulated recombination. The equivalent circuit model of the laser chip in figure 1 illustrates the important parasitic influences in these devices (9). The active layer is shown as the impedance Z and the contact-layer capacitance and resistance as well as the depletion-layer capacitance and bond-wire inductance are also illustrated. In practice, the RC time constant associated with the contact layer is most often the limiting parasitic effect. The use of semi-insulating substrates, however, greatly reduces this effect (9). In this case devices are limited by the basic physics of electron-hole interaction with the lasing field. This interaction gives rise to a small-signal modulation response that has a frequency depen-

dence characteristic of a second-order low-pass network (9). Its form is most easily verified using an approach called parasitic-free modulation (10). In this approach two single-frequency sources are photomixed in the active layer of a test device to generate harmonic modulation. This form of modulation is immune to parasitic effects at all frequencies. Typical response data are shown in figure 2 at three temperatures.

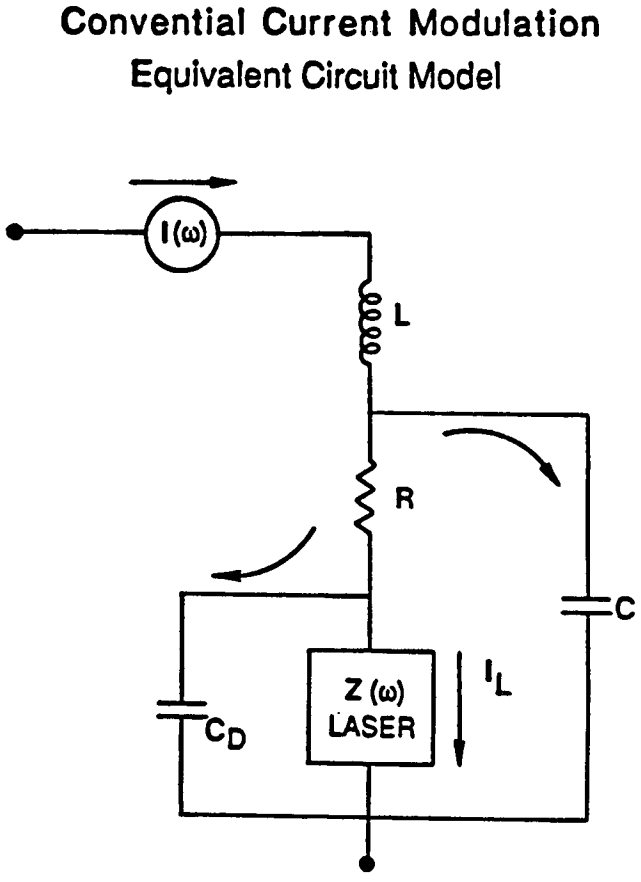

Figure 1 Equivalent circuit model for direct current modulation of a laser diode.

The corner frequency of this response function is called the relaxation oscillation corner frequency and in short wavelength devices it characterizes the useful modulation band width. This corner frequency is given by the geometric mean of two rates: the differential stimulated recombination rate (i.e., the product of differential optical gain and photon density) and the cavity loss rate.

$$\omega = \sqrt{g'p/T}$$

In this expression, ω is the relaxation oscillation corner frequency in units of radians per second, g' is the differential gain, p is the photon density, and T is the photon lifetime. Increased modulation speed can therefore be attained by operation at high power or by degradation of the passive cavity Q. Additionally, higher differential gain will also increase speed. A simple demonstration of the latter approach is given in figure 2. By operating a device at reduced temperature the thermal broadening of the active layer gain spectrum is greatly reduced thereby increasing the gain at a given carrier excitation level and, in turn, modulation speed through its dependence on differential gain. With the advent of quantum well lasers, this same idea can be implemented by using lower-dimensional electronic systems (11). Indeed, the fastest semiconductor laser devices are quantum well devices. In the future, quantum wire and quantum dot structures (two and three dimensional quantum wells) may also be employed to further enhance modulation speed.

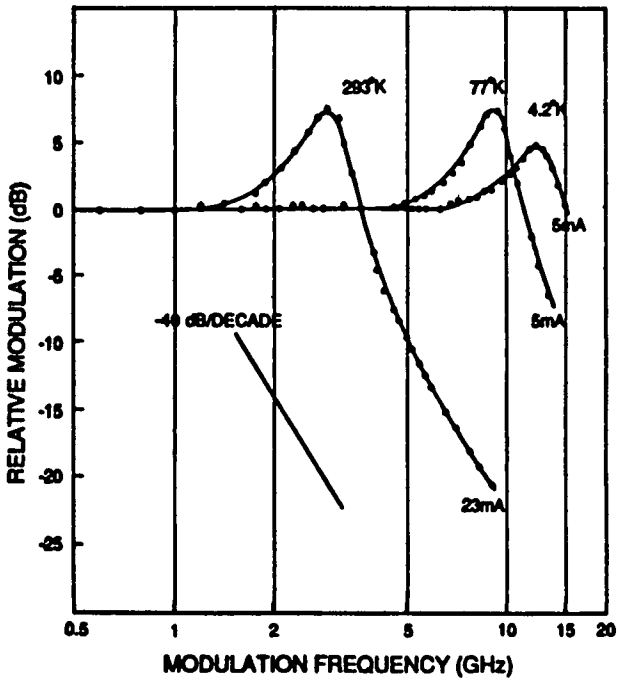

Figure 2 Modulation response of a laser diode in absence of device parasitics. Data is measured at three temperatures.

In long wavelength devices another effect also plays an important role in limiting modulation band width. This goes by the name of "nonlinear gain" and several possible mechanisms have been proposed to explain the effect (12,13). In general, it is observed that at some power level, the modulation response function in these devices is dominated by additional damping effects. The response corner frequency ceases to increase with increasing power as is typical for relaxation oscillation limited behavior. This effect seems more pronounced in quantum well devices and it has been proposed that the injected carrier capture rate into the quantum well is the limiting mechanism. Very recently developed quantum well structures with very high modulation rates indicate that structures can be engineered to minimize this effect (14).

Intensity Noise

At frequencies above a few MHz. state-of-the-art semiconductor lasers exhibit intensity noise that is dominated by quantum effects. There are many different levels from which to attack the problem of quantum intensity noise in semiconductor lasers. For the purposes of this discussion, it is possible to describe two regimes of laser operation and the associated noise behavior: a low-power excess-noise regime and a high-power shot-noise regime (15). The spectral shape of semiconductor laser intensity noise in each of these regimes closely mimics the direct modulation response function (16). In fact, one can view the associated noise spectra as the laser's response to various random modulation sources internal to the device. The most significant of these at low power is spontaneous emission. This source of noise is fixed above threshold and its effect on power fluctuations of the lasing mode diminishes inversely with the photon number in the lasing mode. Hence, for low-power operation the noise power detected into a finite band width varies inversely with device output power. In this regime the fluctuations can be thought of as a random signal superimposed on the amplitude of the optical carrier. In particular, attenuation has the same effect on the noise power and signal power in this regime. It is for this reason noise spectral density is often given in terms of RIN (relative intensity noise). This concept is useful so long as RIN is invariant with respect to attenuation. As discussed below, this is only true for operation in the excess noise regime.

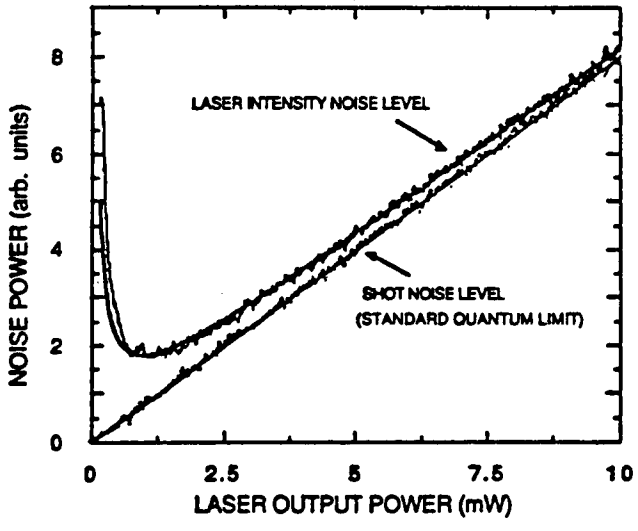

Figure 3 Theoretical and measured intensity noise power versus device output power.

At higher power levels, spontaneous emission noise becomes insignificant and the actual quantum nature of the optical carrier (i.e., photon shot noise) determines the noise level. Detected noise power into a given band width rises linearly with output power in this regime. An intensity noise measurement on a strained quantum well distributed Bragg reflector device is shown in figure 3. Both the excess noise and shot noise regimes are easily seen in the figure. Also displayed is an actual measurement of the shot noise floor (sometimes called the standard quantum limit). For comparison a theoretical intensity noise versus power curve is also displayed for both the laser noise and shot noise levels (solid curves). It is crucial when working in the shot noise regime to have an accurate calibration of this fundamental level. The only unambiguous method for establishing this floor is to use a balanced homodyne receiver (BHR) as diagrammed in figure 4. By a simple change of the circuit configuration used to add or subtract photocurrents in the BHR, one is able to either measure shot noise (subtraction) or the signal noise level (addition) (17).

The particular device measured here exhibited a noise level as low as 0.8 dB above the shot noise floor at an output power of 10 mW. It is important to note that the actual noise level measured at the BHD was much lower than this (see jagged solid curve in figure 3). 0.8 dB is the noise level at the laser facet and accounts for the effect of attenuation between the laser and the BHR (15). Attenuation in this regime affects noise in a less straightforward way than in the excess noise regime, because shot noise cannot be thought of as a signal. An ideal shot-noise limited optical beam would exhibit a detected photocurrent noise power that would vary linearly with attenuation as opposed to quadratically for an excess noise limited beam. In general, a beam exhibits neither pure excess noise or pure shot noise and the effect of attenuation on the noise level lies between these two extremes.

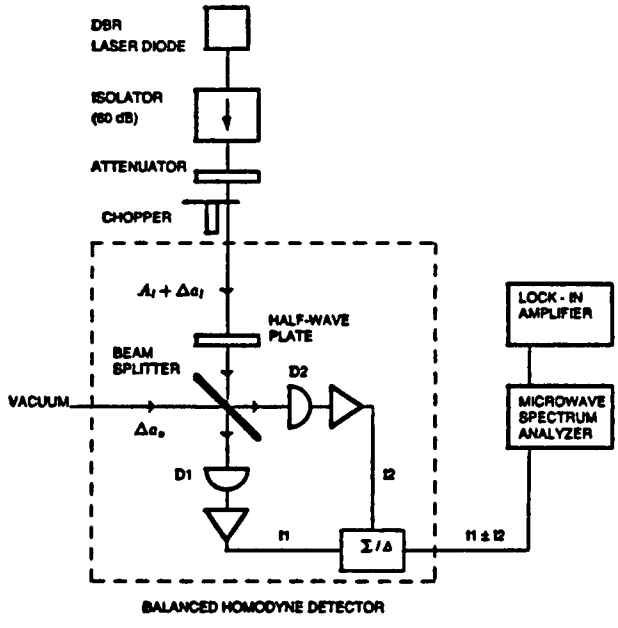

Figure 4 A balanced homodyne receiver for shot noise calibration and laser intensity noise measurement.

In view of the above, RIN is no longer invariant with respect to attenuation in the shot noise regime. Despite this fact, it continues to be used for historical reasons. For completeness, intensity noise in RIN units for the same measurement is displayed in figure 5. We also show the actual RIN at the laser facet resulting from deconvolving loss from the BHR measurement.

Single frequency line width

The fundamental line width of single frequency semiconductor lasers is of considerable importance in systems that utilize phase sensitive detection techniques. The principal source of spectral broadening in these devices is spontaneous emission. Spontaneous photons added randomly to the lasing field create a phase diffusion of the lasing field phase. This diffusion gives the mode spectrum its Lorentzian line shape. The line width at half power varies inversely with power in accordance with the modified Schawlow-Townes formula. As with intensity noise this power dependence reflects the decreasing significance of the fixed spontaneous emission rate with increasing photon number in the lasing mode. A significant additional modification of the Schawlow-Townes formula was recognized as important (16,18) in the early 80's. This work built on earlier work by Haug and Haken showing that detuned operation of a laser oscillator creates amplitude-phase coupling of the lasing field. This coupling, in turn, creates an additional channel for spontaneous noise to couple into the field phase and thereby enhance the line width. The effect is very large in semiconductor lasers and can enhance line width by as much as a factor of 40 (19). Devices having cavity lengths of approximately 300 microns and with uncoated facets exhibit line width-power products in the range of 50 MHz mW.

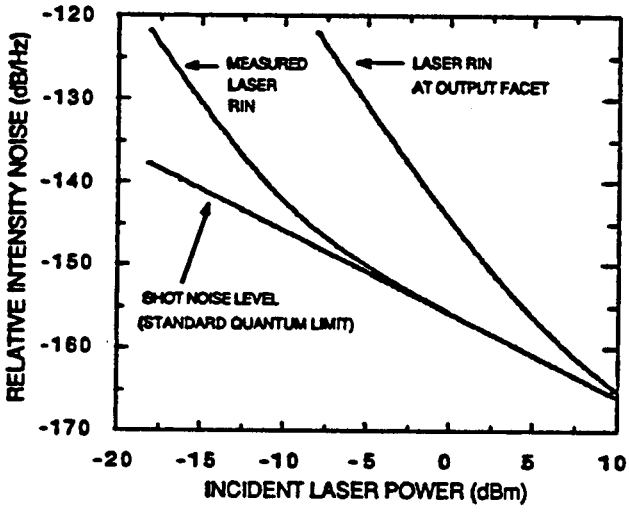

Figure 5 RIN versus laser power for device measured in figure 3. Noise at laser output facet is also displayed.

Several methods for reducing line width are apparent from observation of the fully modified Schawlow-Townes line width formula:

$$\Delta\omega = \frac{S}{2P}(1+\alpha^2)$$

In this expression S is the spontaneous emission rate, P is the number of photons in the lasing mode, and alpha is the so-called line width enhancement factor which characterizes the strength of the amplitude-phase coupling effect (16,18,19). Enhanced facet reflectivity and longer device cavity lengths are both effective ways to reduce line width by increasing the cavity Q (i.e., decrease threshold S). Quantum well active layers can also be tailored to reduce the alpha parameter to values as small as -1 (alpha is typically -4 to -5 in bulk material).

In addition to spontaneous emission, semiconductor laser line width is also influenced by a number of other less fundamental effects. These effects become significant at high power levels where the line width can saturate at a power independent value. For many years a variety of mechanisms thwarted the best efforts of researchers to narrow the line width of solitary semiconductor lasers below 1 MHz. In DFB devices longitudinal variations in modal intensity caused by the DFB mechanism were eventually linked to this high power line width. The resulting spatial hole burning of the gain medium can be suppressed by use of very long cavities. Intensities in these cavities for a given modal photon number are lower than for shorter cavity devices thereby reducing the spatial hole burning effect. By employing long cavity devices in this way and by using quantum well active layers as described above high power line widths as narrow as 50 kHz have been demonstrated in solitary devices.

Before leaving this subject we mention an interesting and potentially useful link between phase and intensity noise in these devices. As mentioned above, the alpha parameter gives a measure of amplitude-phase coupling in the semiconductor laser. Its effect on noise is normally considered undesirable. However, recently we have shown that the correlations between the field amplitude and phase that are created by the alpha coupling can be used to decrease SL intensity noise (20,21). In an approach we call amplitude-phase decorrelation, information about intensity fluctuations that is stored on the field phase is used to damp intensity fluctuations in a simple passive process. Power noise reductions as large as 14.5 dB have been demonstrated using this approach (22).

Wavelength tunability

The amplitude-phase coupling responsible for line width enhancement results from a carrier density dependent component of refractive index in the SL active layer (i.e., gain spectrum detuning). Although undesirable for narrow line width operation, this effect provides a convenient means to electrically tune the wavelength of a semiconductor laser. Wavelength tunability in these devices involves great

fabricational sophistication. Impressive results have been demonstrated by groups in Japan and at AT&T using Bragg grating devices having three contacts to allow independent phase control, grating phase control, and gain control (23,24,25). Seamless tuning over wavelength spans of nearly 10 nm has been demonstrated. A physical limitation on tuning in these devices, however, is the magnitude of the alpha parameter in semiconductor active layers. Until recently it seemed that direct electrical tuning would be limited to the ranges already established. Workers at AT&T, however, demonstrated electrical tuning over 57 nm (not seamless) using a novel Bragg wave guide coupling approach (26). Rather than basing wavelength control on a Bragg grating operating in the reflection mode, these new devices use a Bragg grating to couple two parallel wave guides within the same laser chip. Since the coupling involves a smaller differential wave vector to link modes in each guide, a larger tuning range is possible using the same amount of carrier induced index change.

III. Fiber Lasers:

Overview

Although they are a relatively new in comparison to semiconductor lasers, fiber lasers have evolved very quickly. Beginning with the first simple demonstration of oscillation the field has seen a variety of more sophisticated approaches that have used both ring and Fabry-Perot geometries. Broadband tunability with limited frequency stability in a ring geometry was demonstrated by groups at Bellcore and at NTT (6,26,27). The NTT group used a discrete interference-filter element that was rotated with respect to the fiber axis to achieve tuning. Bellcore demonstrated a novel liquid-crystal birefringent filter as well as a surface acoustic wave filter. Researchers at United Technologies Corporation recently demonstrated a single frequency Fabry-Perot geometry that incorporated newly-developed fiber Bragg filters for mirrors (7). This approach is very elegant since no discrete components are required and lasing action occurs entirely within the fiber. We have recently developed the first single-frequency, ring-geometry fiber laser with long term frequency stability (8). In our approach we have employed for the first time fiber-optic Fabry-Perot Filters (FFP) as frequency selective elements. These filters use a short section of single-mode optical fiber as the resonant cavity for the filter (28). A dielectric stack at the ends of the fiber creates a high finesse and tuning is accomplished by varying the length of the fiber (0 to 15 volts supplied to a piezoelectric element normally scans one free-spectral-range of the device). Our single-frequency ring uses two FFP filters to achieve frequency stability as well as wide wavelength tunability. Its operation and characteristics will be detailed in the next section.

A single-frequency, widely-tunable, fiber ring laser

Figure 6 illustrates the components used in the ring laser. The 980nm output of a titanium:sapphire (or a diode laser) laser was coupled through a wavelength division multiplexer for the pumping source. A pigtailed polarization dependent isolator (isolation 35 dB) was used to prevent spatial hole burning caused by bi-directional operation for more stable single frequency operation. The isolator also served to block feedback from the output port of the system. A polarization controller (PC) was used to match the polarization state to the input polarization of the isolator. The coarse wavelength selective element was a broadband fiber Fabry-Perot (FFP) filter with a 26.1 GHz (0.196nm at 1.5 microns) band width (FWHM) and a 4020 GHz free spectral range (FSR). A second, frequency stabilizing fiber Fabry-Perot is shown in the dashed box and will be discussed momentarily. The total cavity loss (without the second Fabry-Perot) was estimated to be less than 6.5dB from a small signal gain measurement and threshold data. The specific sources of loss were 2.5dB from the FFP, 1dB from the isolator, 1dB from the wavelength division multiplexer and coupler, and 2dB from mode mismatch and splice losses between the erbium fiber and other devices. The threshold was approximately 10 mW. The cavity length was 30 meters corresponding to a free spectral range (FSR) of 6.6 MHz for the laser.

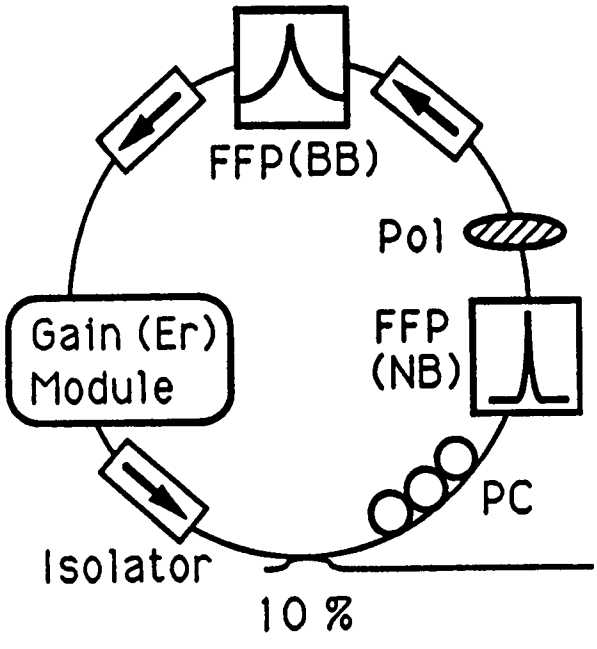

Figure 6 Schematic of single-frequency, tunable erbium ring laser showing broad band (BB) and narrow band (NB) fiber Fabry-Perot filters (FFP).

The laser output was coupled to a 50/50 coupler at 1550nm to enable simultaneous monitoring of the lasing spectrum using both a high resolution scanning Fabry-Perot interferometer and a grating monochromator to determine the lasing wavelength. Tuning was possible by changing the voltage

on the FFP thus scanning the center frequency of FFP over a different longitudinal cavity mode of the ring laser. Tuning over 30nm (corresponding to the FFP filter FSR) between 1530nm to 1560nm was possible by applying 0 to 17 DC Volts. (see tuning curve in figure 7) The tuning range is believed to be limited only by the FSR of the FFP filter. After 17 Volts, it retraced the wavelength at zero applied Voltage. Single frequency operation was observed for periods as long as several seconds although there existed mode hopping under an envelope on the order of 1 GHz, presumably due to cavity instabilities from thermal drift and acoustic noise . Frequency stability was better when using a diode laser pump. We attribute this to gain fluctuation in the erbium fiber due to the pumping source frequency fluctuation, which was more evident in our titanium:sapphire laser. Threshold pump power was between 8.8 mW and 10.4 mW over the entire tuning range. Gain shaping with an additional filter could be applied to further reduce the variation (29).

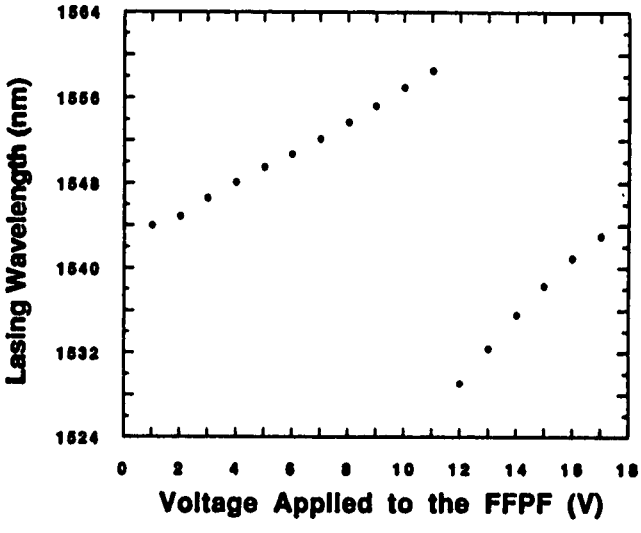

Figure 7 Tuning versus voltage applied to fiber Fabry-Perot filter.

To suppress mode hopping, the second, narrow band width FFP (1.39 GHz, 0.01 nm at 1550 nm, insertion loss 2.5 dB max) was placed in the cavity. The measured threshold pumping power was around 14 mW with the tandem FFP configuration. To prevent inter-etalon interactions, a polarization independent isolator was introduced between the two FFP filters. These interactions were observed to produce additional mode hopping. With the isolator in place, the resulting transmission function from this tandem FFP filter can be considered as the product of two independent transmission functions of FFP filters. Tuning was possible over the entire gain spectrum with 1 nm intervals corresponding to the FSR of the smaller band width FFP. Mode hopping was completely suppressed. Instead, the lasing mode was observed to slowly drift until, after several minutes, oscillation would jump to an adjacent longitudinal mode.

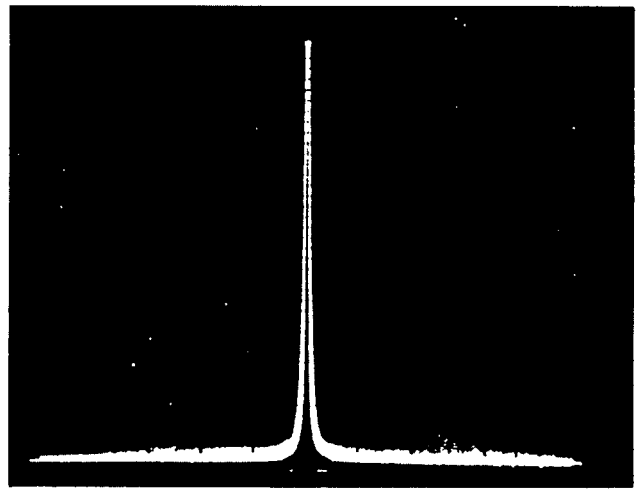

Figure 8 High resolution scan of single frequency ring spectrum. Full width of display is approximately 50 MHz.

Figure 8 shows a lasing spectrum taken using the scanning Fabry-Perot Interferometer (Newport Research Super-Cavity SR-170. FSR 6 GHz.). This device has a resolution of 1 MHz which is sufficient to resolve the 6.6 MHz FSR of the ring laser longitudinal modes. The side mode suppression ratio was measured by detecting the output using a high frequency photodiode and then analyzing the photocurrent using a microwave spectrum analyzer. The measured side mode suppression was higher than 35 dB. Later, we also used another fiber Fabry-Perot with a smaller band width (125 MHz). This produced a side-mode suppression ratio no smaller than 48 dB. A plot of measured side-mode suppression versus tuning for this higher figure is presented in figure 9.

The intensity noise of this device was measured using the balanced homodyne approach described above. In erbium doped fiber lasers, one expects a relaxation oscillation frequency on the order of 10 kHz due to the relatively long fluorescence lifetime of erbium (30). Beyond this frequency, fluctuations in pump power are strongly damped, and the intensity noise power should be dominated by spontaneous emission. The measured noise power (near 310 MHz) showed linear dependence on the output power that was 8.5 dB above the shot noise level. Data showing both laser noise and the shot-noise floor versus output power are given in figure 10.

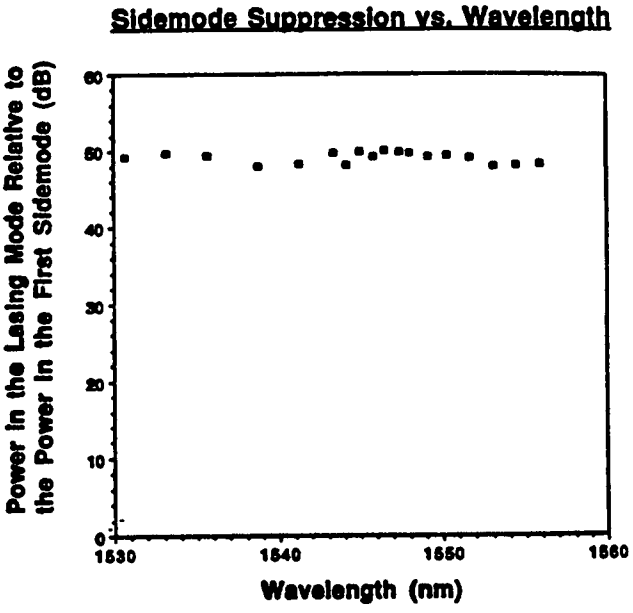

Figure 9 Measured side mode suppression ratio versus tuning in the ring laser.

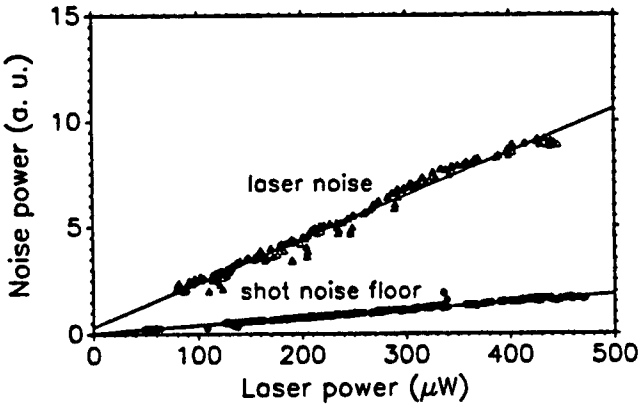

Figure 10 Intensity noise power of erbium ring laser versus laser output power measured relative to shot noise power floor using the balanced homodyne method.

IV. Conclusion

State-of-the-art semiconductor lasers are nearly ideal optical sources. In addition to being reliable and compact, they are low noise, exhibit narrow line widths, and are widely tunable with small applied currents. They are unique among all laser devices in offering the enormous benefit of efficient, high speed, direct current modulation. There is little chance that any other source will ever supplant the semiconductor laser in fiber optic telecommunication systems.

Fiber laser sources, however, despite being incapable of direct modulation, have several advantages of their own over semiconductor devices. The greatest of these is the fact that light generation occurs in the fiber and must never leave the fiber enroute to the transmission cable. Packaging related problems are therefore greatly reduced in such a device. (Although one could argue that packaging of a semiconductor laser still plays a role here except now moved back one level to the optical pump diode.)

In terms of other performance figures of merit, fiber lasers, despite their brief development history, are as nearly as good or exceed the performance of state-of-the-art semiconductor devices. As shown above, intensity noise levels in the ring device we have developed are within 10 dB of the standard quantum limit and can probably be reduced to a few dB above this level. For comparison, state-of-the-art semiconductor lasers operate close to this level. Single-frequency line width in solitary semiconductor lasers has only recently been reduced to values around 50 kHz in specialized structures. For comparison the first fiber ring sources had line widths of less than 10 kHz. Another important property of telecommunication sources is high side mode suppression (SMS). Side mode suppression in the best DFB devices exceeds 60 dB. Typically only 30 dB SMS is required in digital systems and 60 dB is reserved for analog transmission such as in proposed cable television links. To date, the only reported data on SMS in tunable all-fiber sources is by our group for the ring device discussed above. It has an SMS of 48 dB which could potentially be increased to nearly 60 dB with minor modifications now under way.

Finally, as discussed above, wavelength tunability in semiconductor lasers involves extraordinary fabricational sophistication. The tuning range demonstrated in the Caltech single frequency ring is 30 nm (limited by the tuning filter; 50nm should be possible with a new filter). While this tuning involves mode hopping between modes separated by 6 MHz, we believe seamless tuning, if needed, could be accomplished over the same range by introduction of a phase control element into the ring.

It is too soon to make any predictions concerning the possible future role, if any, of fiber lasers in telecommunication systems. However, their performance characteristics to date are impressive despite a much shorter and lower budget cumulative development effort than that seen in the past decade for semiconductor lasers.

References

(1) C.J.Koester, and E.Snitzer, Appl.Opt. vol.3, 1182 (1963).
(2) S.B.Poole, D.N.Payne, and M.E.Ferman, Electron.Lett., vol.21, 737 (1985).
(3) B.Pederson, B.A.Thomrson, S.Zeman, W.J.Miniscalco, and T.Wei, IEEE Photon. Technol. Lett., vol.4, 46 (1992).
(4) Y.Ohishi, T.Kanamori, T.Nishi, and S.Takahashi, IEEE Photon.Technol.Lett., vol.3, 715 (1991).
(5) M.Shimitzu, H.Suda, and M.Horiguchi, Electron.Lett., vol.23, 768 (1987).

(6) D.A.Smith, M.W.Maeda, J.J.Johnson, J.S.Patel, M.A.Saifi, and A.V.Lehman, Opt. Lett., vol.16, 387 (1991).
(7) G.A.Ball, W.W.Morey, and W.H.Glenn, IEEE Photon. Technol.Lett., vol.3, 613 (1991).
(8) N.K.Park, J.W.Dawson, and K.J.Vahala, Appl.Phys.Lett. Vol.59, 2369 (1991).
(9) K. Y. Lau and A. Yariv, IEEE J. Quant. Electron., QE-21, 121 (1985).
(10) K. J. Vahala and M. Newkirk, IEEE J. Quantum. Electron., QE-25, 1393 (1989).
(11) Y. Arakawa, K. Vahala, A. Yariv, Appl. Phys. Lett., vol 45, 950 (1984).
(12) R. Olshansky, P. Hill, V. Lanzisera, and W. Powazinik, IEEE J. Quant. Electron., QE-23, 1410 (1987).
(13) W. F. Sharfin, J. Schlafer, W. Rideout, B. Elman, R. B. Lauer, J. La Course, and F. D. Crawford, Photon. Tech. Lett., vol. 3, 193 (1991).
(14) R. Nagarajan, T. Fukushima, J. E. Bowers, R. A Geels, and L. A. Coldren, Electron. Lett., vol. 27, 1058 (1991).
(15) M. A. Newkirk and K. J. Vahala, Conf. on Optical Fiber Communication, San Diego, March (1991).
(16) K. J. Vahala and A. Yariv, IEEE J. Quant. Electron., QE-19, 1096, 1102 (1983).
(17) B.L.Schumaker, Opt.Lett. vol.9, 189 (1984).
(18) C. H. Henry, IEEE J. Quant. Electron., QE-18, 259 (1982).
(19) D. Welford and A. Mooradian, Appl. Phys. Lett., vol. 40, 865 (1982).
(20) K. J. Vahala and M. A. Newkirk, Appl. Phys. Lett., vol. 57, 974 (1990).
(21) M. A. Newkirk and K. J. Vahala, J. Quant. Electron., QE-27, 13 (1991).
(22) M. A. Newkirk and K. J. Vahala, Appl. Phys. Lett., March 1992 issue.
(23) T. L. Koch, U. Koren, B. I. Miller, Proc. 11th IEEE Int. Conf. on Semiconductor Lasers, Paper J-1, Boston, (1988).
(24) Y. Kotaki, M. Matsuda, M. Yano, H. Ishikawa, H. Imai, Electron. Lett. Vol. 23, 327 (1987).
(25) K. Kondo., M. Kuno, S. Yamakoshi, T. Sakurai, Proc. 11th IEEE Int. Conf. on Semiconductor Lasers, Paper J-3, Boston, (1988).
(26) M.W.Maeda, J.S.Patel, D.A.Smith, C.Lin, M.A.Saifi, and A.V.Lehman, IEEE Photon.Technol.Lett. vol.2, 787 (1990).
(27) K.Iwatsuki, H.Okamura, and M.Saruwatari, Electron.Lett. vol.26, 2033 (1990).
(28) C.M.Miller and F.J.Janniello, Electron.Lett. Vol.26, 2122 (1990).
(29) G.Grasso, F.Fontana, A.Righetti, P.Turner, and P.Maton, Proc. Opt.Fiber Commun.Conference, OFC '1991, FA3
(30) E.Desurvire, J.W.Sulhoff, J.L.Zyskind, and J.R.Simpson, IEEE Photon.Technol.Lett., vol.2, 653 (1990).

Coherent Communications

G. De Marchis
Fondazione Ugo Bordoni
Via Baldassarre Castiglione, 59
I-00142 Roma
Italy

SUMMARY

Coherent lightwave techniques, when compared to direct detection techniques, offer nearly quantum noise limited sensitivity as well as fine tunability similar to that obtained at radio frequencies. These two aspects provide communication systems planners and engineers a means to better exploit the huge bandwidth of single mode optical fibers.

Research activity in this field has started in the early '80 and some laboratory experiments as well as field trials have been performed in last years, showing that such techniques are suitable for transmitting multigigabit per second signals to distances well exceeding hundred kilometers.

On the other hand, coherent multichannel, frequency division multiple access, local area networks have been proposed and experimented worldwide.

The paper will discuss the theoretical advantages and limitations of the various modulation and detection formats together with the state of the art.

Moreover some aspects, related to the introduction of coherent systems in local and metropolitan area networks, will be treated.

Finally some experimental data will be provided and future evolution will be discussed.

1. INTRODUCTION

Over the past several years optical coherent communications have evolved from an esoteric subject, studied in a few research labs, into a paramount importance matter worldwide [1]. This activity is a result of the attainment of real gains in receiver sensitivities and repeaterless transmission spans over those achieved using intensity modulated direct detection systems.

Actually, before the introduction of coherent communications, despite the rapid advance of lightwave technology over almost a decade, the basic operation of an optical fiber communication system had remained essentially unchanged.

In such a system, which is shown in fig. 1, the source, usually a semiconductor laser diode, is directly modulated (on-off keying) varying the driving current, which results in switching on and off the light intensity emerging from the laser itself. At the receiver side, the electrical field exiting the fiber impinges over a semiconductor photodiode (either a pin or an APD, Avalanche Photodiode) which in turns convert the intensity modulated beam into an amplitude modulated photocurrent in the load resistor. Such an operation is the optical equivalent of an old crystal radio in the '20.

Even if recent improvements in device technology (such as external modulators) allow very high bit rates (>4 Gb/s) to be obtained, the receiver sensitivity is far from the quantum limited operation and, moreover, the huge fiber bandwidth is used to convey just one communication channel.

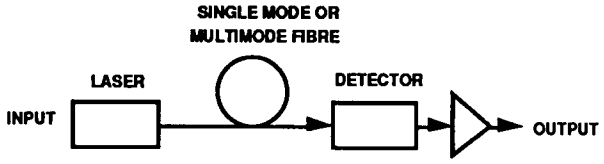

Figure 1 - Block scheme of a IM-DD optical communication system (intensity modulation-direct detection)

Coherent systems were firstly developed to obtain better receiver sensitivities, very close to the quantum limit for the various modulation formats: with the introduction of optical amplification, by means of Erbium doped fiber (used as receiver preamplifier), the same result can be achieved for direct detection systems as well. Nevertheless, the possibility of using coherent techniques in a multichannel environment with frequency division multiple access to the network constitutes an appealing attractive, allowing hundreds of channels to be multiplexed on the same single mode fiber [2] .

The term coherent, in this paper, is used to designate any technique employing nonlinear mixing between two optical waves, as appearing in fig. 2 [3] .

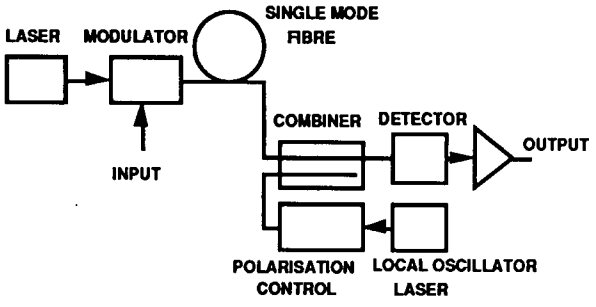

Figure 2 - Block scheme of a system in which the technique of coherent detection is adopted.

One of the two waves, produced by the transmitting laser, is the information bearing signal traveling trough the fiber, the other one is locally generated by a second laser diode (LO Local Oscillator) and the mixing is performed directly by the photodiode which provides an output current proportional to the total power. The resulting photocurrent is an exact replica of the information signal translated from optical to radio frequencies and the receiver is called heterodyne receiver: this kind of operation is the optical equivalent of super heterodyne radio reception.

If the signal wave is $A_S \cos \omega_s t$ and the LO wave is $A_l \cos \omega_l t$ this beating signal can be written

$$I_{ph}(t) = A_s^2 + A_l^2 + 2A_sA_l \cos (\omega_s - \omega_l)t \qquad (1.0.1)$$

The new signal $I_{ph}(t)$ (it is called Intermediate Frequency signal IF) retains any information, in terms of amplitude, frequency or phase modulation, which was present in the original signal wave. Equation (1.0.1) is derived supposing that signal and local waves are perfectly matched in polarization state: it can be shown that, as far as polarization is concerned, a more accurate equation can be considered that removes the above assumption, and polarization modulated signals can be generated and detected as well.

When the signal and LO frequencies coincide, the process is called homodyne detection and the information is translated directly at baseband frequencies as it happens in direct detection systems: the difference is found in the fact that angular modulations (i.e. amplitude, phase, frequency and polarization) can be still detected while they are completely lost in the other case.

It is to be noted in equation (1.0.1) that the signal term power can be made arbitrarily large increasing the LO amplitude: this is a means to overcome the thermal noise which is generated in the electrical front-end of the receiver and which has proven to be the limiting factor for the performance of Intensity Modulated Direct Detection (IM-DD) systems. If the LO power is sufficiently large, the limiting factor in heterodyne and homodyne receivers is represented by the quantum noise affecting the detected photocurrent. As this noise too is increasing with the LO power an asymptotic Signal-to-Noise Ratio (SNR) is reached for large LO, which is called shot-noise limit.

In a heterodyne receiver a further electronic demodulation is needed to obtain baseband signals from which it is possible to estimate the transmitted message. This electronic demodulation can be both synchronous, requiring an electronic PLL, or asynchronous, for example using square law devices. This is why an ASK heterodyne optical system using square law electronic demodulation is called coherent while its microwave equivalent is classified as a non-coherent system.

2. DIRECT DETECTION AND FUNDAMENTAL LIMITS

The photodetector, the basic component of a direct detection receiver, converts the energy contained in light pulses to electrical signals. The detection mechanism is usually referred to as photon counting and is subject to statistical fluctuations: the photon counting is a time varying Poisson process whose intensity function $\lambda(t)$ is proportional to the power (expressed in terms of photons/second, if the values are normalized to hν the photon energy) of the information-bearing signal.

If a binary transmission takes place, the receiver will detect, averaging over a large number of bits, N photons whenever a binary one is sent and 0 photons for a binary zero. Due to the random nature of the time of arrival of the different photons pertaining to the same pulse, the Poisson detection process statistics provides, after some mathematics, the following formula, which assumes that no thermal noise is present

$$p(n) = \frac{(\lambda T)^n e^{-\lambda T}}{n!} = \frac{N^n e^{-N}}{n!} \qquad (2.0.1)$$

Here p(n) is the probability of detecting exactly n photons in a pulse when, on average, each pulse in the stream of duration T seconds contains $\lambda T = N$ photons.
If the binary digits are generated with the same probability (i.e. $\frac{1}{2}$) the chance of making an error is given by $\frac{1}{2}$ p(n=0) which is equal to

$$P_e = \frac{1}{2} e^{-\lambda T} = \frac{1}{2} e^{-N} = \frac{1}{2} e^{-2P} \qquad (2.0.2)$$

where P is the average optical energy, photons per bit.

This is a well known formula providing the so called quantum limit: It implies that in order to achieve a Bit Error Rate (BER) of 10^{-9} it is necessary that at least 10 photons/bit reach the receiver, which is identical to say that each pulse corresponding to a binary one must contain 20 photons.

It is very important to note that such a quantum limit applies to an uncoded, amplitude modulated, binary system: it can be shown that for suitable coding schemes (privileging the number of transmitted zeroes) or modulation formats (Pulse Position Modulation) lower limits, for example 1 photon/bit) can be achieved.
When thermal noise is considered or an APD is used, which introduces one more noise term, called multiplication noise, the practical receiver sensitivity is increased by a factor of 100 (20 dB): this was one of the chief motivation for turning to coherent techniques.

3. IDEAL COHERENT DETECTION

In order to evaluate quantum limits for coherent detection the signal field at the mixer input can be written as

$$s(t) = A \cos (\omega t + \phi) \qquad (3.0.1)$$

where A^2 is proportional to the optical power. In homodyne detection the local oscillator adds, for best performance, a carrier whose amplitude and frequency are exactly the same of the signal wave. It can be shown that the lower quantum limit is obtained for phase modulated signals; in this case the wave impinging onto the detector surface is given by

$$\omega(t) = (A \pm A) \cos \omega t \qquad (3.0.2)$$

where the different signs between parentheses hold for zero and one transmission respectively.

If the bit duration is T, the average transmitted optical energy is A^2T, while the detected energy (photon counts) is either $4A^2T$ or 0. Using equation (2.0.2) the BER can be calculated as

$$P_e = \frac{1}{2} e^{-\lambda T} = \frac{1}{2} e^{-4P} \qquad (3.0.3)$$

This result shows an improvement over the IM-DD quantum limit of 3 dB which is often referred to as super quantum limit. It is, however, to be noted that, to achieve such a

performance, the receiver should be able to know and to track exactly amplitude, phase and frequency of the transmitting laser, what is rather ambitious.

If the constraint on LO amplitude is relaxed, equation (3.0.2) can be written as

$$\omega(t) = (B \pm A) \cos \omega t \qquad (3.0.4)$$

the photon counts are $(B^2+A^2 \pm 2AB)T$, which, after removing a bias term, provide an antipodal pair of signals $\pm 2ABT$ that are Poisson distributed with variance B^2T.

Under these circumstances the BER can be calculated as

$$P_e = \frac{1}{2} \operatorname{erfc} \sqrt{2A^2T} \approx \frac{1}{2} e^{-2P} \qquad (3.0.5)$$

Equation (3.0.5) shows that quantum limit operation can be obtained in homodyne systems using photodiodes without amplification. This is made possible by the availability of a LO with high power, which reinforces the weak signal wave thus overcoming problems related to thermal noise.

In the case of heterodyne detection, the LO frequency is somewhat shifted with regards to the signal wave frequency and the time varying part of the electrical signal after detection is given by

$$i(t) = \pm 2AB \cos \omega_{IF} t \qquad (3.0.6)$$

where ω_{IF}, is the frequency difference between signal and local wave.
After some algebra, in the same hypotheses adopted for the noise in homodyne detection, BER is asymptotically equal to

$$P_e \approx \frac{1}{2} e^{-A^2T} = \frac{1}{2} e^{-P} \qquad (3.0.7)$$

Equation (3.0.7) indicates that to achieve the same BER than in homodyne systems, heterodyne detection needs a double number of photons in signal wave, thus showing 3 dB worse performance.

4. COHERENT OPTICAL SYSTEM STRUCTURE

The general block scheme of an optical coherent transmitter is shown in fig. 3. At the transmitter, the information to be transmitted is coded into the optical field by modulating a semiconductor laser. The modulation can be performed directly both in amplitude and in frequency or by means of an external modulator.

In particular an external modulator is needed when a phase or a polarization modulation is desired. The direct modulation is quite diffused since it allows to avoid the insertion loss of the modulator, however this technique is limited by the modulation bandwidth of the laser and, if amplitude modulation is considered, by the phenomenon of chirping.

At the receiver the incoming optical field is mixed with the local oscillator field by means of an optical front end composed by one or more optical hybrids, as directional couplers, polarization splitters, 90° balanced hybrids and so on, and, if the case, by a polarization control device.

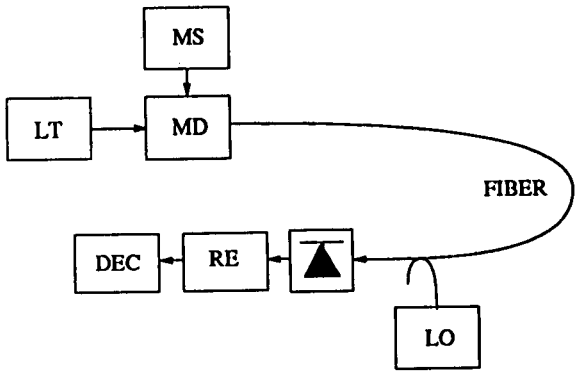

Figure 3 - Block scheme of an optical coherent system (MS=message source, MD=modulation device, LT=laser transmitter, LO=local oscillator, RE= receiver block)

At the output of the optical front end the emerging optical fields are converted into electronic currents by means of some PIN photodiodes. It is to be noted that generally in a coherent system there is no reason to use an APD detector. As a matter of fact the operation near the quantum limit is obtained by means of a high power local oscillator and an APD can only degrade the system performance introducing multiplication noise.

If the local oscillator and the incoming optical carrier have the same frequency the electrical currents at the output of the photodiodes are at baseband and a homodyne receiver is considered. On the other hand if the local oscillator and the received carrier have not the same frequency the electrical currents are frequency translated around an electrical carrier whose frequency is called intermediate frequency (IF). In this case the receiver is called heterodyne. However both in a homodyne and in a heterodyne receiver an automatic frequency control (AFC) of the local oscillator is needed in order to compensate the slow frequency fluctuations of both the local oscillator and the transmitting laser. Generally the AFC is a feedback loop operating on the bias current of the local oscillator whose control signal is derived from the electrical currents.

After the optical to electrical conversion the electrical currents are filtered so to eliminate the constant term due to the local oscillator power and to limit the additive noise and, in the case of the heterodyne receiver, a further electrical demodulation and filtering is performed. At the end of this processing the baseband currents are combined so to obtain a single signal that constitutes the input of a decision device. This last circuit recovers the signal clock from its input by using a baseband PLL and samples the incoming signal at the center of each bit interval. This series of samples are used to estimate the transmitted bits according to the adopted modulation format.
A further specification of the receiver scheme can be obtained by considering a particular optical front end. In the following some of the most common optical front ends will be reviewed.

4.1 Single Branch Receiver

The block scheme of a single channel receiver is shown in fig. 4. The optical front end is constituted by a polarization control device, driven by the electrical current, that transforms the polarization of the received optical field in order to match that of the local oscillator, and by a directional coupler that mixes the signal and the local

oscillator fields. Since a relevant loss of signal power is not acceptable an unbalanced directional coupler is needed.

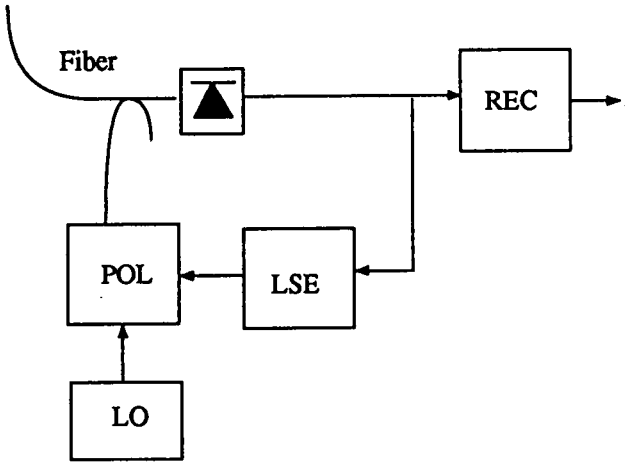

Figure 4- Block scheme of an single channel receiver - The front -end is constituted by a polarization control device (POL=optical polarizator, LO=local oscillator, LSE=level signal estimator, REC=receiver side)

As a matter of fact, assuming the local oscillator linearly polarized along the x axis, after the polarization control device, the signal field $E^s(t)$ and local oscillator field $E^l(t)$ can be written as

$$E^s(t) = A_s(t)\, e^{i[\omega_s t+\phi_s(t)]}\, x$$
$$E^l(t) = A_l(t)\, e^{i[\omega_l t+\phi_l(t)]}\, x \qquad (4.1.1)$$

It is to be noted that, from now on, the amplitudes of the electrical fields will be measured in square root of the power measurement unit so that the square amplitude gives directly the field power. Since the transfer matrix [S] of an unbalanced directional coupler is given by

$$[S] = \begin{bmatrix} \alpha & \sqrt{1-\alpha^2} \\ -\sqrt{1-\alpha^2} & \alpha \end{bmatrix} \qquad (4.1.2)$$

the optical field E(t) at the first output of coupler and at the photodiode input is given by

$$E(t) = \alpha\, E^s(t) + \sqrt{1-\alpha^2}\, E^l(t) \qquad (4.1.3)$$

so that the signal power loss can be made small by designing the coupler in a way that α is very close to one. However in this case the local oscillator power incident on the photodiode is a small fraction of the whole optical power emitted by the local oscillator and could be not sufficient to achieve quantum limited operation.

After the optical to electrical conversion the electrical current is filtered, demodulated in the heterodyne case, and constitutes the input of the decision device.
It is to be noted that, in the case of homodyne detection using a single branch receiver, the front end must incorporate also an optical PLL that is needed to track the phase of the received carrier. The structure of the optical PLL is similar that of an electrical loop but for the absence of an optical device that effectively multiply two optic fields, and will be detailed while analyzing the single branch PSK system.

4.2 Balanced Receiver

An effective way to overcome the problem that in a single branch receiver only a small part of the power of the local oscillator is really used by the receiver, is to adopt a 180° balanced configuration. The block scheme of such a receiver is shown in fig. 5.

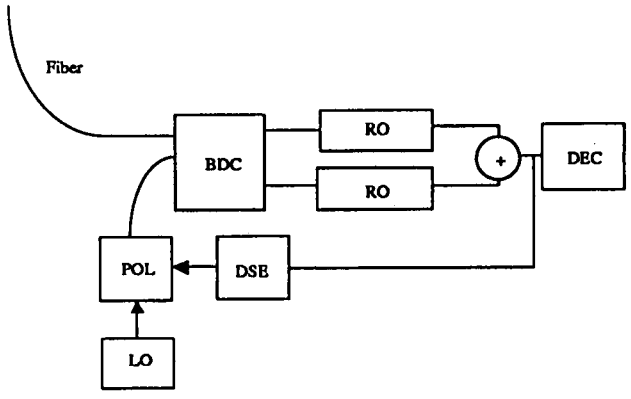

Figure 5 - Block scheme of a system in which the 180° balanced configuration is adopted (BCD=balanced directional coupler, LO=local oscillator, RO=optic receiver which produces base-band signal)

After the polarization control the signal and the local oscillators field, that can be expressed by means of equation (4.1.1), are mixed by using a balanced directional coupler. The transfer matrix of a balanced directional coupler is given by equation (4.1.2) with $\alpha = 1/\sqrt{2}$ so that the optical fields $E^h(t)$ (h=1, 2) at the output of the coupler are given by

$$E^1(t) = \frac{\sqrt{2}}{2}[E^s(t) + E^l(t)]$$
$$E^2(t) = \frac{\sqrt{2}}{2}[-E^s(t) + E^l(t)] \qquad (4.2.1)$$

The fields at the output of the coupler are separately converted into two electrical currents $c_h(t)$ (h=1, 2) by two identical photodiodes. The average values of the electrical currents are given by

$$\langle c_1(t)\rangle = R_p\, A_s(t)\, A_l \cos[\omega_{IF}t + \phi_s(t) + \phi_l] + R_p\, A_l^2$$
$$\langle c_2(t)\rangle = -R_p\, A_s(t)\, A_l \cos[\omega_{IF}t + \phi_s(t) + \phi_l] + R_p\, A_l^2 \qquad (4.2.2)$$

where $R_p = \eta q/h\nu$ represents the photodiodes responsivity being ν the optical carrier frequency, q the electron charge, η the photodiode quantum efficiency and h the Plank constant, and $\langle x\rangle$ the average value of x. Of course equation (4.2.2) holds both in the heterodyne and in the homodyne case, the homodyne case being obtained for $\omega_{IF}=0$.

After the optical to electrical conversion the electrical currents are subtracted so to obtain a single current $c(t)=c_1(t)-c_2(t)$. The average value of c(t) is a signal term equal to that appearing in the case of the single branch receiver with the exception that the whole power of the local oscillator is exploited. However the zero frequency term generated by the local oscillator only is eliminated by the difference between $c_1(t)$ and $c_2(t)$ so that it is no more needed to suppress it by filtering. This is advantageous particularly in homodyne receivers in which the current are

directly at baseband after the optical to electrical conversion.

In contraposition to the above mentioned advantage the 180° balanced receiver requires two identical photodiodes and electrical front end and a perfectly balanced coupler. From equation (4.2.2) it can be easily seen that, if the responsivities of the photodiodes are not identical or if $\alpha=1/\sqrt{2}$,the electrical currents do not combine properly and a performance penalty is induced. However it can be demonstrated that, using ultimate technology, it is possible to obtain 180° balanced receivers with a very low unbalance penalty, requiring however more sophisticated components with respect to a single branch receiver.

4.3 Polarization Diversity Receiver

The principal scope of a polarization diversity receiver is to separately detect the linear polarization components of the received field so to obtain a receiver that is independent of the fiber induced polarization fluctuations of the received field, thus avoiding the need of a polarization control device. However this kind of optical front end is useful also in polarization modulated systems in which, since the information is coded into polarization changes, it is needed to estimate the polarization state of the received field.

The block diagram of a polarization diversity coherent receiver is shown in fig. 6.

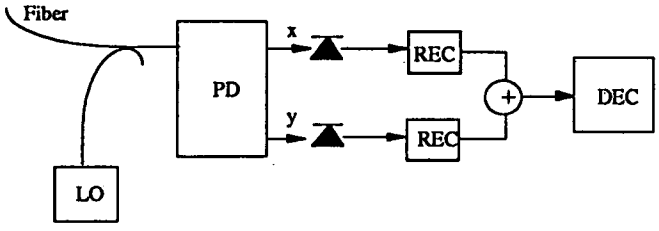

Figure 6: Block scheme of a polarization diversity receiver (PS = Polarization splitter,REC = IF receiver block and demodulator, DEC = decisor)

The received optical field, generally elliptically polarized, and the local oscillator field, that is supposed to be linearly polarized at $\pi/4$ with respect to the receiver reference axes, are mixed by means of an unbalanced directional coupler of the same kind of that used in a single branch receiver. The output of the directional coupler that contains almost all the signal power is used as one input of a polarization splitter.

Since the received and the local oscillator optical fields can be written as

$$E^S(t) = A_S(t)\,\{\cos\phi\ x + \sin\phi\ e^{i\zeta}\ y\}\ e^{i[\omega_S t+\phi_S(t)]} \qquad (4.3.1)$$

$$E^L(t) = \frac{A_L(t)}{\sqrt{2}}\,\{x + y\}\ e^{i[\omega_1 t+\phi_1(t)]}$$

where φ and ζ are angles characterizing the polarization state of the received field, the two output fields $E^1(t)$ and $E^2(t)$ of the polarization splitter can be written as

$$E^1(t) = \{A_S(t)\alpha\cos\phi\ e^{i[\omega_S t+\phi_S(t)]} + \frac{A_L(t)}{\sqrt{2}}\sqrt{1-\alpha^2}\ e^{i[\omega_1 t+\phi_1(t)]}\}\ x$$

$$E^2(t) = \{A_S(t)\alpha\sin\phi\ e^{i\zeta}\ e^{i[\omega_S t+\phi_S(t)]} + \frac{A_L(t)}{\sqrt{2}}\sqrt{1-\alpha^2}\ e^{i[\omega_1 t+\phi_1(t)]}\}\ y \qquad (4.3.2)$$

If these optical field are detected by two identical photodiodes the average values of the currents, after the elimination of the continuous term due to the local oscillator only, are given by

$$\langle c_1(t)\rangle = \sqrt{2}R_p A_s(t)A_l\,\alpha\,\sqrt{1-\alpha^2}\cos\phi\,\cos[\omega_{IF}t+\phi_s(t)-\phi_l]$$

$$\langle c_2(t)\rangle = \sqrt{2}R_p A_s(t)A_l\,\alpha\,\sqrt{1-\alpha^2}\sin\phi\,\cos[\omega_{IF}t+\phi_s(t)-\phi_l+\zeta] \qquad (4.3.3)$$

From equation (4.3.3) it is clear that the complex amplitude of the x-component of the received field can be estimated starting from the current $c_1(t)$ while the y component can be estimated starting from the current $c_2(t)$.

When the polarization diversity scheme is used to achieve polarization fluctuation insensitiveness the two currents are separately processed and the baseband signals are added immediately before the decision device. On the contrary, when the polarization diversity scheme is used to estimate the polarization of the received field the electronic processing generally cannot be divided into two separate parts each involving one electrical current.
It is to be observed that in the case of homodyne detection using a polarization diversity receiver, the front end must comprise also an optical PLL that is needed to track the phase of the received carrier whose structure will be detailed while analyzing PSK systems. Moreover the polarization diversity receiver exploits only a small part of the local oscillator power, as it happens for the single branch receiver. If the power of the local oscillator is to be completely exploited a balanced polarization diversity system can be designed. In this case it can be seen that the average values of the currents at the two electrical outputs of this optical front end are given by equation (4.3.3) in which a = $1/\sqrt{2}$ so that the local oscillator power is completely exploited by the receiver.

4.4 Phase Diversity Receiver

The phase diversity receiver is mainly based on a 90° balanced optical hybrid, whose ideal transfer matrix [S] is given by the following expression

$$[S] = \frac{1}{\sqrt{2}}\begin{bmatrix} 1 & 1 \\ 1 & i \end{bmatrix} \qquad (4.4.1)$$

It is to be noted that phase diversity systems based on other kind of optical hybrids, that is balanced 3x3 hybrids, have been studied and experienced [4]. However this class of receivers has a behavior similar that of 90° balanced receiver and will not be analyzed in this chapter.
The block scheme of a 90° balanced receiver is shown in fig. 7.

After the polarization control, performed by an active optical controller, the received field is mixed with the local oscillator one by means of a 90° balanced optical hybrid.

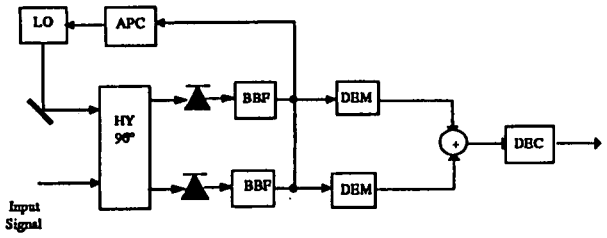

Figure 7: Block scheme of a 90° balanced receiver (LO = local oscillator, HY 90° = 90° optic balanced hybrid, APC = active polarization controller, BBF = base band filter, DEM = demodulator, DEC = decisor)

Since the received and the local oscillator fields can be expressed as in equation (4.1.1), the optical fields $E^1(t)$ and $E^2(t)$ at the hybrids outputs are given by the following equation

$$E^1(t) = \frac{1}{\sqrt{2}}\{A_s(t)\, e^{i[\omega_s t+\phi_s(t)]} + A_l\, e^{i[\omega_s t+\phi_s(t)]}\}\, x$$

$$E^2(t) = \frac{1}{\sqrt{2}}\{A_s(t)\, e^{i[\omega_s t+\phi_s(t)]} + i\, A_l\, e^{i[\omega_s t+\phi_s(t)]}\}\, y \qquad (4.4.2)$$

The fields at the hybrid outputs are detected by two identical photodiodes and, after the elimination of the constant terms due to the local oscillator only, the average values of the output currents are given by the following equations

$$\langle c_1(t)\rangle = R_p\, A_s(t)\, A_l \cos[\omega_{IF} t + \phi_s(t) - \phi_l]$$

$$\langle c_2(t)\rangle = R_p\, A_s(t)\, A_l \sin[\omega_{IF} t + \phi_s(t) - \phi_l] \qquad (4.4.3)$$

As evident from equation (4.4.3) $\langle c_1(t)\rangle$ and $\langle c_2(t)\rangle$ are respectively the real and imaginary part of a complex signal whose expression is

$$s(t) = R_p\, A_s(t)\, A_l\, e^{i[\omega_{IF} t + \phi_s(t) - \phi_l]} \qquad (4.4.4)$$

If the electronic processing is properly designed on the two electrical branches it is equivalent to a processing on the signal s(t) and it is quite important to understand the behavior of the 90° balanced receiver.

As a matter of fact, when a real bandlimited signal is frequency down shifted, it is needed that the new carrier frequency be greater or equal to the signal bandwidth in order to avoid aliasing, that is the superposition of the positive and the negative part of the signal spectrum. For the same reason, if a real bandlimited signal is baseband translated, the operation must be carried out using a demodulation carrier with exactly the same phase of the signal carrier. This allows that, when the positive and the negative part of the spectrum are superimposed at baseband, they are exactly added since each spectral component has the same phase. In the absence of an exact phase tracking the positive and negative frequencies have not the same phase and the consequent interference causes a power loss. However in the case of a 90° balanced receiver the performed operations are equivalent to process the complex signal s(t) whose spectrum contains only positive components. This allows baseband translation without requirements on the phase of the demodulation carrier, that is homodyne detection without the need of an optical PLL. Moreover it is possible to perform a frequency down shift of the received signal around a frequency smaller than the received signal bandwidth without loss of information.

This opportunity can be exploited by down shifting the received signal around a frequency by far smaller than the bit rate. As a matter of fact, one of the most important advantages of the homodyne receiver is that the bandwidth of any electronic devices is one half with respect to a heterodyne receiver. On the other hand, also if a phase tracking circuit is not needed when a 90° balanced optical front end is used, the frequency of the local oscillator must be rigorously equal to that of the incoming carrier, requiring a frequency tracking circuit more sophisticated that that present in a heterodyne receiver. On the other hand, if the incoming signal is to be shifted not exactly at baseband but around a frequency much smaller that the bit rate the electronic filtering can be performed by using a baseband filter with a bandwidth lightly greater than that adopted in the homodyne receiver and the requirements on the automatic frequency control of the local oscillator are the same of a heterodyne receiver. Receivers operating in this way are called intradyne receivers [5].

Phase diversity detection can be combined with polarization diversity detection in order to obtain an optical front end that separately performs a phase diversity detection on each polarization component of the received field. The block scheme of the resulting system is shown in fig. 8 and the electrical currents on the four output electrical branches can be easily obtained.

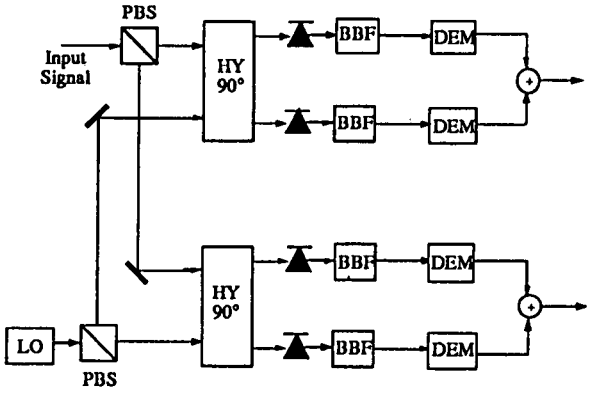

Figure 8 : Block scheme of a phase and polarization diversity system (HY 90° = 90° optic balanced hybrid, BBF = base band filter, DEM = demodulator)

A phase and polarization diversity front end has some very good property, the most important of which is that polarization independent homodyne detection with no need of an optical PLL, is allowed for a certain number of modulation format. The main difficulties in realizing such an optical front end is to realize a perfectly balanced hybrid and four photodiodes, each with the corresponding electrical front end, rigorously with the same characteristics. Perhaps this problem can be solved in a better way by realizing the hybrid, the photodiodes and their electrical front ends all on the same chip using integrated optics techniques; however for the current state

of the art, that is still a difficult task.

The phase diversity optical front end can be also combined with the 180° balanced detection by using a 4x4 optical hybrid whose ideal transfer matrix [S] is given by

$$[S] = \frac{1}{2}\begin{bmatrix} +1 & -i & +1 & -i \\ +1 & -i & -1 & +i \\ +1 & +i & -i & +1 \\ +1 & +i & +i & -1 \end{bmatrix} \qquad (4.4.5)$$

The block scheme of the resulting coherent system is shown in fig. 9.

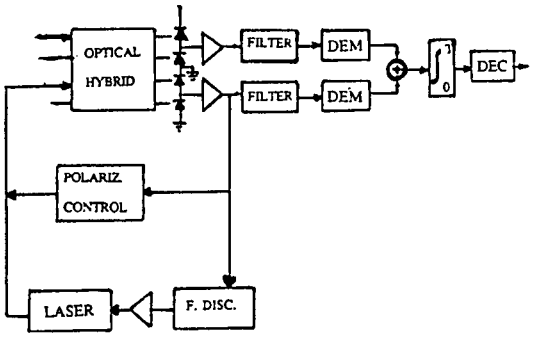

Figure 9: Block diagram of a system with the phase diversity front-end and the 180° balanced detection by using a 4x4 optical hybrid

The average values of the electrical currents on the two output electrical branches are the same of a phase diversity receiver given in equation (4.4.3) so that both homodyne without phase locking and intradyne detection can be performed. However the filtering operation around zero frequency is not needed since the constant term due to the local oscillator only is eliminated by the 180° balanced detection on each branch. Moreover the receiver has other advantages of the balanced detection in eliminating all the disturbing signals that are identical on each optical branch. On the other hand the implementation difficulties are of the same type of the polarization and phase diversity front end.

5. COHERENT SYSTEMS USING PSK MODULATION

One of the first modulation formats to have been investigated for use in coherent transmission systems is the binary Phase Shift Keying (PSK). In this case the optical signal emitted by the transmitting laser is phase modulated by an external modulator so that the field phase is constantly zero during the bit period when a binary zero is to be transmitted and is constantly π during the bit period when a binary one is to be transmitted. In the ideal case a discontinuous phase transition must take place between two adjacent bit periods when commuting from a bit to the other, however in practice it is required that the transition time be much shorter than the bit period.

The power spectral density $S_s(\omega)$ of such a signal can be evaluated using standard methods obtaining, in the hypothesis of equiprobable bits,

$$S_S(\omega) = \frac{A_t^2}{2} T \left\{ \frac{\sin^2[(\omega-\omega_S)T/2]}{[(\omega-\omega_S)T/2]^2} + \frac{\sin^2[(\omega+\omega_S)T/2]}{[(\omega+\omega_S)T/2]^2} \right\} \qquad (5.0.1)$$

where T is the bit period and A_t^2 the transmitted optical power.

5.1 Performance of a Single Branch PSK Homodyne Receiver

The principle scheme of a single branch PSK homodyne receiver is reported in fig. 10.

The received signal is processed by a polarization controller, so to match its polarization state with that of the local oscillator, then it is mixed with the local oscillator field by means of an unbalanced directional coupler. The resulting field is detected by a photodiode.

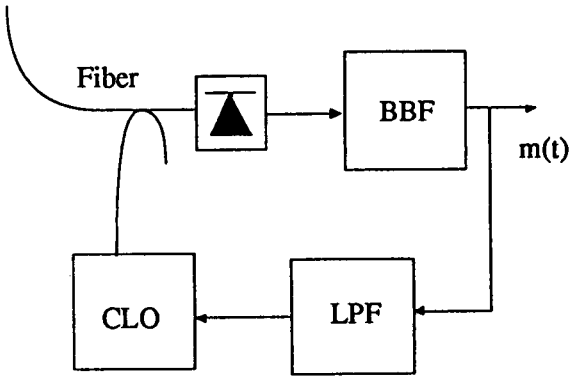

Figure 10: Block scheme of a single branch PSK homodyne receiver (BBF = base-band filter, LPF = low-pass filter, CLO = controllered laser oscillator)

After the polarization controller, assuming the local oscillator linearly polarized along the x axis, the received field has the following expression

$$E_S(t) = A_S \, x \, e^{i[\omega_s t + \phi_s + \pi m(t)]} \qquad (5.1.1)$$

where m(t)=1 if a binary one is transmitted and m(t)=0 otherwise. After the mixing with the local oscillator and the optical to electrical conversion the baseband electrical current c(t) has the following expression

$$c(t) = 2 R_p A_S A_l \alpha \sqrt{1-\alpha^2} \cos[\phi_S(t) - \phi_l + \pi m(t)] + \eta_d(t) \qquad (5.1.2)$$

where $\eta_d(t)$ represents the detection noise process.

In order to obtain the quantum limit of such a receiver the following main hypotheses have been adopted

- the polarization controller ideally matches the polarization states of the received and local oscillator fields;
- the optical PLL ideally estimates the instantaneous phase of the incoming signal carrier and instantaneously reproduces it as phase of the local oscillator field;
- the optical PLL completely ignores the modulation so

that no signal distortion is introduced;
- the directional coupler unbalance factor α is so close to one that the coupling signal loss can be neglected;
- the local oscillator power is so high that there is enough power to achieve quantum limit operation also in the above mentioned hypotheses;
- the photodiode has unit quantum efficiency;
- any electronic components are ideal and do not introduce noise;
- the baseband filter induced signal distortion can be neglected so that its sole effect is to limit the noise power.

On the ground of these hypotheses equation (5.1.2) can be rewritten for a single bit period as

$$c(t) = \pm 2 R_p A_s A_l + \eta_d(t) \qquad (5.1.3)$$

where the plus sign denotes the transmission of a zero, the minus sign that of a one. Moreover the process $\eta_d(t)$ can be assumed to be caused only by the quantum noise and to be a zero mean white Gaussian process whose power spectral density N_Q is given by

$$N_Q = 2 q R_p A_l^2 \qquad (5.1.4)$$

The baseband signal is filtered by an ideal lowpass filter, that is the matched filter if the transmission is performed by means of rectangular phase pulses as in this case, and sampled at the center of the bit time. The sample c_j at the sampling time t_j has the expression

$$c_j = \pm 2 R_p A_s A_l + \eta_{dj}(t) \qquad (5.1.5)$$

The unilateral bandwidth of the lowpass filter can be assumed to be equal to R/2 where R is the bit rate. In this condition the noise sample η_{dj} is a zero mean Gaussian variable with variance $\sigma_\eta^2 = N_Q R/2$. Assuming equiprobable bits, since the distribution of the noise sample is symmetric around zero and does not depend on the transmitted bit, the decision can be performed by comparing the sample c_j with a threshold equal to zero.

The bit error probability P_e is than given by

$$P_e = \frac{1}{2} Pr\{c_j > 0 / m(t_j) = 1\} + \frac{1}{2} Pr\{c_j < 0 / m(t_j) = 0\} \qquad (5.1.6)$$

where Pr{E/F} indicates the probability of the event E conditioned to the event F.

Starting from equation (5.1.6), the error probability can be easily calculated by taking into account that c_j is a Gaussian variable. The result can be expressed in a significant form if it is noted that the signal to noise ratio for the considered case has the following expression

$$\frac{\langle c_j \rangle^2}{\sigma_\eta^2} = \frac{2A_s^2}{h\nu R} = 2n_s \qquad (5.1.7)$$

where n_s is the average number of detected photons per bit. Starting from equation (5.1.7) the bit error probability expression can be written as

$$P_e = \frac{1}{2} \operatorname{erfc} \sqrt{2n_s} \qquad (5.1.8)$$

where erfc(x) is the complementary error function.

In order to compare different system under a performance point of view it is useful to introduce the receiver sensitivity S_n, that is the average number of photons per bit needed to achieve a reference bit error probability. Assuming a reference error probability equal to 10^{-9} the sensitivity of the considered system is about 9 photons per bit. Of course the receiver sensitivity in dBm depends on the bit rate and on the optical carrier frequency.

5.2 Performance of a Single Branch PSK Heterodyne Receiver

The principle scheme of a single branch PSK heterodyne receiver is reported in fig. 11.
The optical front end is similar that of a homodyne receiver but, since the frequency of the local oscillator is different from that of the received signal carrier, there is no need of phase locking.

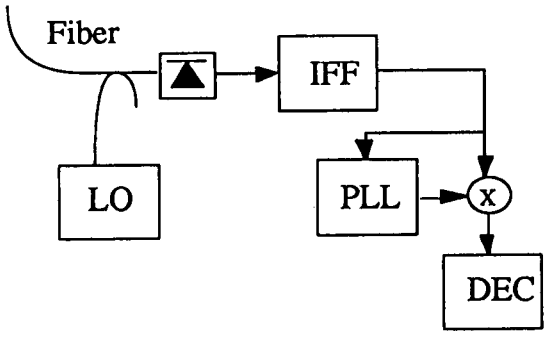

Figure 11: Block scheme of a single branch PSK heterodyne receiver (IFF = intermediate frequency filter, PLL = phase looking loop)

Assuming the same hypotheses considered in the homodyne case, the intermediate frequency current c(t) has the following expression

$$c(t) = 2R_p A_s A_l \cos[\omega_{IF} + \phi_s(t) - \phi_l + \pi m(t)] + \eta d(t) \qquad (5.2.1)$$

where $\eta_d(t)$ represents the detection noise process. The current c(t) is filtered by an ideal bandpass filter of unilateral bandwidth 2R around the angular frequency $2\omega_{IF}$, that is the matched filter in this case, and demodulated by an electrical PLL. The obtained baseband signal is filtered by a wide band filter, whose scope is to eliminate high frequency signal components, and sampled at the center of each bit period.

Assuming an ideal PLL operation, the sample c_j in the instant t_j has the following expression

$$c_j = \pm 2 R_p A_s A_l + \eta_{dj} \qquad (5.2.2)$$

where the noise sample η_{dj}, is a zero mean Gaussian variable. Its variance can be calculated by decomposing the detection noise process, that after the intermediate frequency filtering is a bandlimited Gaussian process, in its

quadratures and multiplying it by the demodulation carrier. It results that η_{dj} is the instantaneous sample of the in-phase component of the quantum noise and its variance is $\sigma_\eta^2 = N_Q R/2$.

Starting from equation (5.2.2) the quantum limit error probability P_e of the PSK heterodyne receiver can be evaluated with a procedure analogous to that used in the homodyne case obtaining

$$P_e = \frac{1}{2}\operatorname{erfc}\sqrt{n_s} \qquad (5.2.3)$$

From equation (5.2.3) and (5.1.8) it is evident that, using a heterodyne receiver, in order to reach an assigned error probability a doubling of the optical power, with respect to the case in which a homodyne receiver is considered, is required.

This behavior is quite different from that of the analogous radio frequency receivers. As a matter of fact at radio frequency a heterodyne and a homodyne PSK ideal receivers have the same performance. This is due to the fact that the performance of an ideal radio frequency receiver are determined by the incoming signal to noise ratio since the noise arrives at the receiver end with the signal. In this situation the fact that a homodyne receiver has half the bandwidth with respect to a homodyne receiver gives no advantage. On the other hand the performance on an ideal PSK coherent optical receiver are determined by the quantum noise, that in a semiclassical analysis is equivalent to an additive white Gaussian noise of given power spectral density that must be added to the electrical signal after the optical to electrical conversion. In this situation, typical of optical coherent systems, the noise power affecting the receiver is proportional to the receiver electrical bandwidth so that a homodyne receiver shows a 3 dB sensitivity gain with respect to the heterodyne one. For example the sensitivity of a heterodyne receiver at an error probability of 10^{-9} is about 18 photons per bit.

5.3 Performance of a PSK Receiver using a Reference Carrier

The most critical element of a PSK receiver is the PLL, needed to reconstruct at the receiver the received signal carrier. A way to avoid the use of such a component is the transmission of a reference carrier with the modulated signal. In this case the reference carrier can be used at the receiver to perform the demodulation, since, being extracted by the same laser, it has the same phase and frequency of the received signal carrier.

A reference carrier can be created at the transmitter both by splitting the optical field emitted by the transmitting laser into two parts, modulating one of them, and than sending the two field into the fiber, or phase modulating the transmitted signal between zero and some phase less than p. In this last case the carrier is not completely suppressed from the spectrum of the modulated signal and can be extracted at the receiver to perform the demodulation.

The transmission of the reference carrier can be performed placing it at the center of the signal spectrum, as in the case of incomplete phase modulation, on a frequency out of the signal bandwidth or on a polarization orthogonal to that of the signal. In this last case, in spite of the polarization evolution along the fiber, the signal and the reference carrier remains separate since the fiber preserve, when in linear propagation regime, the orthogonality between polarization states.

The receiver can perform a homodyne or a heterodyne demodulation. A homodyne demodulation can be for example performed by separating by means of an optical filter the reference carrier placed on a frequency out of the signal bandwidth by the modulated signal, amplifying it by means of an optical amplifier and using it as demodulation carrier in a homodyne receiver. A similar principle can be exploited if the reference carrier is at the center of the signal bandwidth. In this case the optical signal can be amplified by means of an optical amplifier of very narrow bandwidth so to amplify the reference carrier and to induce a negligible signal distortion. The optical field can be than send on a photodiodes that provide the mixing between the amplified carrier and the signal and so the homodyne detection.

In the case of the heterodyne receiver the reference carrier and the modulated signal are both translated at intermediate frequency, divided and than multiplied in order to obtain electrical demodulation.
In this paragraph only one of the numerous different PSK system schemes using a reference carrier demodulation is analyzed in detail in order to obtain some general information on the behavior of the systems belonging to this class. Moreover the chosen system scheme is interesting both for the method used to compensate the fiber induced polarization fluctuations that relies on an electronic tracking algorithm.

The block scheme of the considered system is shown in fig. 12.

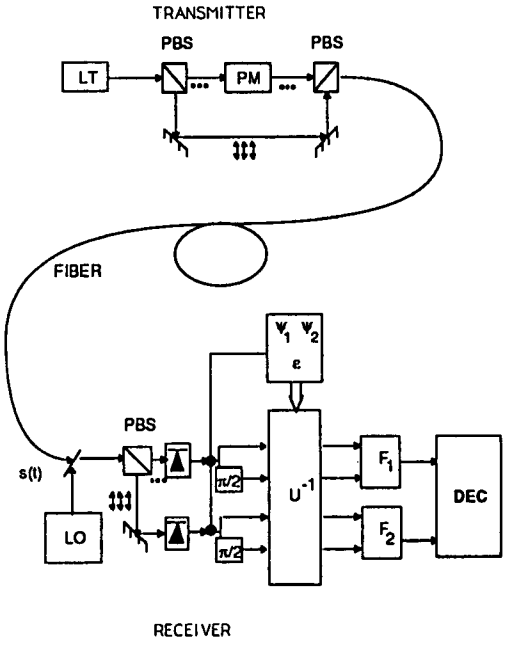

Figure 12: Block scheme of a PSK receiver using a reference carrier (LT = Laser Tansmitter, PBS = polarization beam splitter, PM = phase modulator, F_1, F_2 = intermediate frequency filters)

At the transmitter the laser beam, supposed linearly polarized at a given angle θ with respect to the x reference axis, is divided into its two polarization components. The y component is phase modulated between 0 and π by the message while the x component is used as reference carrier

so that the transmitted signal $E^t(t)$ can be written as follows

$$E_t(t) = A_t[\cos\theta x + \sin\theta\, e^{i\pi m(t)} y]\, e^{i[\omega st + \phi s(t)]} \quad (5.3.1)$$

Considering the transmission through a conventional single-mode optical fibre, the effect due to fibre birefringence can be taken into account by means of the Jones formalism so that the received signal $E^s(t)$ can be expressed as a function of the transmitted signal by means of the unit linear operator [J] so to obtain

$$E^s(t) = e^{-a}[J]\, E^t(t) \quad (5.3.2)$$

where a is takes into account the fiber attenuation.
At the receiver this field is mixed with the optical LO, supposed linearly polarized at $\pi/4$ with respect to the reference axis, by means of a polarization diversity front end.

After detection the analytic signal on both electrical branches is obtained and the operator [J] is inverted by means of an electronic adaptive circuit in order to separate the modulated signal from the reference carrier.
Afterwards the two signals are filtered by intermediate frequency filters F_1 and F_2.

In order to obtain a performance analysis of the considered system it is useful to assume that the reference carrier is not a perfect monochromatic wave so that the corresponding electrical intermediate signal has a spectral width B_c different from zero. Under this condition the current corresponding to the modulated signal has a spectral width equal to $B_m = R + B_c$. There are many physical reasons that can cause a spectral broadening of the carrier, the most important of which is the lasers phase noise so that this hypothesis is realistic. Of course the quantum limit performance can be obtained for B_c tending to zero.

The baseband signal is obtained from the two intermediate frequency currents by means of an electrical beating, this signal is baseband filtered by means of a broadband filter whose scope is to eliminate the high frequency component and sampled at the center of each beat interval to obtain the decision variables.
The general form of the operator [J] is

$$[J] = \begin{bmatrix} \varepsilon_j e^{i\psi_1} & \sqrt{1-\varepsilon_j^2}\, e^{i\psi_2} \\ -\sqrt{1-\varepsilon_j^2}\, e^{-i\psi_2} & \varepsilon_j e^{-i\psi_1} \end{bmatrix} \quad (5.3.3)$$

so that three independent parameters must be estimated: ε_j, ψ_1 and ψ_2. After such estimation the inverse operator can be easily obtained being $[J]^{-1} = [J]^*$.
Starting from equations (5.3.2) and (5.3.3) the received field can be written as

$$E^s(t) = A_s \{[\cos\theta\, \varepsilon_j e^{i\psi_1} + \sin\theta \sqrt{1-\varepsilon_j^2}\, e^{i[\pi m(t)+\psi_2]}]\, x + [\sin\theta\, \varepsilon_j e^{i[\pi m(t)-\psi_1]} - \cos\theta \sqrt{1-\varepsilon_j^2}\, e^{-i\psi_2+}]\, y\}\, e^{i[\omega_s t + \phi_s(t)]} \quad (5.3.4)$$

where $A_s = A_t e^{-a}$ and the received optical power P_{opt} is given, with the assumed measurements units for the field amplitude, by A_s^2.

The intermediate frequency currents before the Jones matrix inversion can be written, in the analytical signal formalism, as

$$\begin{bmatrix} c_1(t) \\ c_2(t) \end{bmatrix} = 2R_p A_s A_l [J] \begin{bmatrix} \cos\theta \\ \sin\theta\, e^{i\pi m(t)} \end{bmatrix} e^{i\phi(t)} + \begin{bmatrix} \eta_1(t) \\ \eta_2(t) \end{bmatrix} \quad (5.3.5)$$

where $\eta_1(t)$ and $\eta_2(t)$ represent complex detection noises. They can assumed to be statistically independent zero mean complex Gaussian processes. The power spectral density of each component of the complex detection noises is $qR_pA_l^2$.
In order to examine the algorithm allowing to estimate the Jones matrix parameters during the transmission it is useful to introduce two independent linear combinations of the phase terms ψ_1 and ψ_2, i. e. $\zeta_1 = (\psi_1 + \psi_2)$ and $\zeta_2 = (\psi_1 - \psi_2)$.

From equation (5.3.5), evaluating the long term average of the electrical power P_1 of the intermediate frequency channel that corresponds to the x component of the received field, the following equation can be obtained

$$\varepsilon_j^2 = \frac{P_1 - P_{opt}\sin^2(\theta)}{P_{opt}\cos(2\theta)} \quad (5.3.6)$$

where the bit values are supposed equiprobable. The average operation is supposed to be performed in a time much longer than the bit rate but much shorter that the fluctuation rate of the Jones matrix elements. If the Jones matrix estimation processor measures P_{opt} and P_1 equation (5.3.6) can be used to estimate ε_j.

Analogously, measuring the peak value of the intermediate frequency signal envelope on the channel one, say $c_{1|max}$, makes it possible to calculate ζ_2 from the equation

$$c_{1|max} = 2\sqrt{P_1 - \varepsilon_j\sqrt{1-\varepsilon_j^2}\sin(2\theta)\cos\zeta_2 P_{opt}} \quad (5.3.7)$$

At last, the parameter ζ_1 can be calculated by measuring the long term average of the beating between the intermediate frequency signals $c_1(t)$ and $c_2(t)$ by means of the equation

$$\langle c_1 c_2 \rangle = 2\,\varepsilon_j\sqrt{1-\varepsilon_j^2}\cos(2\theta)\cos\zeta_1 P_{opt} \quad (5.3.8)$$

Assuming a perfect estimation of the elements of $[J]^{-1}$ and supposing that the signal distortion induced by the intermediate frequency filters can be neglected, the signals after the Jones Matrix Inversion can be written as follows

$$\begin{bmatrix} C_1(t) \\ C_2(t) \end{bmatrix} = \sqrt{2}R_p A_s A_l \begin{bmatrix} \cos\theta \\ \sin\theta\, e^{i\pi m(t)} \end{bmatrix} e^{i\phi(t)} + [J]^{-1} \begin{bmatrix} \eta_1(t) \\ \eta_2(t) \end{bmatrix} * \begin{bmatrix} h_1(t) \\ h_2(t) \end{bmatrix} \quad (5.3.9)$$

where $h_1(t)$ and $h_2(t)$ are the transfer function of the filters F_1 and F_2 respectively.

The decision variable $C_d(j)$ is obtained by the beating between $C_1(t)$ and $C_2(t)$, filtering the obtained signal so to eliminate the high frequency component and sampling at

the center of each bit period in the instants t_j so to obtain

$$C_d(j) = 2\,\mathrm{Re}\,\{C_1^*(t_j)C_2(t_j)\} \qquad (5.3.10)$$

Since [J] is a unitary operator it is straightforward to demonstrate that $C_1(t_j)$ and $C_2(t_j)$ are uncorrelated; as they are Gaussian processes it comes out that they are also statistically independent. Under the assumed hypothesis the variance of the phase and quadrature component of $C_1(t_j)$ is $2qR_pA_{lo}^2B_C$ and that of the components of $C_2(t_j)$ is $2qR_pA_{lo}^2(R+B_C)$.

By substituting to $C_1(t_j)$ and $C_2(t_j)$ their expression in equation (5.3.10) it is possible to see that the decision variable average value is

$$\pm\sqrt{2}\,R_p\,A_s\,A_l\sin(2\theta) \qquad (5.3.11)$$

where the plus sign corresponds to $m(t_j)=0$ and the minus sign to $m(t_j)=1$; moreover the probability distribution of $C_d(j)$ depends on the transmitted bit only by means of its average value.

In this condition, assuming equiprobable transmitted bits, the bit error probability is given by the following expression

$$P_e = \frac{1}{2}\Pr\{C_d(t_j)>0 / m(t_j)=1\} + \frac{1}{2}\Pr\{C_d(t_j)<0 / m(t_j)=0\} \qquad (5.3.12)$$

that using the Marcuum function Q can be written as

$$Pe = \frac{1}{2}[1 - Q(\sqrt{\delta_1},\sqrt{\delta_2}) + Q(\sqrt{\delta_2},\sqrt{\delta_1})] \qquad (5.3.13)$$

where

$$\delta_1 = \frac{1}{2}\left(\sqrt{\frac{A_s\cos\theta}{2B_c}} + \sqrt{\frac{A_s\sin\theta}{2B_m}}\right)^2$$
$$\delta_1 = \frac{1}{2}\left(\sqrt{\frac{A_s\cos\theta}{2B_c}} - \sqrt{\frac{A_s\sin\theta}{2B_m}}\right)^2 \qquad (5.3.14)$$

In order to minimize the error probability the suitable value of the angle θ, that is of the power splitting ratio at the transmitter, must be chosen. Starting from expression (5.3.13) the optimization can be performed only numerically, however a simple expression of the optimum value θ_{opt} can be obtained under the hypothesis of high signal-to-noise ratio if the asymptotic approximation of equation (5.3.13) is considered. As a matter of fact, if the signal-to-noise ratio is high enough on both the channels exploiting the asymptotic expression of the Marcuum function, the error probability can be expressed by the following formula

$$Pe = \frac{1}{2}\,\mathrm{erfc}\left(\frac{\sqrt{\delta_1}-\sqrt{\delta_2}}{\sqrt{2}}\right) \qquad (5.3.15)$$

The optimum value θ_{opt} can be now obtained by maximizing the argument of the error function, obtaining

$$\sin^2\theta_{opt} = \frac{B_m}{B_m+B_c} \qquad (5.3.16)$$

The optimized splitting ratio versus the ratio R/B_c is shown in fig. 13.

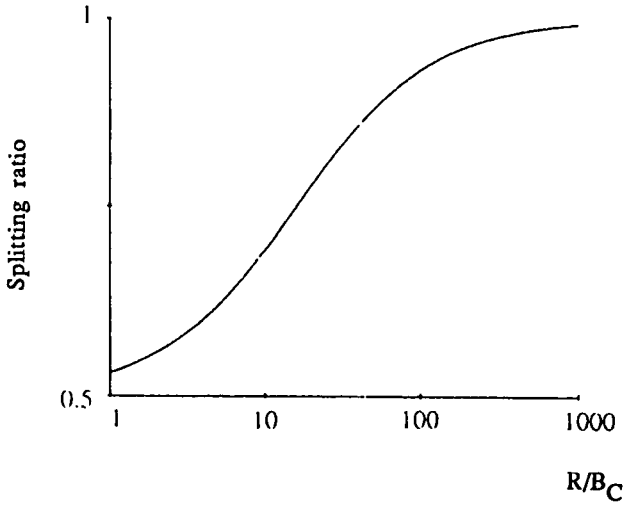

Figure 13: Splitting ratio versus the ratio R/B_C

At the quantum limit, that is in the limit of vanishing reference carrier bandwidth, the power splitting ratio tends to one; in this case a negligible noise power affects the receiver electrical channel corresponding to the reference carrier so that a little optical power is needed to assure the required signal to noise ratio. Almost all the optical power is devoted to the phase modulated channel and the performance tends to that of a single branch PSK receiver.

On the other hand if B_c is by far greater than R it is $B_c \approx B_m$ and about one half of the transmitted power is required by the reference carrier. The bit error probability of the considered system as a function of the average number of received photons per bit is shown in fig. 14 for different values of the ratio R/B_C.

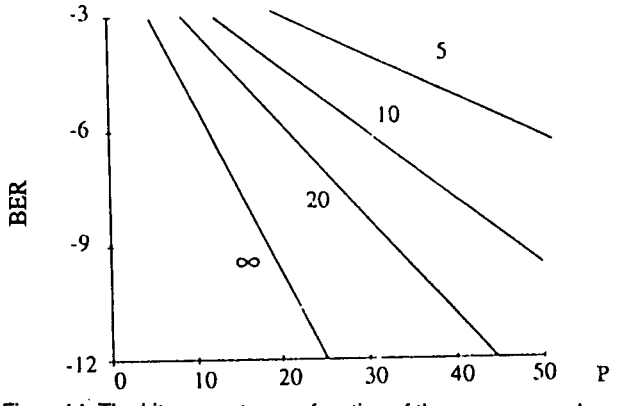

Figure14: The bit error rate as a function of the average number of received photons per bit for different values of the ratioR/B_C

6. COHERENT SYSTEM USING DPSK MODULATION

In section 5 it has been shown that in order to demodulate a PSK modulated signal a demodulation carrier is needed. An

alternative to the use of PSK modulation, allowing phase modulation of the optical signal and asynchronous demodulation at the receiver, is the use of DPSK demodulation. In this modulation format information is encoded not by associating each bit with an absolute value of the field phase but rather by differentially encoding the bit by means of phase changes. For example, assuming that the phase is kept constant in a bit period and is instantaneously changed at the end of this interval, no phase change between tho adjacent bit period can encode a binary zero and a phase change of π a binary one.

At the receiver the decision is performed as if a PSK message would be received and than the obtained bit stream is decoded in order to recover the original message. Of course differential encoding does not alter the spectrum of the transmitted signal that is equal to that of a PSK signal.

In order to analyze the quantum limit performance of DPSK coherent optical systems a general model can be used allowing a unified analysis of all the interesting receiver structures.

The received signal $E^S(t)$ and the local oscillator $E^l(t)$, that can be written as

$$E^s(t) = A_s \{\cos\psi_s x + \sin\psi_s e^{i\zeta_s} y\} e^{i[\omega_s t + \phi_s + \pi m(t)]}$$
$$E^l(t) = A_l \{\cos\psi_l x + \sin\psi_l e^{i\zeta_l} y\} e^{i[\omega_l t + \phi_l + \pi m(t)]} \qquad (6.0.1)$$

are mixed by means of an optical front end. Each considered system structure is determined by the internal structure of the front end, the number M of its output branches and the polarization of the local oscillator that is determined by the parameters φ_l and ζ_l. At the front end output the M optical field are detected by four photodiodes and the resulting currents are filtered by a set of narrowband ideal filters whose scope is to limit the detection noise power affecting the system performances.

If the considered receiver performs a heterodyne detection the filters are ideal bandpass filters centered around the intermediate frequency with unilateral bandwidth 2R, if a homodyne detection is performed the filters are a set of ideal lowpass filters with unilateral bandwidth equal to R. At the filters output the electrical currents can be ordered as the elements of an M-dimensional vector $\underline{C}(t)$. In the case of homodyne detection the vector components are the real values of the baseband electrical currents, in the case of heterodyne detection they are the complex envelopes of the intermediate frequency currents.

After filtering the signals on the electrical branches are demodulated by means of a delay line demodulation. The current at the demodulator input is splitted into two parts of equal power: the first part is transmitted unchanged, the second is delayed by a bit period and then the two currents are multiplied.
This device has the effect to correlate the signals related to adjacent bit periods so to evidence phase transitions in which the transmitted information is encoded.

It is to be noted that this demodulation processing is needed also in homodyne phase diversity receivers. As a matter of fact in this kind of receivers the baseband electrical currents can be represented as complex signals so that a sort of demodulation is needed to reduce them to baseband real currents on which a decision processing can be applied.

After the delay demodulation the baseband signals are added and filtered by means of a wide band baseband filter whose scope is to isolate the baseband component of the signal. The filtered signal is sampled at the center of each bit period so to obtain the decision variable $C_d(j)$.

The hypotheses that are adopted in order to evaluate the quantum limit performance of the DPSK coherent receivers are the following
- if a polarization controller is present in the front end, it ideally match the polarization states of the received and local oscillator fields;
- if the signals are coupled by means of an unbalanced directional couplers its unbalance factor α is so close to one that the coupling signal loss can be neglected;
- all optical hybrids are ideal;
- the local oscillator power is so high that in all the analyzed cases there is enough power to attain quantum limit operation;
- the photodiode has unit quantum efficiency;
- in the heterodyne receivers $(\omega_s - \omega_l)T$ is an integer multiple of 2π;
- all the electronic components are ideal and does not introduce noise;
- the filter induced signal distortion can be neglected so that the only effect of the filters is to limit the noise power and to eliminate the unwanted signal components.

Under these hypothesis the currents vector $\underline{C}(t)$ can be expressed as follows

$$\underline{C}(t) = R_p A_p A_l \underline{X} e^{i[\phi_s - \phi_l + \pi m(t)]} + \underline{n}_D(t) \qquad (6.0.2)$$

where in the homodyne case only the real part of $\underline{C}(t)$ is to be considered. The structure of the front end is completely contained in the complex M-dimensional vector $\underline{X}$ while the vector $\underline{n}_D(t)$ represents the detection noise vector. The elements of $\underline{n}_D(t)$ can be assumed to be zero mean statistically independent complex Gaussian processes whose quadratures have all the same variance σ_η^2 that is determined by the particular system structure.

The decision variable is given by the following expression

$$C_d(j) = \sum_{h=0}^{M} \mathrm{Re}\{c_h(t_j)\, c_h(t_j - T)\} = \underline{C}(t_j)\, \underline{C}^+(t_j - T) + \underline{C}(t_j - T)\, \underline{C}^+(t_j) \qquad (6.0.3)$$

where $c_h(t)$ indicates the h-th component of $\underline{C}(t)$, $T=1/R$ indicates the bit period, + the adjoint, that is the transpose conjugate and $\cdot$ the scalar product.
It can be shown that the following closed form for the expression of the error probability can be obtained

$$Pe = \frac{e^{-V}}{2^{2M-1}} \sum_{j=1}^{M-1} \frac{V_j}{j!} \sum_{h=1}^{M-1} \binom{2M-2-h}{M+j-1} 2^h \qquad (6.0.4)$$

where the inner summation term addendum must be set equal to zero when $j > M-h-1$ and

$$V = \frac{R_p^2 A_s^2 A_1^2}{2s_\eta^2} \|X\| \qquad (6.0.5)$$

In the following equation (6.0.4) will be applied to evaluate the quantum limit performance of some of the most important DPSK system schemes.

6.1 Single Branch DPSK Heterodyne Receiver

The block scheme of the analyzed receiver is shown in fig. 15. The received optical signal is processed by a polarization controller so to match its polarization with that of the local oscillator and is detected by a single branch optical front end. The intermediate frequency electrical signal is filtered and demodulated by a delay line demodulator. After a further filtering by means of a lowpass wide filter the signal is sample at the center of the bit interval so to obtain the decision variable.

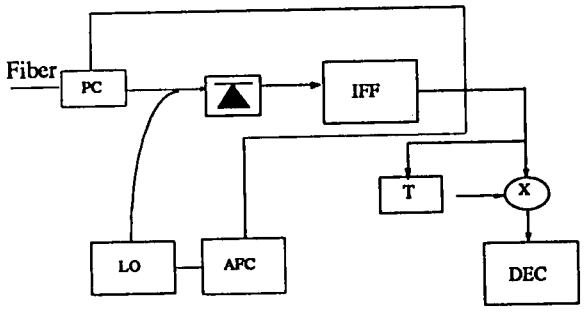

Figure 15: Block scheme of the single branch DPSK heterodyne receiver by using a polarization controller (PC= Polarization Controller, AFC = Automatic Frequency Controller, IFF=intermediate frequency filter)

For this kind of receiver the intermediate frequency current envelope can be written as

$$C(t) = 2R_p A_s A_1 e^{i[\phi_s - \phi_1 + \pi m(t)]} + \eta_d(t) \qquad (6.1.1)$$

so that it is clear that the vector $\underline{X}$ is in this case a scalar equal to 2 and $\sigma_\eta^2 = 4\,q\,R_p\,R\,A_1^2$. Specializing equation (6.0.4) to this case and observing that $n_s = /hv$, where n_s is the average number of detected photons per bit, it is obtained

$$P_e = \frac{1}{2} e^{-n_s} \qquad (6.1.2)$$

From equation (6.1.2) it is evident that the performance of a single branch DPSK heterodyne receiver has almost the same performance of a PSK heterodyne receiver using synchronous electrical demodulation. As a matter of fact the error probability for a heterodyne PSK receiver in the high signal to noise regime can be approximated as $P_e = e^{-n_s}/2\sqrt{\pi n_s}$ so the penalty of the DPSK receiver with respect to the PSK one decreases at the increasing of n_s and, around the error probability of 10^{-9}, is about 0.9 dB. In particular the sensitivity of the considered receiver is $S_n \approx 20$ photons per bit.

6.2 Polarization Diversity DPSK Heterodyne Receiver

The block scheme of the analyzed receiver is shown in fig. 16. The received optical signal is processed by a polarization diversity optical front end and detected by two identical photodiodes. The intermediate frequency electrical signals are filtered and demodulated by identical delay line demodulators. The resulting signals are added and, after a further filtering by means of a lowpass wideband filter, the signal is sample at the center of the bit interval so to obtain the decision variable.

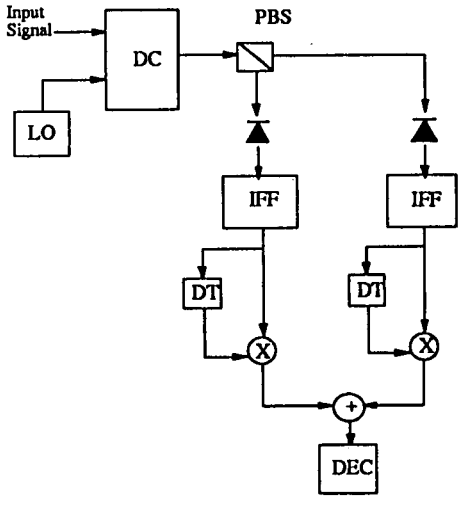

Figure 16: Block scheme of a polarization diversity DPSK heterodyne (DC=Directional coupler, LO=Local oscillator, PBS=Polarization beam splitter, IFF=Intermediate frequency filter, DT=delay line of the T bit time)

Since in the polarization diversity front end the local oscillator is linearly polarized at $\pi/4$ with respect to the receiver axes $\varphi_1 = \pi/4$ and $\zeta_1 = 0$. The complex envelopes of the electrical currents after the intermediate frequency filters can be written as

$$C_1(t) = \sqrt{2} R_p A_s A_1 \cos\psi_s e^{-i[\phi_s - \phi_1 + \pi m(t)]} + \eta_{d1}(t)$$
$$C_2(t) = \sqrt{2} R_p A_s A_1 \sin\psi_s e^{-i[\phi_s - \phi_1 + \zeta_s + \pi m(t)]} + \eta_{d2}(t) \qquad (6.2.1)$$

Comparing equation (6.2.1) with equation (6.0.2) it is obtained

$$X = \begin{bmatrix} \sqrt{2}\cos\phi_s \\ \sqrt{2}\sin\phi_s e^{-\zeta_s} \end{bmatrix} \qquad (6.2.2)$$

and $\sigma_\eta^2 = 2\,q\,R_p\,R\,A_1^2$. Specializing equation (6.0.4) to this case it is obtained

$$P_e = \frac{4+n_s}{8} e^{-n_s} \qquad (6.2.3)$$

It follows that the quantum limit performance of a polarization diversity heterodyne DPSK receiver is independent from the polarization of the received field also if no polarization tracking is adopted. However this property is obtained by doubling all the receiver components but the decision device. The sensitivity at an error probability of 10^{-9} is S_n=22 photons per bit with a penalty of about 0.4 dB with respect to the heterodyne single branch receiver. The cause of this penalty can be understood clearly in the case in which the received field is linearly polarized along a receiver reference axis. In this case one branch of the receiver works exactly as a single branch receiver and the other processes only the detection noise. When the delay line demodulation is performed on this second branch, the noise-noise beating is produced whose power is by far lower than the noise contribution on the signal branch that is mainly due to the signal-noise beating. When the demodulated signals are added a small noise contribution due to the second branch is added to the current at the output of the first branch, that works as a single branch, receiver so that a small penalty is to be expected.

7. COHERENT SYSTEMS USING ASK MODULATION

An alternative to the use of phase modulation is constituted by binary amplitude modulation (ASK), in which the information is linearly encoded in the amplitude of the transmitted field. This modulation format does not require the estimation of the phase of the received field at the receiver allowing asynchronous electrical demodulation that is simpler to implement with respect to synchronous demodulation and less sensitive to the most important degradation causes that are present in coherent systems.

The ASK transmitter is conceptually very simple. As a matter of fact semiconductor lasers can be directly modulated by modulating the driving currents. However the phenomenon of chirping limits the direct modulation speed so that in high bit rate systems an external modulator can be required as for phase modulated systems.

In order to analyze the quantum limit performance of ASK coherent optical systems a general model can be used allowing a unified analysis of all the interesting receiver structures. The general block scheme of an ASK receiver is shown in fig. 17

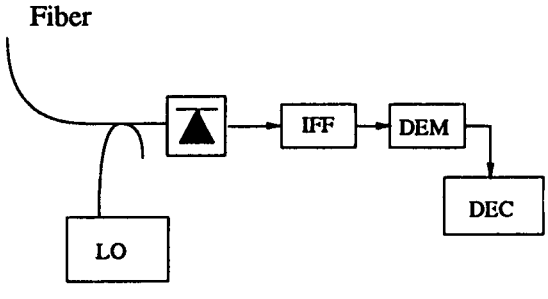

Figure 17: General block scheme of an ASK receiver

The received signal $E^s(t)$ and the local oscillator $E^l(t)$, that can be written as

$$E^s(t) = A_s\, m(t)\{\cos\psi_s x + \sin\psi_s e^{i\zeta_s} y\}\, e^{\,i[\omega_s t + \phi_s]}$$
$$E^l(t) = A_l\, \{\cos\psi_l x + \sin\psi_l e^{i\zeta_l} y\}\, e^{\,i[\omega_l t + \phi_l]} \qquad (7.0.1)$$

are mixed by means of an optical front end. The structure of the front end and of the electrical part of the receiver are similar that of a DPSK receiver but for the fact that the delay line demodulator is substituted by a square law demodulator, that is an ideal electronic device whose output is the square power of the input.

It is to be noted that synchronous demodulation can be also used in single branch and polarization diversity ASK receivers instead of the described asynchronous demodulation. However it can be demonstrated that synchronous demodulated PSK systems have better quantum limit performances with respect to the analogous ASK systems that on the other hand are equally complex to realize and sensitive to a large class of phase affecting degradation phenomena. In this situation if synchronous electrical demodulation is to be adopted PSK modulation is by far preferable and the main attractive feature of ASK systems is the easiness to realize structure of asynchronous receivers that result in feasible and reliable systems.

Another alternative to square law demodulation for single branch and polarization diversity receivers is the envelope demodulation that is realized when the square law demodulator is substituted by a device that present at its output the absolute value of the envelope of its input. If envelope detection is adopted the performance of single branch and polarization diversity ASK systems are practically the same obtained using square law demodulation, however phase diversity receivers cannot be realized.

Under hypothesis similar to that adopted for DPSK systems the electrical currents can be arranged in a vector $\underline{C}(t)$ that can be expressed as follows

$$\underline{C}(t) = R_p A_s A_l \underline{X}\, m(t)\, e^{\,i[\phi_s - \phi_l]} + \underline{n}_D(t) \qquad (7.0.2)$$

where in the homodyne case only the real part of $\underline{C}(t)$ is to be considered. The structure of the front end is completely contained in the complex M-dimensional vector $\underline{X}$ while the vector $\underline{n}_D(t)$ represents the detection noise vector. The elements of $\underline{n}_D(t)$ can be assumed to be zero mean statistically independent complex Gaussian processes whose quadratures have all the same variance σ_η^2 that is determined by the particular system structure.

The decision variable is given by $C_d(j) = \|\underline{C}(t_j)\|$ that can be written as a Hermitian quadratic form of the components of the vector $\underline{C}(t_j)$.

The decision device estimate the transmitted bit by comparing the decision variable with a decision threshold C_{th} and deciding for a transmitted one if $C_d(j) > C_{th}$ and for a transmitted zero otherwise. This leads to the following expression of the error probability

$$P_e = \frac{1}{2} \Pr\{C_d(j) > C_{th} / m(t_j)=0\} + \frac{1}{2} \Pr\{C_d(j) < C_{th} / m(t_j) = 1\} \qquad (7.0.3)$$

where the decision threshold must be optimized in order to obtain the minimum error probability.
Equation (7.0.3) can be computed in the case $m(t_j)=0$; the expression becomes simple can be solved exactly obtaining

$$Pr\{C_d(j)>C_{th}/m(t_j)=0\} = e^{-C_{th}} \sum_{j=0}^{M-1} \frac{C_{th}^j}{j!} \qquad (7.0.4)$$

In the case $m(t_j)=1$ in general the equation cannot be evaluated exactly, although an exact solution can be obtained in some particular case. A general expression for the conditional error probability when a binary one is transmitted can be obtained by applying the saddlepoint approximation.

7.1 Single Branch ASK Heterodyne Receiver

As usual this is the simplest system scheme and first that is to analyze. The intermediate frequency current envelope can be written as

$$C(t) = 2R_p A_s A_l m(t) e^{i[\phi_s - \phi_l]} + \eta_d(t) \qquad (7.1.1)$$

so that the vector $\underline{X}$ is in this case a scalar equal to 2 and $\sigma_\eta^2 = 4 q R_p R A_l^2$. In this case equation 7.0.3 can be solved exactly for both $m(t_j)=0$ and $m(t_j)=1$ so that the following exact expression of the error probability can be derived

$$Pe = \frac{1}{2}[1 - Q(\sqrt{2n_s}, \sqrt{n_{th}})] + \frac{1}{2} e^{-nth/2} \qquad (7.1.2)$$

where n_s is the average number of detected photons conditioned at the transmission of a binary one, that is the peak energy, and n_{th} represents the decision threshold in equivalent photons per bit.

In order to evaluate the quantum limit system performances an optimum threshold should be evaluated. It can be shown that such a value depends on n_s and in particular for $n_s \gg 1$ the optimum threshold tends to $n_s/4$. Once the optimum threshold is evaluated the bit error probability can be computed using expression (7.1.2). However, since the error probability values relevant for optical coherent systems are quite low, an asymptotic approximation of equation (7.1.2) that allows an immediate evaluation of the error probability without the need of numerically evaluate the Marcuum function can be useful. Using the asymptotic expression of the optimum threshold and the asymptotic expansion of the complementary error function the following equation is obtained

$$P_e \approx \frac{1}{2} e^{-n_s/4} \left(1 + \frac{2}{\sqrt{\pi n_s}}\right) \approx \frac{1}{2} e^{-n_s/4} \qquad (7.1.3)$$

From equation (7.1.3) it can be seen that, if the optimum threshold is used, errors occurs predominantly because of noise alone exceeding the threshold rather than signal plus noise failing to do so. Using equation (7.1.3) it is possible to find the quantum limit sensitivity for an error probability of 10^{-9}, which is eual to 80 photons per bit. The same quantum limit evaluated starting from the exact equation results to be about 78 photons per bit, so confirming the accuracy of equation (7.1.3) for high signal to noise ratios.

From the obtained results it can be concluded that the heterodyne ASK single branch receiver suffers of a penalty of about 6 dB with respect to the analogous receiver for phase modulated signals. This penalty can be justified by making two different considerations. Firstly if phase modulation is adopted all the signal power is used to carry information while in the case of ASK modulation only half the average signal power result to be effectively modulated, as demonstrated by the presence of a carrier residue in the transmitted signal spectrum. This phenomenon can be expected to induce a 3 dB penalty. Moreover the significant parameter for the design of the system is not the average signal power but the peak signal power since lasers are characterized by a limitation affecting the maximum instantaneous optical power that can be emitted. Since equiprobable bits are assumed the average power is half the peak power so that another 3 dB penalty is induced for a whole penalty of 6 dB with respect to phase modulated systems.

7.2 Polarization Diversity ASK Heterodyne Receiver

Since in the polarization diversity front end the local oscillator is linearly polarized at $\pi/4$ with respect to the receiver axes $\varphi_l=\pi/4$ and $\zeta_l=0$. The complex envelopes of the electrical currents after the intermediate frequency filters can be written as

$$C_1(t) = \sqrt{2} R_p A_s A_l m(t) \cos\psi_s e^{-i[\phi_s - \phi_l]} + \eta_{d1}(t)$$
$$C_2(t) = \sqrt{2} R_p A_s A_l m(t) \sin\psi_s e^{-i[\phi_s - \phi_l]} + \eta_{d2}(t) \qquad (7.2.1)$$

Comparing equation (7.2.1) with equation (6.2) it is obtained

$$\underline{X} = \begin{bmatrix} \sqrt{2}\cos\psi_s \\ \sqrt{2}\sin\psi_s e^{-\zeta_s} \end{bmatrix} \qquad (7.2.2)$$

and $\sigma_\eta^2 = 2 q R_p R A_l^2$, results that are analogous to that obtained for a DPSK system using a similar receiver. In this case the error probability must be calculated using approssimations by means of equations (7.0.3) and (7.0.4) with M=2 and the expression of the vector $\underline{X}$ given in equation (6.2.2). Since the norm of $\underline{X}$ does not depend on the polarization of the received field the polarization diversity ASK receiver results to be independent of the received state of polarization whichever threshold value is selected.

The optimum threshold value can be evaluated by minimizing the total error probability that yields to a transcendental equation to be solved, however it can be demonstrated that in the high signal to noise ratio the optimum thresholds tends to the same value obtained in the case of single branch receiver. Assuming this value of threshold the quantum limit sensitivity for an error probability of 10^{-9} is S_n=81 photons per bit, with a

sensitivity penalty of 0.2 dB with respect to the heterodyne single branch receiver.

7.3 Phase Diversity ASK Homodyne Receiver

The baseband currents after detection and filtering are given by the following expression

$$C_1(t) = R_p A_s A_l m(t) \cos(\phi_s - \phi_l) + \eta_{d1}(t)$$
$$C_2(t) = R_p A_s A_l m(t) \sin(\phi_s - \phi_l) + \eta_{d2}(t) \qquad (7.3.1)$$

and $\sigma_\eta^2 = q\, R_p\, R\, A_l^2$. As in the case of the analogous DPSK receiver the mathematical model of this receiver turns to be equal to that of the single branch heterodyne receiver also for ASK modulation. The consequence is that all the results obtained for the single branch heterodyne receiver holds also for the homodyne phase diversity receiver.

8. COHERENT SYSTEM USING FSK MODULATION

Frequency shift keying (FSK) systems, convey information by switching the frequency of the transmitting laser between two different values. The receiver, on the other end, has to decide whether

$$A_s \cos(\omega_1 t + \theta)$$
or $$(8.0.1)$$
$$A_s \cos(\omega_2 t + \theta)$$

was transmitted.
We will not insist on FSK detection theory since the BER equation in this case are identical to those for ASK heterodyne detection, yielding a sensitivity of 36 photons/bit.

This result is easily understood if one thinks that an FSK transmitter can be viewed as two complementary ASK binary transmitters operating on different frequencies, the former transmitting binary ones, the latter zeroes. There is an advantage for FSK systems that is not evident from BER equations: these depend only on the average power reaching the receiver not taking into account the average power coupled to the fiber by the transmitter. This power, if a peak-power limited laser is used, as it is normally done, in the case of ASK is only one half of FSK since, statistically, the source is emitting no power for half the number of bits: that means the link attenuation can be 3 dB higher.

An important parameter, in FSK systems, is the modulation index which is defined as the frequency shift normalized to the bit rate

$$m = \frac{|\omega_1 - \omega_2|}{2\pi R} \qquad (8.0.2)$$

The modulation is commonly defined wide deviation FSK whenever m>2, otherwise it is referred to as narrow deviation FSK., in which the single filter receiver is implemented.
The received signal can be processed by a synchronous demodulator, which compare the signal with two reference carriers: in this case a theoretical sensitivity of 36 photons/bit can be obtained and the minimum modulation index which provides orthogonal signal at the decision point is m=0.5 (Minimum Shift Keying).
Since synchronous detection is very difficult to implement in practice, due to the receiver complexity, asynchronous detection is normally used for FSK receivers; the minimum modulation index in this case is m = 1. The theoretical value for receiver sensitivity decreased to 40 photons/bit.

The receiver, which is reported in fig. 18, can be thought as two complementary ASK channels operating at different frequencies, being the separation of the channels accomplished by means of IF filters (dual filter receiver).

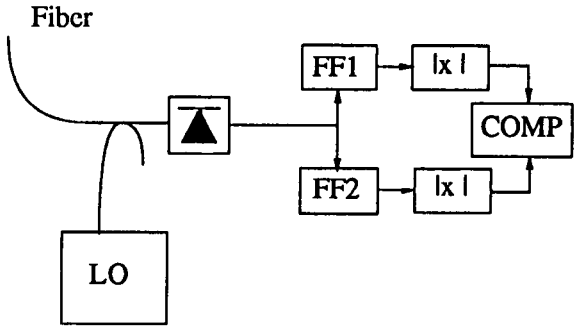

Figure 18 - Block diagram of a large-deviation FSK receiver (LO=local oscillator, FF1,FF2=intermediate frequency filters, |x|=envelope demodulator, COMP=comparator)

Actually, dual filtering is not necessary and just one channel could be implemented trading-off a sensitivity penalty of 3 dB: Nevertheless, since the full gain for dual filtering is very difficult to obtain and, moreover, the required bandwidth for the electrical front-end is far greater, the less complex single filter receiver is often used.
It is to be noted that narrow deviation FSK signals exhibit the narrowest spectrum among binary transmission systems so that it is quite attractive for multichannel frequency division application where total occupied bandwidth is of primary concern.

9. COHERENT TECHNIQUES IN OPTICAL NETWORKS

Coherent optical detection techniques applied to networks implementation can open new directions in networking architectures since they allow FDM of a large number of densely spaced channels so to exploit effectively the nearly 30 THz of bandwidth inherent in conventional single-mode fibres [6], [7]. One of the main advantages of such technique is represented by the ability of each receiver to select one of the FDM channels carried by the fibre by simply tuning its own local oscillator.The best performance can be obtained by combining optical coherent communication techniques with star topology since a star coupler provides nearly ideal means for interconnecting the terminals in a frequency multiplexed network.

In a NxN star network interconnecting N terminals the power P_r required at each receiver is such that

$$P_r \geq FhvR \qquad (9.0.1)$$

being F the receiver sensitivity in terms of photons per bit, h the Planck's constant, v the light frequency and R the bit-rate. Taking into account the star coupler loss and assuming negligible the excess loss the transmitted power P_t

necessary at each terminal is

$$P_t \geq FhvRN \qquad (9.0.2)$$

Assuming that the total throughput NR is limited by the fibre bandwidth B=20 Thz and taking F=100 ph/bit a transmitter power P_t =1 mW is required to realize, in principle, an FDM network with a large number of terminals.

The channel spacing depends upon a lot of factors to be analyzed in network design: bit-rate, intermediate frequency choice, laser linewidth, modulation format, line coding, receiver structure and, for wide deviation FSK systems, frequency deviation. In FDM systems problems have to be faced and solved due to interference among channels: intermodulation and crosstalk.

Intermodulation is due to the quadratic response of the photodiode which generates besides the useful beat signal undesired channel-to-channel and channel-to-LO beat signals whose spectral tails enter the IF filter so to affect signal processing. The influence of intermodulation on multichannel system performance increases with the number of channels and depends on the modulation format. For 100 channels spaced of 5R the induced penalty varies from 1 dB for MSK, characterized by a spectrum more compact than that of the other modulation formats, to about 4 dB for ASK in which the baseband intermodulation components can sensibly contribute to affect the performance. If the penalty induced by intermodulation is too high, a π balanced detection scheme can be adopted at the receiver since it is able to suppress both the intensity noise and the intermodulation terms due to channel-to-channel beating.

Channel crosstalk is due to the extension on the frequency axis of the spectrum tails of the different channels so that the relevant effect is due to the channels adjacent to that to be selected. In a FDM system when a channel is selected the spectrum tails of the other channels can enter the selection filter thus disturbing the signal processing. Theoretically, in the absence of phase-noise, a channel spacing of 2.05R has been evaluated in CPFSK to obtain a 1 dB penalty. The value increases to 2.2R in correspondence to a beat linewidth B_L equal to $2.5\ 10^{-3}R$. About weakly coherent systems (wide deviation FSK, envelope detection ASK), theoretical evaluations have revelead that, as the laser linewidth increases from zero to 0.5R the channel spacing increases from 10R to 32R for ASK and from 12R to 52R for FSK to keep the penalty within 1 dB. Experimental coherent multichannel systems have been demonstrated operating with a channel spacing ranging from 6.6R to 58R [8].

The main problems which have so far limited the realization of coherent optical networks to a few laboratory experiments are represented by the laser phase-noise, the fluctuations of the state of polarization of the optical field at the output of conventional single-mode fibres and, in lesser amount, the laser intensity noise.
Feasibility and reliability of the coherent optical systems are strongly conditioned by laser phase-noise which represents one of the main factors affecting their performance [9], [10], [11]. Moreover it affects the channel spacing in multichannel systems to an extent that is only beginning to be analyzed theoretically [12], [13].

From the point of view of the type of measurement that is made on the received optical field in order to detect the information and consequently of the laser linewidth requirements, three categories of coherent optical systems can be recognized.

The first category is represented by highly coherent systems where the phase of the received field is compared with that of the local oscillator which must be phase-locked to the received signal phase. These systems are the most demanding on laser linewidth being the requirement dictated by the ability of the optical phase-locked-loop to cope with the phase-noise. The linewidth requirement varies from $0.01\text{-}0.05 \cdot 10^{-2}R$ for optical phase-locked-loop to about $0.1\text{-}0.5 \cdot 10^{-2}R$ for synchronous heterodyne PSK .

The second category is constituted by moderately coherent systems in which a differential phase measurement is made on two successive symbols of the signal field. Examples are DPSK and ND-FSK with delay-line discriminator demodulation. The linewidth requirements in these systems are less demanding than in highly coherent systems since the important quantity is the phase-drift over the delay time of the demodulator. Linewidths of $0.3\text{-}0.6 \cdot 10^{-2}R$ are needed and an error rate floor is exhibited for which the only countermeasure is the reduction of the laser linewidth or increasing the bit-rate [11], [14], [15]. In order to carry out differentially coherent systems technical solutions have been proposed to reduce laser linewidth. Semiconductor lasers with external cavities can nowadays provide linewidths in the range from about 1 KHz to several hundreds of KHz however such techniques seem still critical and expensive as engineered solutions that may be used in operational coherent optical networks.

The third category is represented by weakly coherent systems in which the receiver measures the signal power within the bandwidth of the IF filter. Heterodyne detection of ASK and FSK signals with envelope or square-law demodulation are examples. Since the receivers of these systems do not measure the field phase, they are very tolerant to phase-noise. In principle there is no hard limit on the linewidth requirement because it is possible to increase the IF bandwidth to accommodate broad laser linewidths increasing obviously the penalty with respect to the quantum limit. Anyway it has been estimated that a negligible degradation from shot-noise limited sensitivity occurs for linewidths less than 0.1-0.15R and that a penalty within 2 or 3 dB from the shot-noise limit occurs for a linewidth of about 0.5R.

Besides phase-noise the influence of intensity noise of the laser sources on system performance is to be taken into account in designing coherent optical networks. Anyway this problem is not so pressing with the semiconductor lasers nowadays commercially available. Its effect on the receiver sensitivity can be minimized by means of a suitable choice of the local oscillator emitted power. Furthermore, if this were not sufficient the induced penalty can be made in practice negligible by adopting at the receiver end a π balanced detection scheme.

Another important problem which has so far restrained the implementation of the coherent systems in operational optical networks is represented by the fluctuations of the state of polarization of the optical field propagating through a conventional single-mode fibre because of the birefringence of the fibre itself. This phenomenon is due to coupling effects between the two orthogonal states in

which a generic field propagating in a fibre can be decomposed. Such effects arise from mechanisms of both geometrical and physical nature like bending, imperfect circularity of the fibre or dishomogeneities and anisotropies of the dielectrics with which the fibre is made so that even if a perfectly linear polarized optical field is coupled to the fibre within few centimeters its state of polarization will result completely aleatory. Since such coupling mechanisms are dependent on temperature and other environmental conditions, the propagating field polarization undergoes to fluctuations on time scales from several seconds to a few minutes. In order to avoid performance degradation induced by polarization fluctuations perfect polarization matching between the received optical field and the local oscillator must be maintained. Several solutions have been proposed to avoid or control such effect of receiver performance degradation [16]. First of all the use of polarization maintaining fibres allowing the polarization of the output optical field to be kept constant; however their use will be likely limited to a few special applications because of their high attenuation (≈ 2 dB/km against 0.2 dB/km of the conventional single-mode fibres) and cost.

Another approach is based on the use at the receiver end of optical polarization feedback electro-mechanical controllers acting either directly on the fibre (e.g. fibre squeezers) or on the output field (e.g. Faraday rotators, electro-optical crystals) to adjust its polarization in order to match to that of the local oscillator. All these techniques suffer, in different amount, from several problems which make them little reliable in operational systems: insertion loss, endlessness in control, poor temporal response and fatigue in mechanical schemes.

At present the most available techniques to face polarization fluctuations are respectively the polarization diversity detection scheme and the polarization modulation systems.
In a polarization diversity detection scheme, shown in fig. 6 which can be implemented in conventional optical coherent receivers, the polarization components of the received field are separately detected.

The corresponding electrical signals are at first demodulated and then summed before carrying out decision. This receiver scheme, which has been successfully applied in DPSK, FSK and ASK systems, is completely independent of the polarization fluctuations regardless of their evolution rate so that it is suitable not only in point-to-point links, in which fluctuations are very slow, but also in optical networks where fast polarization variations occur when switching among the different subscribers. This is achieved at the expense of a limited penalty with respect to the conventional receiver performance (≈0.5 dB of penalty in the absence of phase-noise) and a doubling of the eletronic processing circuitry.

The polarization modulated systems exploit the property of conventional single-mode optical fibres to preserve at the output orthogonality between input states of polarization. While conventional POLSK systems require an optical polarization control to face polarization fluctuations, a system, called Antipodal Stokes Parameters Shift Keying, ASPSK [17], has been developed which is particularly advantageous since it requires only a feedforward electronic control circuit to achieve insensitiveness to the slow fluctuations due to fibre birefringence. Moreover for network applications a polarization modulation receiver scheme, derived from ASPSK and denominated differential Stokes parameter shift keying (DSPSK), has been proposed in which a differential decision criterion allows complete insensitiveness to polarization fluctuations, whatever the fluctuations rate, at the expense of a 3 dB penalty with respect to ASPSK.

10. EXPERIMENTS

In Table I some of the main coherent optical transmission experiments at intermediate bit-rates are summarized. In one case (*) homodyne detection technique has been carried out using an optical PLL. The length of the point-to-point links achieved without repeaters (290 km at 400 Mb/s and 260 km at 565 Mb/s) show clearly the potentialities of the coherent optical systems in long haul transmissions. The sensitivity values are 5-10 dB far from the quantum limit due mainly to laser phase-noise and imperfections in optical detection and signal electronics processing.

The DPSK system (**) by BRTL is the first field experiment realized using an optical cable 56.3 km long installed between Cambridge and Bedford. More fibres have been connected to obtain a 176 km link and the performed and the performed tests have pointed out a high reliability of the system. The system (***) by KDD has been instead put on a sea trial: a submarine cable 45 km long at a depth of about 6000 m was used to obtain a 90 km transmission line.

In Table II some high bit-rates coherent optical transmission systems are shown. In this case a certain amount of penalty is determined by thermal noise of the receiver whose effect, increasing with the bit-rate, can be no more neglected.

So far the most important experiment of a coherent optical network has been carried out at AT&T by B.S. Glance and his group [18]. The network is constituted of three channels at 1.28 μm, 45 Mb/s narrow-deviation FSK modulated (m=1) and spaced by 300 MHz. The sensitivity is of -61 dBm (113 ph/bit) which is 4.5 dB far from the shot-noise limit. Such result indicates for the proposed system a potential throughput of about 4500 Gb/s. The block scheme of the system is shown in fig. 19.
A 4x4 optical star coupler combines the channels and the beating signal between the channel comb and the LO is detected by means of a π balanced receiver. Demodulation is then performed by a delay-line frequency discriminator. The channel selection is obtained by tuning the LO frequency in such a way to center the wanted channel within the bandwidth of the IF filter which is 100 MHz wide and centered at 225 MHz. The resulting IF is maintained by an automatic frequency control (AFC) circuit controlling the optical frequency of the LO. Frequency stability of the optical signals, which is an essential feature in a densely spaced FDM network, has been obtained by frequency locking each transmitting laser to one of the resonances of a fibre Fabry-Perot resonator. A piece of single-mode fibre 20 cm long with both ends coated with a partially transmitting thin film mirror acts as a Fabry-Perot providing a comb of resonances equally spaced by about 500 MHz with a 3 dB bandwidth of about 50 MHz. As an optical source drifts from the peak of a Fabry-Perot resonance the photodiode detects a baseband signal with the same pattern as the FSK bit-stream modulating the optical source and whose polarity, relatively to the modulating bit-stream, depends on which side of the resonance the frequency drift has occurred. Thus, an error

Modulation Format	Lab.	R Mb/s	λ μm	TX	LO	B_L MHz	S ph/bit (dBm)	L km
ASK-Hom*	BRTL	140	1.523	HeNE⊕ InGaAsP	HeNe	—	—	—
ASK	AT&T	400	1.500	DFB	DFB	—	960 (-43)	—
FSK_WD	NEC	140	1.550	DFB	DFB	17	350 (-52)	243
FSK_WD	Bellcore	560	1.550	DFB	DFB	50	3500 (-36)	
FSK_WD	Fujitsu	600	1.550	DFB	DFB	40	1600 (-39)	140
DPSK	AT&T	400	1.530	ECL	ECL	0.01	45 (-56)	260
DPSK**	BRTL	565	1.534	ECL	ECL	0.01	232 (-47.6)	260
FSK_ND	BRTL	140	1.540	ECL	ECL	0.01	175 (-55)	200
FSK_ND	NTT	400	1.550	ECL	ECL	0.5	195 (-50)	290
FSK_ND	AT&T	400	1.500	DBR	ECL	—	192 (-50)	80
FSK_ND***	KDD	560	1560	ECL	ECL	0.5	888 (-42)	150 90

Table I: Main parameters of some of the most important coherent optical transmission experiments performed at intermediate bit-rates. The symbol R stands for bit-rate, I light wavelenght, TX transmitting laser, LO local oscillator, B_L beat linewidth, S receiver sensitivity and L trunk lenght. FSK_WD and FSK_ND stand for respectively wide-deviation and narrow-deviation FSK and ECL for external cavity laser.

Modulation Format	Lab.	R Gb/s	λ μm	TX	LO	B_L MHz	S ph/bit (dBm)	L km
DPSK	AT&T	1	1.530	ECL	ECL	0.01	230 (-45.2)	200
DPSK	NEC	1.2	1.540	ECL	ECL	1.8	200 (-45)	170
DPSK	Fujitsu	1.2	1.540	ECL	ECL	—	290 (-43.5)	190
DPSK	AT&T	2	1.530	ECL	ECL	0.02	480 (-39)	170
FSK_ND	Bellcore	1	1.500	DFB	ECL	8	1500 (-37)	100
FSK_ND	NTT	2	1.550	ECL	ECL	1	1260 (-35)	197
FSK_ND	NTT	2	1.550	DFB	DFB	12	535 (-38.6)	202
FSK_ND	NTT	4	1.550	DFB	DFB	---	1445 (-31.3)	155
FSK_ND	NTT	2.5	1540	DFB	DFB	8	100 (-44.9)	290
FSK_ND	NTT	8	1550	DFB	DFB	15	693 (-31.5)	202

Table II: Main parameters of some of the most important coherent optical transmission experiments performed at high bit-rates. The adopted symbols are the same of Table I.

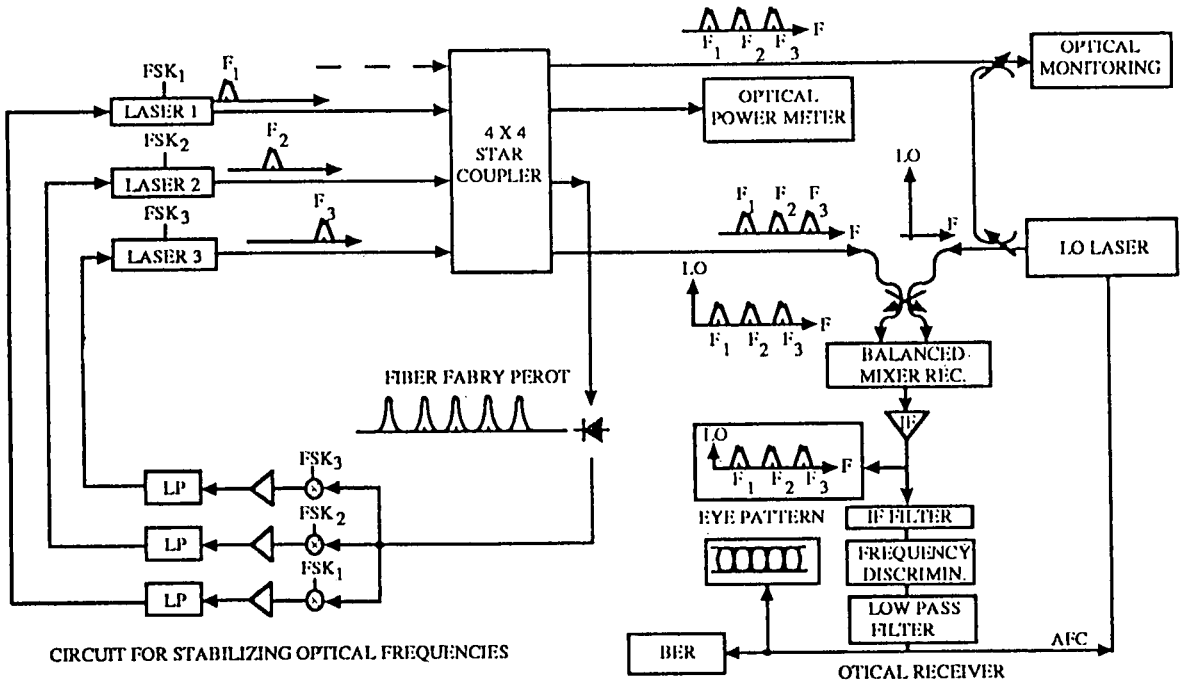

Figure 19: Schematic block diagram of an FDM system with frequency stabilization of optical signals originating from the same location

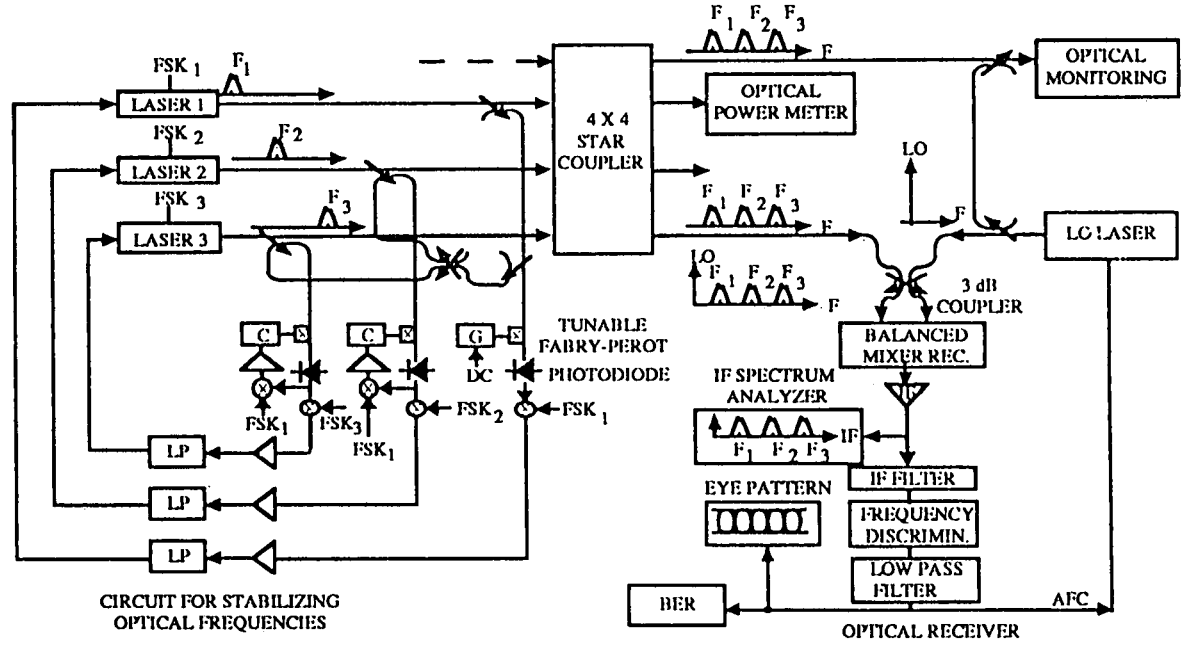

Figure 20:Variant of Figure 19 block diagram, in which one of the optical transmitted signal is used to synchronize the Fabry-Perot resonators of the other optical channels.

signal can be simply obtained by multiplying the FSK modulating bit-stream by the detected signal and filtering the resulting amplified product by a low-pass filter. The error signal is then used to lock the transmitting laser frequency to the selected Fabry-Perot resonance. The use of this simple scheme is nevertheless limited to a network where the optical sources are at the same location.

An approach allowing this problem to be solved is based on the use of a central Fabry-Perot acting as a master for the whole system. The variant introduced in the scheme is shown in fig. 20.

Each laser is frequency locked to a separate tunable fibre Fabry-Perot. The set of resonances is made the same for all the transmitting lasers by synchronizing the Fabry-Perot resonators. This is obtained by feeding two optical signals to the Fabry-Perot: one is supplied by the transmitting laser, the other originates from a central optical source frequency-stabilized by its own Fabry-Perot. This reference signal is frequency modulated by a known frequency tone supplied to each station. Therefore two error signals are detected by each local Fabry-Perot of which one is used to frequency lock the laser, the other is utilized to frequency lock the local Fabry-Perot to the master.

A coherent optical FDM experimental broadcasting system has been developed at NEC for CATV distribution service [19]. The schematic diagram of the system is shown in fig. 21.

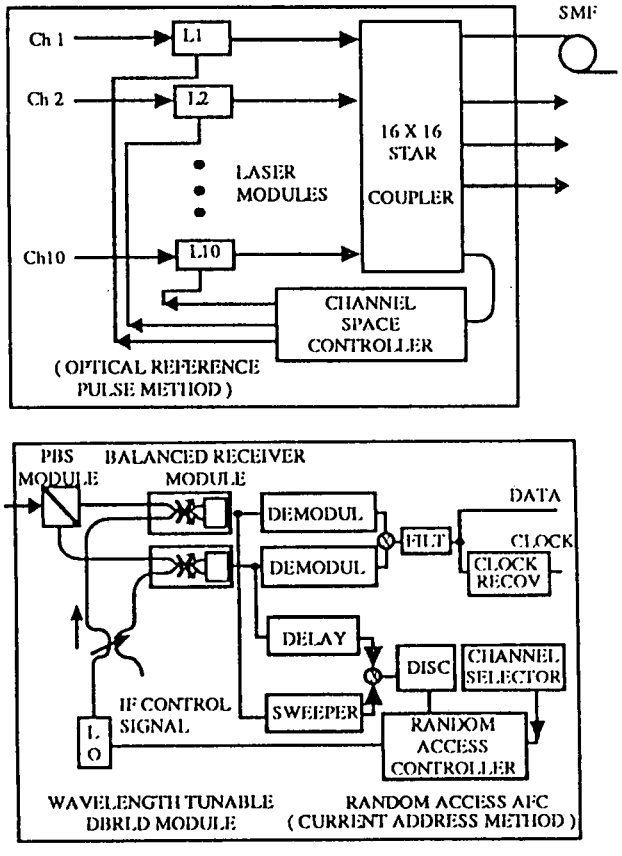

Figure 21: Schematic block diagram of 10-channel coherent optical FDM CATV exsperimental equipment.

At the transmitter ten 1.54 μm tunable DBR lasers are wide-deviation FSK modulated (m=3) at 400 Mb/s. The channel spacing has been stabilized to 8 GHz by a control technique denominated "reference pulse method". As shown in fig. 22 it is based on a tunable DBR laser acting as sweep laser whose frequency is swept over a range of about 100 GHz.

A Fabry-Perot resonator with an 8 GHz free-spectral-range and finesse of 20 is used as channel spacing standard. The resonance frequency is stabilized within 100 MHz by means of temperature control.

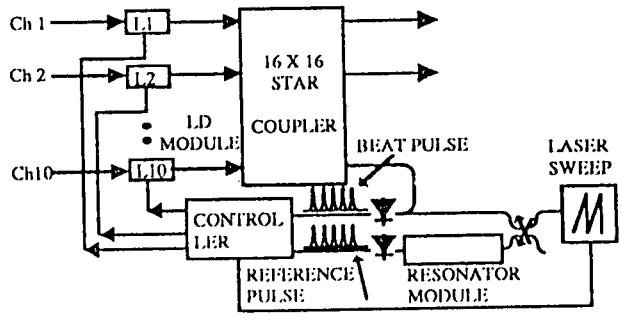

Figure 22: Block diagram of channel space locking system, based on reference pulse method.

Transmitter frequencies are controlled in such a way that the generation times of the bit pulses between the transmitter optical signal and the sweep laser signal coincide with the time of the reference pulses generated by the sweep laser signal through the Fabry-Perot. With this scheme every transmitter frequency refers to the Fabry-Perot resonance frequency with 8 GHz free-spectral-range. A polarization diversity receiver realizes single-filter FSK demodulation and random access automatic frequency control according to the "current address methods". The random access AFC consists of an IF discriminator, a sweeper, a channel selector and a random access controller. In the initialization procedure the controller scans the local oscillator frequency over the entire tuning range (about 100 GHz) and memorizes local lasers control current value when the beat pulse is detected at the square law-pass filter in the IF discriminator. Each memorized value corresponds to the current address of a channel. When a channel call is sent to the channel selector the controller can directly access the memorized address current corresponding to the called channel. Then the sweeper scans the local frequency over the 1 GHz range, searching for and locking the called channel IF into the capture range of the IF discriminator. A 114 GHz capture range, an 80 GHz lock range and a random channel selection time less 1 ms have been obtained while the receiver sensitivity was -45 dBm at 400 Mb/s for all ten channels. The system has been estimated to be able to distribute about 80 high definition TV channels to 2000 subscribers by 500 GHz frequency tunable DBR laser diodes.

REFERENCES

[1] A review of some of the principal studies on advanced fiber optic networks can be found in the monographic number: AT&T Technical Journal, vol. 66, n° 6, 1987.

[2] O. E. DeLange,"Wide-band Optical Communications Systems: Part II Frequency-Division Multiplexing", Proceedings of the IRE, vol.58, N°10, 1970, pp.1683-1690.

[3] T. Okoshi, K. Kikuchi, *Coherent Optical Fiber Communications*, KTK Scientific Publishers/Tokyo, Kluwer Academic Publishers, Dordrecht, 1988.

[4] Davis A.W., Pettitt M.J., King J.P., Wright S., "Phase Diversity Techniques for Coherent Optical Receivers", IEEE-J. of Lightwave Tech., vol. LT-5, n° 4, pp. 561-572, 1987

[5] G.L.Abbas, V.W.S. Chan, T.K.Yee "A Dual-Detector Optical Heterodyne Receiver for Local Oscillator Noise Suppression" IEEE-J. of Lightwave Tech., vol. LT-4, pp. 1110-1122, 1986

[6] N.A. Olsson, J. Hegarty, R.A. Logan, L.F. Johnson, K.L. Walker, L.G. Cohen, B.L. Kasper, J.C.Campbell, "68.3 km transmission with 1.37 Tbit·km/s capacity using wavelength division multiplexing of ten single-frequency lasers at 1.5 μm", Elect.Lett., vol.21, 1985, pp.105-106.

[7] R.A. Linke, A.H. Gnauck, "High-Capacity Coherent Lightwave Systems", IEEE J. Lightwave Tech., vol.6, N°11, Nov.1988, pp.1750-1769.

[8] L.G. Kazovsky, "Channel Spacing in Coherent Optical Transmission Systems", Proc. Fourth Tirrenia International Workshop Digital Comm., Tirrenia (Italy), September 19-23, 1989.

[9] I. Garrett, G. Jacobsen, "The Effect of Laser Linewidth on Coherent Optical Receivers with Nonsynchronous Demodulation" IEEE J. Lightwave Tech., vol.5, N°4, April 1987, pp.551-560.

[10] I. Garrett, D.J. Bond, J.B. Waite, D.S.L. Lettis, G. Jacobsen, "Impact of Phase Noise in Weakly Coherent Systems: A New and Accurate Approach", IEEE J. Lightwave Tech., vol.8, N°3, March 1990, pp.329-337.

[11] J. Salz, "Coherent Lightwave Communications", AT&T Tech. J., vol.64, 1985, pp.2153-2209.

[12] D. Zaccarin, D. Angers, T. H. Huynh, "Performance Analysis of Optical Heterodyne PSK Receivers in the Presence of Phase-Noise and Adjacent Channel Interference", IEEE J. Lightwave Tech., vol.8, N°3, March 1990, pp.353-366.

[13] S. Betti, G. De Marchis, E. Iannone, M. Todaro, "Crosstalk in a DPSK FDM System Affected by Laser Phase-Noise", Microwave and Optical Technology Lett., vol.3, N°5, May 1990, pp.141-144.

[14] G. Nicholson, "Probability of error for optical heterodyne DPSK system with quantum phase-noise", Elect.Lett., vol.20, 1984, pp.1005-1007.

[15] L.G. Kazovsky, G. Jacobsen, "Bit error ratio of CPFSK coherent optical receivers", Elect.Lett., vol.24, 1988, pp.69-70.

[16] T. Okoshi, "Polarization-State Control Scheme for Heterodyne or Homodyne Optical Fibre Communications", IEEE J. Lightwave Tech., vol.3, N°6, Dec.1985, pp.1232-1237.

[17] S. Betti, F. Curti, G. De Marchis, E. Iannone, "Phase Noise and Polarization State Insensitive Optical Coherent Systems", IEEE J. Lightwave Tech., vol.8, N°5, May 1990, pp.756-767.

[18] B.S. Glance, J. Stone, K.J. Pollock, P.J. Fitzgerald, C.A. Burrus, B.L. Kasper, L.W. Stulz, "Densely Spaced FDM Coherent Star Network with Optical Signals Confined to Equally Spaced Frequencies", IEEE J. Lightwave Tech., vol.6, N°11, Nov.1988, pp.1770-1781.

[19] S. Yamazaki, M. Shibutani, N. Shimosaka, S. Murata, T. Ono, M. Kitamura, K. Emura, M. Shikada, "A Coherent Optical FDM CATV Distribution System", IEEE J. Lightwave Tech., vol.8, N°3, March 1990, pp.396-405.

HIGH SPEED LOCAL AREA NETWORKS

by

H. Hodara and **E. Miles**
Tetra-Tech Inc.
9645 Scranton Road
Suite 200
San Diego, CA 92121
United States

1. INTRODUCTION

Radical changes are taking place in the computer architecture landscape. The big, centralized machines known as computer mainframes are being replaced by networks of microcomputers distributed over a wide geographical area.

The "brain" of the mainframe, the central processing unit or CPU performs four basic functions: it communicates with humans through dumb terminals, it communicates with machines by means of software and Input/Output (I/O) ports, it manages data files, it executes programs. These functions are time-shared, and controlled by the operating system. Mainframes lack flexibility, and are expensive to operate. Furthermore, the operating system is proprietary and does not lend itself to interfacing with software applications residing on other machines, without major reprogramming. Mainframes belong to the "Old Order".

During the last decade, three technical breakthroughs have contributed to the demise of the old order, and brought significant changes to computer architecture .
Processors are much smaller and capable of carrying out mathematical operations much faster. The old CPU has been reduced to a microprocessor embodied in a chip, the size of a fingernail. Clock rate, a measure of how rapidly the CPU chip performs operations or carry out instructions, has increased from 5 MHz to 50 MHz in a span of ten years.
In addition, storage or memory capacity is also undergoing exponential growth: the same size chip that packed 4 megabits of memory in 1988 is now approaching 64 megabits!
Such increase in speed and memory now demands a communication medium capable of transmitting data at rates exceeding gigabits per second (Gb/s). For instance, the information content of an 8 1/2"x 11" color page is approximately 20ϕ megabits(Mb). To scan or "dump" that information in 1/10 second requires 2 Gb/s data rate. The low loss, low dispersion optical fiber is the third breakthrough that makes high data rate transmission a reality.

2. What's a LAN?

The last decade breakthroughs have allowed small, autonomous microcomputers to attain speed and memory capacity exceeding that of the old mainframes. Microcomputer users can now execute operations quickly and locally. As the demand for access and transmission of information over widespread geographical areas increases, it becomes necessary to share resources, rather than duplicating them at each location. This is particularly true in parallel processing. Such resources include application softwares, data bases, peripheral equipment (printers, displays, etc.), specialized CPUs like file servers or routers. The result is a network of specialized microcomputers, each dedicated to a specific task, capable of accessing data and executing operations at some other distant computer. It is called Client-Server architecture: Users or client computers, such as PC (Personal Computers) and Workstations (more powerful PCs) act as "windows" into and array of computing resources distributed geographically and provided by a network of specialized server computers. The network of distributed clients and servers makes up the " New Order" that is displacing mainframes; the resultant sharing of resources among microcomputers with specialized tasking reduces cost and increases reliability.

This collection of interconnected, autonomous computers within distances of the order of a few kilometers (within a building or a block of buildings) is called a local area network, abbreviated LAN.

3. What's in a LAN?

The LAN consists of computers and peripherals (printers, displays, etc.) known as stations interconnected by means of a communication network. One way to characterize a LAN is in terms of three major elements:

Topology, describes the geometrical configuration of the communication network that interconnects the stations. Some examples are shown in Fig.1. Note from the figure that all networks consist of branches and nodes, regardless of the topology. ' Nodes are the stations access points to the net, and branches are the transmission links that connect them. Why is topology important? Because with N nodes, if one would resort to brute force connections by linking each node to every other node, N(N-1)/2 branches would be needed. For large N, cable cost would increase as the square of the number of nodes. In telephone circuits, some of the nodes are not stations, but only perform a switching function for routing purposes. In some LANs, the switches are eliminated or reduced to one (as we shall see in the case of star topology), and replaced by a set of established rules of communications called protocols; nodes and stations are now coincident, and the connective topology between stations can be simplified. The basic LAN topologies, shown are the star (Fig.1A), the ring (Fig.1B) and the bus (Fig.1c); and a generalization of the bus called tree (Fig.1D). They are discussed further on.

The communication medium, the physical link between nodes usually consists of electric wires or optical fibers, although in some cases it can be an air link (wireless and fiberless). Wires can be twisted pairs or coaxial cables; fibers are usually multimode; for very high data rates singlemode fibers are used. Further on, we compare their relative performance, in terms of a figure of merit that combines data rate and length: For coaxial cables data rate-length squared product $\mathcal{R}L^2$, and for fibers data rate-length product $\mathcal{R}L$.

Protocols are the set of rules stations must obey in order to communicate across the network. For instance, the rules a station follows in order to send bits of information through the net without interfering with another station, are called access control protocols; the rules for reliable communications between stations by means of error detection and error corrections are called link control protocol; at the fundamental level of the operation, the format of the data being sent is also a protocol. Thus a protocol can be as basic as data format (bits configuration) and voltage levels, or as complex as algorithms embodied in program software or firmware designed to provide communications between application softwares residing on different machines. How protocols are implemented and standardized in order to allow communication between different machines and software applications is discussed further on.

4. TOPOLOGIES

Figure 1 shows examples of various topologies.

In the star topology (Fig.1A), all stations communicate with each other via a central switch, the control element. A circuit or connection between two stations is established through the switch for the duration of the message transmission. This type of communication is called circuit switching. A drawback of circuit switching is in the case of messages that are not continuous, but have a large fraction of idle time; in this case the communication becomes inefficient, as it ties up the channel and prevents other stations to communicate during idle periods.

The ring (Fig.1B) is nothing else than point-to-point links

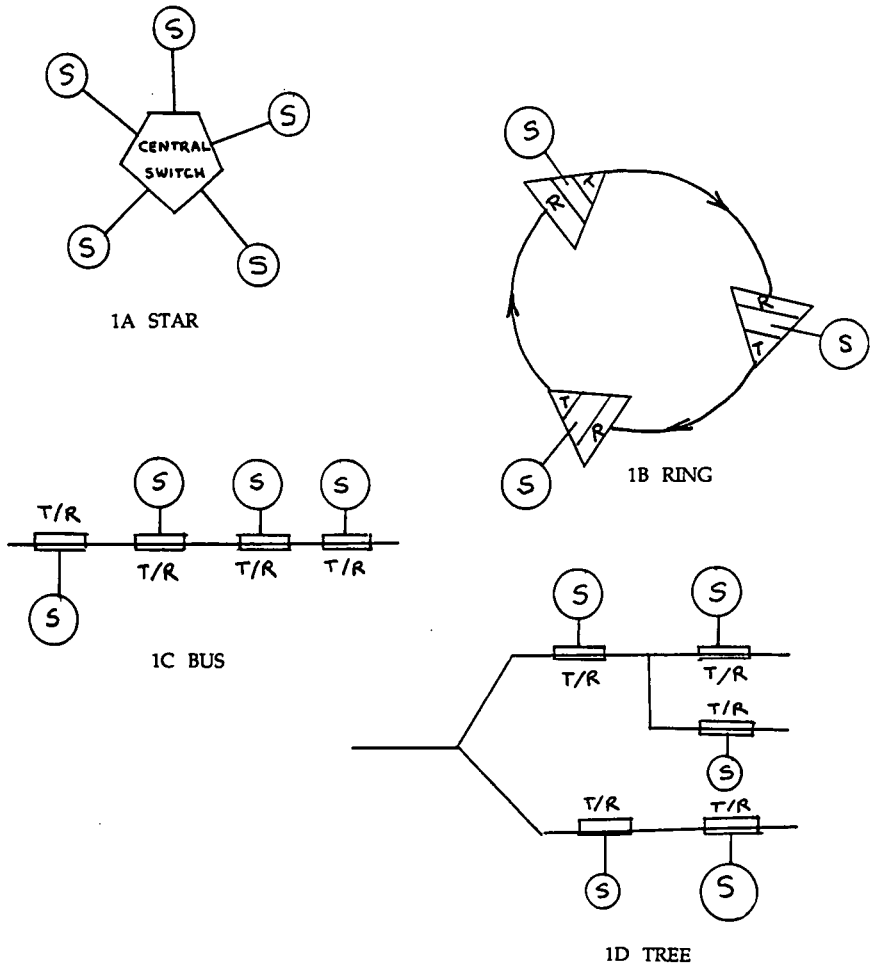

FIG. 1 LAN TOPOLOGIES
(S = Station, T = Transmitter, R = Receiver)

cascaded through repeaters. Each station is connected to the ring at the repeater. A message sent by one station, circulates through all the repeaters, and is read by every station. Thus a connection needs not to be established between two stations for the duration of the message, as in circuit switching. If the message has idle times, that time can be used by other stations to communicate among themselves. This is achieved by breaking up all messages, into smaller units of a few thousand bits called packets. However, it now becomes necessary for each packet to show destination address, and carry some form of control information that allows orderly access to the ring by other stations in need of communicating. Access control logic and addressing are part of the set of rules or protocols that must be established. This type of communication called Packet Switching is commonly used for computer data; it consists of short data blocks or packets handled in an interactive mode.

The bus topology (Fig.1C), unlike the previous topologies needs no central switch or repeaters. Stations are connected to the bus at the nodes, through interface processors. Control circuitry in the processor is handled by protocols, which ensure orderly transmission among the various stations. Bus topology, like the ring operates in a broadcast mode, i.e. messages are received and read by everybody, and both topologies favor packet switching. The tree topology (Fig.1D), an extension of the bus is often used in cable television.

5. PROTOCOLS

In order to communicate between different software applications and/or different computers and peripherals, it becomes necesssary to:
1) Break up the communication functions into a hierarchy of smaller, manageable, self-contained sets of tasks called layers, with minimal coupling betwen the layers. Coupling between layers takes place through the form of elementary software operations called services.
2) Standardize each layer's communication functions that interface with adjacent layers. The set of conventions or algorithms needed to carry out these functions make up the protocols.
Together, layers and protocols define the architecture of the network.

Standardization has been developed by the International Standards Organization, ISO. The standards, although not complete should allow different equipments and software applications to communicate with each others. Those standards are embodied into the Open Systems Interconnection model, OSI of layered architectures.

Each layer has its own set of protocols. All protocols must fulfill two functions 1) timely and correct delivery of the data, i.e. synchronization and error detection/correction, 2) reformatting of the data to ensure recognizable delivery at destination . The first is handled by network protocols; the second by higher-level protocols. Figure 2 illustrates the hierarchy. The two groups of protocols are further broken down in sublayers, which in the OSI model add up to seven, with each layer tasked to support these functions. For LAN operation, only the network layers are relevant; they are three, with their own standards developed by IEEE (Institute of Electronic Engineers) that conform loosely to the OSI model, as they are now described.

Refer to Figure 2 which shows the three layers. The protocols of the lowest layer, the physical layer ensure the transmission of raw bits over the physical link, wire or fiber. As such, they handle bit duration, voltage swing, as well as mechanical specifications such as the number of pins.

The next layer up, the medium access control provides the protocols that allow data access to the network. Two principal

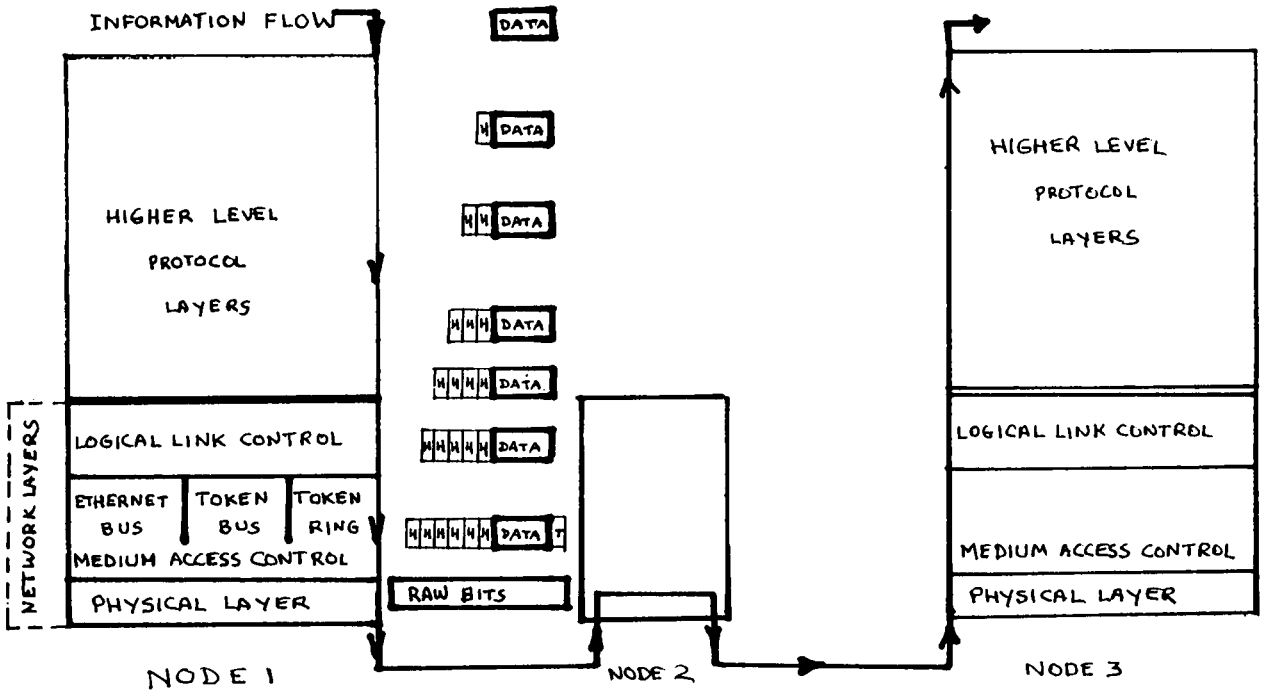

FIG. 2 LAYERED ARCHITECTURE FOR LANs
(H = Header Bits, T = Trailer Bits)

functions are: formatting the data packets into frames that carry source and destination addresses; and controlling the sequence of operations required to transmit a packet, while simultaneously avoiding interference with other stations. The protocols in this sublayer follow different IEEE standards depending on the topology of the LAN: Ethernet bus, Token passing bus, and token ring.
The third layer, Logical Link Control (LLC for short) has protocols that are independent of the topology. It provides mostly interface functions between the layer below and the higher level protocol layers above; it also breaks up the information from the upper layer into small blocks of data or frames that consist of data packets and control bits.

All these protocols are implemented by adding control bits at the beginning or end of the data block (see Fig.2). They are called headers and trailers respectively (abbreviated H and T in the figure). These added bits carry the control information embodied in the protocol. As the information travels down through the layers, each layer adds control bits that implement the respective protocols. The process illustrated in Fig.2 is called encapsulation. A common analogy is mailing a letter. The contents of the letter are part of the message, only one packet. The page number on the particular letter is the next encapsulation that identifies the packet sequence. The next level encapsulation is the envelope that carries the house address. Additional encapsulations could include the name of the recipient, and so on.

So far we have discussed LAN topologies, protocols and standards in the context of electrical networks. When one tries to adapt electrical LAN concepts to fiberoptic networks, several problems arise because the transmission media are radically different. We now address these problems.

6. PROBLEMS WITH PRESENT HIGH SPEED LANs

For high speed LANs to transmit data at Gb/s rates, single mode optical fibers are needed. Coaxial cables at these frequencies incur skin-effect losses that limit the useful transmission distance to tens of meters. Table I lists a useful invariant quantity; for coaxial cables it is the product of data rate and squared length. For instance, a 1/2" coaxial cable has a data rate-length squared product, $\mathcal{R}L^2$= 4 Mb/s-km^2. At 4 Gb/s, the useful transmission distance is reduced to $(4/4000)^{1/2}$x 1000 m, or 30m. On the other hand, an optical fiber, with $\mathcal{R}L$~40Gb/s-km carries the same data rate over 10km.

Until recently, all-optical implementations of high speed LANs have had two serious drawbacks: Branching losses and directionality of fiberoptic couplers.

Branching Losses

Of the three basic LAN topologies, bus, ring and star only the repeatered ring (Fig. 1B) so far lends itself to fiberoptic implementation, when it comes to serving a large number of nodes (several hundreds). Unlike their electrical counterparts, buses and stars run out of photons after serving a limited number of stations due to cumulative branching losses. The reasons are both theoretical and practical.

Theoretically, with only passive coupling, the maximum number of stations that can be served by a bus is calculated as follows: Refer to Fig.1C, with communication established between the two stations that are furthest apart. No loss is assumed in the cable; the power tapped off at each station is not a fixed ratio, but a constant amount sufficient to overcome receiver noise, kTB in the electrical case and hνB at optical frequencies; (B is bandwidth, k Boltzmann's constant, T receiver temperature, h Planck's constant and ν optical frequency).

TABLE I

PERFORMANCE OF COAXIAL CABLES AND OPTICAL FIBERS

TRANSMISSION MEDIUM	COAX $\mathcal{R}L^2$	OPTICAL FIBERS $\mathcal{R}L$
COAX		
1/4" DIAMETER	1.0 Mb/s-km^2	
1/2" DIAMETER	4.0 Mb/s-km^2	
OPTICAL FIBERS		
MULTIMODE STEP INDEX		40 Mb/s-km
MULTIMODE GRADED INDEX		400 Mb/s-km
SINGLE MODE FIBER		Tens of Gb/s-km

For electrical LANs, the number of stations supported by unity power is

(1) $N_e = 1/kTB$

On the other hand, for the same bandwidth, a unit of optical power supports a number of stations

(2) $N_0 = 1/h\nu B$.

It is clear from the above that many more stations can be passively coupled to an electrical LAN since,

(3) $N_e/N_0 = h\nu/kT >> 1$ (~30)

The same results apply to the bus because the power can also be distributed equally between all stations. It is done by using variable couplers, of increasing tap fraction downstream along the bus, in just the right amount to compensate for cumulative branching losses. The theoretical distribution loss, for N (N_e or N_0) stations coupled passively and optimally to either stars or buses is 10logN optical decibels, or 20logN electrical decibels.

On the practical side, the ratio N_e/N_0 is even greater than Eq.(3). This is because, until recently only electric bus or star coupling losses could be overcome with amplification. Electronic amplifiers are much more common than optical amplifiers. In fact, a typical electrical bus such as Ethernet (Fig.1C), actively couples to the cable via transceivers, and can support thousands of stations.

Before optical amplifiers entered the picture, fiberoptic LANs could not support a large number of stations except by converting back to electronic, and electronic amplification. For instance, a star topology requires an active NxN electronic switch, with electro-optic conversion at 2N ports; a ring topology must be made up of point-to-point links, with electronic repeaters, optical receivers and transmitters at each node. Both topologies suffer from a common weakness: single point of failure; the switch in the star, any one repeater in the ring. This weakness is in part remedied with redundancy and by-pass switches. Fig.3 shows a fiberoptic ring and lists one of the problems inherent to this topology.

Fiberoptic Coupler Directionality

On an electrical bus, any connecting branch transmits signals in both directions: the connection is bidirectional. A linear electrical bus is a viable topology since any station can reach all other stations by transmitting either in one or the other direction; it is in fact the basis of the Ethernet bus. Fig.4 shows a bus, lists the advantages of the electric version and the problems inherent to its fiberoptic counterpart.

An optical coupler is inherently unidirectional. Consequently, it favors a closed loop topology. Fig.5 shows couplers (as circles) on a fiber loop to which optical amplifiers (shown as triangles) have been added in order to make up for branching losses. The amplifiers are incidental to this discussion; the point to note is that if transmitter and receiver use a common coupler, then only one direction of propagation can be supported by the loop. The closed loop topology however introduces an added complexity: it requires that the optical couplers be switchable. Several problems arise if they are not:

- Data keeps recirculating around the loop; although attenuated, it can be a significant source of interference.

- Each transmitter saturates its station receiver during the transmission of a data packet. For high throughput, the packet length is longer than the loop; as a result, the saturated receiver misses part of the return transmission which indicates acknowledgement by the packet recipient.

7. SUMMARY OF PROBLEMS AND SOLUTIONS

We summarize below the two problems with the corresponding solutions just discussed, and add a third solution.

PROBLEM	SOLUTION
Branching losses	Optical amplifiers
Unidirectionality	Closed loop with switchable couplers
	Open loop with fixed couplers

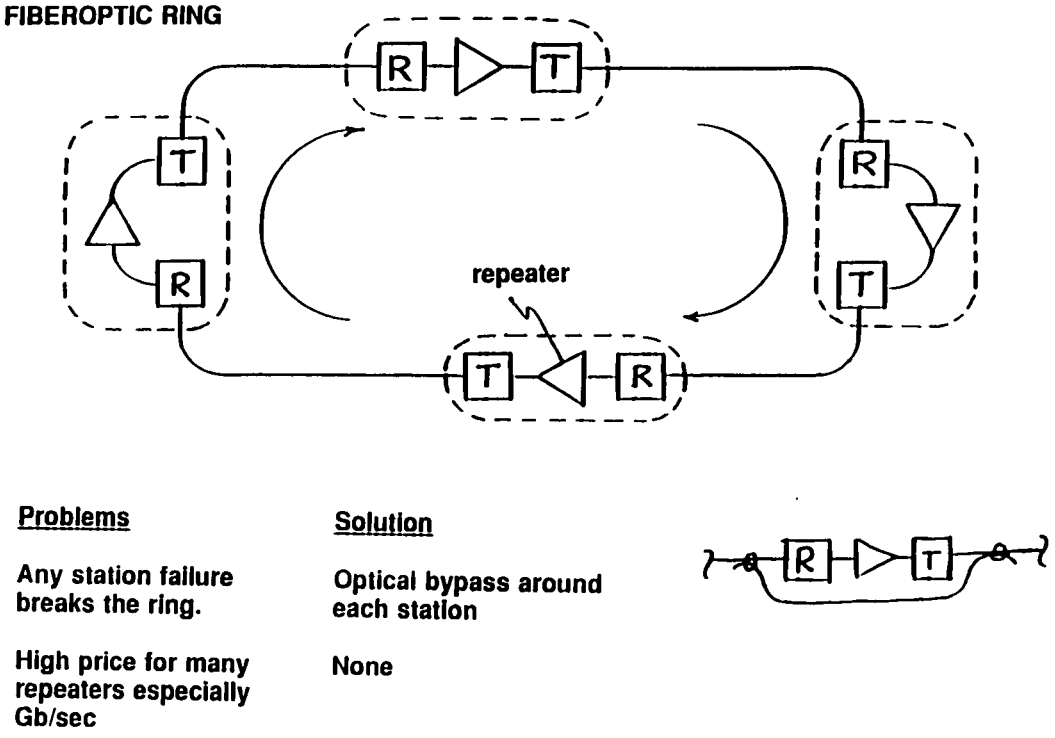

FIG. 3 REPEATING RING NETWORK

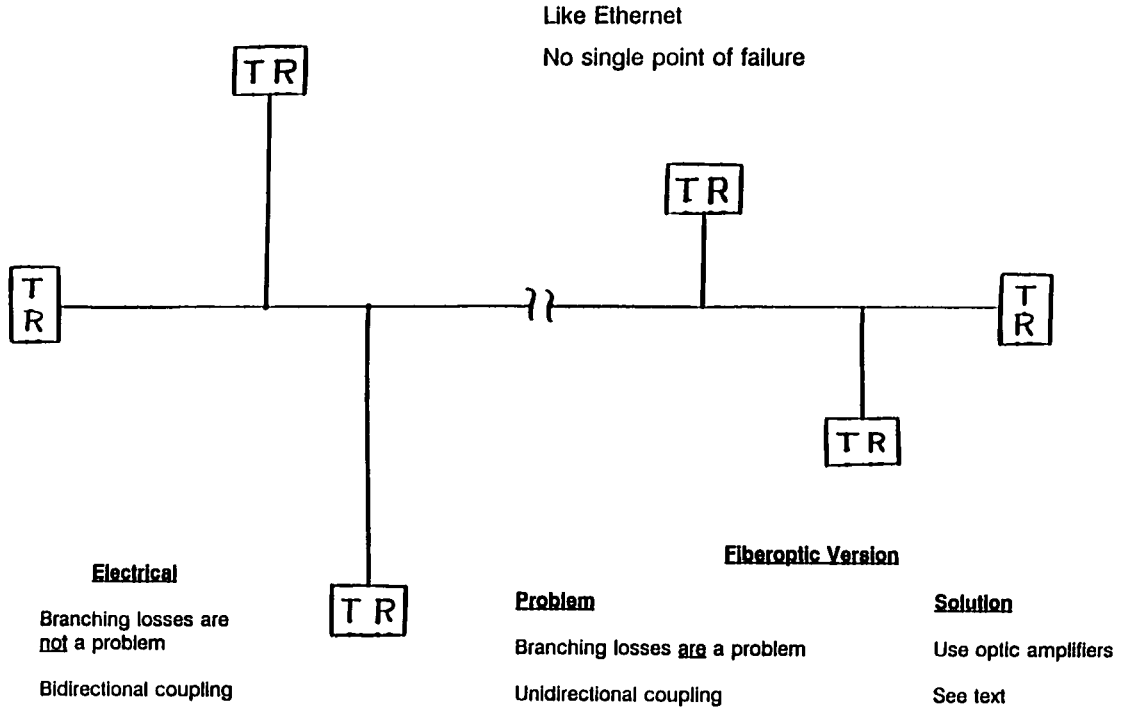

FIG. 4 LINEAR BUS TOPOLOGY WITH SHARED MEDIUM

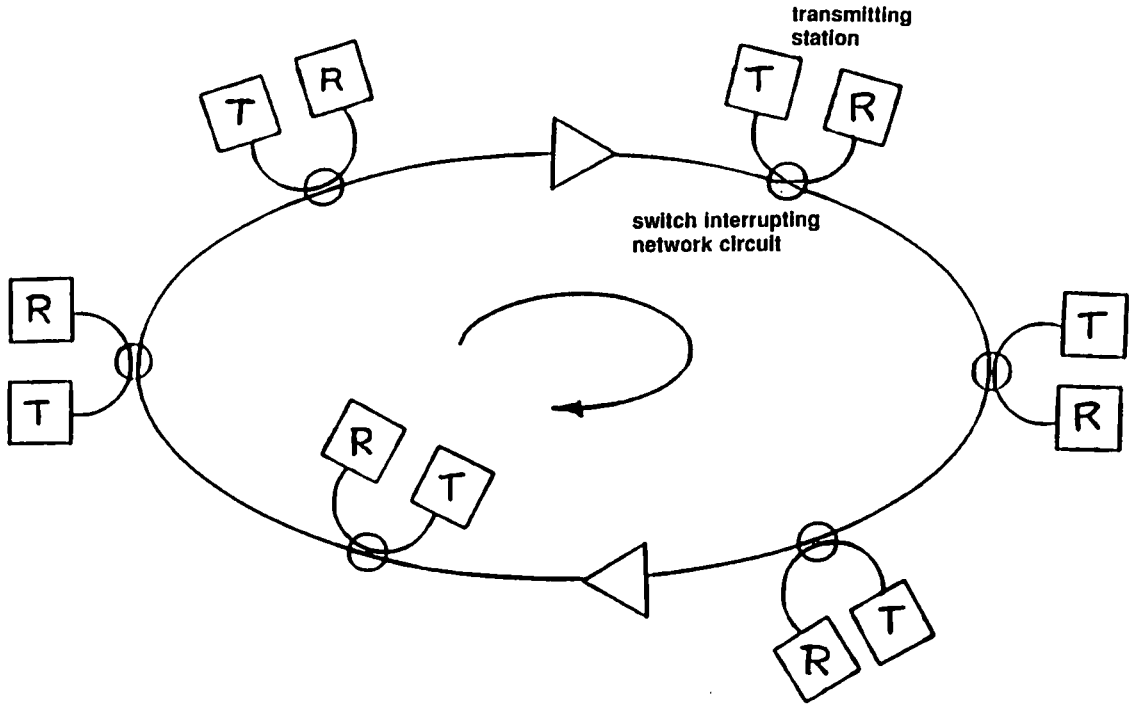

FIG. 5 CLOSED-CIRCUIT BUS WITH GAIN

We shall discuss two possible implementations, one with switchable couplers, the other with fixed couplers, both using optical amplifiers. As a preliminary, we first review the characteristics of two key optical components, switchable couplers and optical amplifiers.

8. SWITCHABLE COUPLERS

Switchable couplers eliminate these problems. Switching must set the coupler in one of three states shown in Fig.6:
- Interrupt state breaks the loop continuity for the duration of the transmission (Fig.6a).
- On-line state for reception (Fig.6b).
- Fail-safe state, so that the main bus is not interrupted (Fig.6c).

The speed of the switch must be able to accomodate the data rate and packet duration. At 6b/s, nanosecond switch times are

needed; this rules out electro-mechanical solutions, and favors Lithium Niobate electro-optic switches. Such switches have been demonstrated; an important feature is that they derive control information locally from the medium access protocol.

The coupling element in the switchable coupler consists of two waveguides deposited on a substrate whose properties can be modified by applying an electric field. When two waveguides are in close proximity (a few wavelengths apart) (see Fig.7) , under certain circumstances, power is transferred back and forth along the length. The process is a resonance phenomenon, much like the one that takes place between two coupled pendulums. Resonance occurs if the propagation constants or wavenumbers β_1 and β_2 are equal. We denote the mismatch between wavenumbers,

(4) $\Delta = \beta_1 - \beta_2$,

as this is one of the parameters that determines the fraction of light power transferred from one guide to the other. The other parameter is the coupling constant κ; it depends on the mode field distribution and the separation between the guides. If guide 1 is excited, the light fraction transferred to guide 2 is a function of the interaction length L (also called coupling length), that is the length over which the guides run close to each other; it is also a function of the coupling constant κ, and the mismatch parameter Δ. The resultant expression is well known; it is the solution to two first order coupled differential equations and is given by

(5) $F = \{1+(\Delta/\kappa)^2\}^{-1/2}\sin^2\{[1+(\Delta/\kappa)^2]^{1/2}\kappa L\}$

A plot of the fractional power coupled into waveguide 2 as a function of the normalized coupling length κL, for different values of the parameter Δ/κ is shown in Fig.8. For full power transfer, the wavenumbers must be equal, i.e. $\Delta=0$, and the normalized length, $\kappa L=(2n+1)\pi/2$. Because the substrate is quite lossy, in practice we choose n=0, which makes the interaction length $L = \pi/2\kappa$; L is typically of the order of 1 cm. In order to transfer all the power back to guide 1 over this coupling length, F of Eq.(5) must vanish. That corresponds to $\Delta/\kappa = (3)^{1/2}$, obtained by making the argument of the sine function equal to π. How does one change Δ/κ? By fabricating the coupler out of electro-optical material in which titanium strip guides are diffused onto a $LiNbO_3$ substrate, and electrodes are deposited over it (Fig.7). Applying a voltage between the two electrodes creates an electric field in one of the guides that changes the refractive index, and consequently the wavenumber. A simple expression relating the change in wavenumber as a function of the applied voltage V and the guide separation w has been worked out by Hammer (Integrated Optics, T.Tamir Editor, Springer-Verlag, New York 1979):

(6) $\Delta/\kappa = 6.33E{-}2\ V\ e^{w}$

where w is expressed in μm and V in volts. Fig.9 gives a plot of light power transfer as a function of voltage, for a guide separation w=3μm. The switch exhibits two states:

Cross state at 0 volts; all power transferred to guide 2
Bar state at 1.4 volts; all power transferred back to guide 1.

A "mixed" state also occurs between 0 and 1.4V; any coupling ratio can be obtained by varying the voltage between these two values, with partial power transfer taking place. As we shall see, it has important applications in close loop LANs.

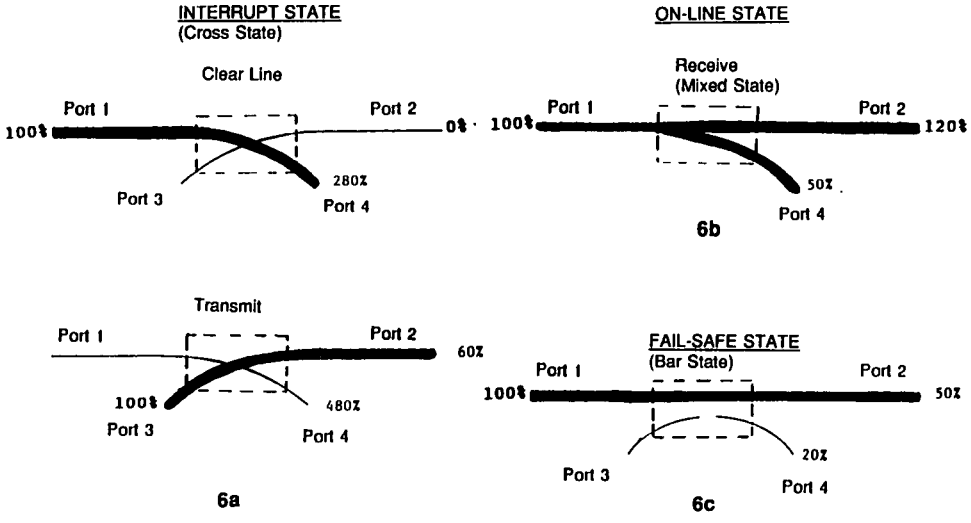

FIG. 6 SWITCH STATES

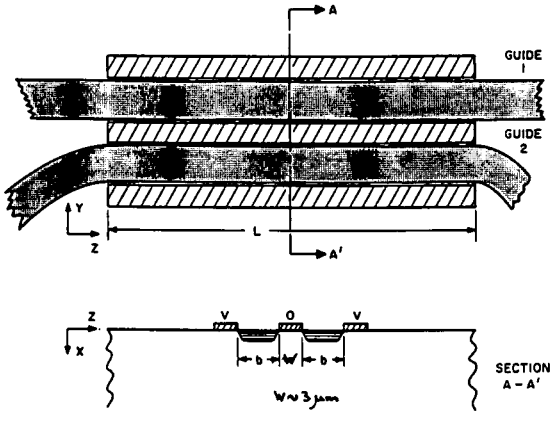

FIG. 7 WAVEGUIDE SWITCH
(Hammer, op. cit.)

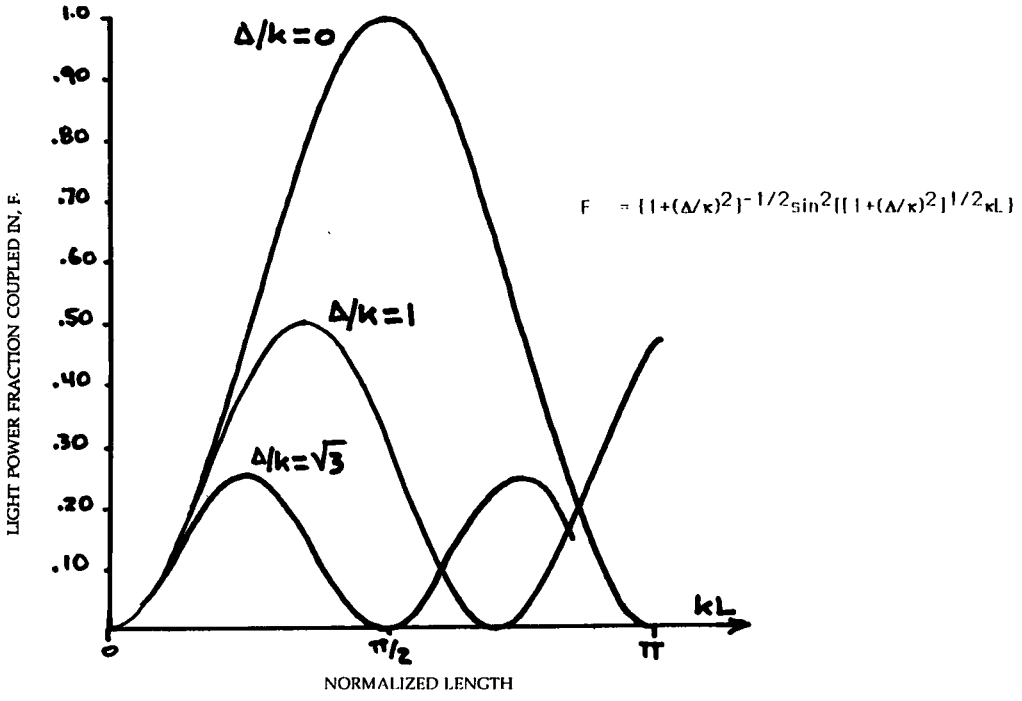

FIG. 8 POWER TRANSFER IN $LiNbO_3$ SWITCH

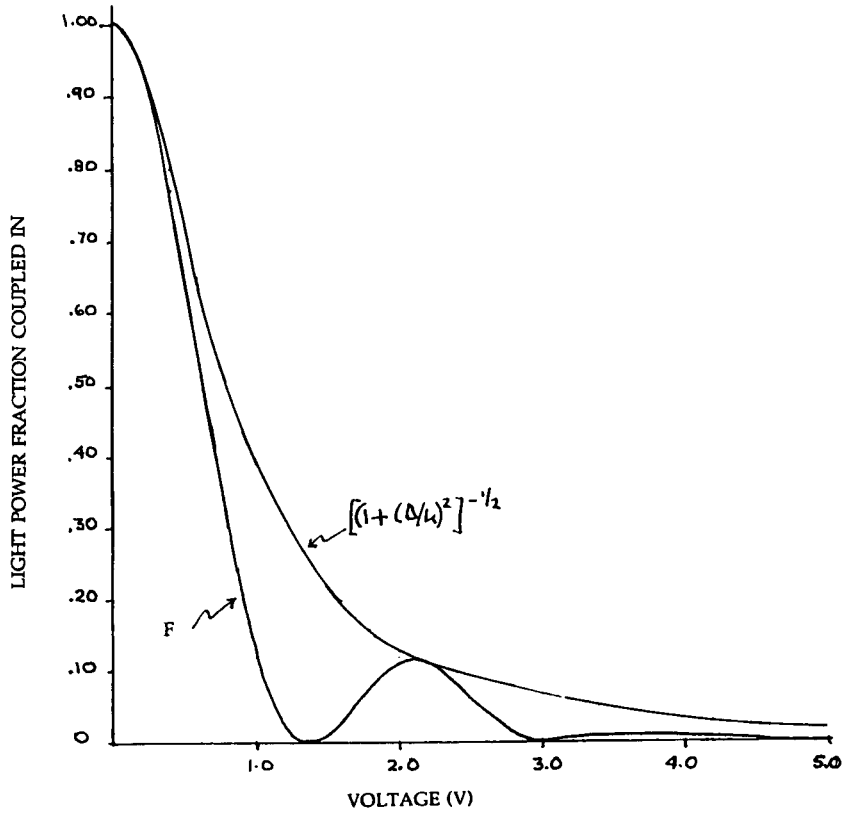

FIG. 9 LIGHT POWER TRANSFER AS A FUNCTION OF VOLTAGE

9. OPTICAL AMPLIFIERS

Optical amplifiers have been around since the laser came into existence. Until recently, only the semiconductor amplifier was commercially available; its cost is prohibitive and unlikely to come down because the number of applications are limited. All this has changed with the emergence of the erbium-doped fiber amplifier, EDFA for short. It uses the same glass fiber employed in telecommunications, except that it is doped with rare earth materials, such as erbium. The dopant atoms are optically pumped with a laser at wavelengths 980 nm or 1480 nm, slightly shorter than the signal wavelength 1300 or 1550 nm. Since the erbium atoms resonate at the signal wavelengths, the incoming signal stimulates emissions that add up coherently to it, and result in amplification. Although the EDFA cost is presently just as high as the semiconductor amplifier, it has such a potential for large volume applications in all fiber systems that its cost is expected to come down by orders of magnitude. In addition, its ease of fabrication and its ability to operate as a distributed amplifier (with light doping) makes it an ideal candidate for distributed networks.

In working with EDFA's, a few parameters need to be introduced in order to predict the performance of network systems. We begin with gain.
Gain is distributed through the length of the amplifier medium as the result of optical pumping. It follows that gain is an exponential function of length z in the medium,

(7) $G(z) = e^{\gamma z}$

γ, the gain per unit length is the net result of the competition between amplification per unit length, g and fiber intrinsic attenuation, α over the same path; in short,

(8) $\gamma = g - \alpha$;

γ is normally expressed in dB/m,

(9) $\gamma_{dB} = 10 \log(e^{\gamma}) = 4.34\ \gamma$

The gain per meter g is a strong function of the difference between the number of atoms pumped to the excited state N_2 and the number in the ground state, N_1; the difference N_2-N_1 is called population inversion. When $N_2 >> N_1$ the gain reaches saturation. When the difference is zero, the gain is unity, and when the difference is negative, the medium becomes an absorber. It is also a function of the erbium, the dopant density. For dopant concentration of the order of parts per million, the gain is in dB/m; for concentrations down to parts per billion, it is less than 1dB/km. The exponential increase in gain with length is limited by the fact that the medium attenuates the pump signal, and eventually one runs out of gain. This is well illustrated in Fig.10. (Payne and Laming, Optical Fibre Amplifiers, OFC Conference Proceedings, 1990) which shows pump power exponential decay with fiber length; Fig. 11 (obtained by Miles of our laboratory) illustrates gain dependence with length, for various pump powers.

Another set of important parameters for communication systems is the one that describes the various noise contributions. They arise in good part from the incoherent light glow, or amplified spontaneous emission, ASE for short as it beats against the signal (signal-spontaneous beat) and against itself (spontaneous-spontaneous beat) in the detector. Recall that a photodetector, in the language of communication theory is a square law detector to the electric field, and the beats come from squaring the sum of the various noise field components. There are also two shot terms, one due to signal fluctuations and the other caused by background fluctuations, or ASE. The expressions for noise at the amplifier output are well known and have been derived many times. We use the forms presented by Nakagawa (IEEE JLT,9, No2,1991; p198) for the components of beat noise, after converting them to detected current fluctuations, via the sampling theorem $2B_eT=1$.

We begin with the expression for ASE, P_{sp}:

(10) $P_{sp} = n_{sp}\ (G-1)\ h\nu B_o$

The population inversion parameter, $n_{sp} = N_2(N_2-N_1)^{-1}$ is a measure of the pumping efficiency. With full population inversion, $N_1=0$ and $n_{sp}=1$,its minimum theoretical value. At a pump wavelength of 14800nm, it is of the order of 1.5. B_o is the optical bandwidth, and the other terms have already been defined. Note that in general, $g >> \alpha$ in (10). Following are the various noise contributions expressed as mean square detector current fluctuations:

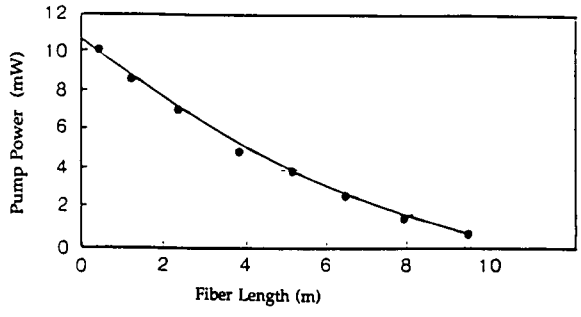

FIG. 10 ATTENUATION OF PUMP POWER ALONG FIBER

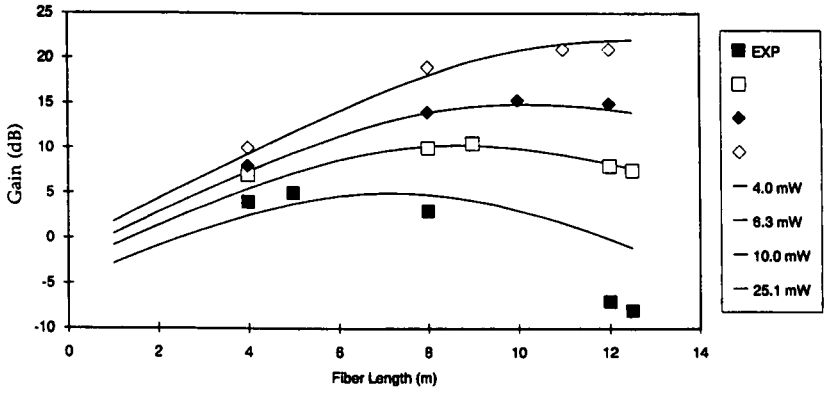

FIG. 11 GAIN VS. LENGTH WITH PUMP POWER AS PARAMETER

SHOT NOISE

(11) $\langle \Delta i^2_{sh} \rangle = 2\eta e^2 B_e (h\nu)^{-1} [P_{in} G + n_{sp}(G-1) h\nu B_o]$

The first term in the bracketed expression is due to signal and the second caused by ASE. B_e is the electronic bandwidth, P_{in} the input signal optical power to the amplifier, and η the detector efficiency.

SIGNAL-SPONTANEOUS BEAT NOISE

(12) $\langle \Delta i^2_{s-sp} \rangle = 4 n_{sp} (\eta e)^2 (h\nu)^{-1} P_{in} G(G-1) B_e$

SPONTANEOUS-SPONTANEOUS BEAT NOISE

(13) $\langle \Delta i^2_{sp-sp} \rangle = 4(\eta e)^2 B_e B_o n_{sp}^2 (G-1)^2$

The expressions above are all measured at the amplifier output.

Payne and Laming (op.cit.) have calculated the relative noise contributions and measured total noise. Fig.12 shows output current spectral noise densities (i.e the preceding expressions divided by the optical bandwidth) as a function of input signal power, P_{in}. For signals larger than a few microwatts, the significant contribution comes from the signal-spontaneous beat noise.

Having reviewed the principles of operation of the two building blocks of high speed LANs, switchable couplers and erbium-doped fiberoptic amplifiers (EDFA for short), let us proceed with with two examples of fiberoptic LANs configured around these elements. We discuss two loop topologies, closed and opened; recall that fiberoptic couplers are unidirectional, and the loop rather than the bus is the natural topology.

10. CLOSED LOOP LAN

The $LiNbO_3$ switch described above applies directly to the example of Fig.5. The closed loop demands 1) a switchable coupler in order to prevent recirculation of data, and 2) optical amplifiers to make up for the significant attenuation in $LiNbO_3$.

In the past, semiconductor amplifiers on the main bus were frowned upon because they are single points of failure. However, EDFAs have the same long reliability as fibers; the most likely failure is the pump, and redundant pumps can be added. The possibility even exists of doping the $LiNbO_3$ with erbium to achieve gain (Helmfrid, Elec.Lett., 27, 23 May 1991; p.913. Brinkman, Elec.Lett., 27, 28 Feb.1991; p.415).

Fig.13A (Hinton,IEEE Spectrum, Feb.92; p.42) illustrates a standard electro-optic switch and the two states in which it operates: By-pass, called Bar in the telephone parlance, and interrupt or Cross. The splitting of the electrodes is not relevant to this discussion. Fig.13B shows the switch placement in a network node; T and R stand for the node transmitter and receiver. The coupler is built with an interaction length corresponding to $\pi/2$ radians and matched wavenumbers ($\beta 1 = \beta 2$), under zero applied voltage. This is the shortest distance, for which complete power transfer occurs.(See Figs. 8 and 9). Thus the cross state which occurs under zero voltage is also a fail-safe state; in case of failure the bus is not interrupted. On the other hand, the switching state, which here is a Bar state occurs with application of 1.4V in the example of Fig.9. In this state, the transmitter sends its packet, while the other stations listen in a "mixed" state, with applied voltage between zero and one volt, depending on the fraction of light that needs to be coupled into the receiver. We thus have 3 states for loop operation:

Interrupt or Bar State
Fail-safe or Cross State
Receive or Mixed State

The problem with switches is the insertion loss, which typically runs into several decibels, of the order of 5dB per switch. The loss is compensated with optical amplifiers. Gain for these amplifiers is of the order of 20 dB, which means one amplifier every four nodes. Unfortunately, amplifiers are noisy, and the higher the gain, the noisier they are. With so few nodes per amplifier, the signal-to-noise ratio degrades rapidly, inversely with the number of cascaded amplifiers. The open loop topology that follows removes these limitations: No switching necessary, and more nodes per amplifier.

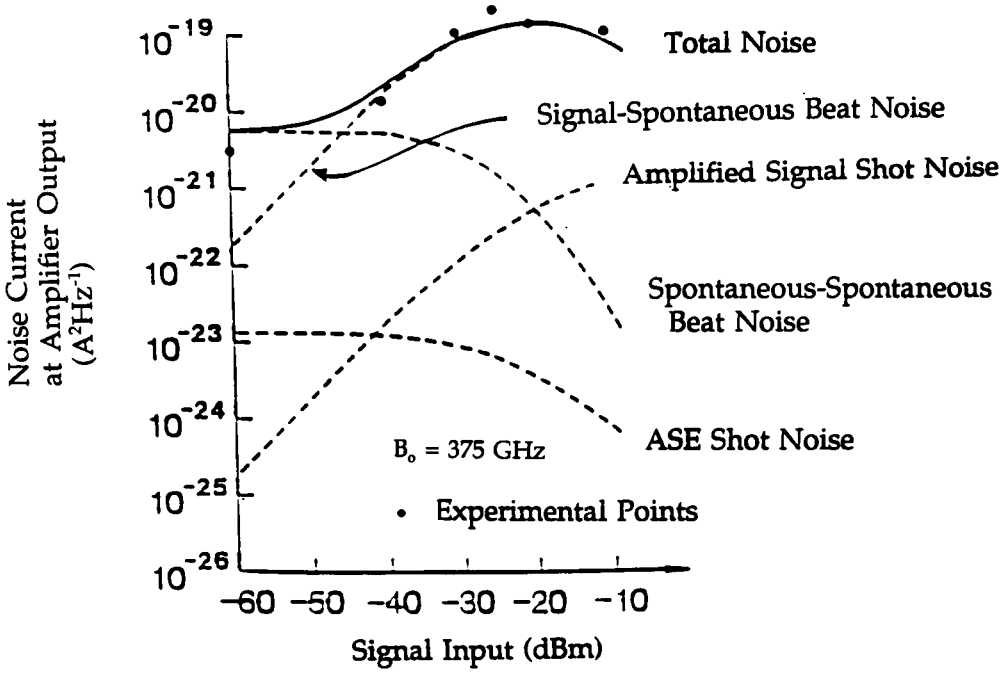

FIG. 12 RELATIVE NOISE CONTRIBUTIONS IN EDFAs
(Payne and Laming, op. cit.)

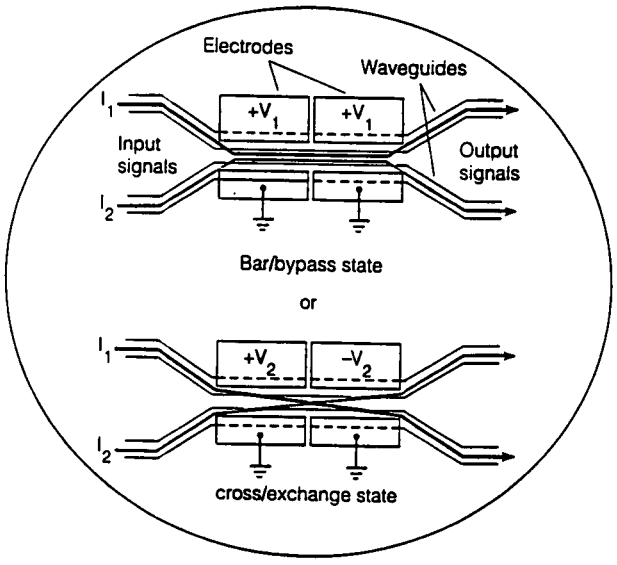

A. TWO STATE SWITCH
(Hinton, IEEE SPECTRUM, Feb. 92, p. 42)

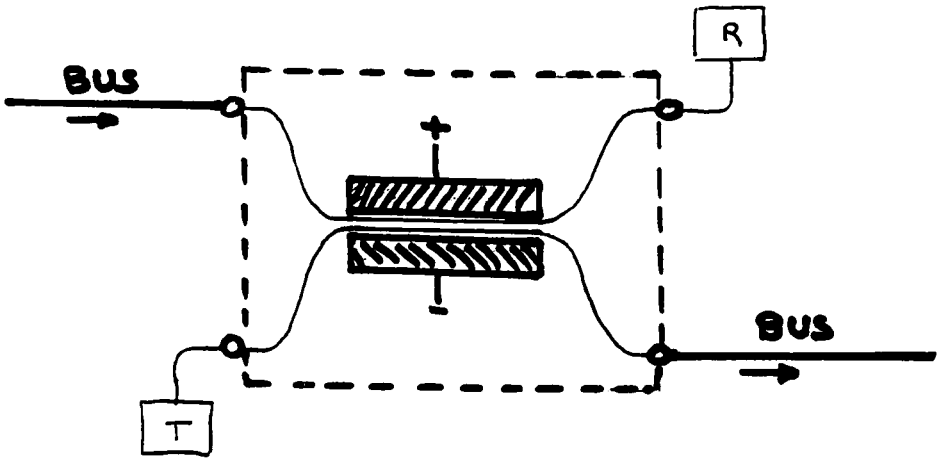

B. IMPLEMENTATION OF SWITCH: Cross State = OV
Bar State = 1.4V

FIG. 13 SWITCHABLE ELECTRO-OPTIC COUPLER

OPEN LOOP LAN

Figs.14 illustrate a novel topology that eliminates the problem of data recirculation encountered in closed loops; as a result, a switching coupler is no longer necessary. The optical path is folded, so that all the transmitters are at one end, and the receivers at the other.

Medium access control is local, at the node. A fraction of the light is tapped at each node and the packet address is read by all receivers. The addressed node has then local authority, subject to a protocol, to turn on its transmitter and send a message.

The couplers are passive, and the branching losses are compensated by EDFAs. There are various ways to connect the amplifier pumps, but this a subject in itself and will not be discussed here.

Consider now the network of Fig.14B, with transmitters on the top leg of the figure, and receivers on the bottom one. Each span between amplifiers supports m transmitter or receiver nodes, except for the first and last span. All spans are made equal in length, an so is the link length between nodes. (The link between nodes is often called a branch). The end spans carry m+1 nodes, and the end transmitter and receiver are fused directly onto the fiber bus, with negligible coupling losses. All other nodes are coupled to the bus, with coupling ratio C (of the order of 10%) and efficiency η_c (of the order of 80%).

To calculate the number of nodes per span, m and the number of cascaded amplifiers M, we proceed as follows:

Let P be the power input to the fiber from any transmitter. One way to design the LAN is to have amplifiers with gain that compensates exactly the losses across the span, so that the power appearing at the output of each amplifier is P. The losses are mostly branching losses; the fiber attenuation, of the order of 0.3dB/km is negligible over the span. The gain of each amplifier is accordingly,

$$(14a)\quad G = [\eta_c{}^m (1-C)^m]^{-1}$$

For instance, setting the gain at 20 dB, the permissible number of nodes with coupler ratio 10% and efficiency 80% is m = 14. The result follows after recasting the preceding expression into:

$$(14b)\quad m = \_ (10 \log G)/(10 \log[\eta_c(1-C)])$$

Fixing G and m imposes constraints on the maximum number of amplifiers that can be cascaded, and the amount of power

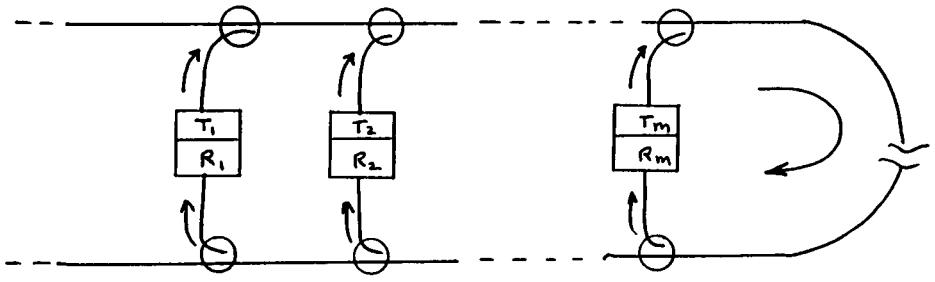

A. OPEN LOOP CONFIGURATION

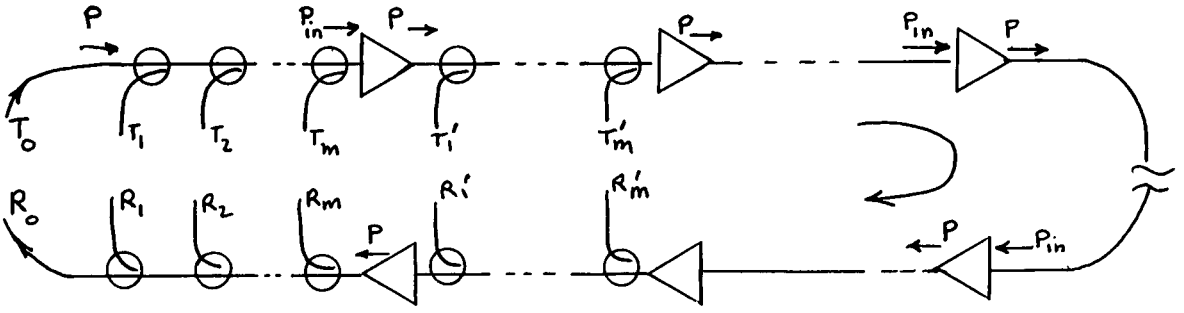

FIG. 14 OPEN LOOP LAN WITH FIXED RATIO PASSIVE COUPLERS AND EDFAs

required. This is readily understood by considering the worst case, transmission between T_1 and R_1. The received power

(15) $P_R = P\,\eta_c C[\eta_c(1-C)]^{m-1}$

must be large enough to meet a signal-to-noise ratio that ensures minimum error probability; one must also verify that P_R exceeds or equals the receiver sensitivity. The calculations that follow use the electrical signal-to-noise ratio,

(16) $K = \langle i_s^2\rangle/\langle \Delta i_n^2\rangle$

where the numerator is the square of the receiver signal photocurrent,

(17) $\langle i_s\rangle = (\eta e/h\nu)\,P\,[\eta_c(1-C)]^m$

and the denominator, the mean square noise photocurrent. It is the sum of the mean square noise contributions given by Eqs(11), (12) and (13), but corrected to account for the cumulative increase caused by cascading amplifiers. The noise arises from interaction between signal power and ASE. The latter (Eq.10), becomes

(18) $P_{sp} = Mn_{sp}(G-1)h\nu B_0$

Wherever P_{sp} occurs in the noise equations, it must be replaced by Eq.(18). Note that the beat noise of Eq(12) is proportional to the product PP_{sp}, while the beats of Eqs(13) are proportional to $(P_{sp})^2$. The resultant noise expressions, take into account the fact that $P = P_{in}G$, and that both, P and P_{sp} are attenuated by $G^{-1} = [\eta_c(1-C)]^m$ between last amplifier output and receiver:

(19a) $\langle \Delta i^2_{sh}\rangle = 2\eta e^2 B_e(h\nu)^{-1}[P+Mn_{sp}(G-1)h\nu B_0]\eta_c C[\eta_c(1-C]^{m-1}$

(19b) $\langle \Delta i^2_{s-sp}\rangle = 4Mn_{sp}(\eta e)^2(h\nu)^{-1}P(G-1)B_e(\eta_c C)^2[\eta_c(1-C)]^{2(m-1)}$

(19c) $\langle \Delta i^2_{sp-sp}\rangle = 4(\eta e)^2 B_e B_0(Mn_{sp})^2(G-1)^2(\eta_c C)^2[\eta_c(1-C)]^{2(m-1)}$

To reduce noise induced by ASE, optical filters are used at the output of each amplifier. Typical filters have bandpass of 1nm, or equivalent frequency band B_0=125 GHz, with insertion loss of a couple of dBs. The effect is to reduce the effective amplifier gain by that amount. As long as the number of amplifiers, M is below several hundreds, signal-spontaneous beats are the dominant form of noise, provided that some filtering is used. In this case, using Eqs.(17) and (19b), the signal-to-noise ratio at all receivers, following the last amplifier, and thermal noise neglected, is

(20) $K = (P/h\nu B_e)\,/4Mn_{sp}(G-1)\}$

The preceding equation omits the fact that in some digital transmissions, the absence of a pulse indicates a "0". During this interval, there is no beat noise; for equal distribution of "1's" and "0's", K above is greater by 3dB. However, if we take into account that receiver thermal noise (which we have neglected) is always present, regardless of the presence or absence of the pulse, Eq.(20) is justified for conservative design.

To ensure bit error probability < E-9, then K > 36. Setting K=36 and n_{sp}=1.5, we have

(21) $M=3.6E4\,[P(mw)/B_e(GHz)](G-1)^{-1}$

Note that the laser power at each station is $P_L \equiv C^{-1}P$. The total number of nodes served is

(22) $N = m(M+1)$

corresponding to N/2 stations or transmitter-receiver pairs.

N must be an even number for this type of LAN. In order not to be unduly restrictive, either m must be even or M must be odd. The latter choice is less constraining on the design. We now give a design example.

Design Example: We use four basic equations repeated below for convenience:

(14b) $m = \_\,(10\log G)/(10\log[\eta_c(1-C)])$

The first one determines the number of nodes per amplifiers and the next one the number of amplifiers, both as a function of gain.

(15) $P_R = P\,\eta_c C[\eta_c(1-C)]^{m-1}$

(21) $M=3.6E4\,[P(mw)/B_e(GHz)](G-1)^{-1}$

Note that it is the signal-spontaneous beat noise in Eq.(21) that sets the limit on the maximum gain that can be had, for a bit error probability not exceeding E-9. However, the maximum gain is often below this limit, as another constraint comes in: receiver noise which determines its sensitivity, that is the minimum power, P_R necessary to meet the bit error rate of E-9. Typical sensitivities are -35dBm at 1Gb/s (0.5 GHz) and -40dBm at 200Mb/s (100 MHz). Receiver sensitivity is related to gain through,

(15) $P_R = P\,\eta_c C[\eta_c(1-C)]^{m-1}$

Finally the total number of stations follow from the last equation below:

(22) $N/2 = m(M+1)/2$

The various quantities of interest m, M and N/2 are plotted in Figs.15A and B for the parameters C, η_c, P and B_e.

Consider now a LAN operating at 1Gb/s, and decide on N/2=200 stations. The first step in the design is to determine the required amplifier gain. Fig.15A shows that for 200 stations, the number of amplifiers, M=22 and the corresponding gain, G=25dB are limited by signal-spontaneous beat noise. The number of nodes per amplifier read off the curve is m=18. However, the receiver sensitivity constraint, Eq.(21) with P_R equal to -35dBm, together with the acceptable number of nodes per amplifier, Eq.(14b) establishes a maximum limit on gain, which calculates to G=15dB. The receiver noise limit, at this gain is shown on the figure, and the corresponding number of nodes, m=10. To meet the prescribed number of stations under this more stringent condition, M=39. This is no problem, since as the gain decreases, so does beat noise and M increases. At 15dB gain, we see from the figure that M can exceed 200, and the total number of stations that can be supported exceed 1000.

Summarizing, the network consist of 40 cascaded amplifiers, each of 15dB gain, with 10 nodes between amplifier spans. Fig.15B illustrates the same set of curve, with only one change, reduced data rate to 200 Mb/s.

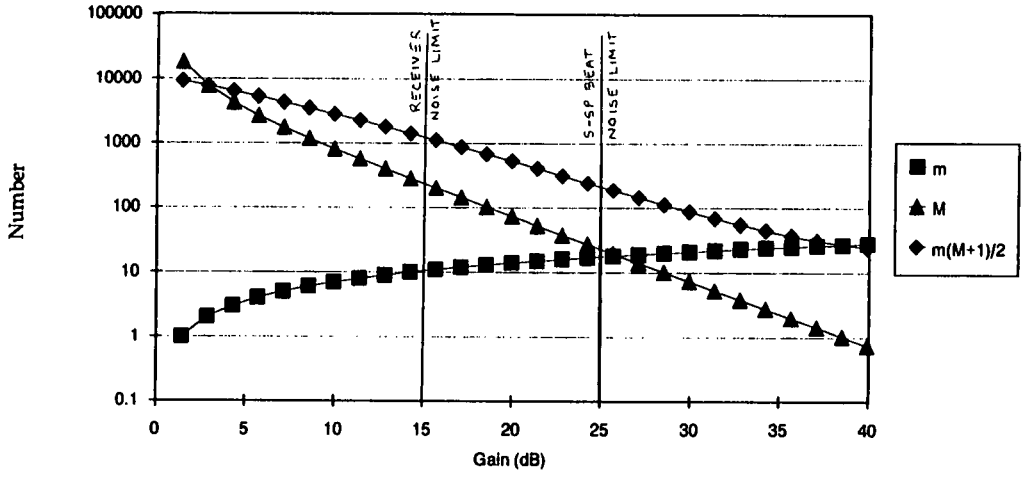

FIG 15A NUMBER OF NODES PER AMPLIFIER m, AMPLIFIER M, AND STATIONS m (M + 1)/2 AS A FUNCTION OF GAIN, WITH PARAMETERS:

C = 10% η_c = 80% P = 0.1mw B_e = 0.5 GHz (1 Gb/s)

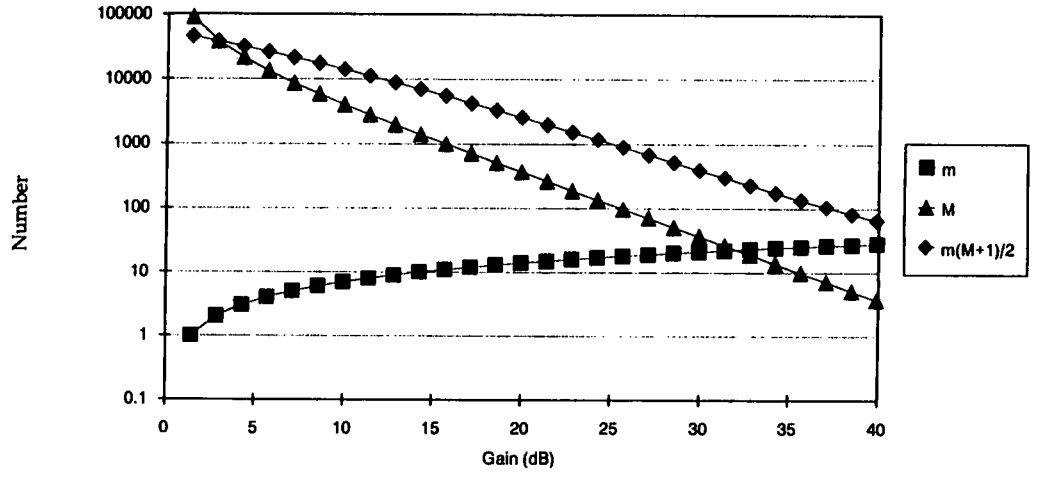

FIG 15B NUMBER OF NODES PER AMPLIFIER m, AMPLIFIER M, AND STATIONS m (M + 1)/2 AS A FUNCTION OF GAIN, WITH PARAMETERS:

C = 10% η_c = 80% P = 0.1mw B_e = 0.1 GHz (200 Mb/s)

NONLINEAR EFFECTS IN OPTICAL FIBERS

Bruno Crosignani
Dipartimento di Fisica,
Universita' di Roma "La Sapienza",
00185 Roma, Italy
and
Fondazione Ugo Bordoni, 00142 Roma, Italy

SUMMARY: The basic differential equations necessary to represent nonlinear propagation of short and ultrashort optical pulses in dielectric waveguides are derived. After introducing fundamental and higher-order soliton solutions of the nonlinear Schroedinger equations, the possibilities of realizing soliton-based communication systems are discussed. Higher order nonlinear effects associated with self-Raman gain and optical amplification in connection with the use of active fibers are also described.

1. INTRODUCTION

Third-order nonlinear optical effects such as optical Kerr effect, Stimulated Raman Scattering (SRS) and Stimulated Brillouin Scattering (SBS), turn out to play a relevant role in fiber optics, despite the extremely low nonlinear coefficients of silica, due to the long interaction length provided by the diffraction-free optical waveguide. This circumstance can be both beneficial or detrimental, according whether these effects are exploited for conceiving new kind of optical devices or intrude in an unwanted way in the operation and performances of other devices. Luckily, in many cases, nonlinear effects can be put to work to advantage. This is particularly true for the case of optical telecommunication systems, in whose frame one of these effects, namely the Kerr one, can be successfully used to compensate for the unavoidable distortion introduced by the chromatic dispersion of glass, thus allowing for the transmission of very large bandwidth over extremely long distances. It is accordingly understandable the choice of finalizing the present analysis to the description of the influence of the Kerr nonlinearity on the propagation of very short pulses, keeping also in mind the possibility of employing active fibers (to which a whole lecture is devoted in our Lecture Series) for the purpose of amplification and regeneration.

2. GENERAL FORMALISM FOR NONLINEAR PROPAGATION

The approach developed in this Section is purely phenomenological, that is the microscopic processes responsible for the nonlinear interaction are modeled by means a "constitutive relation" connecting the electric polarization $\mathbf{P}$ and the electric field $\mathbf{E}$ through the introduction of the linear and nonlinear susceptibility, $\chi^{(1)}$ and $\chi^{(3)}$ respectively. More precisely, adopting the convention of summation over repeated indices and dropping, for simplicity, the dependence on the spatial variable $\mathbf{r}$, one has

$$P_i(t) = \varepsilon_0 \int_{-\infty}^{t} dt' \chi_{ij}^{(1)}(t-t') E_j(t') + \varepsilon_0 \int_{-\infty}^{t} dt' \int_{-\infty}^{t} dt'' \int_{-\infty}^{t} dt''' \chi_{ijkl}^{(3)}(t-t', t-t'', t-t''') E_j(t') E_k(t'') E_l(t''') \quad , \quad (1)$$

the term containing the product of two electric fields being absent because of the spatial inversion symmetry of silica.

The problem of describing nonlinear pulse propagation in such a medium is then equivalent to finding the appropriate solutions of Maxwell's equations

$$\nabla \times \mathbf{E} = -\mu_0 \frac{\partial \mathbf{H}}{\partial t} \quad , \quad (2)$$

$$\nabla \times \mathbf{H} = \frac{\partial \mathbf{D}}{\partial t} \quad , \quad (3)$$

where

$$\mathbf{D} = \varepsilon_0 \mathbf{E} + \mathbf{P} = \varepsilon_0 \mathbf{E} + \mathbf{P}_L + \mathbf{P}_{NL} . \quad (4)$$

This task can be accomplished either resorting to the "wave equation" approach [1] or to "coupled-mode" theory. [2,3,4]

In the first one, Maxwell's equations, together with (4), are manipulated to give the wave equation

$$\nabla^2 \mathbf{E} - \frac{1}{c^2} \frac{\partial^2}{\partial t^2} \mathbf{E} - \nabla(\nabla \cdot \mathbf{E}) = \mu_0 \frac{\partial^2}{\partial t^2} \mathbf{P} \quad , \quad (5)$$

where c is the light velocity *in vacuo*. Next, the field is expanded in terms of the modes of the structure (see fig. 1), that is monochromatic solutions of the kind

$$\mathbf{E}_m(x,y;\omega) e^{i\omega t - i\beta_m(\omega) z}$$

which satisfy, together with the appropriate boundary conditions, Eq.(5) when $\mathbf{P} = \mathbf{P}_L$. In this case,

$$\mathbf{D}_\omega(\mathbf{r}) = \varepsilon_0 [1 + \chi_\omega^{(1)}(\mathbf{r})] \equiv \varepsilon_\omega(\mathbf{r}) \mathbf{E}_\omega(\mathbf{r}) \equiv \varepsilon_0 n_\omega^2(\mathbf{r}) \mathbf{E}_\omega(\mathbf{r}) \quad , \quad (6)$$

where the subfix ω stands for Fourier transform (we consider, from now on, isotropic situations and assume $n_\omega(\mathbf{r})$ to be a scalar). Performing this expansion, that is

$$\mathbf{E}_\omega(\mathbf{r}) = \sum_m c_m(z,\omega)\mathbf{E}_m(x,y;\omega)e^{-i\beta_m(\omega)z} \quad , \quad (7)$$

and inserting it into the Fourier transform of Eq.(5) yields, after adopting the so-called "slowly varying approximation" (SVA),

$$\left| \frac{d^2 c_m}{dz^2} \right| << \beta_m \left| \frac{dc_m}{dz} \right| \quad , \quad (8)$$

the following equations of evolution for the c_m's

$$e^{-i\beta_m z}\frac{dc_m}{dz} + \frac{i\omega}{4p_0}\int_{-\infty}^{+\infty} dx \int_{-\infty}^{+\infty} dy (\mathbf{P}^{(T)}_{NL,\omega}\mathbf{E}^{(T)}_m - P^{(z)}_{NL,\omega}E^{(z)}_m) = 0 \, , \quad (9)$$

where

$$2p_0\delta_{nm} = \int_{-\infty}^{+\infty} dx \int_{-\infty}^{+\infty} dy \, (\mathbf{E}^{(T)}_m \times \mathbf{H}^{(T)*}_m)\cdot \mathbf{e}_z \quad (10)$$

and the superscript (T) and (z) indicate the transverse and longitudinal (with respect to the direction $\mathbf{e}_z$ of propagation) parts of the corresponding quantities.

In the coupled-mode approach, the expression (7) of the electric field (together with an analogous one for the magnetic field) is inserted into Maxwell's equations and Eq.(9) is derived without the necessity of resorting to the SVA (actually, it can be shown that the SVA is redundant ,[5] and that its artificial necessity stems from having deduced from first-order Maxwell's equations the second-order wave equation). Thus, we assume in the following that the set of Eqs.(9) are valid without any approximation.

3. THE NONLINEAR POLARIZATION

Many physical mechanisms contribute to $\chi^{(3)}$ and a particularly good description of their microscopic origins and behavior can be found in Ref.(6). For the purpose of our development, it is sufficient to recall that a rather general expression of $\mathbf{P}_{NL}$ is given by

$$\mathbf{P}_{NL}(t) = \varepsilon_0 \chi^{(3)} \mathbf{E}(t)\, \mathbf{E}(t)\cdot\mathbf{E}(t) + \mathbf{E}(t) \int_{-\infty}^{t} d\tau \, a(t-\tau)\mathbf{E}(\tau)\cdot\mathbf{E}(\tau) \, . \quad (11)$$

The first term in Eq.(11) represents the fast responding (time scale of 1-10 fetmoseconds) electronics contributions arising from a direct distortion of the electronic clouds from their region of linear response under the influence of the propagating field. The second term models slower nuclear nonlinearities which arise as a consequence of electric field induced changes in the dynamics of the nuclei.

The optical Kerr effect is associated with the contributions of the nonlinear polarizability which vibrate at approximately the same frequency of the propagating field (other contributions, as the one giving rise to third-harmonic generation, are generally negligible in optical fibers for phase-matching reasons). They can be easily identified introducing the "analytic signal" of the field , that is

$$\hat{E}(r,t) = 2\sum_m \int_0^{+\infty} d\omega\, c_m(z,\omega) E_m(x,y;\omega) e^{i\omega t - i\beta_m(\omega) z} \quad , \quad (12)$$

in terms of which

$$E = \frac{\hat{E} + \hat{E}^*}{2} \quad . \quad (13)$$

In fact, after noting that the analytic signal is of the form

$$\hat{E}(r,t) = e^{i\omega_0 t} V(r,t) \quad ,$$

where $V(r,t)$ varies on a time scale much larger than $1/\omega_0$ (ω_0 being the mean frequency of the field), and considering for simplicity the case of a field linearly polarized in a direction orthogonal to the z-axis, it is immediate to verify that the significant contribution arising from the first term on the right side of Eq.(11) is

$$P_{NL}(t) = \frac{3}{4} \varepsilon_0 \chi^{(3)} |\hat{E}(t)|^2 E(t) \quad , \quad (14)$$

where $|\hat{E}(t)|^2$ is called the "instantaneous optical intensity".

Equation (14) allows one to define a nonlinear refractive index n_ω. To this end, it is expedient to realize the existence of two largely different time scales (the one associated with E(t) and the one with $|\hat{E}(t)|^2$), so that, by taking the Fourier transform of both sides of Eqs. (4) and (14), one approximately has

$$D_\omega = [\varepsilon_\omega + \frac{3}{4} \varepsilon_0 \chi^{(3)} |\hat{E}(t)|^2] E_\omega \, . \quad (15)$$

From Eq.(15) it is immediate to define the nonlinear refractive index

$$\tilde{n}_\omega \cong n_\omega + n_2 |\hat{E}(t)|^2 \, , \quad (16)$$

where n_ω is the linear refractive index and $n_2 = (3/8)\chi^{(3)}/n$ the so-called "nonlinear refractive index coefficient" ($n_2 = 2 \times 10^{-22}$ $m^2 V^{-2}$ for silica). Equation (16) can be written in the equivalent form

$$\tilde{n}_\omega = n_\omega + N_2 I(t), \quad (17)$$

where I(t) is the optical intensity (Watt/cm^2) and N_2 = 3.2 x 10^{-16} cm^2/Watt.

Equation (15) represents the optical Kerr effect in its simplest form, that is for linearly polarized light and having neglected the non-instantaneous response of the medium. This last effect can be included by taking into account the second term on the right side of Eq.(11). Its contributions to the nonlinear polarization vibrating at approximately the frequency of the field are

$$E(t)\int_0^\infty d\tau a(\tau)E(t-\tau)E(t-\tau) \Rightarrow \{\frac{3}{2} b_0[\hat{E}(t)\hat{E}^*(t)] - b_1 \frac{d}{dt}[\hat{E}(t)\hat{E}^*(t)] + \frac{1}{2} b_2 \frac{d^2}{dt^2}[\hat{E}(t)\hat{E}^*(t)] + ..\}E(t), \quad (18)$$

where

$$b_n = \frac{1}{2}\int_0^\infty \tau^n a(\tau)d\tau \quad , \quad (19)$$

so that

$$P_{NL}(t) = \{[\frac{3}{4}\varepsilon_0\chi^{(3)} + \frac{3}{2}b_0][\hat{E}(t)\hat{E}^*(t)] - b_1 \frac{d}{dt}[\hat{E}(t)\hat{E}^*(t)] + \frac{1}{2} b_2 \frac{d^2}{dt^2}[\hat{E}(t)\hat{E}^*(t)] + ..\}E(t) \equiv S(t)E(t), \quad (20)$$

where S(t) contains the slowly-varying contribution.

4. THE PROPAGATION EQUATION

The equation of evolution obeyed by the field amplitude in a medium possessing a nonlinear polarization expressed by Eq.(20) can be written by resorting to Eq.(9). To this end, let us first write the electric field, which we assume purely transverse, inside a single-mode optical waveguide as

$$\hat{E}(\rho,z,t) = 2\int_0^\infty d\omega\, \tilde{c}(z,\omega)E(\rho;\omega)e^{i\omega t - i\beta z}, \quad (21)$$

where ρ=(x,y). If we assume its bandwidth $\delta\omega$ to be much smaller than its central frequency ω_0, Eq.(21) can be rewritten as

$$\hat{E}(\rho,z,t) = 2E(\rho;\omega_0)e^{i\omega_0 t - i\beta(\omega_0)z}\int_0^\infty d\omega\tilde{c}(z,\omega)e^{i(\omega-\omega_0)t - i[\beta(\omega)-[\beta(\omega_0)]z} \equiv E(\rho;\omega_0)e^{i\omega_0 t - i\beta(\omega_0)z}\phi(z,t), \quad (22)$$

where $\phi(z,t)$ is a slowly-varying modal amplitude.

After recalling Eq.(20), the set of Eqs.(9) reduces, for the only mode present, to

$$\frac{d\tilde{c}(z,\omega)}{dz} = -i\frac{\omega}{4p_0}\int_{-\infty}^{+\infty} dx \int_{-\infty}^{+\infty} dy e^{i\beta(\omega)z} E(\rho) P^{(T)}_{NL,\omega} \quad , \quad (23)$$

where $E(\rho)$ stands for $E(\rho;\omega_0)$ and $P^{(T)}{}_{NL,\omega}$ is the Fourier transform of the quantity of the right side of Eq.(20). If we now multiply both side of Eq.(23) by the factor $\exp\{i(\omega-\omega_0) - i[\beta(\omega)-\beta(\omega_0)]z\}$ and integrate over the positive values of ω we obtain, recalling the definition of ϕ (see Eq.(22),

$$2\int_0^{\infty} d\omega \frac{d\tilde{c}(z,\omega)}{dz} e^{i(\omega-\omega_0)t - i[\beta(\omega)-[\beta(\omega_0)]z} = \left(\frac{\partial}{\partial z} + \frac{1}{V}\frac{\partial}{\partial t} - \frac{i}{2A}\frac{\partial^2}{\partial t^2} - \frac{1}{3!B}\frac{\partial^3}{\partial t^3} + ..\right)\phi \quad , \quad (24)$$

where

$$V = \left(\frac{d\beta}{d\omega}\right)^{-1}_{\omega_0} , \quad A = \left(\frac{d^2\beta}{d\omega^2}\right)^{-1}_{\omega_0} , \quad B = \left(\frac{d^3\beta}{d\omega^3}\right)^{-1}_{\omega_0} \quad (25)$$

represent respectively the group velocity, the second order group - dispersion and the third order group - dispersion. On the right-hand side of Eq.(23) we have, following the same procedure,

$$-\frac{i}{2p_0}\int_{-\infty}^{+\infty} dx \int_{-\infty}^{+\infty} dy E(\rho) \int_{-\infty}^{+\infty} d\omega e^{i(\omega-\omega_0)t - i[\beta(\omega)-\beta(\omega_0)]z} \omega e^{i\beta(\omega)z} P^{(T)}_{NL,\omega}$$

$$= -\frac{1}{4p_0} e^{i\beta(\omega_0)]z - i\omega_0 t} \int_{-\infty}^{+\infty} dx \int_{-\infty}^{+\infty} dy\, E(\rho) \frac{\partial}{\partial t} P_{NL}(t) \quad (26)$$

so that, recalling Eqs.(20), (22), and (24), we have

$$\left(\frac{\partial}{\partial z} + \frac{1}{V}\frac{\partial}{\partial t} - \frac{i}{2A}\frac{\partial^2}{\partial t^2} - \frac{1}{3!B}\frac{\partial^3}{\partial t^3} + ..\right)\phi(z,t) =$$

$$-\frac{i\omega_0}{4p_0}\int_{-\infty}^{+\infty} dx \int_{-\infty}^{+\infty} dy E^2(\rho) S(t)\phi(z,t) - \frac{1}{4p_0}\int_{-\infty}^{+\infty} dx \int_{-\infty}^{+\infty} dy E^2(\rho) \frac{\partial}{\partial t}[S(t)\phi(z,t)] \quad . \quad (27)$$

By the very definition of p_0 (see Eq.(10)) and taking advantage of the relation

$$\mathbf{e}_z \times \mathbf{H}_m^{(T)} \equiv \sqrt{\frac{\varepsilon_0}{\mu_0}}\, n\mathbf{E}_m^{(T)} , \quad (28)$$

it is easy to show that

$$2p_0 = n(\varepsilon_0/\mu_0)^{1/2}\int_{-\infty}^{+\infty} dx \int_{-\infty}^{+\infty} dx E^2(\rho) = n\,(\varepsilon_0/\mu_0)^{1/2} , \quad (29)$$

where the last equality follows from normalizing to one the integral of the square of the transverse spatial configuration of the mode.

By introducing into Eq.(27) the expression of p_0 furnished by Eq.(29), together with that of S(z,t) provided by Eq.(20), we finally obtain

$$\left(\frac{\partial}{\partial z} + \frac{1}{V}\frac{\partial}{\partial t} - \frac{i}{2A}\frac{\partial^2}{\partial t^2} - \frac{1}{3!B}\frac{\partial^3}{\partial t^3} + ..\right)\phi(z,t)$$

$$= -iR|\phi|^2\phi - \frac{R}{\omega_0}\frac{\partial}{\partial t}[|\phi|^2\phi] - iRb_1\phi\frac{\partial}{\partial t}|\phi|^2 - \frac{Rb_1}{\omega_0}\frac{\partial}{\partial t}[\phi\frac{\partial}{\partial t}|\phi|^2] + \ldots , \quad (30)$$

with

$$R = k_0 n_2 \int_{-\infty}^{+\infty} dx \int_{-\infty}^{+\infty} dy E^4(\rho) \equiv \frac{k_0 n_2}{\sigma} \quad (31)$$

where $k_0 = \omega_0/c$ and σ is the "effective area" of the mode.

It is worthwhile to recall at this point that we have only considered the longitudinal (i.e., along z) evolution of the field. Actually, the nonlinear part of the refractive index can also affect the transverse configuration of the field inside the fiber through a mechanism known as "self-focusing" This effect, for whose description we should have introduced the "radiation modes" of the structure, is negligible at the powers usually employed in the frame of fiber-optic telecommunications.

Equation (30) describes the propagation of an optical pulse in a single-mode lossless fiber. The physical meaning of the terms on its left-hand side containing second, third and higher-order time derivatives is associated with chromatic dispersion, that is with the fact that different frequencies of the wave-packet travel at different group velocities; they become more and more important as the pulse narrows because of the associated wide bandwidth. The terms on the right-hand side represent the nonlinear response of the medium. More precisely, the first one is associated with the intensity dependent part of the refractive index (see Eq.(16)) and gives rise to "self-phase modulation" while the second is responsible for "self-

steepening" of the pulse edge; the third one causes the pulse spectrum to shift toward lower frequencies , a process termed "self-frequency shift".

Equation (30) does not account for stimulated inelastic scattering processes as SRS or SBS in which energy can be transferred from a pump field either to a propagating or counterpropagating signal pulse, provided that the peak power of the former is above the corresponding threshold levels and that its wavelength lies within the bandwidth of the gain spectrum of the pump.. It can be, however, suitably modified to include the contributions due to these effects (see Sect. 7).

5. THE NONLINEAR SCHROEDINGER EQUATION AND ITS SOLITON SOLUTIONS

The equation obtained from Eq. (30) by retaining, on its right-hand side, only the first term and by dropping, on the left side, the terms containing time derivatives of order higher than the second , that is

$$\left(\frac{\partial}{\partial z}+\frac{1}{V}\frac{\partial}{\partial t}-\frac{i}{2A}\frac{\partial^2}{\partial t^2}\right)\phi = -iR\left|\phi\right|^2\phi \ , \quad (32)$$

is usually referred to as the nonlinear Schroedinger equation (NSE) and is able to describe fairly well propagation of pulses of temporal width larger than 100 fs. It is often written, in a frame of reference moving with velocity V and after introducing the dimensionless variables $\zeta = z/(T^2|A|) = z/L_D$, $\tau = (t-z/V)/T$ and $u = (RT^2|A|)^{1/2}\phi$, where T is the width of the pulse at z=0, in the normalized form

$$i\frac{\partial}{\partial\zeta}u + \mathrm{sgn}(A)\frac{1}{2}\frac{\partial^2}{\partial\tau^2}u - |u|^2u = 0 \ , \quad (33)$$

where sgn is the sign function.

For a wide class of well-behaved initial values ($u(\zeta=0,\tau)$) problems, Eq.(33) can be solved exactly by means of the inverse scattering method.[8] We will consider here, in the relevant case of anomalous second order group - dispersion (that is A<0), a particular class of solutions, termed "bright" solitons, which evolve without change in their intensity profile or with at most a periodic change (actually, to deserve this name , these solutions must have the property of passing through each other without change in their amplitudes and to be stable with respect to small perturbations).

The simplest of such solutions is the fundamental soliton, which propagates undistorted without change of shape for arbitrarily long distances (obviously, an attractive feature for information transmission in optical telecommunication systems). It reads

$$u(\zeta,\tau) = e^{-i\zeta/2}\mathrm{sech}(\tau) \quad (34)$$

or, equivalently,

$$\phi = \phi_0 e^{iz/2AT^2} \operatorname{sech}\left(\frac{t - z/V}{T}\right), \quad (35)$$

provided that

$$-\frac{1}{AT^2} = R|\phi_0|^2 . \quad (36)$$

The peak power P required, according to Eq.(36), for exactly balancing the broadening effect of chromatic dispersion through the narrowing one of the nonlinearity turns out to be quite reasonable. For example, for typical values of the fiber parameters and at an wavelength of the carrier of 1,55 μm, P = 50 mW for T = 10 ps .

If one considers a boundary condition which is the superposition on N (integer) single solitons, that is

$$u(\zeta=0,\tau) = N \operatorname{sech}(t) , \quad (37)$$

one obtains a class of higher-order solitons $u(\zeta,\tau)$ whose intensity $|u(\zeta,\tau)|^2$ is periodic with period $\zeta_0 = \pi/2$ (that is $z_0 = \pi T^2|A|/2$). For the numerical values given above, z_0 = 8 Km.

The temporal evolution over half soliton-period of the second (N=2) order soliton and over one soliton-period for the third (N=3) and fourth (N=4) order ones is shown in figs. 2, 3 and 4, respectively. The pulse structure acquires more and more complexity as N is increased.

In general, if the initial pulse shape or peak power do not satisfy Eq.(37), the pulse is still able to evolve into a soliton. More precisely, if the normalized input peak power does not correspond to an integer N but to a value N + η, with $|\eta| < 1/2$, the pulse becomes, asymptotically in ζ, a soliton whose order is N. If it is the input pulse shape which does not match the hyperbolic secant shape, then the problem has to be investigated by solving numerically the NSE. For example, in fig. 5 it is shown as a Gaussian pulse ($u(\zeta=0,\tau) = \exp(-\tau^2/2)$) adjusts its width and shape to evolve asymptotically into a fundamental soliton.

The presence of losses may be accounted for by introducing on the right-hand side of Eq.(32) the term $-(\alpha/2)\phi$, where α is the attenuation coefficient of the waveguide at the carrier frequency. The NSE can then be rewritten to include this term and reads

$$i\frac{\partial}{\partial\zeta}u + \operatorname{sgn}(A)\frac{1}{2}\frac{\partial^2}{\partial\tau^2}u - |u|^2u = -i\Gamma u , \quad (38)$$

where $\Gamma = (\alpha/2)|A|T^2$. By considering this term as a weak perturbation, Eq.(38) can be approximately solved thus getting, for an input pulse of the type $u(\zeta=0,\tau) = \mathrm{sech}(\tau)$ and in the case of anomalous dispersion,

$$u(\zeta,\tau) = e^{-2\Gamma\zeta} e^{i\sigma} \mathrm{sech}(e^{-2\Gamma\zeta}\tau) \ , \quad (39)$$

where $\sigma = (1/8\Gamma)[1- \exp(-4\Gamma\zeta)]$.

According to Eq.(39), the pulse width increases exponentially with the traveled distance z,

$$T(z) = T e^{\alpha z} \ , \quad (40)$$

while accurate numerical solutions[9] show that actually increases with a rate slower than that of a linear medium (see fig 6).

6. TELECOMMUNICATIONS WITH OPTICAL SOLITONS

The rationale underlying the employement of optical solitons for the purpose of transmitting a digital information is obviously associated with the fact that fundamental solitons preserve their shape over long propagation distances, a circumstance allowing to avoid the pulse overlapping due to chromatic dispersion As far as higher-order solitons are concerned, the existence of a structure does not lead to a significant broadening of the energy half width (as it can be seen, for example, in fig. 7 for the N=2 soliton); besides, the fact that the pulse width of higher-order solitons decreases initially can be used to advantage for compensating the loss-induced soliton broadening. In this perspective, the aim of a soliton-based communication system is simply to increase the spacing between electronic repeaters; it can be achieved by employing the low power-levels available from semiconductor lasers and leads to an increase of a factor of 2 in the repeater spacing (typically, of the order of 100 Km at a bit rate of 8 Gbit/sec).

In a more advanced perspective, the exploitation of optical solitons is envisioned to make possible the transmission of optical data at bit rates of tens of Gb/s over many thousand of kilometers, without the necessity of relying any longer on electronic devices for performing the necessary signal processing. This approach relies on the possibility of overcoming losses, a result which can be achieved either by means of an optical amplifier or by employing Raman gain to amplify the soliton through the use of a pump wave which is injected into the fiber and propagate with the signal. [10]

In this last and more promising scheme, the fundamental soliton is amplified by the interaction with a pump wave (up-shifted in frequency with respect to the soliton signal), thus being able to maintain its N=1 value (see fig. 8). Its feasibility has been actually demonstrated in an experiment where 55 psec long solitons where circulated in a fiber loop covering,

without a significant increase of their width, a distance of about 4000 Km.[12]

There are many other aspects which need to be discussed in the frame of soliton propagation because of the role they can play in setting fundamental limits on the performance of a telecommunication system. Among them, the influence of the often unavoidable phase modulation (or frequency chirp) present in the signal $u(\zeta=0,\tau)$ injected at the fiber input, the interaction among neighboring pulses which sets a lower limit on their separation time interval T_B (and thus on the bit rate $B = 1/T_B$) and the spontaneous-emission noise which coexists with Raman scattering. The reader particularly interested in these subjects is referred to Ref. 7 for an excellent discussion.

7. HIGHER ORDER NONLINEAR EFFECTS AND OPTICAL AMPLIFICATION

The purely phenomenological approach adopted in Sect. 2 has allowed us to write down the nonlinear equation of evolution of an optical pulse propagating in a single mode fiber. It contains, besides the terms responsible for self-phase modulation and self-steepening associated with the optical Kerr effect, high order nonlinear terms which become important when the pulse duration is shorter than 100 fsec, that is when its spectral width becomes comparable with the carrier frequency ω_0. In this Section, we first elucidate the physical mechanism responsible for these nonlinear terms, which is associated with Raman gain, and then generalize our equation of evolution to include the amplification mechanism which is present when the fiber, doped with rare-earth ions pumped by a suitable laser field (active fiber), can act as an active medium [13]

To this end, the nonlinear polarization is usually written as the sum of three terms,

$$P_{NL} = P_e + P_m + P_i \ , \quad (41)$$

where P_e represents the fast-responding electronic part responsible for the optical Kerr effect and P_m and P_i those associated respectively with stimulated molecular oscillations and with the resonant contributions of rare-earth ions.

The Raman contribution to P_m can be shown to give rise, as long as the pulse duration T is larger than $T_R = 1/\pi\Delta\nu_R$ (where $\Delta\nu_R$ is the bandwidth of the spontaneous Raman scattering; typically, T_R = 100 fsec) to a term completely similar to that given by Eq.(14), which corresponds to the phenomenological term containing b_0 in Eq. (20). If T becomes smaller than T_R , then P_m contributes also a term of the kind $(Rt_R)(d/dt)|E(t)|^2$ (with t_R a parameter, of the order of a few femtoseconds, related to the slope of the Raman gain around $\omega = \omega_0$) completely analogous to the phenomenological one proportional to b_1 in Eq. (20). Its physical meaning is that, for very short pulse duration, its spectral width is wide enough that the Raman gain can amplify the low frequency components by extracting energy from the high

frequency ones which act as a pump . This results in an average frequency decreasing, as observed experimentally, in which the pulse spectrum shifts toward the red side (self-frequency shift). In terms of the dimensionless variables u, ζ, and τ introduced in Sect. 5, Eq.(30) reads (by assuming A<0)

$$[i\frac{\partial}{\partial\zeta} - \frac{1}{2}\frac{\partial^2}{\partial\tau^2} - i\delta\frac{\partial^3}{\partial\tau^3}]u = |u|^2u - is\frac{\partial}{\partial\tau}(|u|^2u) + \tau_R u\frac{\partial}{\partial\tau}|u|^2 \quad , \quad (42)$$

where $\delta = |A|/6BT$, $s = 1/\omega_0 T$ and $\tau_R = t_R/T$.

The dynamics of the nonlinear polarization P_i associated with the presence of active ions can be accounted for by describing them as two-level sytems obeying Bloch's equations. At zero frequency-detuning (that is for $\omega_0 = \omega_{12}$, where ω_{12} is the resonance frequency of the two-level system) and neglecting the population variation induced by the pulse propagation , the contribution of P_i results, for pulse durations T > 100 fsec, in the addition of other local terms on the right-hand side of Eq. (42) which takes the form

$$[i\frac{\partial}{\partial\zeta} - \frac{1}{2}\frac{\partial^2}{\partial\tau^2} + ..]u = |u|^2u + ...+ i\frac{G}{2}(1 - \gamma_a\frac{\partial}{\partial\tau} + \gamma_a^2\frac{\partial^2}{\partial\tau^2})u \quad , \quad (43)$$

where G is an amplification parameter (given by the ratio between $T^2|A|$ and the amplification length) and $\gamma_a = T_{bw}/T$, where $T_{bw} = 1/\pi c\Delta\nu$ is the relaxation time of the excited level associated with the amplification bandwidth $\Delta\nu$.

The results of a numerical integration[14] of Eq. (43) (neglecting contributions of chromatic dispersion not included in A), are reported in fig. 9 for the case of one soliton pulse [$u(\zeta=0,\tau) = \mathrm{sech}(\tau)$] for a small value (G=0.2) of the amplification parameter. In this regime, the soliton amplitude and the group delay increase while its width undergoes a reduction; the pulse spectrum monotonically shifts to the low-frequency region and may eventually reach a situation where no overlapping is present with the amplification bandwidth.

We wish finally to write down, for the sake of completness and in view of the fact that Raman amplification has been proposed as a possible way of compensating losses in optical soliton propagation (see Sect. 6), the system of equations governing the evolution of the pump and signal waves (ϕ_p and ϕ_s, respectively). It reads [7,15]

$$i(\frac{\partial}{\partial z} + \frac{1}{V_s}\frac{\partial}{\partial t})\phi_s + \frac{1}{2A_s}\frac{\partial^2}{\partial t^2}\phi_s = R(|\phi_s|^2 + 2|\phi_p|^2)\phi_s - \frac{i}{2}(\alpha_s - g_s)|\phi_p|^2)\phi_s$$

$$i\left(\frac{\partial}{\partial z}+\frac{1}{V_p}\frac{\partial}{\partial t}\right)\phi_p+\frac{1}{2A_p}\frac{\partial^2}{\partial t^2}\phi_p = R\left(|\phi_p|^2+2|\phi_s|^2\right)\phi_p - \frac{i}{2}(\alpha_p+g_p)|\phi_s|^2)\phi_p \quad , \quad (44)$$

where $\alpha_{s,p}$ are the linear loss rate and g_s and g_p are the coupling coefficients of the Raman process ($g_s = g_R / \sigma$, $g_p = (\omega_p/\omega_s)g_s$, g_R being the Raman-gain coefficient, see fig. (10)).

If one neglects pump depletion, then, under stationary conditions,

$$|\phi_s(z)|^2 = |\phi_s(0)|^2 \, e^{g_s|\phi_p(0)|^2 L_{eff} - \alpha_s z} \quad , \quad (45)$$

where $L_{eff} = (1/\alpha_p)[1 - \exp(-\alpha_p z)]$, so that the amplification gain G_A is given by

$$G_A = \frac{|\phi_s(z)|^2}{|\phi_s(0)|^2 e^{-\alpha_s z}} = e^{g_R P_0 L_{eff}/\sigma} \quad , \quad (46)$$

with P_0 the pump power at the fiber input.

8. CONCLUSIONS

We have introduced a formalism which provides an accurate mathematical description of nonlinear propagation of optical pulses in dielectric waveguides.

Pulse evolution obeys a nonlinear partial differential equation which takes into account different effects (such as chromatic dispersion, self-phase modulation, self-steepening, self-frequency shift an so on), whose relative importance depends on the pulse temporal width.

Its solution, which in general requires a direct numerical integration, is expedient both for modeling soliton-based telecommunication systems, in which active fibers can be employed for amplification and regeneration of the signal, and for investigating the formation and compression of very short pulses to be used for the analysis of ultrafast phenomena.

REFERENCES

1. A. Yariv, "Quantum Electronics", 3rd Ed.(Wiley, New York, 1988).
2. H. Kogelnik , "Theory of dielectric waveguides" in "Integrated Optics", T.Tamir ed., (Springer, Berlin, 1989).
3. D. Marcuse, "Theory of Dielectric Optical Waveguides" (Academic Press, New York, 1974).
4. S. Solimeno, B. Crosignani, and P. Di Porto, "Guiding, Diffraction, and Confinement of Optical Radiation" (Academic Press, New York, 1986).
5. B. Crosignani, P. Di Porto, and A. Yariv, Opt. Commun. **78**, 237 (1990).
6. A. Owyoung, "The origins of the nonlinear refractive indices of liquids and glasses", Ph.D. Thesis (California Institute of Technology, 1971, unpublished).
7. G.P. Agrawal, "Nonlinear Fiber Optics" (Academic Press, San Diego, 1989).
8. V.E. Zakharov and A.B. Shabat, Sov.Phys. JETP **34**, 62 (1972).
9. K.J. Blow and N.J. Doran, Opt.Commun **52**, 367 (1985).
10. A. Hasegawa, Opt.Lett. **8**, 650 (1983).
11. L.F. Mollenauer, R.H. Stolen, and M.N. Islam, Opt.Lett. **10**, 229 (1985).
12. L.F. Mollenauer and K. Smith, Opt.Lett. **13**, 675 (1988).
13. see D. Payne, this Lecture Series.
14. V.V. Afanasjev, V.N. Serkin, and V.A. Vysloukh, "Amplification and compression of femtosecond optical solitons in active fibers",Soviet Lightwave Communication (to be published).
15. A. Hasegawa, Appl.Opt. **23**, 3302 (1984).
16. R.H. Stolen, Proc. IEEE **68**, 1232 (1980).

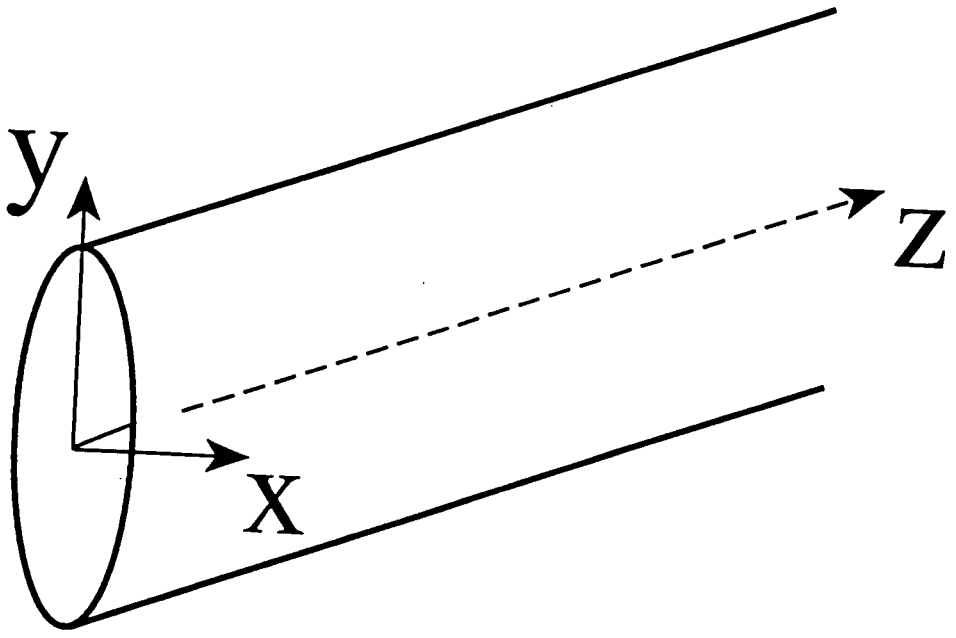

fig. 1 Waveguide geometry.

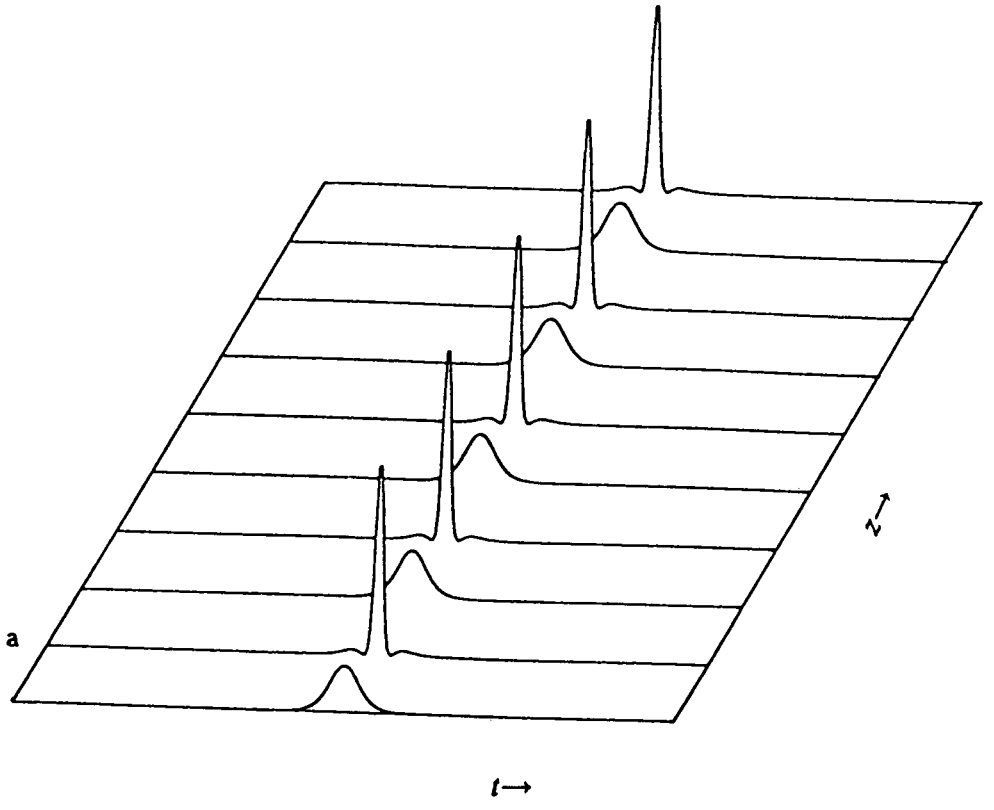

fig.2 Evolution of an N = 2 soliton.

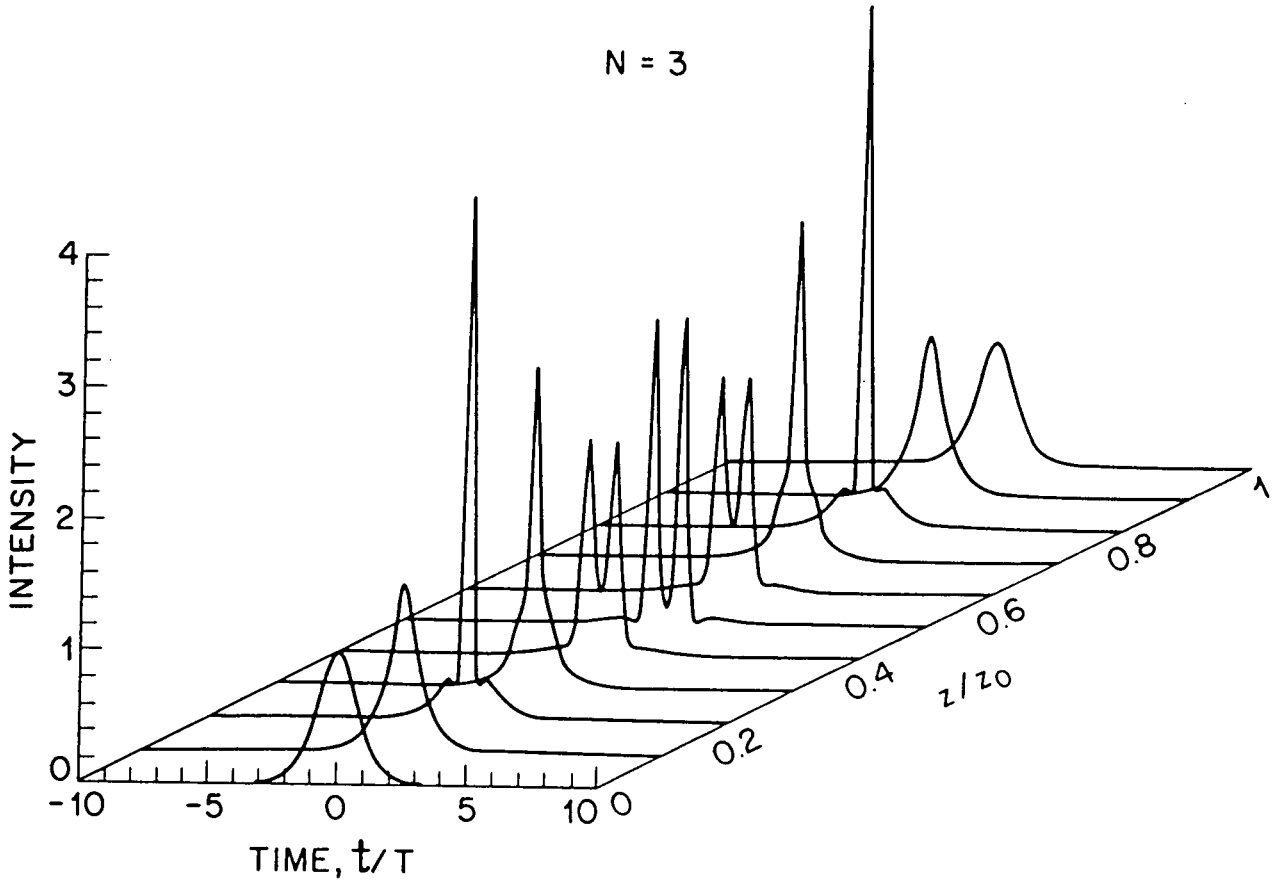

fig. 3 Evolution of an N = 3 soliton.

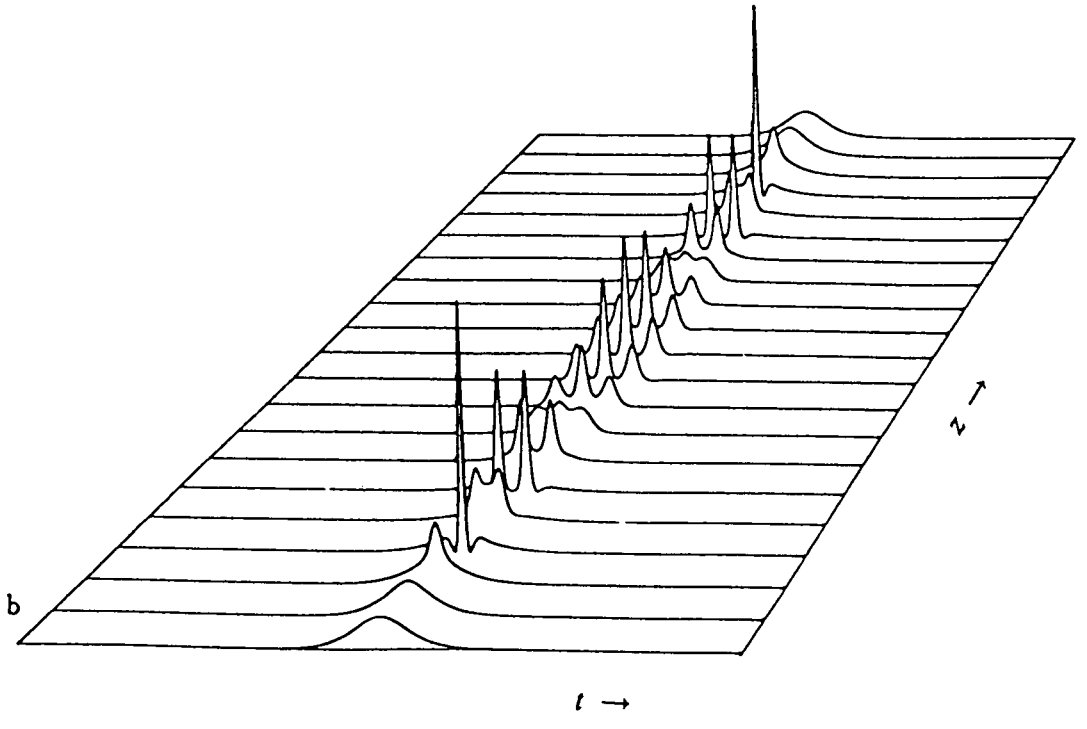

fig. 4 Evolution of an N = 4 soliton.

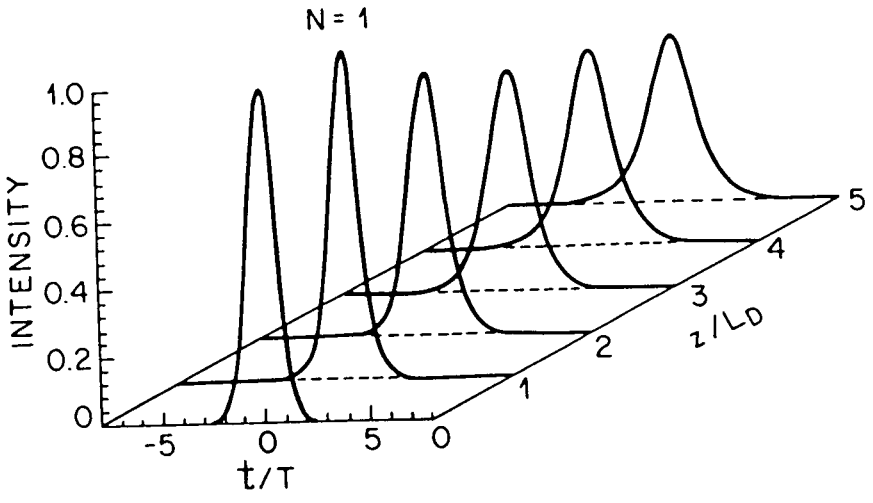

fig. 5 Evolution of a Gaussian pulse in the anomalous dispersion regime.

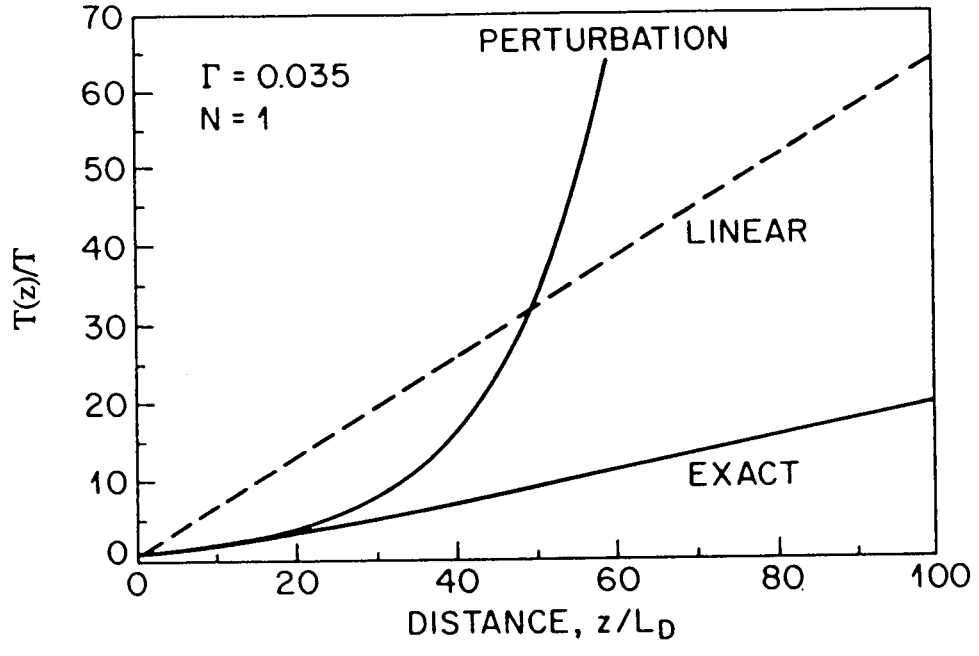

fig. 6 Behavior of the pulse width with distance in the presence of losses (after ref.9).

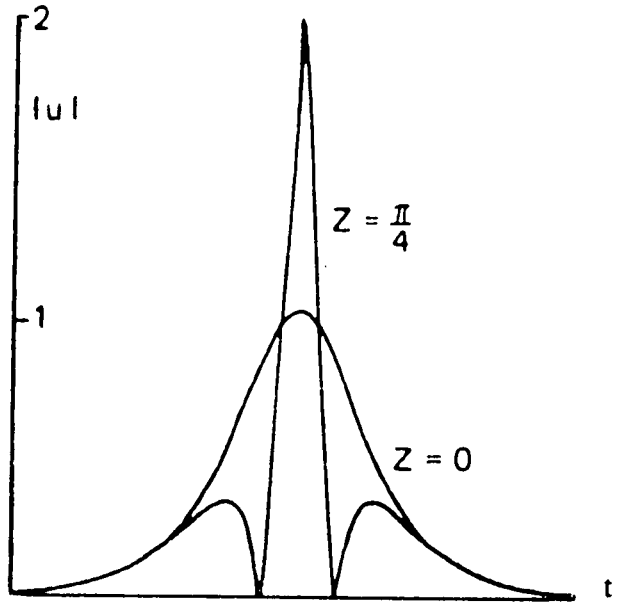

fig. 7 Pulse shape at $\zeta = 0$ and $\zeta = \pi/4$ for the N = 2 soliton.

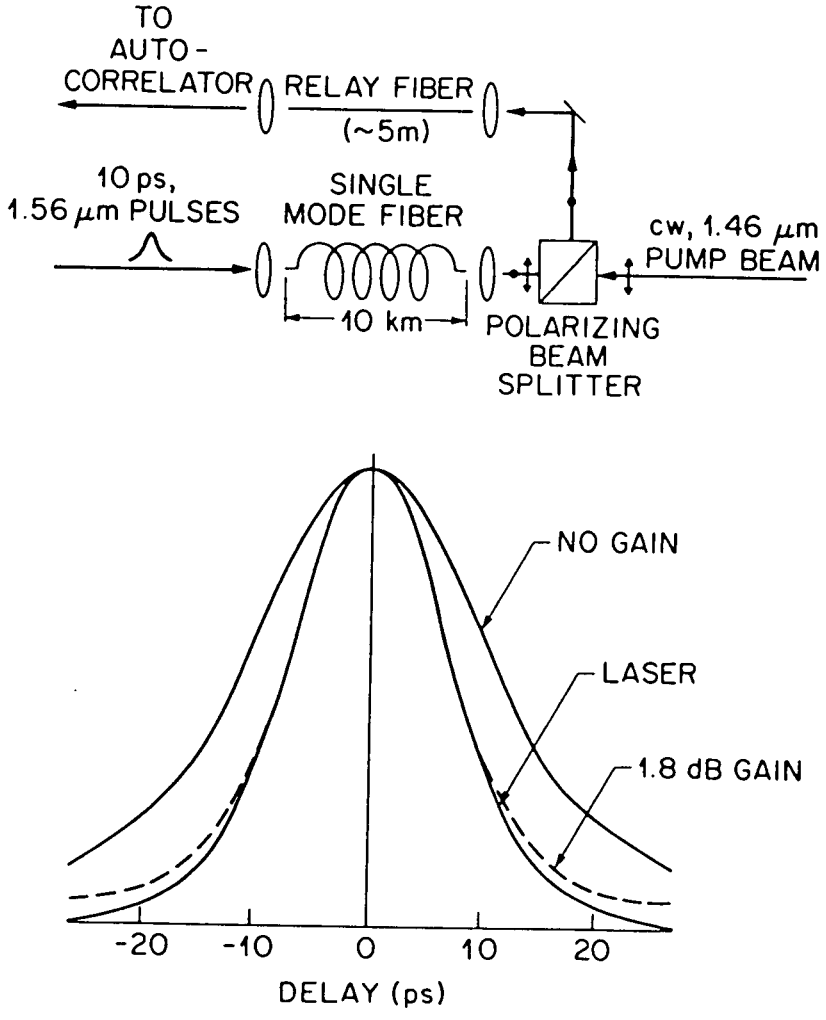

fig. 8 Experimental setup and results for a fundamental soliton propagating in a 10-km-long fiber in the presence of Raman gain (after ref.11).

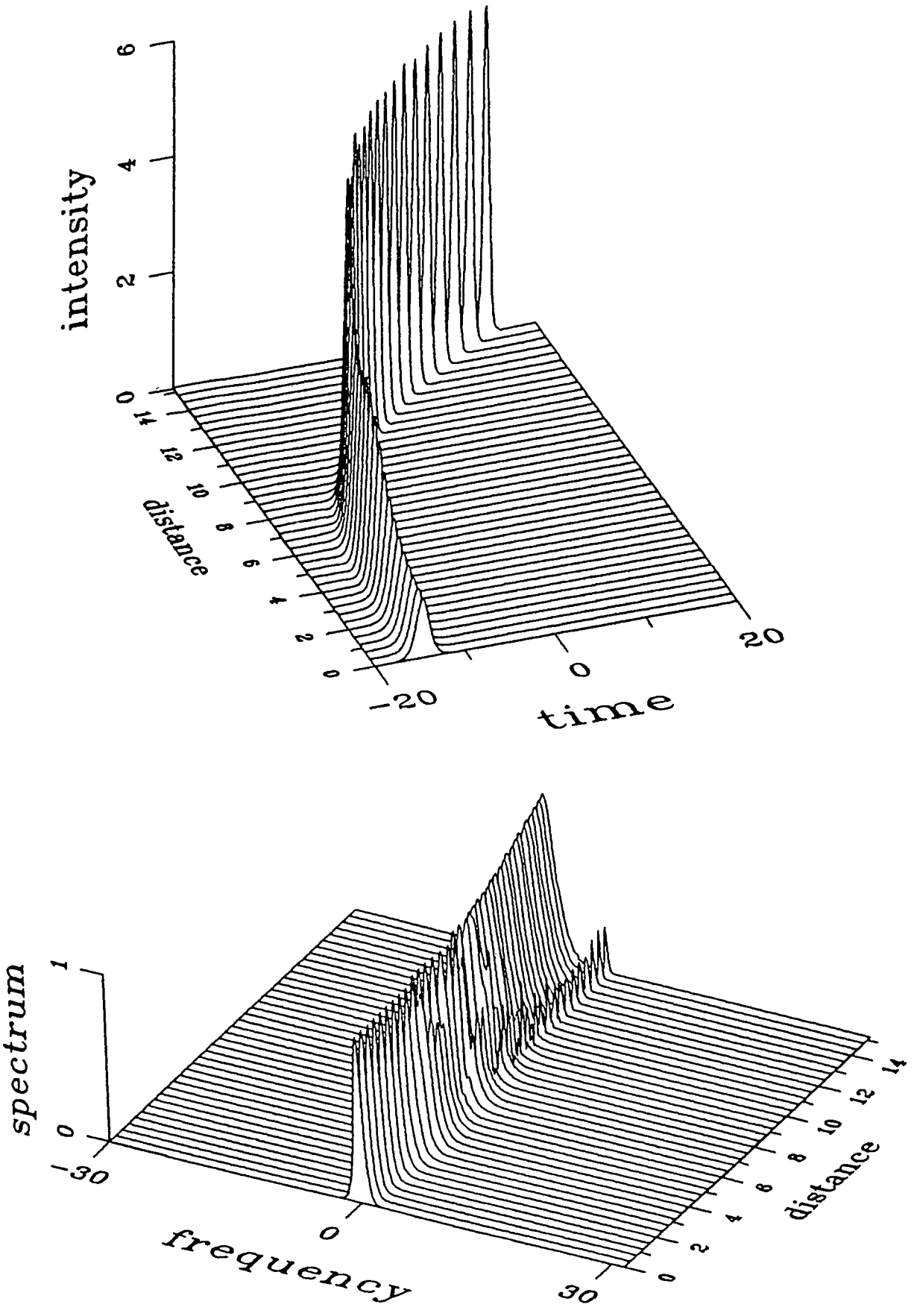

fig. 9 Evolution of the fundamental soliton for T = 100 fs, γ_a = 1 and G = 0.2; a) intensity, b) spectrum.

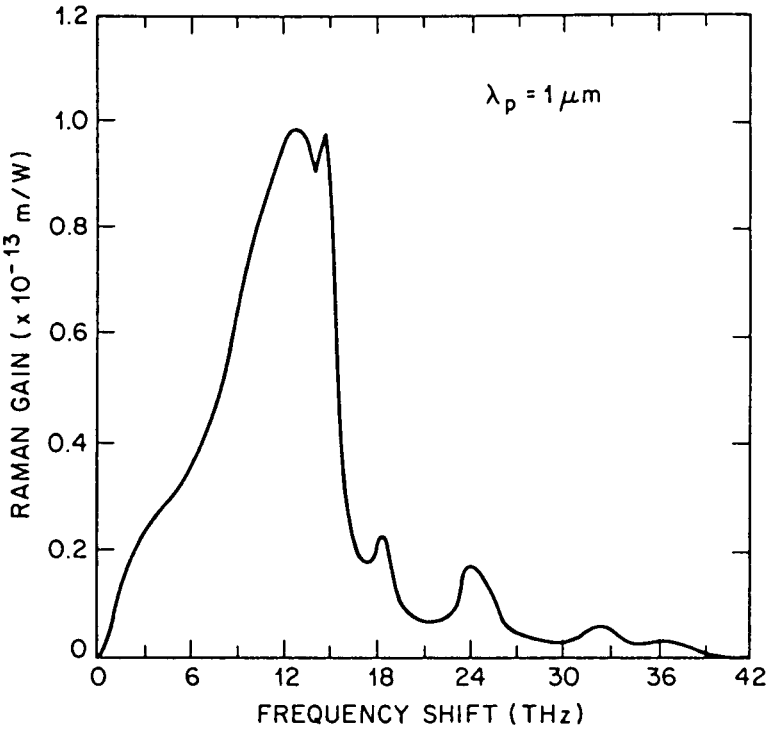

fig. 10 Raman gain spectrum of silica (after ref. 16).

ACTIVE FIBRES AND OPTICAL AMPLIFIERS

David N Payne

Optoelectronics Research Centre,
The University, Southampton, S09 5NH

INTRODUCTION

The incorporation of rare-earth ions into glass fibres to form fibre lasers and amplifiers is not a recent development. In fact the first glass laser ever demonstrated (Ref 1) was flash-pumped in the form of an optical fibre, a configuration which was used to overcome the difficulties of obtaining high-quality glass in bulk form. Apart from a report (Ref 2) in 1974 of laser operation in an Nd^{3+}-doped silica multimode fibre, the idea of guided-wave glass lasers attracted little attention for the next 24 years. The idea resurfaced (Ref 3) in 1985 because both optical fibre and laser-diode technologies had advanced to a stage where low-loss, rare-earth-doped, single-mode fibres could be made and high-power semiconductor sources were available to pump them. In addition, low-cost fibre components (couplers, polarisers, filters) were available which allowed construction of complex, all-fibre ring and Fabry-Perot resonators (Ref 4) to form a unique and powerful new fibre-laser technology. Even so, it was only the announcement in 1987 of a high-gain, erbium-doped fibre amplifier (EDFA) (Ref 5) operating in the third telecommunications wavelength-window at 1.54μm that sparked widespread interest in rare-earth-doped fibres in the optical telecommunications community. From that moment, frenzied worldwide activity has brought numerous new fibre amplifier developments and in 1990 resulted in several commercial products appearing, a time-lag of only three years after the first research announcement.

The fibre laser, on the other hand, is only now beginning to receive widespread attention as a possible contender for a well-controlled, stable light source for telecommunications, lidar, sensors and metrology, despite its obvious advantages of high-power pulsed operation, single-frequency capability, ease of access to the resonator and compatibility with communications fibre. Much of the current interest stems from the unique ability of a fibre laser to generate high-purity soliton pulses of a few picoseconds in duration for potential application in the soliton-based, long-haul high-capacity communications links of the future.

The small core size of the single-mode fibre allows high pump intensities for modest ($\sim$ mW) pump powers. Moreover, the intensity can be maintained over long lengths and this leads to ultra-low lasing thresholds and permits cw diode-laser-pumped operation of three-level lasers without the usual thermal problems. In conjunction with the long fluorescent lifetime of rare-earths in glass, the high pump intensity also allows efficient, high-gain ($>$30dB) operation of fibre amplifiers with good saturation properties. In addition, compatibility with existing fibre components is excellent, allowing all-optical circuitry to be assembled with both active and passive components. This is particularly beneficial for the fibre amplifier, where splicing of the active fibre into the telecommunication link virtually eliminates troublesome Fresnel-reflection feedback which normally limits the gain in semiconductor laser amplifiers.

ERBIUM-DOPED FIBRE AMPLIFIERS

The erbium-doped fibre amplifier (EDFA) is now established as the preferred amplifier for operation in the third telecommunications window at 1.54μm. It has high polarisation-insensitive gain ($>$40dB), low crosstalk between signals at different wavelengths, good saturation output power which increases with pump power and a noise figure close to the fundamental quantum-limit

(~3dB). The excellent noise characteristics allow hundreds of amplifiers to be incorporated along the length of a fibre telecommunication link, which can then span more than 10,000km. Compared to the alternative of a transmission link with electronic repeaters, an all-optical link has the merit that it is transparent to the transmission code format and bit rate. It can thus be uprated by changing only the transmitter and receiver, and not the repeaters.

A simplified schematic diagram of an EDFA is shown in Figure 1, while Figure 2 shows a more realistic optical configuration. The latter emphasises the compatibility of fibre amplifiers with the numerous fibre components which have been developed for telecommunications use and which are now being applied to the construction and control of amplifiers. Note particularly the requirement for optical isolators at the input and output to prevent feedback from reflections or Rayleigh scattering into the amplifier which could result in undesirable laser oscillation.

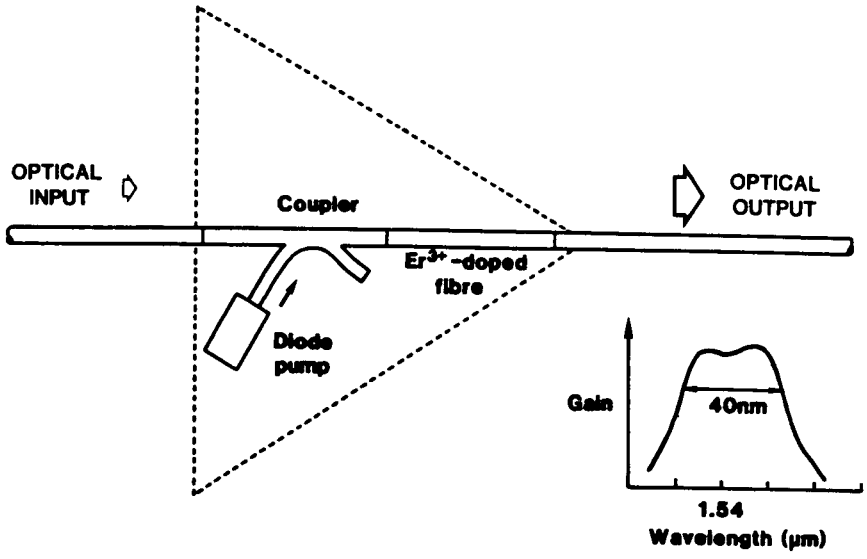

Figure 1 : Schematic of Erbium-Doped Fibre Amplifier (EDFA)

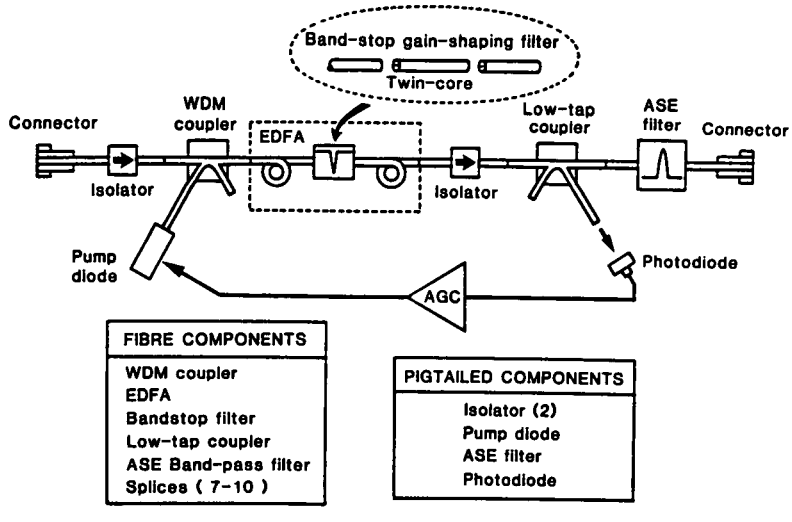

Figure 2 : EDFA showing fibre components employed

Pumping the EDFA

In order to obtain an Er^{3+} population inversion and associated signal gain, the fibre amplifier is optically pumped by a diode laser via a wavelength-division-multiplexing (WDM) coupler, as shown in Figures 1 and 2. There are a number of possible pump wavelengths corresponding to the well-known Er^{3+} ground-state absorption bands (Figure 3). Of these, potential diode-pumping wavelengths are 807nm, 980nm and 1480nm. Unfortunately, the 807nm pump band suffers pump excited-state absorption (ESA), leading to a relatively-low pump efficiency. The effect occurs when a further transition is present above the (highly-populated) upper laser level with an energy difference corresponding to that of the pump photons. In this case an additional absorption (i.e. ESA) occurs at the pump wavelength which drains pump power and limits the available gain. Nevertheless, careful choice of fibre parameters and pumping at the edge of the band (827nm) to minimise ESA has allowed a pump efficiency of 1.3dB/mW to be obtained (Ref 6). For the 980nm and 1480nm bands, maximum pump efficiencies (Refs 7, 8) of 11dB/mW and 5.1dB/mW have been obtained respectively. The result for in-band pumping at 1480nm i.e. pumping into one of the many of the Stark components of the broad signal band, are lower than for 980nm pumping because it is not possible to fully invert the erbium gain medium. However, a compensation for this lower efficiency is that the gain passband for 1480nm pumping is flatter than for 980nm pumping.

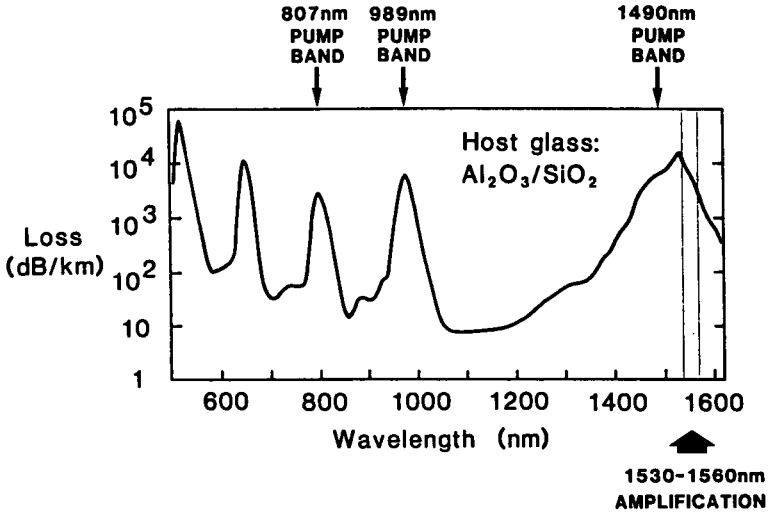

Figure 3 : Pump absorption bands of Er^{3+} in $Al_20_3Si0_2$ glass fibres

Factors which have emerged as important in achieving maximum gain for minimum pump power (max. dB/mW) are fibre numerical aperture, erbium concentration and confinement, and background loss, particularly at the pump wavelength. Unfortunately, these factors are interrelated; it is found experimentally that increasing the numerical aperture increases the fibre background loss, especially for high erbium concentrations. The best reported result of 11dB/mW (Ref 7) was for a fibre made by the VAD process. Results which exceed this value have yet to be reported, although fibres made in our laboratory using the MCVD fabrication process have achieved 8.9dB/mW. Results showing gain against pump power are shown for two such fibres in Figure 4, together with the fibre parameters. However, it should be recognised that a trade-off exists between gain efficiency and amplifier noise figure (Ref 9) owing to backward-travelling ASE which saturates the input to the amplifier and reduce its gain. Just as with electronic amplifiers, reducing the gain of a low noise amplifier front-end is always detrimental to the noise performance. We calculate that amplifiers with a gain efficiency in excess of 10dB/mW will have noise figures exceeding 4dB.

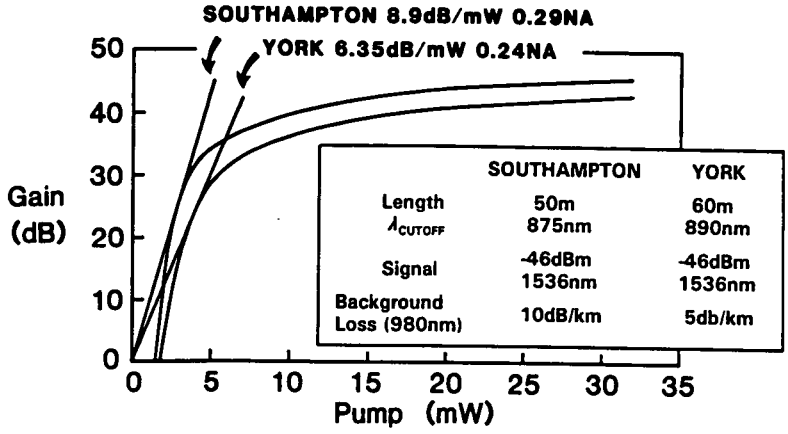

Figure 4 : Gain vs. pump power for two erbium-doped fibres with the characteristics shown

The optimum choice of pump wavelength remains an issue to be resolved, but could well depend on the intended amplifier application, i.e. as a pre-, power or line amplifier. The 980nm wavelength gives the best pump efficiency and noise figure, but pump diode lasers have yet to prove their long-term reliability, although this looks promising. Pump laser diodes at 1480nm benefit from a longer development time and have proven reliability. However, their electrical efficiency is worse than that of 980nm diodes and the amplifier electrical power consumption is therefore considerably higher, especially when one takes into account the requirement for a higher optical pump power at 1480nm because of the lower amplifier pump efficiency.

Noise

Excited states in rare-earth-doped media are subject to spontaneous as well as stimulated emission. The noise in an optical amplifier arises from the presence at the output of amplified spontaneous emission (ASE), which is given by:

$$P_{ASE} = 2\mu.\Delta\mu.h\nu\ (G-1)\ ,$$

where μ is the amplifier inversion factor, $h\nu$ the photon energy, $\Delta\nu$ the ASE spectral width and G the amplifier gain. This ASE falls on the detector along with the amplified signal, whereupon the two components are mixed to give signal/spontaneous "beat" noise. The noise is so-called because the signal acts similarly to the local oscillator in a homodyne receiver and beats with the photon noise of the cw ASE power. In addition, the ASE beats with itself (spontaneous/spontaneous beat noise) and, of course, there are the usual shot noise terms associated with both signal and ASE. Assuming a detector of unit quantum efficiency, the noise power spectral density due to amplified signal and ASE is:

$$\langle i^2 \rangle = \frac{2e^2}{h\nu}\ (A+B+C)$$

where $A = P_S + P_{SP}$ - shot noise term
$B = 2\mu P_S\ (G-1)$ - signal/spontaneous beat term
$C = 2\Delta\nu.h\nu[\mu(G-1)]^2$ - spontaneous/spontaneous beat term

where P_S and P_{SP} are the signal and spontaneous optical powers at the amplifier output. For most applications, especially if $\Delta\nu$ is made small by narrow-band filtering of the ASE at the amplifier output to match the signal bandwidth, B dominates and the noise figure is:

$$NF = \frac{\text{Input signal to noise power ratio}}{\text{Output signal to noise power ratio}} = \frac{P_{in}}{P_{out}} \frac{Noise_{out}}{Noise_{in}} = \frac{1}{G^2} \frac{B}{P_S/G} \approx 2\mu$$

Thus for a fully inverted amplifier ($\mu = 1$), the NF is 2, or 3dB.

We see that the best noise figure obtainable in an optical amplifier is quantum-mechanically determined to be 3dB and is limited by ASE which mixes with the signal on a detector to produce signal/spontaneous beat noise. It can be shown that this NF translates into a best possible sensitivity of 39 photons/bit in a digital receiver, assuming a bit error rate of 10^{-9}. It should be remembered, however, that the 3dB figure is an optimum and is dependent on the population inversion at the input to the amplifier. Although it is possible to approach a noise figure of 3dB in the amplifier by careful attention to fibre parameters, ASE filtering and pump power to ensure full inversion at the amplifier input, the results for a complete receiver are usually limited by the losses incurred at the input to the amplifier which add to the noise figure. For example, the WDM coupler and isolator shown in Figure 2 can easily add an additional 2-3dB to the noise figure. The best reported noise figure for a complete optical pre-amplifier/receiver is 137 photons/bit, which corresponds to a noise figure of 8.6dB (Ref 10). Thus improvements in front-end component losses are necessary to take full advantage of the optical fibre pre-amplifier, at which point the pre-amplifier/receiver will have much the same sensitivity as the rival coherent heterodyne detection system, with less complexity.

Output power

An important characteristic of an optical amplifier is its saturation output power. Unlike a diode amplifier, an EDFA has both a saturation output power which increases with pump power, as well as an ability to operate deep in saturation without signal distortion and interchannel crosstalk (Ref 11). As a consequence of these two attributes, when EDFAs are employed as power (post) amplifiers where the input signal is large and the amplifier heavily saturated, near quantum-limited differential pump-to-signal conversion efficiencies are possible (Ref 12).

When operating under deep saturation in the power amplifier mode, up to 93% quantum efficiency (Ref 12) and 77% absolute pump-to-signal conversion efficiency (Ref 13) have been respectively obtained for the two preferred pump wavelengths (980nm and 1.48μm). These results indicate that the amplifier is operating as a near-perfect photon convertor and little further improvement is possible.

EDFA's capable of high output powers (>20dBm) are needed to compensate splitting losses incurred in large-scale subscriber distribution networks and in analogue transmission of multiple TV channels. The search for EDFA's with high output power depends largely upon the availability of a sufficiently-powerful and practical pump source. Approaches vary from the use of multiple-diode lasers (Ref 14), to the adoption of Nd:YAG mini-lasers (Ref 15) and Nd^{3+}-doped fibre lasers (Ref 16). The latter two emit at a wavelength around 1.06μm and can give output powers in excess of 1 Watt, thus showing considerable potential as pumps for EDFA's with output power approaching +30dBm. Erbium does not possess a pump absorption band at 1.06μm and cannot therefore normally be pumped at this wavelength. Co-doped fibres are an attractive means of alleviating constraints on the pump source wavelength by using a sensitiser with a broad absorption band. Ytterbium is especially attractive in this regard as it exhibits an intense broad absorption between 800nm-1080nm, spanning several convenient pump wavelength source options, including Nd^{3+}-doped lasers. Figure 5 shows the pump absorption bands of Er^{3+} in silica, with the Yb^{3+} absorption superposed (c.f. Figure 3). The relevent energy levels for Er^{3+} and Yb^{3+} are shown

in Figure 6. Energy is transferred from Yb^{3+} to Er^{3+}, the efficiency of which depends strongly on the glass host. In bulk phosphate glasses this efficiency can be 85%, principally due to the reduced probability of back transfer (Er^{3+} to Yb^{3+}) for this host. We have found that SiO_2/Al_2O_3 fibres made by the MCVD process can mimic a phosphate glass provided sufficient P_2O_5 is added as a dopant. Such silica-based fibres show considerably improved transfer efficiency.

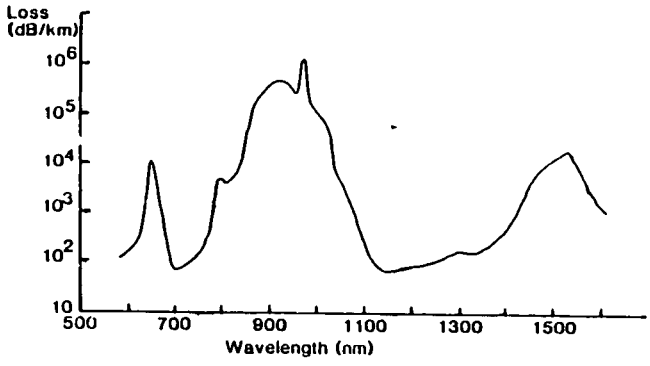

Figure 5 : Absorption spectrum of Er^{3+}/Yb^{3+} co-doped fibre. Note large absorption centred at 900nm caused by Yb^{3+}

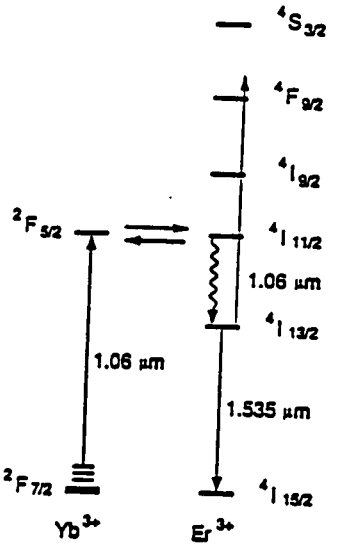

Figure 6 : Er^{3+} and Yb^{3+} energy levels showing the energy-transfer pumping scheme

To construct a power amplifier using these fibres, a high-power, diode-pumped, Nd:YAG laser operating at 1064nm is used to pump into the long-wavelength tail of the Yb^{3+} absorption. Such mini-YAG lasers are commercially available with output powers exceeding 1 watt, and are potentially scalable to even higher powers (Ref 17). The Er^{3+}/Yb^{3+} fibre approach therefore shows considerable potential for EDFA's with output power approaching +30dBm. Although not as mature as Nd:YAG mini-lasers, the cladding-pumped Nd^{3+}-doped fibre laser (Ref 16) has been shown to give an output of 1W using a similar multi-stripe pump diode to the Nd:YAG and therefore the fibre laser shows even greater promise as a pump source for an all-fibre, high-power EDFA.

Gain spectrum flattening

A number of schemes have emerged to flatten the broad (>35mm) but unequal EDFA gain spectrum (Figure 7) which causes problems in multichannel WDM transmission systems. Some progress can be made with choice of fibre materials, particularly Al_2O_3 co-doping and the use of ZBLAN fibres, although the most promising approach appears to be the use of an internal compensating filter within the amplifier (Ref 18). This approach has the merit that the gain spectrum can be shaped and flattened without loss of pump efficiency and dynamic range, leading to an amplifier characterised by a gain in excess of 25dB and a 3dB bandwidth >30nm for a pump power of <50mW. The technique can be understood by imagining that the front half of the EDFA acts as a pre-amplifier and the remainder as a power amplifier. As is common is audio amplifiers, response-shaping is best done in the pre-amplifier, thereby preventing the power amplifier from saturating and wasting power. The spectrally-shaped gain profile is shown in Figure 7 for an amplifier with a compensating bandstop filter placed within its length in order to attenuate the gain

peak which occurs at 1536nm. However, even with spectral shaping, for long amplifier chains involving large numbers of EDFA's, some form of spectral AGC will be required to precisely balance individual channels across a wide spectral range and prevent an accumulation of channel imbalance.

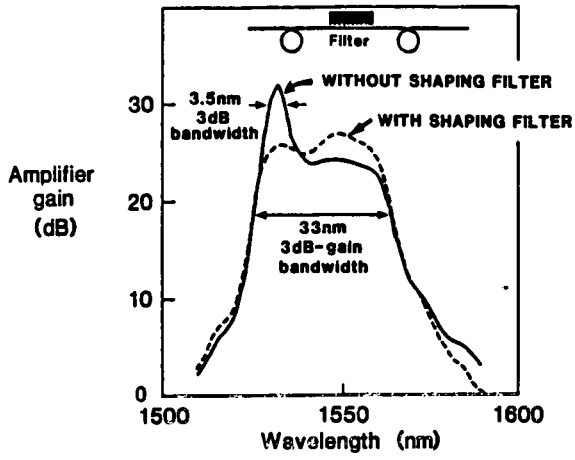

Figure 7 : EDFA spectral gain profile, showing gain flattening by addition of a shaping filter within the amplifier length

Erbium-doped planar-waveguide amplifiers

Although the planar waveguide approach to erbium-doped amplifiers is attractive, particularly for lossless splitting of a signal into a large number of output ports (Figure 8), the search for a planar "EDFA" is plagued by erbium concentration effects which result in a large loss of radiative quantum efficiency once the erbium concentration exceeds a few hundred ppm, an effect known as concentration quenching. This effect limits the minimum length of the amplifier to around a metre before a severe loss of efficiency occurs. Figure 8 shows the results obtained to date for the radiative quantum efficiency of Er^{3+} ions in various glass hosts and it can be seen that a severe reduction occurs for concentrations of Er^{3+} above about 300ppm, with fluoride glasses being the most benign host. Note that this problem is peculiar to Er^{3+} and occurs to a far smaller degree in other rare-earths, such as Nd^{3+}. The search continues to find a glass host which is able to accept a higher level of erbium doping from which amplifiers of a few cm in length can be fabricated.

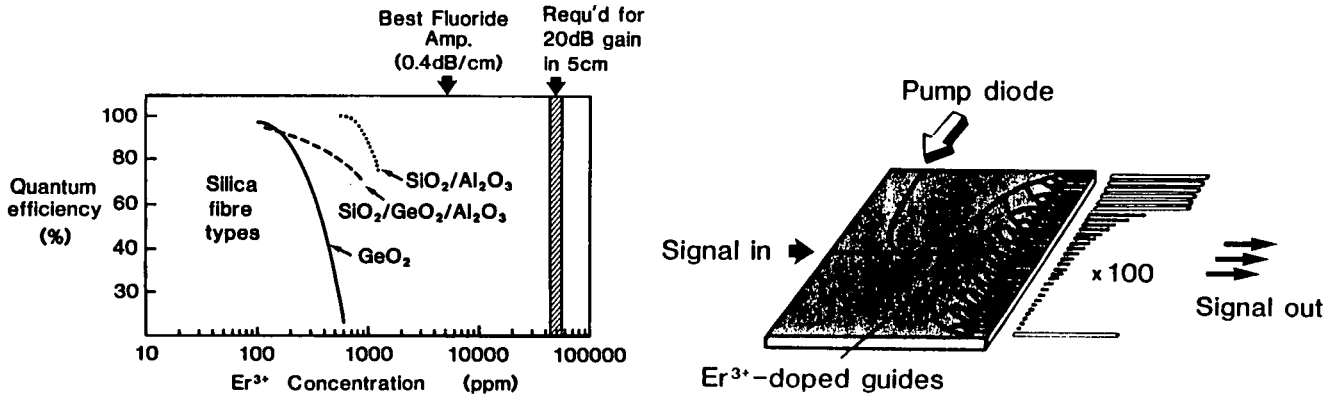

Figure 8 : Lossless splitting scheme in an erbium-doped planar waveguide amplifier (left). Right shows the reduction in quantum efficiency which results from the high Er^{3+} doping required to make a short amplifier

Fibre amplifiers at 1.3μm

As can be seen from the above, the EDFA provides almost the ideal amplifier for 1.55μm operating wavelengths. Unfortunately, 1.55μm systems are still predominantly laboratory experiments and although they will undoubtedly form the systems of the future, by far the largest proportion of currently operational optical transmission systems operating in the 1.3μm wavelength window. A 1.3μm fibre amplifier would be extremely useful for upgrading or extending existing systems. Two candidates have emerged, neodymium and praseodymium-doped fibre amplifiers. In the case of neodymium-doped fibre, a transition exists between the $^4F_{3/2}$ and $^4I_{13/2}$ levels which gives rise to fluorescence near 1.32μm. Unfortunately, (i) a signal ESA band exists near 1.3μm and (ii) strong competing transitions from the same level occur at 0.9μm and 1.06μm. The effect of the ESA is to prevent gain at wavelengths shorter than about 1.36μm, whereas the competing transitions cause large gain to build up at other wavelengths which must be reduced to prevent ASE losses and eventually lasing. In fluoride (ZBLAN) glass the ESA spectrum is shifted to shorter wavelengths and 10dB gain at 1.345μm has been reported for only 50mW pump power (Ref 19). Thus to date the gain is too low and the wavelength too long for telecommunications requirements.

Perhaps the most exciting recent development has been reports of a praseodymium-doped fluoride fibre amplifier. Pr^{3+} exhibits fluorescence at 1.3μm on the $^1G_4$ - $^3H_5$ transition, but this is heavily quenched by multi-phonon decay to the underlying $^3F_4$ level in all but the lowest phonon-energy glasses, hence the choice of ZBLAN (Ref 20). Even in ZBLAN glass, the radiative quantum efficiency has been measured at only a few percent, which leads to a low amplifier pump efficiency. To compensate this, small core, high-numerical aperture fibre designs have been developed in an attempt to achieve high gains at pump powers obtainable from diode lasers. Miyajima et al (Ref 21) have demonstrated a 32dB true amplifier gain for a pump power of 300mW at 1.01μm and a peak pump efficiency of 0.2dB/mW (Figure 9). This compares poorly with the 11dB/mW obtained for the EDFA. However, these are early days and much effort is underway worldwide to improve the Pr^{3+}-doped fibre amplifier. The most promising approach apart from high-NA designs is to find a glass host with even lower phonon-energy than exhibited by ZBLAN to inhibit the multi-phonon decay process. Several groups are working on modified fluoride glass compositions for this purpose. However, even if successful in improving pump efficiency, there are a number of engineering issues yet to be solved involving strength, environmental stability and splicing of ZBLAN glasses to silica communications fibre.

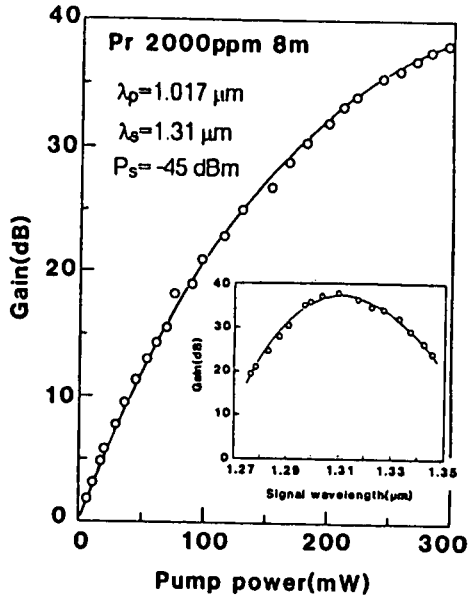

Figure 9 : Gain vs. pump power for a Pr^{3+}-doped ZBLAN glass fibre. Inset shows spectral gain (Ref 21)

Systems applications

From the foregoing it can be seen that the EDFA exhibits a performance close to that of an ideal amplifier. It is efficient, diode-pumpable, broadband, has both low noise and a high-output power and is fully compatible with fibre systems. Although undoubtedly requiring quite different amplifier designs, EDFA applications fall into three groups.

Line-amplifiers, which replace conventional electrical repeaters in long-haul telecommunications links, particularly undersea routes. A major difference between electrical repeaters and optical amplifiers is that the optically-amplified link becomes "transparent" in an electrical as well as an optical sense. The medium is no longer specific to bit-rate and format, nor even (within limits) to the wavelength of the signal, thus allowing multichannel transmission. The link is thus truly an optical conduit; a system upgrade can be achieved by changing only the terminals and not the numerous repeaters of the conventional link.

Power (Post) Amplifiers, which allow boosting of weak transmitter signals to the required power level. They also find extensive use in multi-way splitting and reamplification (so-called lossless splitting). This latter application is particularly important as fibre telecommunications moves towards subscriber applications. Pump-to-signal power conversion efficiency is clearly the prime requirement and we have noted earlier the advances in efficient, high-power amplifiers.

Pre-Amplifiers, allow sensitive, near quantum-limited detection in (especially) very high bit-rate systems, where electrical amplifier performance is poor. Here low noise and pump efficiency are prime requirements. Progress in these areas has also been dealt with above.

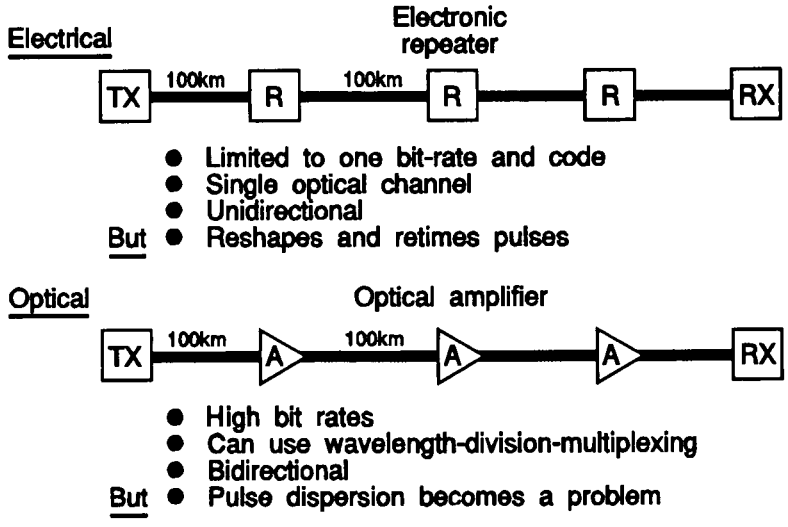

Figure 10 : Comparison between electrical and optical amplification for transmission

The advent of EDFA line amplifiers has raised some interesting new issues in long-haul system design. The differences between electrical and optical amplification for transmission are shown schematically in Figure 10. Whereas long-haul transmission links were hitherto always loss-dominated, the advent of the EDFA has effectively eliminated this and virtually- lossless links of 10,000km or more can now be contemplated. However, the one merit of electrical repeaters is that they retime and regenerate the incoming signal before retransmission and thus are able to correct any dispersion experienced by the pulses. By contrast, the optical amplifiers in a transmission link faithfully reproduce a dispersed pulse, and the designer now has to cope with up

to 10,000km (i.e. the trans-Pacific distance) of dispersion. Although adopting dispersion-shifted fibre helps considerably, it is unlikely that fibre manufacturers will be able to adjust the dispersion parameters of the fibre sufficiently accurately to ensure sufficiently low dispersion over these distances. Nonetheless, it is thought that a bit-rate of 1Gb/sec is achievable over a distance of 10,000km provided the dispersion in the fibre can be kept to below an average of 2.5ps/nm.km. There is also some hope that dispersion equalisation can be achieved using a compensating fibre at the end of the link having a large opposite dispersion characteristic to that of the ensemble. The bit-rate-distance projections for dispersion-shifted and non-dispersion-shifted fibre are shown in Figure 11, which also shows that there exists a solution to the problem of dispersion, namely, the use of non-linear transmission.

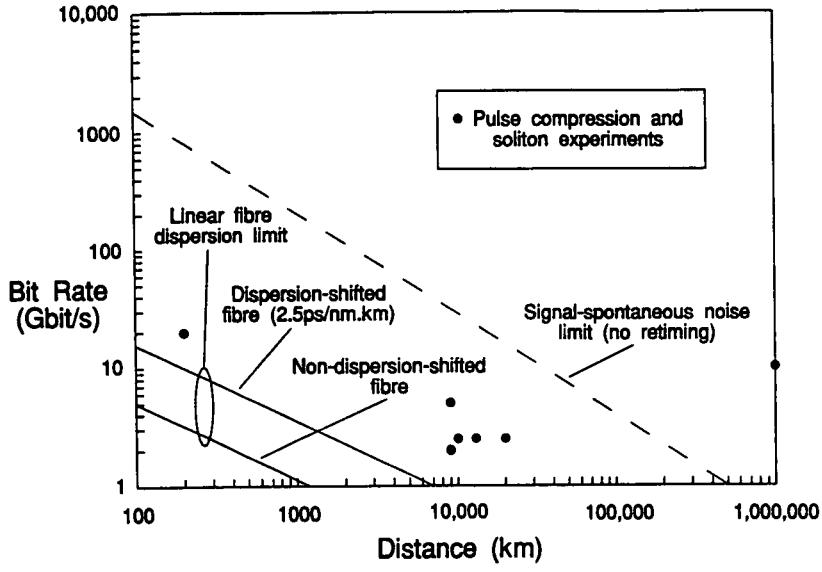

Figure 11 : Bit-rate vs. distance for dispersion-shifted and non-dispersion shifted fibres. Also shown are reported non-linear transmission experiments, together with the Gordon-Haus limit for amplified links

Non-linear transmission involves the use of soliton pulses. The refractive-index of glass varies slightly with optical intensity, about 10^{-13} per mW propagating in the core of a typical fibre. A consequence of this is that a pulse propagating in a glass fibre sees a moving "valley" of higher refractive-index material which travels with it. This refractive-index "valley" tends to cause bunching of high-intensity light, slowing the faster (blue) components of the pulse and speeding up the slower (red) components. It transpires that there is a critical pulse intensity and duration for which the non-linear refractive-index change can exactly balance the natural dispersion of the fibre. Such pulses are called optical solitons and are characterised by a peak power P_s given by:

$$P_s = \frac{0.0763\, A\lambda^3}{Cn_2} \cdot \frac{D}{\tau^2}$$

where A is the core-mode effective area, λ the operating wavelength, D the fibre dispersion, C the speed of light, n_2 the non-linear index and τ the soliton FWHM duration. For a typical pulse duration of 50ps and a fibre dispersion of 2ps/nm.km, the peak pulse intensity required is about 1mW, which is easily attainable using diode lasers. In theory, an optical soliton will propagate indefinitely without dispersion. Unfortunately, in practice the soliton intensity decays along the fibre owing to the fibre loss, until once below a critical intensity, the pulse suffers normal dispersion effects and rapidly broadens.

The advent of optical amplifiers has made soliton transmission a real possibility, since the soliton intensity can be boosted every 20km or so to ensure that it does not fall below the critical dispersion threshold. Although it sounds unlikely, it transpires that the soliton pulse is a remarkably stable pulse form and proves resistant to perturbations in fibre dispersion, multiple repeated amplification and (to a limited extent) amplifier ASE noise. The latter effect causes a variance in pulse arrival times and provides the ultimate limit (the Gordon-Haus limit) to soliton bit-rate distance capability, shown by the dashed line in Figure 11. Also shown in the figure are results for recent multi-amplifier, soliton transmission experiments, most of which have been performed in recirculating loop configurations. From the figure it can be seen that up to two orders of magnitude improvement in distance-bit-rate product can be obtained by non-linear transmission using solitons and several experiments have proved the concept. Also noted in Figure 11 is a single experimental point indicating the possibility of 10Gbit/sec transmission over one million kilometres (Ref 22), an extraordinary result which appears to exceed the Gordon-Haus limit, an achievement which was made possible by optically reshaping the pulse periodically, as an the electrical repeater.

The advent of EDFA's has made soliton transmission a reality, although there exists a variety of opinions as to whether practical telecommunications links using solitons are practical. One school of thought believes that non-linearities in fibre will inevitably be encountered in long-haul transmission and therefore should be harnessed to advantage, while the other argues that non-linear transmission is too complex to engineer reliably and that adequate transmission capacity can be obtained in the linear regime.

FIBRE LASERS

Fibre lasers are essentially photon convertors. They use the "raw" photons emitted by diode lasers to excite rare-earth ions contained within the fibre core which subsequently emit a stable, well-controlled laser beam. Because of the guiding properties of the fibre, the diode-laser pump light is tightly confined over the distance required for absorption and this leads to a high population-inversion density. This large inversion density is readily obtainable in both three and four-level laser systems at modest pump powers and gives a high single-pass gain without the usual thermal problems associated with bulk-glass lasers. The high gain, often tens of dB, allows complex resonators to be designed without undue attention to the loss of the components employed in the construction, such as couplers, isolators and modulators. The fibre laser output is well-defined, having a beam profile which is close to a diffraction-limited Gaussian. The fibre laser resonator is stable, and provides a rugged, well-confined and easily-accessed laser cavity. The diode-laser designer, on the other hand, now freed of the need to produce an optical output suitable for telecommunications, can concentrate on efficient optical power generation. This freedom of design has led to pump lasers becoming available with output powers >30W for pumping mini-YAG lasers, and we can expect similar developments at wavelengths suitable for pumping a variety of fibre lasers.

The fibre laser geometry allows a compact, flexible layout, easy connection to optical components and a stable, optically-confined laser beam. While much of the commercial interest is likely to be in sources based on Er^{3+}, Pr^{3+} and Nd^{3+} for optical communications, it is also important to realise that four other rare-earths have successfully been incorporated into silica hosts and operated as fibre lasers, namely, samarium, ytterbium, thulium and holmium. An indication of the optimal pumping environment provided by the fibre laser is that laser action of Pr^{3+} and Sm^{3+} in glass has only been achieved in fibre form.

Fibre-laser oscillation covers the range 651nm (Sm) to beyond 2μm (Tm, Ho). Figure 12 shows the laser lines which have been reported to date, together with the loss windows of silica and

fluoride-glass fibres. Erbium sits conveniently at wavelengths of 1.54μm and 2.7μm, both close to the lowest loss wavelengths of these two fibre types. Furthermore, Er^{3+}-doped fibre lasers can operate with close to unity quantum efficiency (Ref 23) when pumped at 980nm and an output power of 5mW is readily-obtainable for launched pump powers as low as 15mW, a power well within the range of pump diodes. A typical fibre laser Fabry-Perot resonator is shown in Figure 13. Numerous resonator configurations are possible based on fibre-optic fused couplers, for example, ring resonators, anti-resonant-ring reflectors (fibre-loop mirrors) and Fox-Smith resonators, as well as hybrid versions of these. A useful review of fibre laser configurations is given in Ref 24.

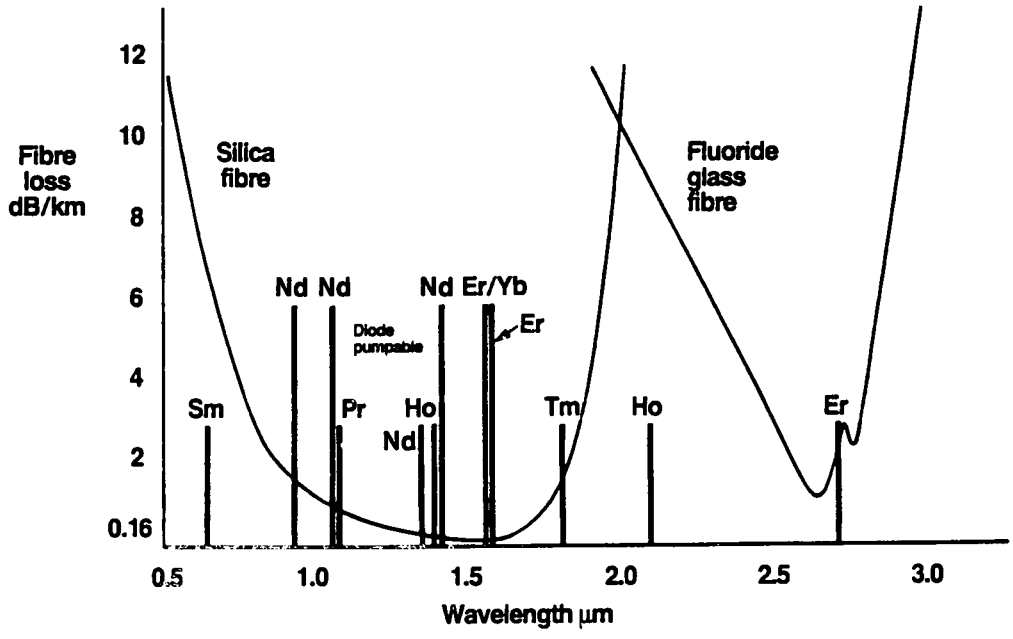

Figure 12 : Reported fibre laser wavelengths compared to silica and fluoride glass fibre transmission windows

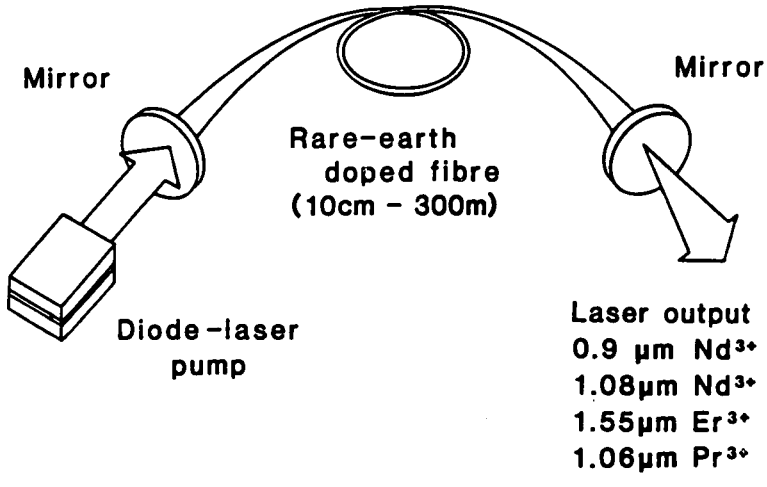

Figure 13 : Fibre laser Fabry-Perot configuration

Current worldwide fibre-laser research covers a broad spectrum. As just one example of recent results (Ref 25), the tuning range obtained for a Tm^{3+}-doped fibre lasers is shown in Figure 14 for both an Al_2O_3-SiO_2 fibre and a GeO_2-SiO_2 fibre. The tuning range is extremely broad, being almost 300nm (1.66μm to 1.86μm) for the Al_2O_3-SiO_2 host glass. Also noteworthy is the strong effect of

the host glass composition (see curve for GeO_2-SiO_2 glass), a characteristic of glass-based lasers which can be usefully employed to adjust the emission wavelength of fibre lasers.

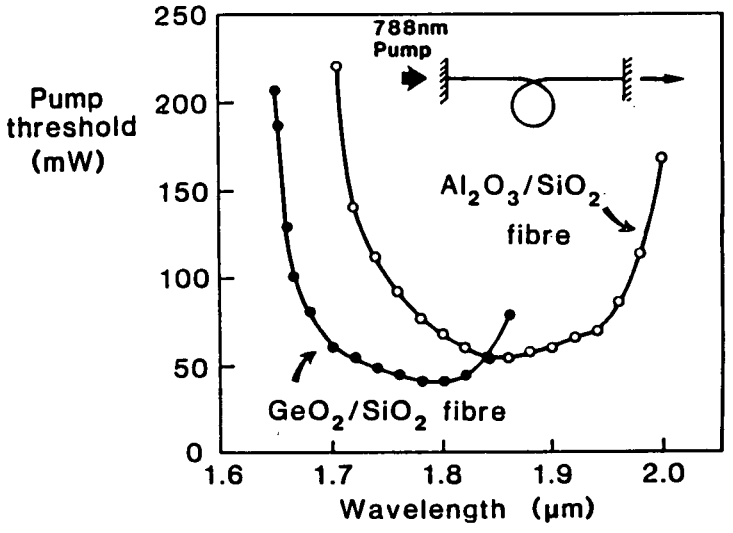

Figure 14 : Tuning curves for Tm^{3+}-doped fibre lasers using either Al_2O_3 or GeO_2 as a co-dopant

The thulium-doped fibre laser covers an extremely valuable part of the spectrum which is eye-safe. Strong interest in this wavelength region has recently emerged for gas sensing (particularly of hydrocarbons), lidar, windshear detection and volcanic ash cloud sensing. The wavelength can be extended to over 2μm and high-power lasers emitting in excess of 1W should be possible.

High-power fibre lasers

It is commonly thought that fibre lasers are low-power devices and therefore not competitive with diode-pumped bulk crystal lasers. However, by employing special glass fibre technology and novel inner-cladding geometry, it is possible to construct a Nd^{3+}-doped, single-mode fibre laser emitting an output power of 1.07W at a wavelength of 1.057μm. The laser is pumped with a 3W GaAlAs multi-stripe, laser-diode array and has several advantages over its similarly-pumped Nd:YAG counterpart. For example, the broad absorption line of Nd^{3+} in glass obviates the need for selection and temperature stabilisation of the pump-diode wavelength. The waveguide nature of the fibre resonator makes mirror alignment simple, eliminates thermal focussing and ensures perfect transverse-mode selection. The laser cavity is therefore substantially immune from environmental effects. In addition, fibre lasers are broadly tunable and, by the use of a variety of well-established fibre technique, can give high-power, Q-switched output, femtosecond mode-locked pulses and narrow-linewidth operation. The technique of cladding-pumping (Ref 26,27) allows pumping of single-mode fibre lasers with a multimode diode array, thus allowing the fibre laser to exploit the increasingly-available, high-power, diode-pump sources. Since the output of multistripe diode arrays is not uniphase, it cannot be efficiently launched into the core of a single-mode fibre laser. This problem is overcome by launching into the cladding of the fibre which is designed to guide the multimode light from the diode array by the addition of a further outer cladding, as shown in Figure 15. To optimally match the diode emission to the fibre requires careful choice of materials and design of the fibre cross-sectional geometry. The fibre utilises compound glass technology to obtain both an optimal geometry and a high radiative cross-section. The fibre geometry is shown in Figure 16 (inset) and comprises a heavily Nd^{3+}-doped (3wt%) core located centrally within a rectangular, highly-multimode, undoped, inner-cladding waveguide of

lower-index glass into which the pump light is injected. This inner cladding was in turn clad with a further lower index glass to give a high numerical aperture (0.42) and a circular fibre cross-section. The inner cladding was thus designed to match the large diode diffraction angle and emitting area, whilst minimising the core/inner cladding area ratio, thus optimising pump absorption in the core and minimising the laser threshold (Ref 28).

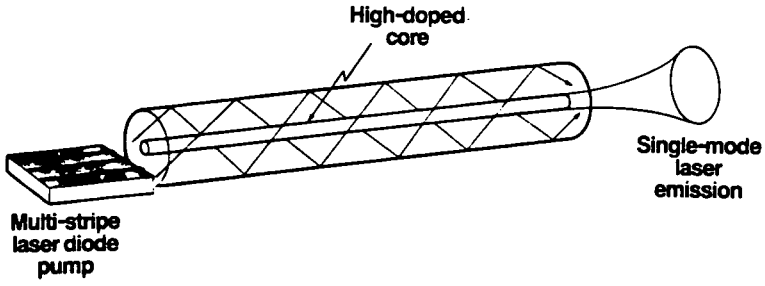

Figure 15 : High-power cladding-pumped single-mode fibre laser

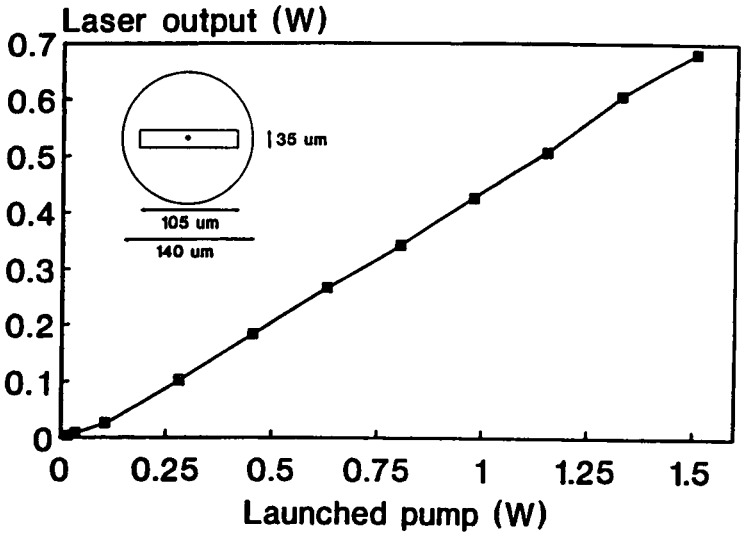

Figure 16 : Nd^{3+}-doped cladding-pumped fibre laser characteristic. Inset shows fibre cross-section

Pump light at 808nm from a 3W diode array was launched into the rectangular inner cladding of the laser fibre through a highly-reflective dichroic mirror butted to the endface, the other mirror being simply a cleaved fibre endface giving 4% Fresnel reflection. With the pump diode laser operating at full power, the fibre laser gave 1.07W output power at a peak wavelength of 1.057μm. As shown in Figure 16, the slope efficiency with respect to absorbed power was around 50%, which is close to the maximum attainable.

Owing to its simplicity and robustness, the high-power fibre laser provides a competitor for diode-pumped Nd:YAG lasers in many applications, being potentially cheaper and widely tunable. Furthermore, fibre compatibility allows ready exploitation of the wide range of fibre devices available and permits integration into complex fibre optical circuits. As an example of this, the above high-power fibre laser has been used as a pump source for a high-power, Er^{3+}/Yb^{3+} fibre telecommunications amplifier at 1.54μm, using an all-fibre, tandem-pumping arrangement (Ref 29).

Tunable, single-frequency fibre lasers

One of the consequences of the very broad fluorescence linewidth of rare-earth and glass fibres is that fibre laser output emission is in general broadband, usually around 10nm or so. Although this is of no significance in some applications, for telecommunications, metrology or sensing the requirement is usually for only one of the numerous possible resonator modes to oscillate. This so-called "single-frequency" operation inhibits intensity noise generated by both intermode competition and mode-hopping and provides a highly monochromatic output with very-low relative intensity noise. The spectral linewidth for single-frequency operation is that of just one of the resonator modes and is given by the Schawlow-Townes limit which indicates, amongst other factors, that the linewidth is inversely proportional to the resonator length. Since typical fibre lasers are metres in length, whereas diode-lasers are submillimetre, fibre lasers can exhibit single-frequency operation with linewidths in the kilohertz region, whereas diode lasers have megahertz linewidths. This is a very attractive attribute of fibre lasers.

A less helpful consequence of the long fibre laser resonator is the close frequency spacing Δf of the axial laser modes, given by:

$$\Delta f = \frac{c}{2Ln}$$

where c is the speed of light, L the resonator (fibre) length and n the core refractive index. Obtaining single-frequency operation requires the selection of just one of these dense comb of oscillating laser lines. Two approaches can be taken:

1. The use of a short Fabry-Perot resonator to space the axial modes as widely as possible, in conjunction with a very narrowband Bragg reflector as one of the laser feedback mirrors (Ref 30).

2. The adoption of a travelling-wave resonator (Ref 31) which automatically encourages single-axial-mode operation by elimination of spatial hole-burning. Spatial hole-burning occurs only in standing-wave resonators and, as the name implies, "burns" out the population inversion periodically along the gain medium, thus leaving some gain unused. It transpires that the immediately-adjacent axial mode to that causing the spatial hole-burning then sees higher available gain and will oscillate, since it can effectively fill in the spatial gaps left by the first oscillating mode. It is this spatial hole-burning which encourages the laser to operate in multiple axial modes, rather than just one, and its elimination immediately disposes the laser towards single-frequency operation.

Both of the above approaches require narrowband optical filters which ideally are fibre-based. Because the Fabry-Perot resonator approach has a standing optical wave in the resonator, the requirements for the frequency-selective component are more stringent, since the natural tendency of the laser must be overcome. On the other hand, the travelling-wave approach exploits the predisposition of the laser to operate in single-axial mode and the frequency-selective component is used largely as a tuning element. Three main narrowband filter types have emerged with quite different characteristics and each has been used to produce single-frequency fibre lasers. These are the fibre-relief grating (Ref 32), photorefractive Bragg-grating (Ref 33) and the miniature fibre Fabry-Perot (FFP) (Ref 34). The fibre-relief grating applies a physical corrugation on the side of the fibre and is made by removing the fibre cladding by polishing to obtain access to the core evanescent field, or by employing a D-section fibre. Photoresist is then applied and exposed holographically using a short-wavelength laser. A grating is subsequently etched into the fibre using either a dry or wet process. An index-layer is then normally applied to "lift" the field and

optimise its interaction with the grating corrugations. Fibre-relief gratings act as a narrowband Bragg-reflector and reflectivities as high as 95% with a bandwidth between 25-1800GHz have been reported (Ref 35). Excess losses are low (<0.5dB) and limited tunability (3nm) can be obtained by temperature-tuning or changing the index of the grating overlay.

An exciting recent development in narrowband filters is the technique of directly writing photorefractive-Bragg gratings within the core of a single-mode fibre (Ref 33). An interference pattern of ultra-violet light at around 240nm is focussed onto the core of a germanium-doped silica fibre. After exposure of a few minutes, a distributed-Bragg reflector is created at a wavelength corresponding to the periodicity of the interference pattern. Using this transverse holographic technique, photorefractive gratings can be written at any wavelength and can have reflectivities up to 98%. The origin of the effect is the subject of much controversy with several theories available. There appears to be agreement that it is associated with Ge E' centres within the core which absorb strongly at 240nm. Fortunately, writing the gratings is accompanied by an increase in absorption of only 0.2% at 1.55μm. Reflection linewidths of 20-100GHz are obtainable and the filters exhibit limited tunability (2nm) using either temperature or strain (Ref 36). The main appeal of photorefractive grating filters is the ease with which they can be made, their very low loss and the non-invasive nature of the fabrication process.

Fibre Fabry-Perot filters (Ref 37) have been around for a number of years, but have recently come to prominence with the development of widely-tunable commercial devices. Several configurations are possible, the most popular being to deposit highly-reflective, multi-layer dielectric mirrors on the ends of a short (<2nm) stub fibre which is then glue-spliced between fibre pigtails. Tuning is achieved by piezo-electrically stretching the short fibre length, which incorporates a gap for this purpose. The inclusion of a fibre waveguide within the Fabry-Perot resonator is crucial, since it prevents beam walkoff and allows a high finesse (>100) to be achieved in a compact, robust device.

Fabry-Perot filters differ from grating filters (either relief or photorefractive) in that they have a bandpass characteristic, reflecting the stopped light. In common with all Fabry-Perot etalons, they exhibit multiple passbands, with typically bandwidths of 1-100GHz and a free spectral range (FSR) of 100-100,000GHz. Excess losses are <3dB and tunability over one or more FSR is possible.

Two examples of travelling-wave, single-frequency fibre lasers are shown in Figures 17 and 18, one using the photorefractive Bragg-reflector or fibre-relief grating and the other using a fibre Fabry-Perot filter. Travelling-wave operation of the resonators is ensured by incorporating an isolator to prevent counter-propagating resonances. In both cases spectral linewidths of <20kHz are achieved with very low amplitude noise and a tunability over 40nm. These attributes make this type of laser a very strong contender for telecommunications WDM sources. Compared with DFB diode lasers they have narrower linewidth, lower noise and a higher output power. However, an as-yet unsolved problem is that of mode-hopping from axial mode to axial mode which occurs when the filter precisely straddles two laser resonator modes.

It remains to be seen whether the single-frequency fibre laser will rival DFB diode lasers as the preferred narrow-linewidth telecommunications source, particularly in areas which require highly-stable, narrow-band tuning capability, such as in dense WDM systems.

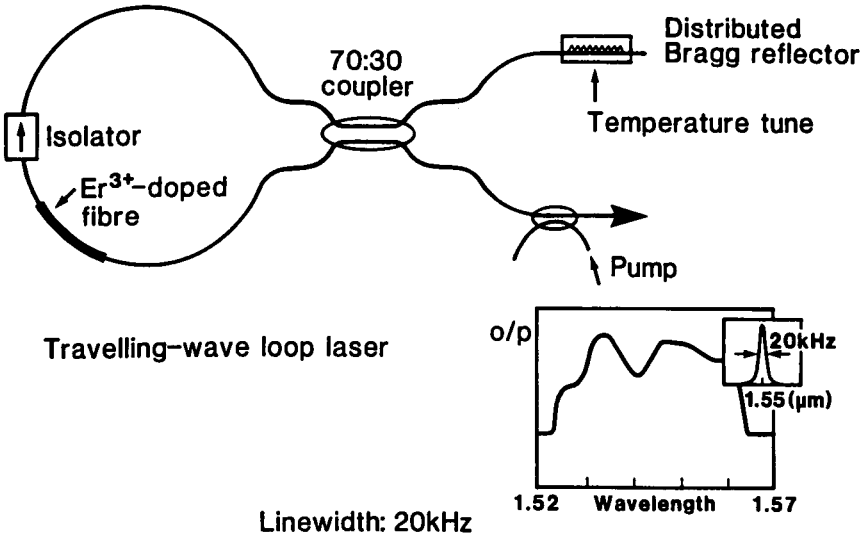

Figure 17 : Tunable single-frequency loop laser using a Bragg grating as a tuning element

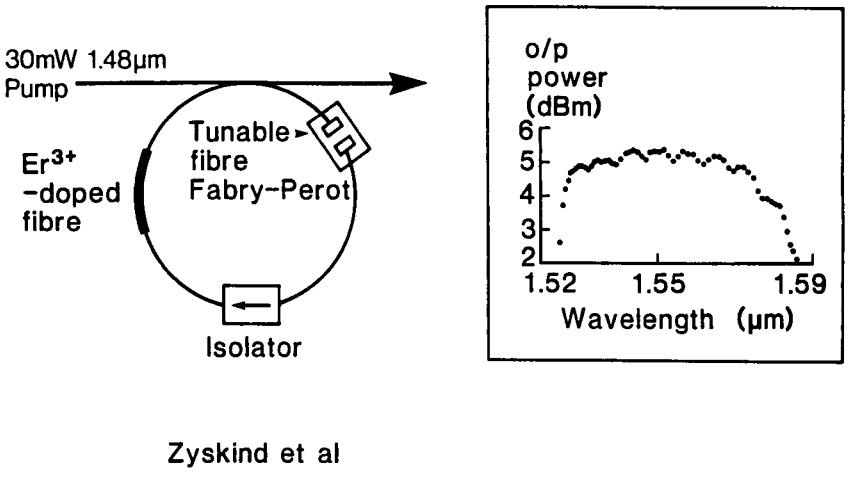

Zyskind et al

Figure 18 : Tunable single-frequency travelling-wave ring laser using a fibre Fabry-Perot tuning element

Mode-Locked Fibre Lasers

As with conventional lasers, fibre lasers can be Q-switched or mode-locked to produce short, high-power pulses. An advantage of the fibre configuration is that the peak-power handling capability (set by the material damage) is tens of kilowatts, a figure which considerably exceeds that obtainable from diode lasers. Thus fibre lasers can be used to convert the low-level light from a diode-laser pump into the short, high-power pulses required for lidar, non-linear switching and ranging. A few milliwatts of average output power from a fibre laser can have peak powers of many kilowatts in a pulse train.

Numerous publications have emerged which describe mode-locking and Q-switching of fibre lasers by conventional laser techniques, such as phase, amplitude or intra-cavity modulation (Ref 38).

At the power levels obtainable from mode-locked fibre lasers, especially if subsequently amplified, non-linear effects in fibres are easily accessable. Moreover, with the plethora of fibre components now available, it is relatively-easy to assemble complex fibre circuits to include fibre lasers and

amplifiers. Recently, this has led to a number of fibre laser/ amplifier configurations emerging which combine non-linear switching, soliton propagation and mode-locking. It is our purpose here to examine just one of these as illustrative of the advantages to be gained by combining non-linear and amplifying effects.

Fibre switches

Much work has done been to develop all-optical switches compatible with optical fibre technology. The physical mechanisms employed have been based on third-order, non-linear effects such as Self-Phase and Cross-Phase Modulation (SPM and CPM respectively), which have response times of the order of a few femtoseconds. This ultrafast response time is tantalising for switching and routing in ultra-high bit-rate telecommunications schemes, high-speed optical processing and in the generation of ultra-short pulses. We will first describe the operation of an all-fibre, ultrafast switch, the Non-Linear Amplifing Loop Mirror (NALM) and then show how such a switch can be used within a laser cavity to act as a passive mode-locker. We will then detail the results of experiments on a passive, self-starting, fibre laser capable of generating solitons with durations as short as 320fs.

A number of all-fibre switching schemes have been developed based on third-order, non-linear phenomena, i.e. the small change of refractive-index which occurs with optical intensity. All of these schemes require some form of dual-path interferometer (or polarimeter) in order to detect the small phase change which is induced by the third-order non-linearity. The power levels required to obtain maximum switching contrast in any interferometric switching scheme are determined by the precise design and details of the system, but can be roughly estimated from:

$$IL = 500 ,$$

where I is the optical power in Watts and L the interaction length in metres. It can be seen that either high power levels or long interaction lengths are required to get appreciable switching effects. In order to obtain switching powers commensurate with any practical communications or signal-processing system, i.e. <1W, we require switches with correspondingly-long interaction lengths ($L > 500$m). Such long interaction lengths lead to severe problems with environmental stability for any interferometric device owing to the difficulty of maintaining a long-term phase balance between the two optical paths involved. However, if we adopt a scheme based on the fibre Sagnac interferometer (Figure 19) in which the two "arms" of the interferometer are common to the same piece of fibre, the system will be inherently stable to perturbations, provided that they occur on a time scale which is long compared to the time taken for light to travel through the interferometer, typically a few microseconds. Since the Sagnac interferometer when operating linearly returns light to the port from which it came, it is frequently referred to as a "loop mirror" (Ref 39).

A recent development is to incorporate an EDFA within the loop mirror (Refs 40,41) as shown in the figure. Since the amplifier is located at one end of the loop, the counter-clockwise propagating light traverses the loop at lower intensity than the clockwise propagating light, and the amplifier provides the necessary switching asymmetry.

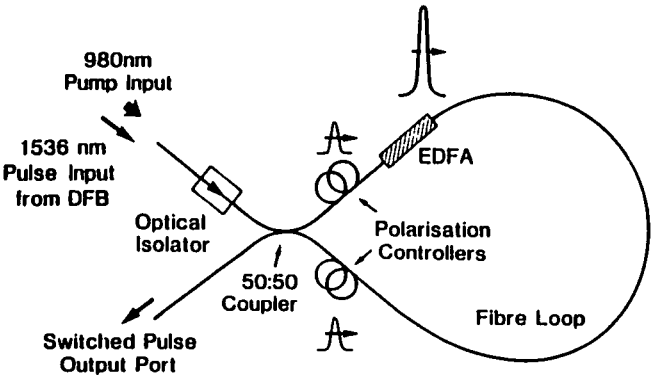

Figure 19 : Fibre Non-Linear Amplifying Loop Mirror switch configuration

The non-linear response of the system can be obtained by evaluating the response of the coupler (which has equal power-splitting) to light incident at the input port (optical intensity I_1). Considering quasi-cw operation, i.e. a regime in which dispersive effects can be neglected, and assuming an amplifier gain G with an effective-path length L, the net phase difference $\Delta\phi$ between counter-propagating pulses is:

$$\Delta\phi = (G\text{-}1)n_2 I_1 kL$$

where k is the propagation vector and n_2 is the non-linear refractive-index ($n=n_0+n_2I_1$). This net phase difference generated after propagation around the loop causes switching of the light from the input to the output ports according to:

$$I_2 = GI_1\sin^2(\Delta\phi) \ ,$$

and gives 100% of the input light switched to the outport port at $\Delta\phi=(2n+1)\pi$, $n=0,1,2...$ Effectively, the loop mirror reflection decreases with input intensity. The high gain available with erbium-doped fibre amplifiers (G > 40dB) reduces input switching powers of fibre switches from the Watt to the microwatt regime. Note that the NALM has inherent gain which has potential for use as a mode-locking element within a laser cavity.

We have assumed here that the light remains in a linear state of polarisation throughout its traversal of the interferometer. This is unlikely to be the case and the NALM loop is almost certain to possess a degree of birefringence. It can be shown that the net effect is to add a linear-phase-bias to the nonlinear phase shift. By appropriate birefringence control (corresponding to an equivalent linear phase shift of π) the NALM switching characteristic can be completely reversed, i.e. the loop-mirror reflectivity can be made to increase with intensity, in which form it can be useful as a non-linear feedback element for a mode-locked laser.

The input/output power transfer characteristic for a high gain (46dB) NALM is shown in Figure 20. The loop length was 306m and the input signal source a DFB laser operating at a wavelength of 1536nm. The interferometric nature of the switch is evident from the sinusoidal characteristic. Note that full switching occurs at an input of only 100μW peak power.

Since the degree of NALM switching is power-dependent and has a transfer function given above, passing a pulse with a given intensity profile through the device leads to strong pulse-shaping effects. It transpires that the only pulses which do not suffer shaping and losses on switching are

solitons, since they are the only pulse form (with the exception of square pulses) which has an overall phase factor which applies equally across the entire pulse envelope. It is this unusual attribute which permits low-energy- loss soliton switching in the NALM. This further lends credence to the statement that solitons are the natural bits for communications and switching. The operation of the NALM in the soliton regime has been analysed for a relatively low-gain system (of the order 3dB) in Ref 42, where it is concluded that solitons should be well switched by the NALM.

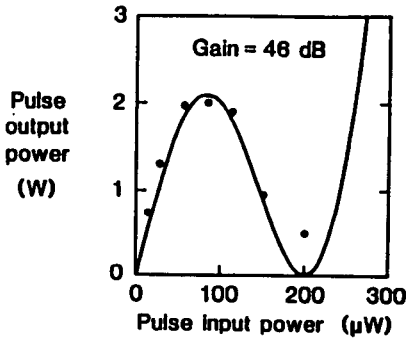

Figure 20 : Transfer characteristic of the NALM fibre switch

Mode-locked fibre lasers

It is well-known from bulk laser theory that the incorporation of non-linear elements, such as saturable absorbers, within a laser cavity can lead to passive mode-locking of the system and generally yields very short pulses. Provided it is biased using birefringence, the NALM characteristic on the first switching cycle is similar to that of a saturable absorber, only in this case the NALM acts as a mirror whose reflectivity increases with intensity. Such a non-linear mirror can be used as one end mirror in a Fabry-Perot cavity (Ref 43) to produce mode-locking. However the birefringence control required to bias the NALM leads to environmental instability. A more complex scheme, known as the Figure-8 laser (Ref 44,45,46) does not require birefringence bias of the NALM and is therefore potentially more stable.

The Figure-8 laser scheme is shown in Figure 21. The system consists of two discrete loops, one a unidirectional ring containing an isolator and the other a NALM loop. At low intensity, light incident at port A is reflected back to port A by the loop mirror and is therefore ultimately lost within the isolator. However, if the light intensity is high, as might occur for mode-locked pulses, the NALM switches light to port B, whereupon it is able to circulate within the isolator loop, providing feedback for the laser.

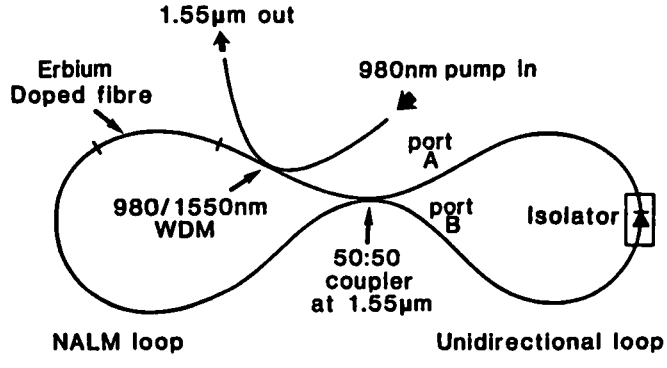

Figure 21 : Figure-8 self-starting, mode-locked fibre-laser scheme

If we consider light propagation in the quasi-cw regime, then the cavity loss vs. light intensity has the form shown in Figure 22, where it is seen that there is a well-defined intensity which produces minimum laser resonator loss.

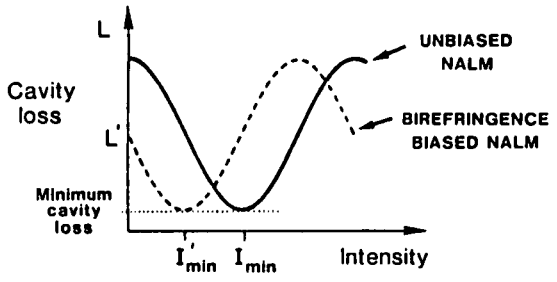

Figure 22 : Resonator loss in the Figure-8 laser as a function of intra-cavity (pulse) intensity, showing how the loss can be adjusted by means of birefringence

Since the laser system is predisposed to operate in a mode which minimises internal losses, it favours high-intensity, pulsed operation, i.e. mode-locking. As we saw above, the NALM loop switches with minimum loss pulse waveforms which are either square or solitons, since both of these waveforms have the characteristic that they generate uniform, non-linear phase profiles across their entire pulse envelope. We would therefore expect the laser to favour these pulse forms. Furthermore, the low input powers required to switch a NALM operating at high gain enables the pulsed operation to build up from noise at the NALM input. The process is assisted by allowing a degree of cw lasing at low input pump powers, either by using a coupler with an asymmetric coupling ratio, or by biasing the NALM by means of birefringence, as in Figure 22. Thus the laser operates in pulsed mode without the need for any external modulator and is found to undergo a variety of different types of pulse behaviour (Ref 47). Both square pulse and soliton pulse generation have been observed with the system operating at 1.56μm. The square pulses are relatively long in duration (150psec).

The more interesting soliton regime can be entered by adjusting the NALM phase-bias (Figure 22) and the resulting solitons can have a duration as short as 320fsec. The autocorrelation trace and optical spectrum obtained in this case are shown in Figure 23. Note the large blue-shifted component of the spectrum, the origin of which is believed to be due to splitting of the pulse into soliton and non-soliton components during the amplification and propagation processes. These components separate both temporally and spectrally, since the soliton pulse will be red-shifted by the soliton self-frequency shift. The dynamic balance between the self-frequency shift and the gain-pulling effect of the amplifier push the pulse out to the long-wavelength edge of the erbium gain-spectrum. The large blue-shift component is not observed when generating solitons with durations $> \sim 600$fsec.

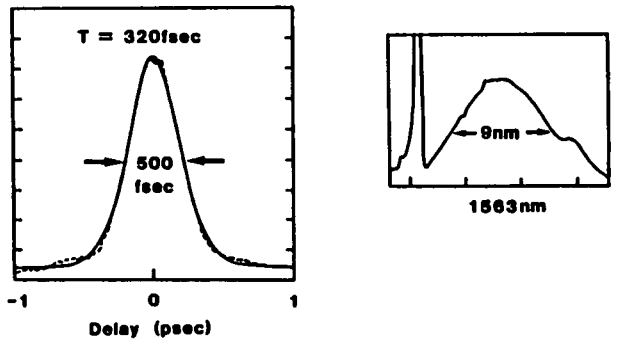

Figure 23 : Autocorrelation trace and spectrum of a 320fs soliton pulse obtained at the output of the Figure-8 laser. Solid line represents the calculated soliton profile

Because the laser operates without external modulation, the soliton repetition rate can be complex. Bunches of solitons repeating at the cavity round-trip frequency have been observed, with pulse repetition rates as high as 100GHz within the pulse bunches. The system can also operate in a regime in which the solitons are no longer bunched, but occur seemingly randomly-distributed over the entire cavity round-trip period, the pulse patterns repeating at the round-trip frequency. Note that since the energy of a soliton is fixed, i.e. quantised, more pulses must circulate in the cavity if the pump power is increased. Thus the average repetition rate must increase in order to obtain more output power. It is also possible to obtain pure harmonic mode-locking in which an integral number of precisely-spaced pulses occur within a round-trip period.

Despite the very broad gain-bandwidth of erbium ions in silica, the effect of soliton self-frequency shift restricts the minimum possible pulse duration to around 300fsec, as noted above. By combining the Figure-8 laser and the EDFA, it is possible to generate even shorter pulses by exploiting the pulse compression which occurs during soliton amplification in a fibre amplifier (Ref 48). In this case the Figure-8 laser was configured to stably produce bandwidth-limited soliton pulses with a duration of 450fsec, using just 20mW of launched pump power at 980nm, a power easily-obtainable from a laser diode. The average output power was 120μW with approximately 10 pulses circulating within the laser cavity. The pulses were fed to an external EDFA with a length of 5.5m. Since a small amount of power was tapped from the full-power solitons circulating within the Figure-8 laser, the input to the amplifier fibre was only about one tenth the peak power required for a soliton. Thus over the first few metres of the amplifier the pulses increase their energy without experiencing significant non-linear effects. However, when the pulse under amplification attains an energy close to that of the fundamental soliton, non-linear effects in its propagation become significant and the amplification process becomes more complicated. At a certain pulse energy corresponding to a higher-order soliton, multi-soliton compression occurs and the pulsewidth decreases abruptly. With a pump power of 320mW in the following EDFA, a total power gain of 29dB was obtained and pulse compression down to 90fsec was observed at the fibre output. The time-bandwidth product of these pulses was 0.3, in reasonable agreement with that expected for a sech^2 soliton pulse shape. Thus, during soliton amplification and propagation we are able to transform 450fsec fundamental solitons into 90fsec fundamental solitons.

A number of interesting further effects could be observed at higher EDFA gains, such as high-order soliton break-up into coloured solitons due to soliton self-frequency shift (Ref 48). These experiments serve to show both how powerful the combination of fibre lasers and amplifiers can be, as well as the ability of the EDFA to support pulses as short as 90fsec.

CONCLUSIONS

We have seen how the simple expedient of incorporating rare-earth ions into optical fibres has produced a whole new active-fibre technology. The most obvious immediate impact of the technology is in fibre amplifiers which have revolutionised telecommunications systems design, particularly in undersea routes. The fibre amplifier is generally acknowledged as the most significant development in telecommunications in recent years. Its impact will be to hasten the transference of satellite-based telecommunications to optical fibre transmission for international telephone traffic. The full impact of readily-available optical amplification has yet to be felt in telecommunications systems architectures and we can expect radical new proposals in the future, particularly involving soliton transmission and dense wavelength-division-multiplexing.

The fibre laser has still to make as great an impact. Although stable, compact and rugged, its application as a telecommunications source has yet to materialise. A disadvantage is the need for an external modulator, although for high-speed systems this is essential even for diode lasers in order to prevent frequency chirp and the accompanying dispersion. Thus it may be that fibre lasers will find application only in the high-capacity systems of the future where frequency stability is

valued and an external modulator is no disadvantage. On the other hand, it is clear that the wide tunability and the variety of emission wavelengths make the fibre laser very attractive for sensing, metrology and military applications. In addition, the fibre laser is capable of orders of magnitude higher peak-pulse power than the diode laser and is thus well-suited to ranging, OTDR and non-linear optics. It should not be forgotten, however, that many of the high-power advantages can also be gained by following a gain-switched diode laser with an EDFA, at least for the 1.55μm spectral region.

A unique attribute of fibre lasers is their ability to produce solitons when mode-locked. It would appear that solitons are the natural bits for both transmission and switching. Since the required soliton pulse form, peak power and duration are determined by the transmission fibre characteristics, there is a certain logic in generating them within the fibre. We have also shown that combinations of fibre lasers, amplifiers and components can be used to construct complex fibre circuits and it is clear that an integrated fibre device technology is emerging. Using this technology, in the future we can expect high-power cw fibre lasers to rival today's miniature, diode-pumped, crystal lasers.

ACKNOWLEDGEMENTS

I would like to thank all my colleagues at Southampton University, much of whose work is reported here.

REFERENCES

1. Snitzer, E., "Optical maser action of Nd^{3+} in a barium crown glass", Phys. Rev. Lett., Vol. 7, p. 444, 1961.

2. Stone, J. and Burrus, C.A., "Neodymium-doped fiber lasers: room temperature cw operation with an injection laser pump", Appl. Opt., Vol. 13, p. 1256, 1974.

3. Poole, S.B., Payne, D.N. and Fermann, M.E., "Fabrication of low-loss optical fibres containing rare-earth ions", Electron. Lett., Vol. 21, p. 737, 1985.

4. Mears, R.J., Reekie, L., Poole, S.B. and Payne, D.N., "Neodymium-doped silica single-mode fibre lasers", Electron. Lett., Vol. 21, p. 738, 1985.

5. Mears, R.J., Reekie, L., Jauncey, I.M. and Payne, D.N., "High-gain, rare-earth-doped fibre amplifier at 1.54μm", Proc. OFC 1987, Reno, Paper WI2.

6. Horiguchi, M., Shimizu, M., Yamada, M., Yoshino, K. and Hanafusa, M., Electron. Lett., Vol. 26, pp. 1733-1759, 1990.

7. Shimizu, M., Yamada, M., Horiguchi, M., Takeshita, T. and Okayasu, M., Electron. Lett., Vol. 26, pp. 1641-1643, 1990.

8. Nakazawa, M., Kimura, Y. and Suzuki, K., Proc. Topical Mtg on Optical Amplifiers & their Applications, Paper PDP1, Monterey, 1990.

9. Zervas, M.N., Laming, R.I. and Payne, D.N., "Trade-off between gain efficiency and noise figure in an optimised fibre amplifier", Proc. OFC '92, San Jose, February 1992.

10. Gnauck, A.H. & Giles, C.R., "2.5Gb/s and 10Gb/s transmission experiments using a 137 photon/bit erbium fibre preamplifier receiver", Proc 17th European Conference on Optical Communication, Vol. 3, pp. 60-63, Paris, 1991.

11. Laming, R.I., Reekie, L., Morkel, P.R. and Payne, D.N., "Multichannel crosstalk and pump noise characterisation of Er^{3+}-doped fibre amplifier pumped at 980nm", Electron. Lett., Vol. 25, pp. 455-456, 1989.

12. Laming, R.I., Payne, D.N., Meli, F., Grasso, G. and Tarbox, E.J., "Highly-saturated erbium-doped-fibre power amplifiers", Proc Topical Meeting on Optical Fibre Amplifiers and their Applications, Vol. 13, pp. 16-19, Monterey, Ca., August 1990.

13. Craig-Ryan, S.P., Massicott, J.F., Wilson, M., Ainslie, B.J. and Wyatt, R., Proc. ECOC '90, Amsterdam, 1990.

14. Takenaka, H., Okuno, H., Fujita, M., Odagiri, Y., Sunohara, Y. and Mito, I., "Compact size and high output power Er-doped fiber amplifier modules pumped with 1.48μm MQW LDs", Proc. Second Topical Meeting on Optical Amplifiers and Their Applications, pp. 254-257, Snowmass, Colorado, June 1991.

15. Grubb, S.G., Windhorn, T.H., Humer, W.F., Sweeney, K.L., Lelabady, P.A., Townsend, J.E., Jedrzejewski, K.P. & Barnes, W.L., "+20dBm erbium power amplifier pumped by a diode-pumped Nd:YAG laser", Proc. Second Topical Meeting on Optical Amplifiers and Their Applications, Paper PDP 2-1, Snowmass, Colorado, June 1991.

16. Minelly, J.D., Laming, R.I., Townsend, J.E., Barnes, W.L., Taylor, E.R., Jedrzejewski, K.P. and Payne, D.N., "High-gain fibre power amplifier tandem-pumped by a 3W multi-stripe diode", Proc. OFC '92, San Jose, February 1992.

17. Townsend, J.E., Barnes, W.L., Jedrzejewski, K.P. and Grubb, S.G., "Yb^{3+}-sensitised Er^{3+}-doped optical fibre in silica host with very high transfer efficiency", Electronics Letters, Vol. 27, pp. 1958-1959, 1991.

18. Tachibana, M., Laming, R.I., Morkel, P.R. and Payne, D.N., "Erbium-doped fibre amplifier with flattened gain spectrum", Photonics Technology Letters, Vol. 3, pp. 118-120, 1991.

19. Miyajima, Y. et al., "Nd^{3+}-doped fluoride fiber amplifier module with 10dB gain and high pump efficiency", Proc. Second Topical Meeting on Optical Amplifiers and Their Applications, Snowmass, Colorado, June 1991.

20. Ohishi, Y. et al., "Pr^{3+}-doped optical fiber amplifier operating at 1.3μm", Proc. Optical Fibre Communications Conference, San Diego, 1991.

21. Miyajima, Y. et al., "38.2dB amplification at 1.31μm and possibility of 0.9μm pumping in Pr^{3+}-doped fluoride fiber", Electronics Letters, Vol. 27, 1706-1701, 1991.

22. Nakazawa, M., Yamada, E., Kubota, H. & Suzuki, K., "10Gbit/s soliton data transmission over one million kilometres", Electronics Letters, Vol. 27, p. 1270, 1991.

23. Barnes, W.L., Morkel, P.R., Reekie, L. & Payne, D.N., "High quantum efficiency Er^{3+} fibre lasers pumped at 980nm", Opt. Lett., Vol. 14, pp. 1002-1004, 1989.

24. Urquhart, P., "Review of rare-earth-doped fibre lasers and amplifiers", IEE Proc. Part J., Vol. 135, p. 385, 1988.

25. Barnes, W.L. & Townsend, J.E., "Highly tunable and efficient diode pumped operation of Tm^{3+}-doped fibre lasers", Electron. Lett., Vol. 26, pp. 756-747, 1990.

26. Snitzer, E., Po, H., Hakimi, F., Tumminelli, R. & McCollum, B.C., "Double-clad, offset core Nd fibre laser", Proc. Conference on Optical Fibre Communications, New Orleans, Paper PD5, 1988.

27. Po. H., Snitzer, E., Tumminelli, R., Zenteno, L., Hakimi, F., Cho, N.M. & Haw, T., "Doubly clad high brightness Nd fibre laser pumped by GaAlAs phased array", Proc. Conference on Optical Fibre Communications, Houston, 1989.

28. Minelly, J.D., Taylor, E.R., Jedrzejewski, K.P., Wang, J. & Payne, D.N., "Laser- diode-pumped neodymium-doped fibre laser with output power in excess of 1 watt", to be published in Proc. Conference on Lasers and Electro-Optics, Paper CWE6, Anaheim, May 1992.

29. Minelly, J.D., Laming, R.I., Townsend, J.E., Barnes, W.L., Taylor, E.R., Jedrzejewski, K.P. & Payne, D.N., "High-gain power amplifier tandem-pumped by a 3W multistripe diode", Proc. Conference on Optical Fibre Communications, Paper TuG2, San Jose, 1992.

30. Jauncey, I.M., Reekie, L., Townsend, J.E., Payne, D.N. & Rowe, C.J., Electronics Letters, Vol. 24, pp. 24-26, 1988.

31. Morkel, P.R., Cowle, G.J. & Payne, D.N., Electronics Letters, Vol. 26, pp. 632-634, 1990.

32. Sorin, W.V. & Shaw, H.J., Journal of Lightwave Technology, Vol LT-3, pp. 1041-1043, 1985.

33. Meltz, G., Morey, W.W. & Glenn, W.H., Optics Letters, Vol. 14, pp. 823-825, 1989.

34. Stone, J. & Marcuse, D., Journal of Lightwave Technology, Vol. LT-1, pp. 382-385, 1986.

35. Bennion, I., Reid, D.C.J., Rowe, C.J. & Stewart, W.J., Electronics Letters, Vol. 22, p. 341, 1986.

36. Morey, W.W., Proc. OFS'90, p. 285, Sydney, Australia, 1990.

37. Stone, J. & Stulz, L.W., Electronics Letters, Vol. 23, pp. 781-782, 1987.

38. See for example France, P.W. (Ed), "Optical Fibre Lasers and Amplifiers", Chapter 9, Blackie & Son, London, 1991, ISBN 0-216-93157-6.

39. Doran, N.J., Blow, K.J. & Wood, D., "Soliton logic elements for all-optical processing", SPIE Vol. 836, Optoelectronics Materials, Devices, Packaging, and Interconnects, pp. 238-243, 1987.

40. Richardson, D.J., Laming, R.I. & Payne, D.N., "Very low threshold Sagnac switch incorporating an erbium doped fibre amplifier", Electronics Letters, Vol. 26, pp. 1779, 1990.

41. O'Neill, A.W. & Webb, R.P., "All optical loop mirror switch employing an asymmetric amplifier/attenuator combination", Electronics Letters, Vol. 26, pp. 2008-2009, 1990.

42. Fermann, M.E. et al, "Nonlinear amplifying loop mirror", Optics Letters, Vol. 15, pp. 1217-1224, 1990.

43. Avromopolous, H.E. et al, "A passively mode-locked erbium fibre laser", Topical Meeting on Optical Amplifiers & Their Applications, Monterey, Paper PDP8, 1990.

44. Richardson, D.J. et al, "Self-starting passively mode-locked fibre laser based on the amplifying Sagnac switch", Electronics Letters, Vol. 27, pp. 542, 1991.

45. Duling, I.N. III, "All-fiber ring soliton laser mode-locked with a nonlinear mirror", Optics Letters, Vol. 16, pp. 539-541, 1991.

46. Bulshev, A.G., Dianov, E.M. & Okhotinov, O.G., "Self-starting mode-locked laser with a nonlinear ring resonator", Optics Letters, Vol. 16, pp. 88-90, 1991.

47. Richardson, D.J. et al, "Pulse repetition rate effects in a passively mode-locked erbium doped fibre laser", Electronics Letters, Vol. 27, pp. 1451-1453, 1991.

48. Richardson, D.J., Grudinin, A.B. & Payne, D.N., "Passive, all-fibre source of 30fs solitons" Proc. Topical Meeting on Non-Linear Guided Wave Phenomena, Paper PDP8, Cambridge, September 1991.

OPTICAL FIBER SENSORS

Eric Udd
McDonnell Douglas Electronic Systems Company
Santa Ana, California 92705

SUMMARY

Fiber optic sensors are finding increased usage in aerospace guidance and control applications due to their light weight, immunity to electromagnetic interference, high bandwidth and sensitivity, and solid-state, all-passive nature. This paper reviews fiber optic sensors with particular emphasis on aerospace applications.

1. INTRODUCTION

Fiber optic communication links have revolutionized the telecommunication industry by providing low cost, high fidelity and very high transmission rate capability. In a similar manner the emerging optoelectronic industry has brought us such products as compact disk players and laser printers. As a result of these developments a second revolution is taking shape as fiber optic sensors that take advantage of components developed in association with the telecommunication and optoelectronic industry begin to enter the market. These sensors offer a series of advantages of particular importance to the aerospace industry, including small size and weight; immunity to electromagnetic interference, which also reduces the cost of shielding; environmental ruggedness; high multiplexing potential; and potentially low costs due to complementary developments in the telecommunication and optoelectronic industries. Aerospace applications for these fiber optic sensors include fiber optic rotation sensors,

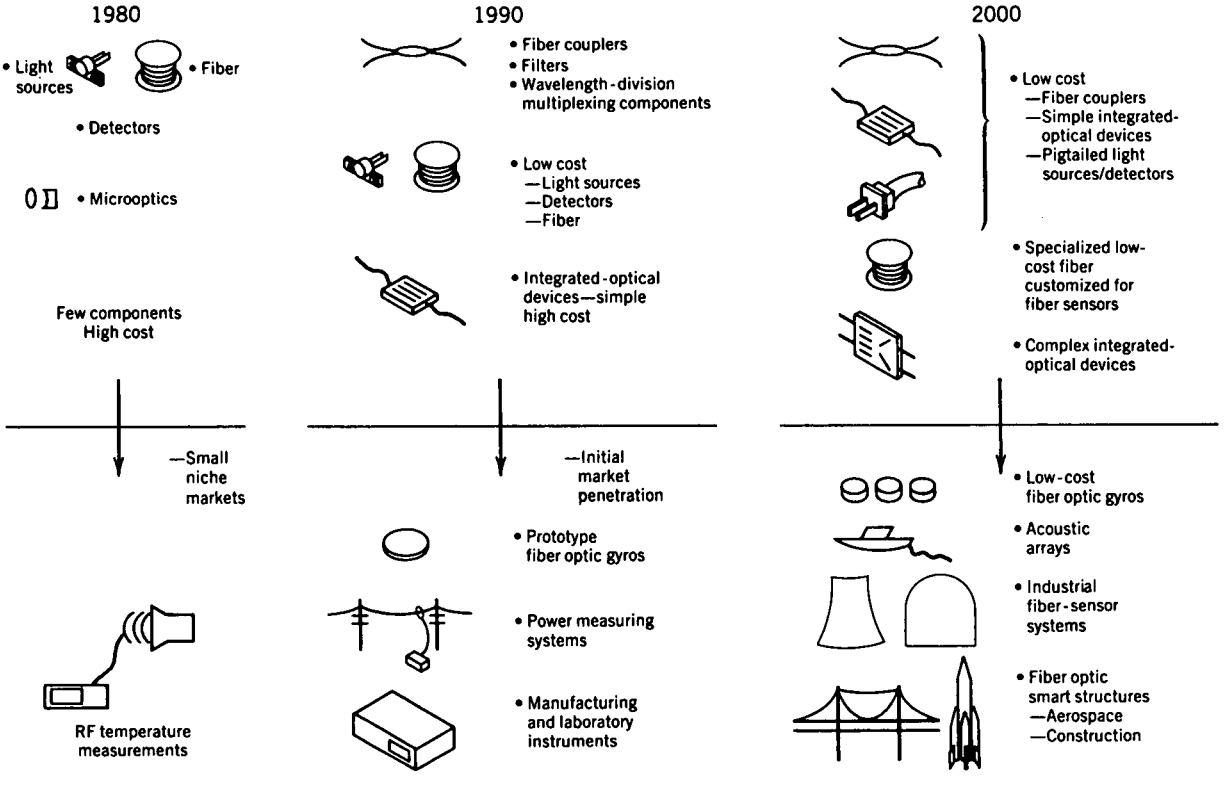

Figure 1. As key components become available at lower cost fiber optic sensors will penetrate many more markets [After Reference 4].

accelerometers, vibration sensors, smoke detectors, linear and angular position sensors, and strain, temperature, and electromagnetic field sensors.

The trends for fiber optic sensors are illustrated by Figure 1. In the early 1980s few components were available and they were expensive. This situation resulted in fiber optic sensors being used in only a few niche markets where their advantages were overwhelming. For example these sensors were used to make temperature measurements in radio frequency environments. By 1990 the number of components had dramatically increased, the cost of many items had dropped by an order of magnitude or more while the quality and performance dramatically increased. Important examples include (1) the cost of laser diodes dropping from about $3000 each to $3 each while lifetimes went from a few hours to tens of thousands of hours and (2) the cost of single-mode fiber dropping from $10/m to $0.10/m with lower attenuation, greater concentricity of the core and cladding, and improved jacketing material. In the same time frame new components such as fiber couplers, wavelength division multiplexing elements, and integrated optical devices became commercially available. The net result was that many more fiber optic sensors became available, penetrating such markets as inertial rotation, power system monitoring, and manufacturing and process control. By the year 2000 it can be expected that many more components, integrated optical devices, pigtailed light sources, and fiber couplers will be available at low cost. The result will be the widespread proliferation of fiber optic sensors and their use in industrial control systems and the rapidly evolving area of smart structures that includes health maintenance and diagnostic systems for aerospace vehicles and civil structures. Figure 2 graphically portrays the emergence of fiber optic sensor technology as the continually decreasing costs of an increasing number of high quality components allows fiber optic sensor designers to produce competitive products to meet the needs of current and future markets.

The paper provides a brief overview of fiber optic sensor technology with emphasis on its application to aerospace platforms. The field is covered in much more depth by References 1 through 3.

2. FIBER OPTIC SENSOR TECHNOLOGY

Fiber optic sensors are often categorized as being either extrinsic or intrinsic. Extrinsic or hybrid fiber optic sensors have an optical fiber carry a light beam to and from a "black box" that in response to an environmental effect modulates the light beam. Intrinsic or all fiber optic sensors are sensors which measure the modulation of light by an environmental effect within the fiber. These types of sensors are shown in diagrammatic form by Figure 3. A series of representative examples of extrinsic sensors and the type of environmental effects

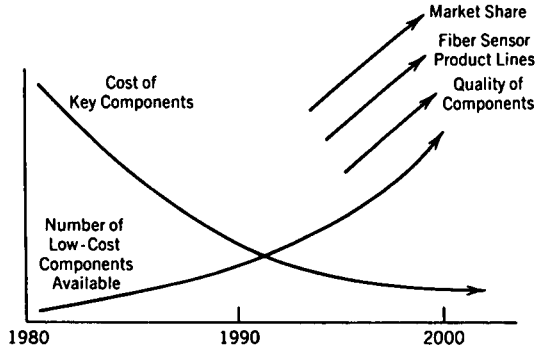

Figure 2. Low cost high quality components are key drivers to increase fiber optic sensor market share [After Reference 4].

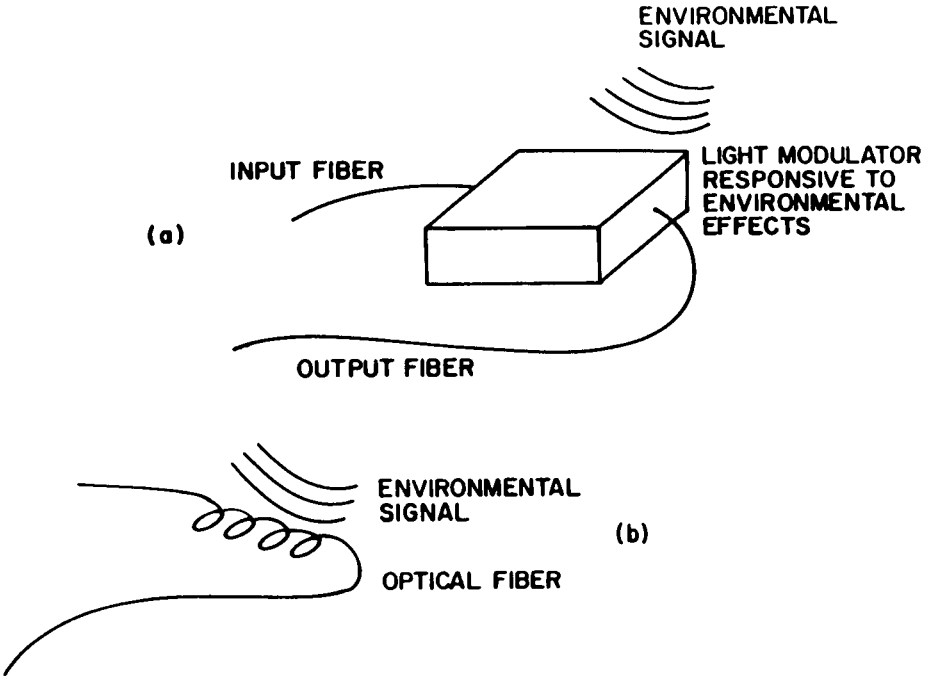

Figure 3. (a) Extrinsic or hybrid fiber optic sensors consist of fibers that bring light to and from a black box where light is modulated in response to an environmental effect. (b) Intrinsic or all fiber optic sensors rely on environmental modulation within the fiber itself. [After Reference 5].

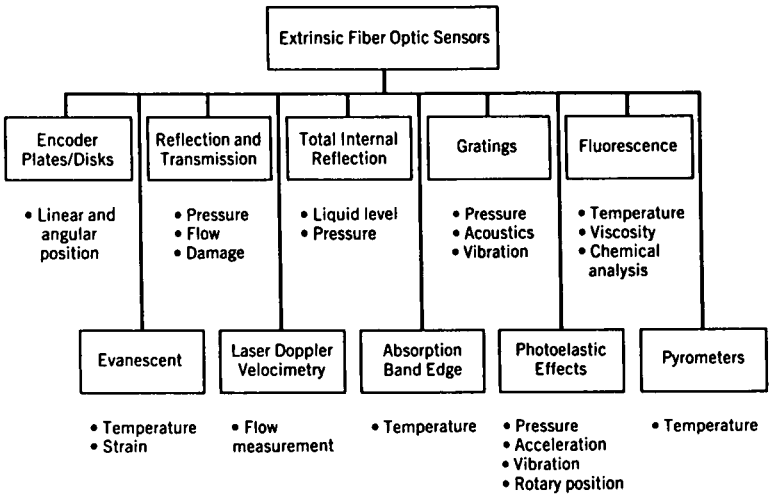

Figure 4. Partial listing of extrinsic fiber optic sensors and typical sensing applications [After Reference 4].

they are used to sense are listed in Figure 4. A corresponding chart for intrinsic fiber optic sensors is shown in Figure 5. An important subclass of intrinsic fiber optic sensors are the interferometric sensors, of Figure 6, which often exhibit high sensitivity and are competing with conventional high value sensors. Representative examples will be given in this section for extrinsic, intrinsic and interferometric fiber sensors.

Some of the simplest, although very useful extrinsic fiber optic sensors are based on the coupling of light that propagates out of an optical fiber and reflects off a mirror. Because the light that exits the fiber is dispersed into a cone which depends on the numerical aperture of the fiber, the proximity of the reflective mirror to the fiber determines the intensity of the light reflected back into it. This type of sensor, illustrated by Figure 7, is useful for such applications as proximity sensors for door and hatch closure as well as vibration sensor applications where high sensitivity is not a key issue.

Another application of using fibers to monitor reflectivity are linear and angular position sensors that can be used to support actuators. Here bundles of optical fibers are used to monitor the reflectivity of plates with gray scale codes. Light injected into the fiber is then reflected back and the resulting signal is used to interpret position. Alternatively optical fibers can be used in a transmission mode to support position sensors as is shown in Figure 8. Here an optical fiber is used to carry light to the plate and a second collector fiber is used to monitor transmission through the gray scale encoded plate.

It is also possible to monitor position by using a combination of a moving optical fiber end and collection fibers. In Figure 9 the case is illustrated where two fibers are used as collection optics; as can be seen from the resultant output, it is possible to interpolate the input fiber position to a very small fraction of the fiber diameter, which is on the order of 100 microns.

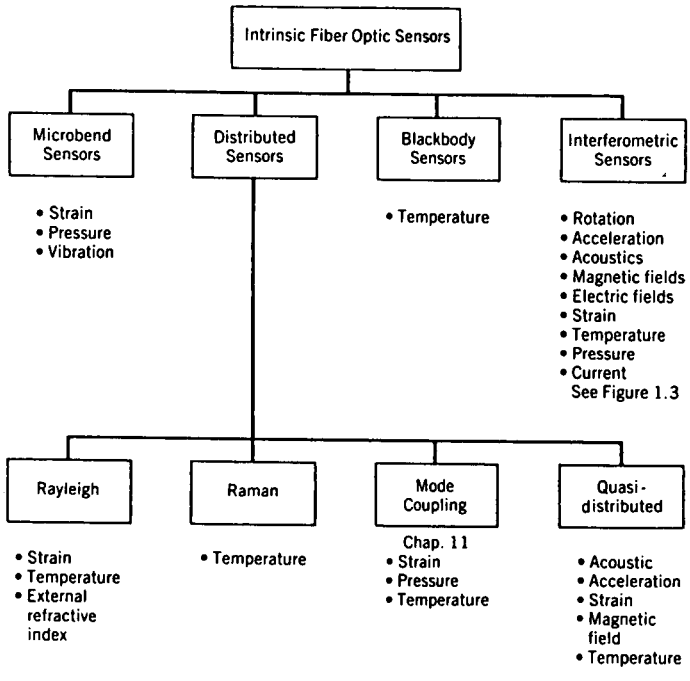

Figure 5. Partial listing of intrinsic fiber optic sensors and typical environmental sensing applications [After Reference 4].

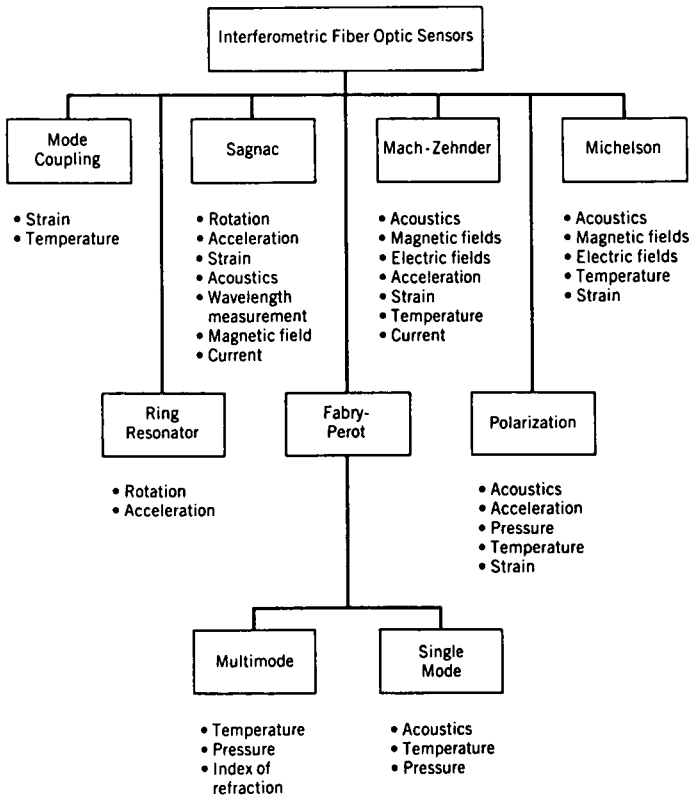

Figure 6. Partial listing of interferometric fiber optic sensors and typical environmental sensing applications [After Reference 4].

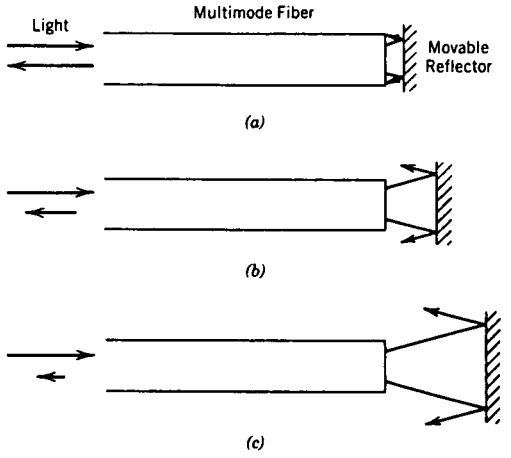

Figure 7. Extrinsic fiber optic sensor based on a movable reflective mirror [After Reference 6].

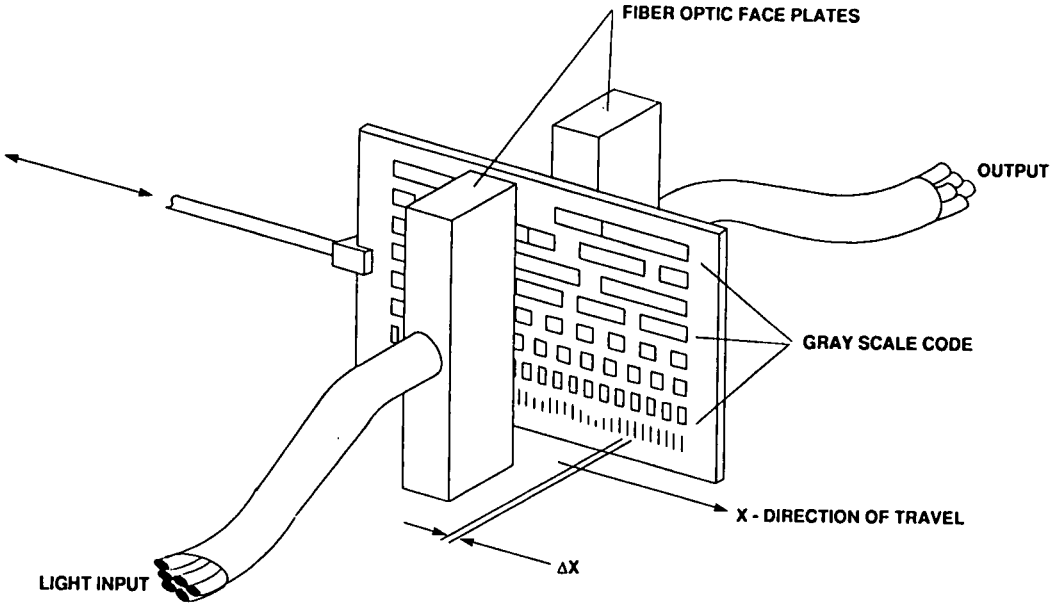

Figure 8. Linear encoder based on transmission through an encoder plate [After Reference 7].

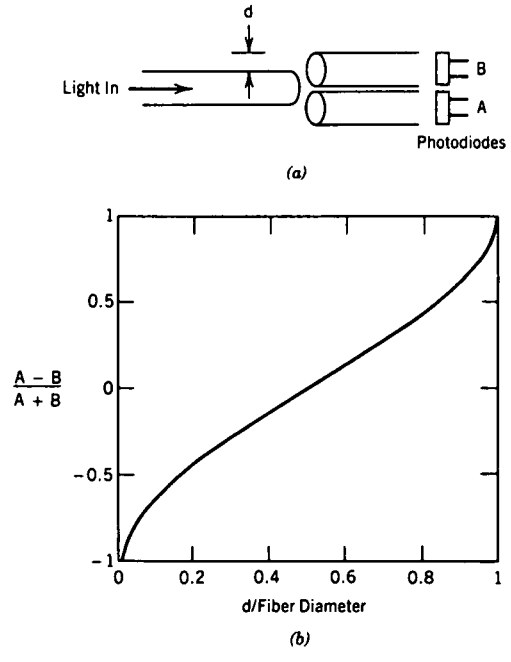

Figure 9. Position sensor based on a movable input fiber and fixed collection fibers [After Reference 6].

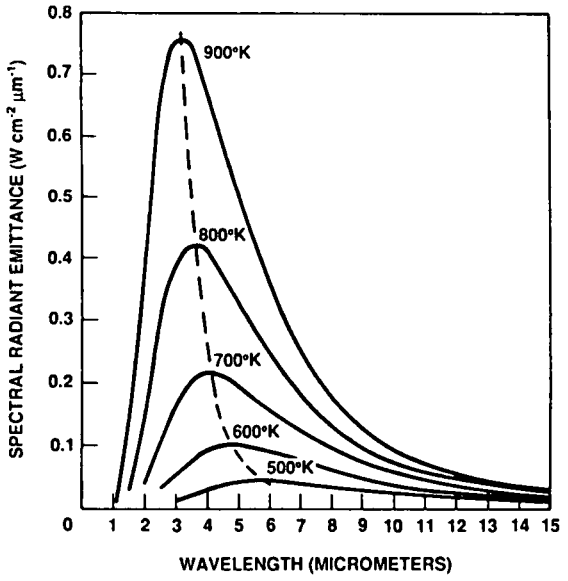

Figure 10. Blackbody radiation [After Reference 7].

Simple point extrinsic sensors to measure temperature may be made using blackbody radiation and fluorescence. These sensors were among the first to be commercialized. The principle upon which the blackbody sensor is based is shown in Figure 10. When an object is heated the spectral content of the emitted light shifts and also changes in intensity. By monitoring the spectral shift the temperature may be determined. Figure 11 shows schematically an Accufiber temperature sensor that uses a blackbody cavity at the end of the fiber and a spectral analyzer based on narrowband filters to measure temperature. Another commercial approach applied by Luxtron is to measure the fluorescent decay of light emitted from the end of an optical fiber coated with a phosphor elastomer after being subjected to a light pulse. Figure 12 shows the coated fiber end, while Figure 13 illustrates a typical fluorescent decay curve that is temperature dependent. Both of the above techniques have the important advantage of being independent of the light intensity. This is important as it allows the usage of connectors and other variable intensity elements between the sensing region and the output detectors necessary for many aerospace applications.

Changes in the index of refraction may also be used to support extrinsic sensors. An important application is their usage as liquid level sensors. Figure 14 illustrates a liquid level sensor based on the principle of total internal reflection. When the prism is dry the index of refraction difference between the prism and the gas medium is large and the light beam emitted from one fiber is directed back into the output fiber. When the prism is immersed in liquid the index of refraction is more nearly matched and the light beam escapes into the liquid, greatly attenuating the return light beam. Figure 15 shows another system used to measure the presence of steam in an industrial setting. In this case green and red light beams are passed through a prismatic chamber containing either water or steam. The refraction of the light beams then results in a green (water) or red (steam) light indication to the observer.

It is also possible to use optical fibers to carry a light signal to a media and measure properties of the media based on the returning light beam signature. As an example Figure 16 shows an optrode which uses a short wavelength light source and an optical fiber to deliver a light beam to a sampling region. The media then fluoresces in response to the light beam and the fluorescent signal is carried back to a spectrometer and data acquisition and processing unit where it is analyzed. This type of sensor has been used to monitor chemical species, water content, viscosity and many other important properties of materials and

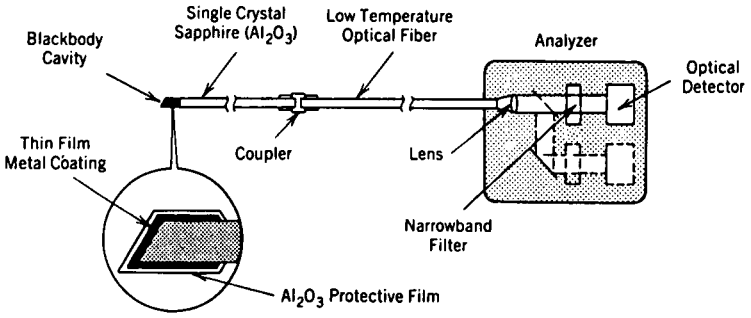

Figure 11. Accufiber temperature sensor using blackbody radiation [After Reference 7].

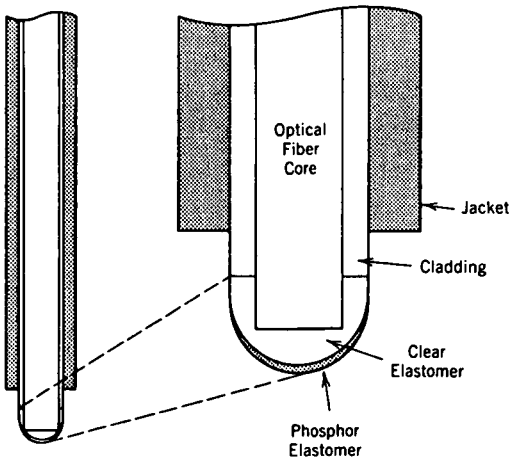

Figure 12. Luxtron fiber optic temperature sensor based on fluorescent decay [After Reference 7].

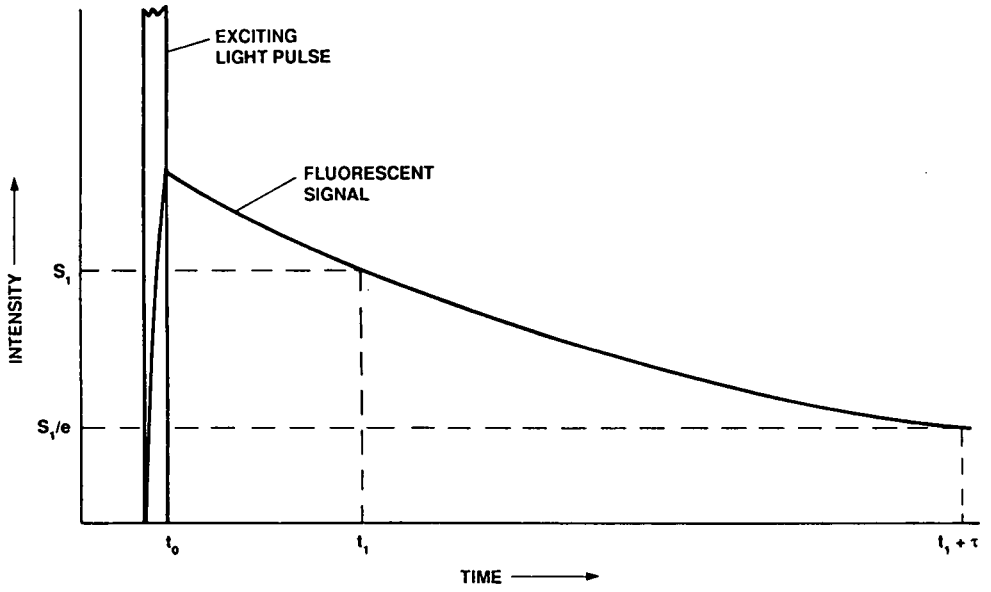

Figure 13. Fluorescent decay used to support temperature sensing [After Reference 7].

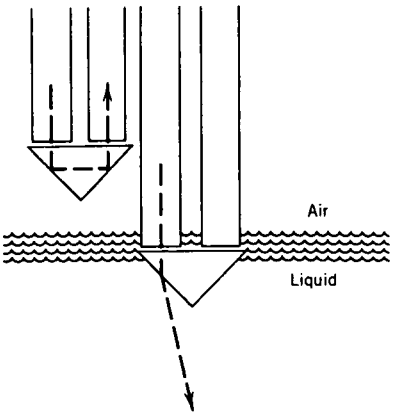

Figure 14. Liquid level sensor based on total internal reflection [After Reference 6].

a) DEVIATION OF BEAMS WHEN LIGHT PASSES THROUGH WATER

b) UNDEVIATED BEAMS WHEN LIGHT PASSES THROUGH STEAM

Figure 15. Liquid level indicator based on refraction [After Reference 7].

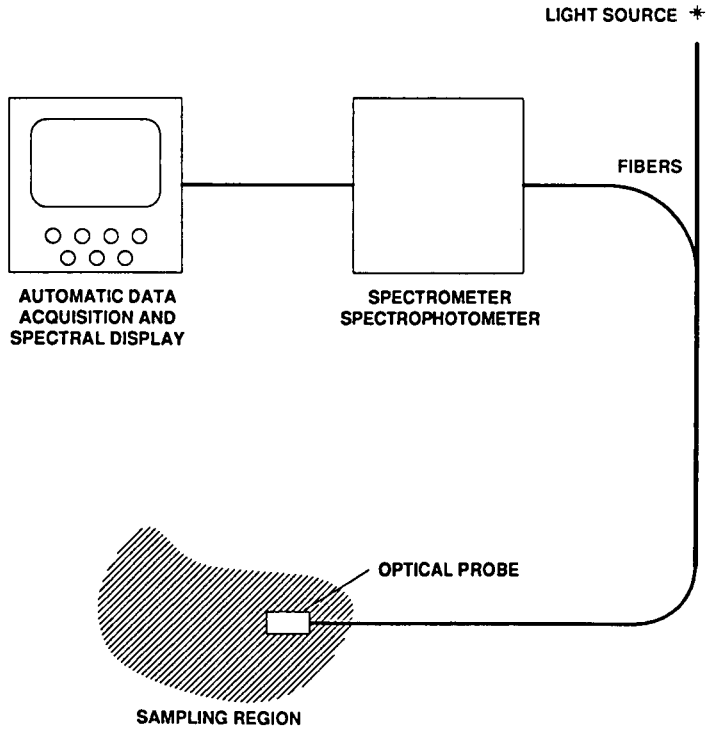

Figure 16. Fiber optic sensor used to monitor material properties based on fluorescence [After Reference 7].

media [Reference 8]. A second example of this type of fiber sensor is the laser doppler velocimeter system of Figure 17. Here two input fibers are used in combination with a lens to establish an interference pattern in a fluid flow. As particles move through the fluid flow they cause a modulated light signal that is collected by the lens and directed back into the output fiber. The resultant output signal frequency can then be used to determine the component of velocity of the particle perpendicular to the interference pattern.

Intrinsic or all fiber sensors measure environmental effects through their effect on light propagating through the optical fiber. This can be as simple as the measurement of loss of light due to bending of an optical fiber such as that used in the microbend accelerometer of Figure 18. Another class of fiber sensor uses changes in the mode profile of light beams propagating through optical fibers resulting in evanescent coupling or loss due to strain or bending [Reference 9]. These intensity modulated sensors have the advantages of being low cost and relatively simple. The main limitations are low sensitivity, linearity and dynamic range. Many of the higher performance intrinsic fiber sensors fall into the class of interferometric sensors. These sensors may be implemented in extrinsic (hybrid) or intrinsic (all fiber) form. As an example of an extrinsic interferometric sensor MetriCor has developed a series of etalon-based fiber sensors that may be used to measure pressure, temperature, and index of refraction as shown in Figure 19. These devices rely on spectral modulation of an incoming light beam that depends on the separation of the two mirrors forming the etalon. Because the information is spectrally encoded, difficulties associated with connector and fiber cable losses are minimized. To distinguish between the types of environmental effects the transducers are designed to respond primarily to the desired effect while minimizing undesired responses. It is also possible to form the etalon sensor in an intrinsic all-fiber mode by putting mirrors directly into the optical fiber. There are also many other types of interferometric sensors, three of which are shown in Figure 20. Each of these interferometric sensors is used to accurately determine changes in the phase of a light beam

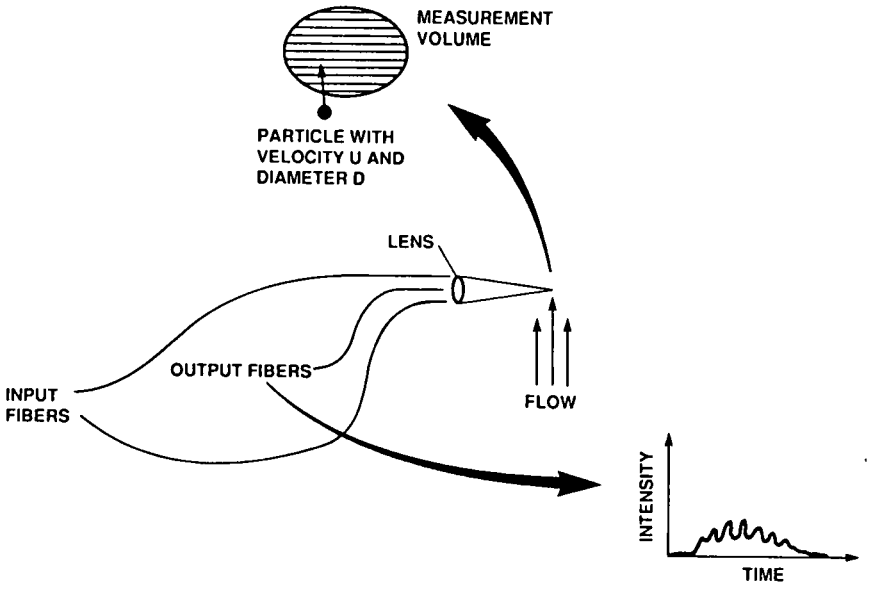

Figure 17. Fiber optic laser doppler velocimeter [After Reference 7].

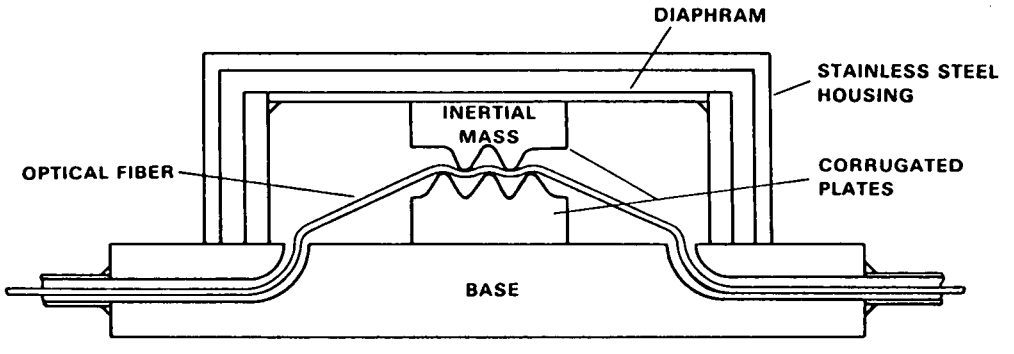

Figure 18. Accelerometer based on fiber optic microbending [After Reference 7].

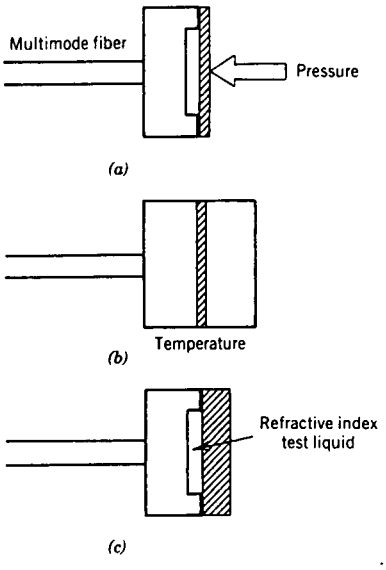

Figure 19. Fiber optic etalon based (a) pressure, (b) temperature and (c) refractive index sensors.

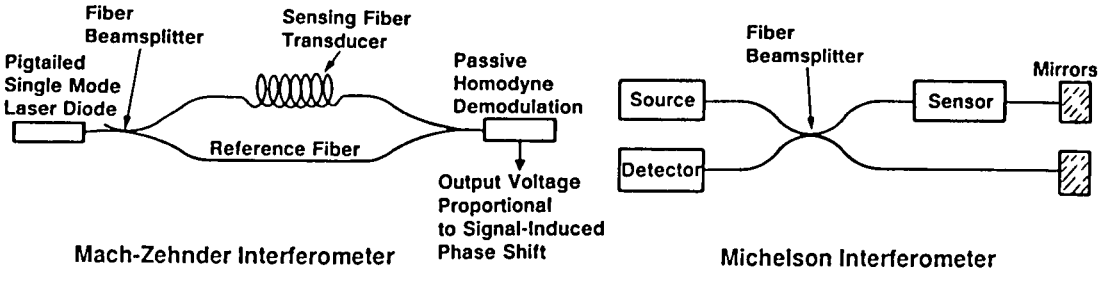

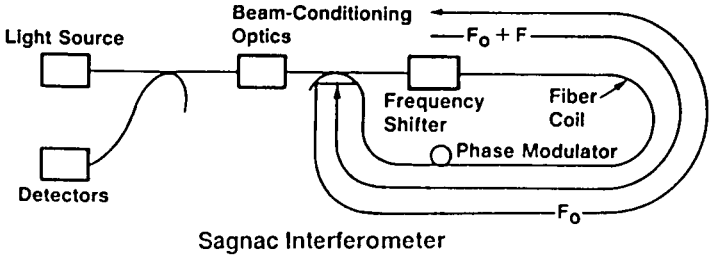

Figure 20. Interferometric fiber optic sensors.

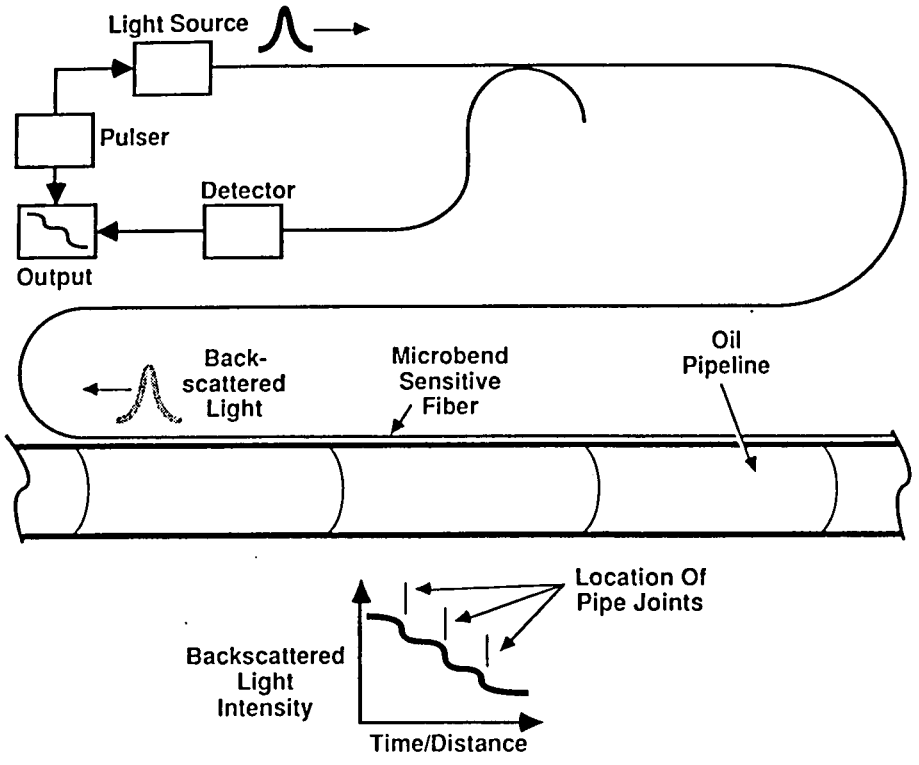

Figure 21. An application of time division multiplexing to support microbend sensors monitoring strain in a pipeline.

propagating through an optical fiber. Because environmental effects change the effective length of an optical fiber a measurable phase change results. The Mach-Zehnder interferometer [Reference 10-11] consists of a light source whose output is split by a fiber beamsplitter into two optical fiber paths. One of the paths is optimized to respond to the environmental effect while the other is shielded from it. When the two beams are combined and the phase shift is measured to determine the environmental effect. The Michelson interferometer is similar to a Mach-Zehnder that has effectively been cut in half with mirrors placed on the fiber ends to fold back the light beam toward the light source and detector. In general this type of interferometer has lower sensitivity than the Mach-Zehnder due to excess noise generated by feedback into the light source. One of the advantages of the Michelson is that it is single ended which can be useful for some applications. The last type of interferometer to be discussed is the Sagnac interferometer [References 12-15] that has been used to support fiber optic gyros. This interferometer has the unique feature of comparing light beams that propagate along nearly identical paths in opposite directions in a fiber optic coil. This feature allows the first-order cancellation of many environmental effects when the interferometer is properly configured for rotation sensing thereby allowing fiber optic gyros to be a major application of fiber optic sensor technology. This interferometer may be configured to sense acoustics, strain, and temperature as well to act as an instrument for measuring wavelength of a light source and fiber dispersion characteristics.

3. MULTIPLEXING

One of the important features of fiber optic sensors is that they can be multiplexed along a single line of optical fiber. Multiplexing techniques [References 16-17] that have been used include time domain, frequency, wavelength, coherence, and polarization multiplexing. The three techniques that are most commonly used are time domain, frequency, and wavelength division multiplexing. Figure 21 illustrates the

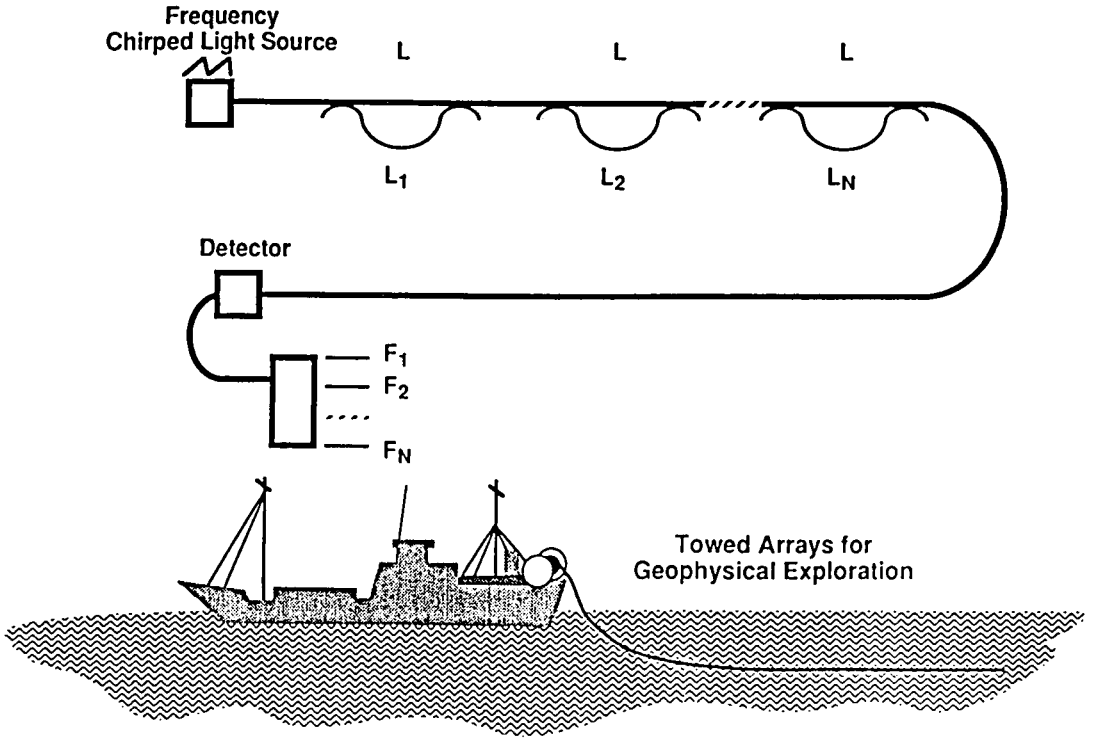

Figure 22. Frequency division multiplexing to support an array of Mach-Zehnder based acoustic sensors.

application of time division multiplexing in combination with microbend sensitive fiber to monitor stress in an oil pipeline. In this case a light pulse is sent down the fiber and the return backscattered light analyzed with respect to time. Because excess stress increases microbending loss, the location of stress points can be measured. An example of frequency division multiplexing methods is shown in Figure 22. Here a light source is chirped in frequency (this can be done by modulating the current in a laser diode for example) and a series of Mach-Zehnder interferometers are placed along a single fiber line with predetermined length differences between the two fiber interferometer legs. Each of these differences result in a carrier frequency F1 to FN that is separate and distinct from the other interferometers resulting in separable signals. An example of wavelength division multiplexing is shown in Figure 23. Here a broadband light source is used and split into several fiber paths by a star coupler. The end of the reference leg has a broadband mirror that reflects most of the light. The various sensor legs have mirrors that reflect only a specific portion of the broadband light sources spectral envelop. When the light beams are recombined a dispersive element is used to separate out the spectral signals from each of the sensors. These multiplexing techniques may be used separately or combined to support larger numbers of sensors.

4. AEROSPACE APPLICATIONS

Advanced aerospace platforms are ideal candidates for the widespread usage of fiber optic sensor technology [References 18-21] in that they require lightweight, low-power sensor systems capable of withstanding severe environments. Figure 24 shows areas where fiber optic sensors could be applied to a launch vehicle. At the rocket nozzle, temperatures and vibrations are such that conventional electronic sensors would fail well before meaningful measurements could be made. Fiber optic sensors have been demonstrated at operating temperatures of over 1000 degrees centigrade and by using sapphire based sensors have the potential to go much higher. At the same time they have demonstrated the ability to withstand

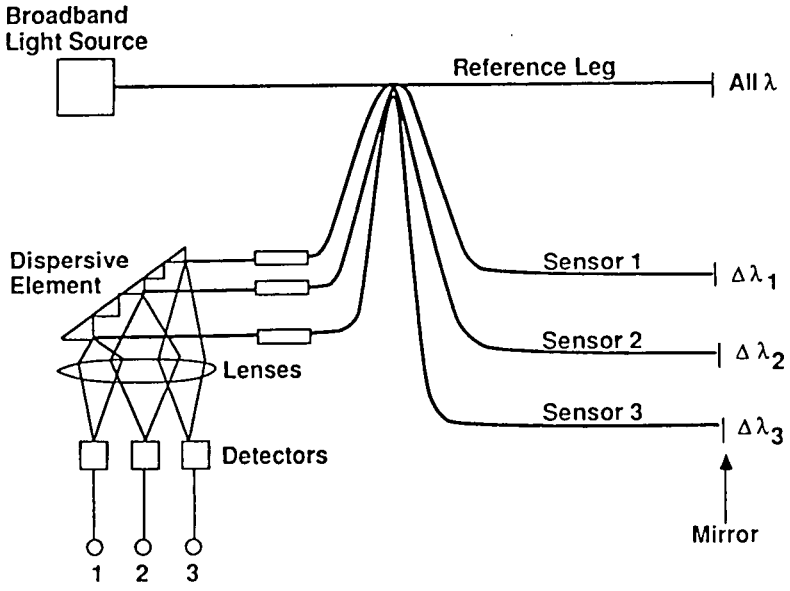

Figure 23. An example of wavelength division multiplexing.

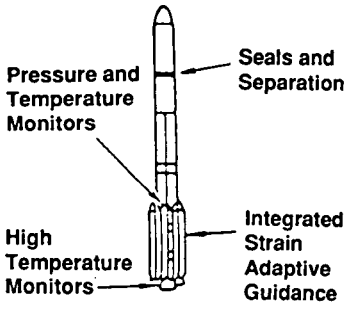

Figure 24. Application of fiber optic sensors to a launch vehicle.

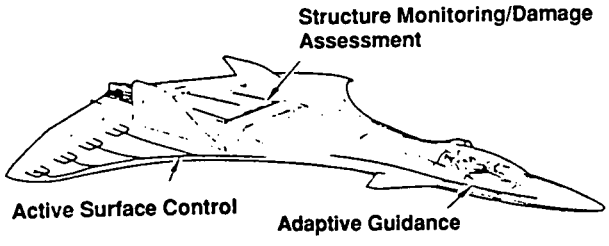

Figure 25. Application of fiber optic sensors to an aircraft.

high shocks and g loading necessary to support launch vehicles. Other applications include monitoring cryogenic tanks for leaks as well as pressure and temperature at critical locations.

For aircraft as shown in Figure 25 fiber optic systems could be used to support smart structure health monitoring systems to continually assess structural integrity. The sensor could also be used to support active surface control systems and adaptive guidance.

One of the issues for space platforms of Figure 26 is that as they become increasing advanced the structure can be expected to be lighter. Active control of the platform may then become necessary to damp out undesired vibrations and prevent oscillations. Fiber optic sensors could then be used to form a nervous system throughout the structure that in combination with actuators could control the structure. A network of fiber optic sensors could also be used to assess the health of the structure, payloads and habitats as well as be used to support data networks.

As an example of how fiber sensors may be used to support an aerospace platform consider the case of the cryogenic composite tank illustrated by Figure 27. Fiber sensors are wound into the structure as it is being built to monitor such parameters as degree of cure, temperature, pressure, water content, and residual strain. After the part is built the sensors may be used to support nondestructive evaluation techniques including acting as embedded acoustic sensors to support ultrasonic evaluation. Once the part is installed the sensors may become part on a health monitoring system used to support the platform prior to and after launch.

5. CONCLUSION

An overview of fiber optic sensors has been provided with reference to aerospace applications. It can be expected that the usage of these sensors will become increasingly important as advances are made in optoelectronic components and fiber optic communication systems.

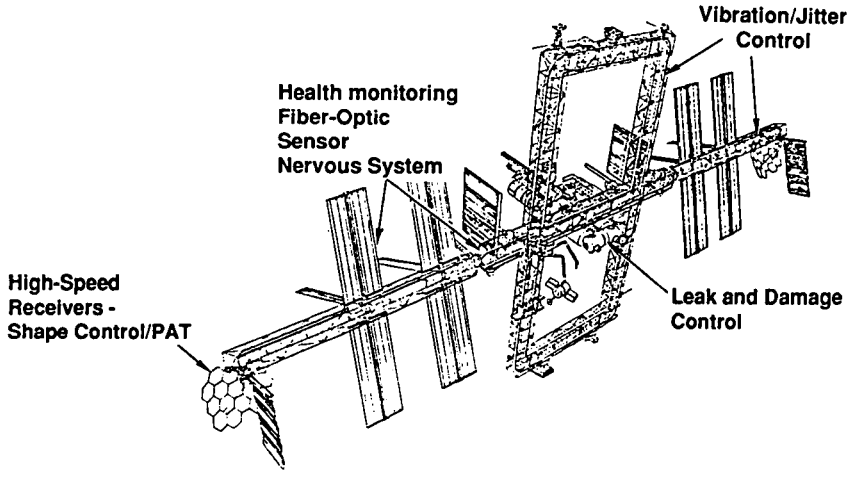

Figure 26. Application of fiber optic sensors to a space platform.

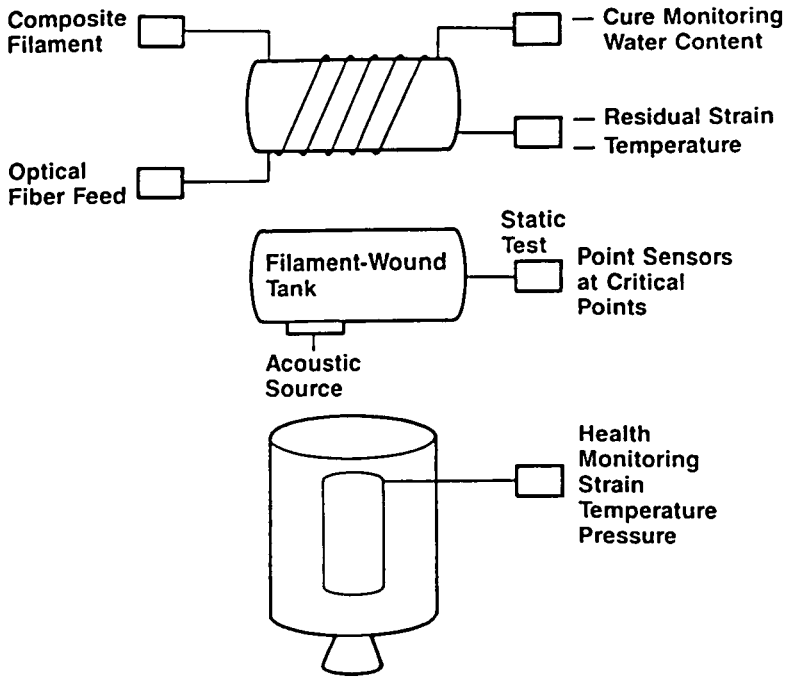

Figure 27. Usage of a fiber optic sensor to support the manufacture testing and deployment of a health monitoring system on a pressurized tank.

6. REFERENCES

1. E. Udd, Editor, "Fiber Optic Sensors: An Introduction for Engineers and Scientists", Wiley, New York, 1991.

2. J. Dakin and B. Culshaw, Editors, "Optical Fiber Sensors: Principles and Components", Vol. 1, Artech House, Boston, 1988.

3. B. Culshaw and J. Dakin, "Optical Fiber Sensors: Systems and Applications", Vol. 2, Artech House, Norwood, Mass., 1991.

4. E. Udd, "The Emergence of Fiber Optic Sensor Technology", in "Fiber Optic Sensors: An Introduction for Engineers and Scientists", Edited by E. Udd, Wiley, 1991.

5. D.A. Nolan, P.E. Blaszyk and E. Udd, "Optical Fibers", in "Fiber Optic Sensors: An Introduction for Engineers and Scientists", Edited by E. Udd, Wiley, 1991.

6. G. Mitchell, "Intensity-Based and Fabry-Perot Interferometer Sensors", in "Fiber Optic Sensors: An Introduction for Engineers and Scientists", Edited by E. Udd, Wiley, 1991.

7. J.W. Berthold, "Industrial Application of Fiber Optic Sensors", in "Fiber Optic Sensors: An Introduction for Engineers and Scientists", Edited by E. Udd, Wiley, 1991.

8. R.A. Lieberman, Editor, "Chemical, Biochemical and Environmental Sensors III", Proceedings of SPIE, Vol. 1587, 1991.

9. T.E. Clark and M.W. Hall, "Thermally Switched Couplers", Proceedings of SPIE, Vol. 986, p. 164, 1988.

10. A. Dandridge, "Fiber Optic Sensors Based on the Mach-Zehnder and Michelson Interferometers", in , Edited by E. Udd, Wiley, 1991.

11. A. Dandridge and A.D. Kersey, "Overview of Mach-Zehnder Sensor Technology and Applications', Proceedings of SPIE, Vol. 985, p. 34, 1988.

12. S. Ezekial and H.J. Arditty, Editors, "Fiber Optic Rotation Sensors", Springer Series in Optical Sciences, Vol. 32, Springer-Verlag, New York, 1982.

13. E. Udd, Editor, "Fiber Optic Gyros: 10th Anniversary Conference", Proceedings of SPIE, Vol. 719, 1986.

14. S. Ezekial and E. Udd, Editors, "Fiber Optic Gyros: 15th Anniversary Conference", Proceedings of SPIE, Vol. 1585, 1991.

15. E. Udd, "Fiber Optic Sensors Based on the Sagnac Interferometer and Passive Ring Resonator", in "Fiber Optic Sensors: An Introduction for Engineers and Scientists", Edited by E. Udd, Wiley 1991.

16. A.D. Kersey and J.P. Dakin, Editors, "Distributed and Multiplexed Fiber Optic Sensors", Proceedings of SPIE, Vol. 1586, 1991.

17. S.D. Kersey, "Distributed and Multiplexed Fiber Optic Sensors" in "Fiber Optic Sensors: An Introduction for Engineers and Scientists", Edited by E. Udd, Wiley, 1991.

18. R.M. Measures, "Smart Structures with Nerves of Glass", Progress in Aerospace Science, Vol. 26, p. 289, 1989.

19. C.J. Mazur, G.P. Sendeckyj, and D.M. Stevens, "Air Force Smart Structure/Skins Program Overview", Proceedings of SPIE, Vol. 986, p. 19, 1988.

20. R.O. Claus and E. Udd, Editors, "Fiber Optic Smart Structures and Skins IV", Proceedings of SPIE, Vol. 1588, 1991.

21. E. Udd, "Fiber Optic Smart Structures", in "Fiber Optic Sensors: An Introduction for Engineers and Scientists", Edited by E. Udd, Wiley, 1991.

Acknowledgement

Figures 1-19 are drawn from the book Fiber Optic Sensors: An Introduction for Engineers and Scientists, edited by Eric Udd, Copyright 1991 by John Wiley and Sons, Inc. Permission to use these figures has been granted by John Wiley and Sons, Inc. and is gratefully acknowledged.

Smart Structures - The Relevance of Fibre Optics

Brian Culshaw
Peter T. Gardiner

Smart Structures Research Institute
University of Strathclyde
204 George Street, Glasgow G1 1XW
Scotland, U.K.

ABSTRACT

The concept of the smart structure integrates structural engineering, sensing, control systems and actuation to provide a mechanical assembly which is capable of responding to its environment and/or loading conditions. The realisation of the smart structure requires integration of skills in a variety of scientific and engineering disciplines ranging from mechanical engineering through materials science into signal processing, data analysis, sensing and actuation.

The sensing technology must have a number of key features of which the ability to take distributed measurements of various parameters throughout the structure is paramount. Fibre optics technology therefore promises to have a significant role to play in the evolution of the smart structures concept. This paper analyses this role in detail, presents an assessment of the current state-of-the art in fibre optic technology related to smart structures and presents a scenario for future developments.

1. INTRODUCTION

The smart structure integrates mechanical engineering, control systems, signal processing and actuation in a way which can be visualised with reference to Figure 1. The essential concepts are that the actuators and sensors are embedded within the actual structure and therefore form an integral part of its behavioural characteristics rather than an "add on" which would typify the more instrumented structure. The smart structure may then respond by adapting its dimensions, its stiffness, its vibrational characteristics, its damping constant, etc, in response to environmental and/or loading conditions. The realisation of a truly smart or adaptive structure requires advanced technology in sensing, processing, control and actuation and to date they have only been brought together at a relatively simplistic level for specialised applications such as space vehicles [Ref. 1].

The first step in the realisation of the generalised smart structure is the incorporation of the necessary sensor arrays to obtain the essential data concerning the state of the structure. In general this requires precision distributed measurements of the strain, temperature and sometimes chemical composition throughout the structure. Careful analysis of loading requirements and the structural characteristics can limit the number of sensory elements required, but in general, a complex sensing array is essential. This paper focuses on the needs in this sensor array and discusses these needs with reference to the properties of fibre optics systems, thereby demonstrating that fibre optics will have an important but not exclusive role to play in the evolution of smart structures.

Potential applications for smart structures may be viewed either by the industrial sector under consideration or through the properties of the materials from which a particular structure is fabricated. There are potential applications in aerospace (especially for zero gravity structures), civil engineering, marine engineering, automotive engineering, and in the longer term, when the technology costs are pruned, in consumer products such as toys, leisure goods and domestic appliances. A discussion based upon market sectorial requirements would entail analysis of factors such as performance, materials, structural dimensions and environmental requirements. Categorising smart structures is probably simpler if the analysis is centred upon their use in three principal materials: plastics, especially fibre reinforced composites, structural metals, including steels and alloys, and building materials, especially concrete. These materials possibilities cover all the requirements in the industrial sectors mentioned previously and consequently this paper will concentrate on a materials based critique of the smart structure system. Aerospace use is focussed on composites and metals, but an analysis of concrete is included for comparison.

The remainder of the paper is divided into four major sections. Initially the basic needs appropriate to each of these applications is analysed. This then leads into a critique of the sensor options available. We then continue to discuss the range of fibre optic sensors available and their potential role in this context. Finally, an assessment of future problems and future prospects for fibre optics and smart structures is presented.

2. MATERIALS APPLICATIONS

2.1 Introduction

The reasons for approaching the analysis of smart structures on a materials basis have already been outlined. However before going into the materials based discussion it is useful to briefly distinguish the applications sectors. The difference is primarily concerned with structural sizes. In discussing structural sizes there are two factors of interest. The first is the overall dimension. It is also important to analyse the characteristic distance between stiffeners and supports within the structure since this determines the effective maximum resonant frequencies which can be expected within it. The other main features concern response times, bandwidths and environmental requirements. Table 2.1 presents a broad brush summary of these parameters for aerospace, civil engineering, marine engineering and automotive applications.

TABLE 2.1 - Structural Monitoring Characteristics of Various Applications

Sector	*Size*	*Characteristic Dimension*	*Environment*	*Accessibility*	*Time Constants*	*Costs*
Aerospace	5-50m	0.5m	Severe	On-board	msecs-secs	Can be high
Civil	100-1km	10m	Moderate-Severe	can be remote	days	moderate to high (no research tradition except Japan
Marine	10m-500m	1-5m	Moderate - Severe	can be remote	minutes	moderate to high
Automotive	< 10m	< 1m	Moderate (except engine components)	On-board	seconds	must be low

TABLE 2.2 - COMPOSITE MATERIALS

Measurand / *Application*	*Temperature*	*Strain*	*Delamination and Fracture*	*Chemical Sensing*	*Water and Moisture*	*pH*	*Comments*
Fabrication	0-200°C ± 1°C (to 400°C PEEK)	20,000$\mu\epsilon$ ± 100$\mu\epsilon$	n/a	Cross-linking of resin matrix (often indirectly via mechanical changes	n/a	n/a	Cure monitoring potentially important. All sensors must survive cure process.
Test	-55°C to +125 ± 1°C	As above	Detect delamination ≈ 1cm². Cracks ≈ 50μm wide.	n/a	Opinons vary. 0.1% moisture content sufficient to cause concern.	n/a	Testing primarily mechanical and thermal. Moisture useful for R.H. testing
In-Service Monitoring	As above	As above	As above	n/a	As above		In service monitoring needs long life version of test sensors
Comments	Usually important to correct other measurands	Strain histories and signatures potential indicator of structural deterioration	Can also be in principle detected by, e.g. modal frequency analysis ultrasonic testing		Effect of moisture on composites not well documented		Sensor EMBEDDING preferred and well developed

TABLE 2.3 - STRUCTURAL METALS

Measurand / *Application*	*Temperature*	*Strain*	*Delamination and Fracture*	*Chemical Sensing*	*Water and Moisture*	*pH*	*Comments*
Fabrication							Temperatures too high for *conventional* embedded sensors. No obvious gains from measurements.
Test	-55°C to +125°C ± 1°C	1000$\mu\epsilon$ ± 10$\mu\epsilon$	50μm crack widths	n/a	n/a	n/a	Fibre optics offers simple way to instrument complex test pieces
In-service monitoring	As above	As above	As above	Corrosion conditions and corrosion products, esp for steels	n/a	Presence of pH < 7.5 to permit corrosion of steels	Metal (especially steel) structures also important in concrete (see Table 2.4).
Comments		Optical fibre has breaking strain ten times that of metals	The NMI/Cranfield tell tale one of the first in this area (≈ 1978)	Chemical may here be most effective using point sensors in strategic spots			All sensors must be SURFACE MOUNTED

TABLE 2.4 - CONCRETES

Measurand / *Application*	*Temperature*	*Strain*	*Delamination and Fracture*	*Chemical Sensing*	*Water and Moisture*	*pH*	*Comments*
Fabrication	n/a	n/a	n/a	n/a	n/a	n/a	Setting times, etc, depend on input mixture control
Test	-50°C to +80°C ± 1°C	Strain to fracture low ($\approx 100\mu\epsilon$) STRESS important only in tension	Cracks > 100μm	n/a	n/a	n/a	Structures designed to be in compression. Sample testing for quality control. Load models of full structure.
In service monitoring	-50°C to +80°C ± 1°C	Detect vibrational spectra or displacement under load	as above	n/a	Ingress can stimulate ice damage	pH < 8 gives signal for corrosion of reinforcement elements	Gradual lowering of pH from $\approx$ 12.8 to 8 in service viewed as good indicator
Comments	Represents outdoor extremes	Commercial sensors already available for function				Point sensors for pH on vulnerable re-inforcing bars seems optimum	Building industry promising as first application area

2.2 Composite Materials

Composite materials embrace mainly carbon or glass fibre reinforced polymer resin matrix systems and the more advanced ceramic and metal matrix systems. To date smart structures work has concentrated upon polymeric systems and no significant information has been gathered concerning their possibilities in metal and ceramic matrix composites. Since these are primarily aimed at high temperature applications there are obvious potential difficulties with the survivability of coating materials, though of course, metal covered optical fibres should be totally compatible.

A key element in composite structure instrumentation is that sensors can be embedded within the material and they should also be able to withstand the temperature and strain excursions under which the material itself can operate. These particular requirements make fibre optics sensors especially useful in this context since the optical fibre is entirely compatible with the reinforcing fibres in the material and can withstand similar mechanical and thermal excursions. These requirements are summarised in Table 2.2.

2.3 Structural Metals

The first steps in structural integrity monitoring using fibre optics were aimed at examining metallic materials, especially those used in the fabrication of off-shore structures [Ref. 2]. This device, first described in 1978, relies upon the appearance of cracks in the structure breaking optical fibres at predetermined breaking strains. By monitoring which fibres had broken the development of cracks could be measured. However, since the strain tolerance of metals is small compared to that of fibres, this breakage technique only detects damage. For the more general situation, the requirements are those summarised in Table 2.3.

One specific generic feature worthy of mention is that any sensor array will have to be attached to the outside of a metallic structure since the forming conditions for most metallic structures whether they are cast, machined or forged cannot be tolerated by any embeddable sensor technology. Recently [Ref.3] embedding in cast aluminium has been reported.

2.4 Concrete

Although concrete is not extensively used in aerospace, it is interesting to see the requirements because the overall situation in concrete is very different. The forming temperatures are relative modest - though concrete can become significantly warm during the setting process due to an exothermic reaction - but the mechanical conditions which may be experienced by any embedded sensor system are obviously extreme. To date most instrumentation in concrete structures has been embedded in channels after the major part of the structure has been fabricated or incorporated into composite reinforcing members. There have been a few trials with fibres made up in concrete while it is being poured and occasionally the fibre survived. The overall requirements for concrete structures are shown in Table 2.4.

2.5 Other Materials

Whilst the preceding discussion covers most of the structural materials of interest, there are obviously some potential exceptions. The most obvious is the "smart rope" currently being investigated as a project within the Smart Structures Research Institute at Strathclyde. Here the prime material constituent is high strength nylon and the need is to indicate areas in which the nylon has been excessively stressed. There may also be other applications specific material requirements and these are likely to occur in the consumer markets if and when the technology reaches that particular arena.

3. SENSOR TECHNOLOGIES

3.1 Essential Needs

The basic requirements of the sensor system may be summarised as follows:

- It must have the necessary spatial and temporal bandwidths dictated by the structural size and the maximum modal frequency expected within the structure. As a guide-line the sensory structure which measures 10 points per characteristic dimension (see table 2.1) is likely to prove to have adequate spatial bandwidth. The equivalent temporal bandwidth will involve going up to a few harmonics of the resonant frequency corresponding to the characteristic dimension. Typically the speed of sound is in the region of 5,000 metres per second in many solids so the corresponding maximum frequency of interest is of the order 25,000-x Hz, where x is a characteristic dimension. Depending upon the structure the frequency may be significantly lower since often transverse rather than longitudinal waves are appropriate, but occasionally it may be higher if the structure is subjected to heavy tensile load.

- The sensor must be compatible with the materials which form the structure. In particular the sensor must withstand the mechanical and environmental excursions for which the structure is designed.

- Simple systems are preferred and in particular sensor multiplexing is an almost inevitable requirement. This could be effected using distributed sensors or a conventional communication bus could be embedded and connected to intelligent local sensor systems.

- Embedding is preferred since intimate contact with the material itself is ensured. For some materials, especially metals, the necessary attachment procedures must be specified.

- The cost of the sensor system must be small compared to the cost of the structure and must be capable of realising significant savings in either the design, the installation or the operation of the structure.

3.2 Candidate Sensor Technologies

There remains significant interest in the potential of surface mounted sensor technologies whilst in the longer term embedded systems are probably preferable since they permit intimate examination of the material properties. Consequently it is useful to categorise candidate technologies in terms of surface and embeddable approaches. Finally there are a number of probing technologies which may be used in conjunction with or independently of the sensor arrays. These are all outlined.

3.2.1 Surface Inspection Technique

The principal ones are:

- conventional strain gauges which must be attached to the structure and individually wired to a separate monitoring unit.
- conventional thermocouples which require similar wiring.
- visual NDT which is obviously only suitable for off-line use.
- visual indicators such as the colour changes observed in some liquid crystals with changes in temperature. The measurands which can be addressed using these techniques are limited to temperature and stress and these are indicators only rather than accurate measurement devices.
- chemically reactive surface treatments responding to changes in local pH, CO_2 content etc.

The first two of these options are really not considered as prime candidates for smart structures use. However, the possibility for a small sensor with compact local signal processing, transmitting onto a digital data bus has not been addressed in the literature and appears to offer the potential for rugged, attached system sensing technologies.

3.2.2 Embeddable technologies

Here there are three prime possibilities:

- fibre optic sensors which form the subject of the remainder of the paper
- acoustic waveguide sensors which have been tried but suffer from acoustic loss during transmission and are also very much at the pre-laboratory prototype stage.
- embedding resistant intelligent electronic systems could be conceived but have not been realised with sufficient ruggedness and adequately low cost for incorporation in any other than extremely special material systems.

3.2.3 Probes

It seems likely that probing techniques will complement sensor arrays and the combination of the two could prove to be extremely powerful. Examples could include:

- ultrasonic signature analysis combining a known probing function with the responses of the sensor arrays in the structure.
- analytical systems involving the use of radioactive isotopes and the analysis of their signatures.
- acoustic emission, typically produced during structural damage, whose occurrence could be built into a watching brief for the sensing network.

3.3 Observations and Conclusions

There are clearly many options for the sensor technologies to be incorporated in smart structures. Current realisations of the overall concept rely almost exclusively on "conventional" sensor technologies such as silicon strain gauges and thermocouples for their implementation. However, the limitations of these approaches both in terms of material compatibility and system complexity do inhibit their long term potential.

A range of sensor approaches will be necessary in the final realisation of any smart structure complex. Here the focus sits upon the fibre optics technologies and these must have an important part to play since embedded fibre optics can realise single point, multiplexed or distributed sensing and is compatible with most material systems. Furthermore an embedded fibre optic sensor array can be implemented in conjunction with appropriate probe technologies to provide advanced non destructive evaluation procedures. Additionally, the array can be programmed to recognise the onset of acoustic emission due to damage during operation so that the alarm function for this, and indeed, other events can be built into the system configuration.

Preliminary fibre optic systems have been operated in carbon and glass fibre composites and in concrete structures. Experience gained from these systems will lead to significant future developments. The following sections review the technologies available and the developments which may accrue.

4. FIBRE OPTIC SENSOR TECHNIQUES: BASIC PRINCIPLES

A complete review of the principles of fibre optic sensors may be obtained elsewhere [Ref. 4]. For the purposes of this discussion it is useful to review the principal mechanisms underlying fibre optic sensors and very briefly describe their potential in terms of measuring particular physical valuables. Fibre optic sensors may be categorised in a wide variety of schemes. In this context examining "discrete" and "distributed" techniques provides the most relevant information on the smart structures application. Here a discrete sensor is one which measures at a single point or to be more exact measures a single variable either at a single point or averaged along a specific length of optical fibre. The distributed measuring system measures a particular variable along the length of the fibre but includes the possibility for analysing the variation of this variable along the fibre's length.

4.1 Discrete Sensing Techniques

The principal systems include:

- Interferometers including polarimeters and mode/interference systems (Figure 2) all rely upon measuring the effective optical length of the fibre and relating this to the measurand of interest, typically temperature or strain. The measurement of the total absolute length (interferometry) is an extremely sensitive indicator of strain and is often too sensitive for practical use. In polarimetry and mode-mode interferometers the system measures the differential between the delays of two closely spaced propagating modes within the fibre. This second order measurement is usually sufficiently sensitive for most purposes. It is important to realise that both temperature and mechanical strain produce the same effect (namely a change in delay) so that if temperature and strain occur in the same temporal bandwidth a dual measurement is essential to separate one from the other. Dynamic measurements of strain can be made unambiguously and the technique is intrinsically precise and repeatable since the measurement is referred back to the wavelength of the laser used to radiate the fibre.

- Microbend sensors (Figure 3) rely upon mechanically induced perturbations to the external profile of the fibre to induce loss along the fibre length. Therefore a measurement of the attenuation along the fibre gives and indication of the mechanical condition of the fibre. Typically this indication is only repeatable to a 10% level for a given mechanical perturbation and intense local strain may produce an equivalent signal to a much smaller distributed strain. The process is inherently non-linear but can be used to good effect in areas where the strain is known to be limited (for example concrete bridges) and is also useful for dynamic measurements involving the determination of, for example, modal frequencies.

- "Tell-tale" sensors involve the breakage of an optical fibre. The detection of this breakage is an indication of damage to the structure to which the fibre is attached or in which it is embedded. The problem is that most glass or silica optical fibres have a breaking strain in excess of 5% which exceeds that of most structural materials. The surface can be treated to reduce the breaking strain of the optical fibre but the repeatability and reliability of this process can be called into question. The technique has however been used as a damage monitoring concept.

- Index matching cladding (Figure 4) can be used as a means to monitor the distribution of refractive index along an optical fibre and this basic idea has been put to good effect in a gas leakage cryogenic alarm. The fibre ceases to guide when the cladding index equals or exceeds the core index. Thus the cryogenic alarm operates by exploiting differential thermal coefficients of refractive index between the core and the cladding. In smart structures this approach has been used to monitor the curing of epoxy resins whose index increases at the phase transition point. Therefore a fibre with appropriate core index embedded within the matrix will cease to transmit when the matrix is set. Careful choice of materials can also realise a range of temperature alarms using the same technique.

- Chemical measurements (Figure 4) can be realised using a very wide variety of approaches. Chemical measurements in smart structures are acknowledged to be important especially in the fabrication phase and also as a tool in corrosion monitoring. However, the ideal technique whereby the concepts may be adapted into the smart structures area remains to be identified. With the exception of the index matched cladding approach there have been no reports of embedded chemical sensing.

4.2 Distributed Sensing and Array Technologies

Much has been said on the topic of distributed sensing [Ref. 5]. To date there has been relatively little field experience with such systems since there are undeniable problems associated with the accurate single valued definition of the relationship between the measurand of interest and the effect observed on the fibre. The distributed sensor (Figure 5) must be distinguished from the multiplexed sensor array (Figure 6), also discussed in detail in Ref. 6. In the distributed sensor the fibre itself is a sensor material and no attempt is made within the fibre path to distinguish between particular elements along that path. In the multiplexed system the sensor may be the fibre or may be a material attached to the fibre. However some topological distinctions are incorporated within the network to ensure that one particular sensor section can be identified from others typically by its position defined as a time delay through the network or as a geographical route through the network.

Both approaches are relevant for smart structures.

One obvious requirement for smart structures is the need for a simple fibre network within the structure. In general this implies a single fibre length operating as a sensing element. If we accept this as a requirement then in principle the unperturbed approach typifying distributed sensing is probably preferable. However, some form of multiplexing approach has significant advantages. In particular the signal from a specific sensing element can be enhanced and there is substantially greater flexibility in the spatial resolution obtainable with multiplexed concepts rather than distributed ones.

This leads to the need for new techniques to delineate sensor arrays along the length of a single fibre (Figure 7). To date the following have been the principal candidates:

- localised fusing of a fibre to change the characteristics of the fibre along the short length. This has been particularly useful in producing polarisation coupling between the fundamental modes of a polarisation maintaining fibre.

- photo-refractively induced Bragg gratings which rely upon the photo-refractive effect in germania doped silica core fibres to produce a coupling determined by the periodicity of the Bragg grating.

- Mechanical strain introduced at specific points to produce coupling.

Of these, the first two proved to be relatively successful and have survived the embedding process quite well. The last is subject to fluctuations during embedding.

Perhaps the most successful distributed sensing technique is the Stokes/anti-Stokes temperature measurement system shown in Figure 8. This can measure with resolutions of degrees centigrade over distances of the order of metres and integration times of the order of minutes. The technique has the advantage that it relies upon fundamental properties of the fibre for its operation and is therefore self calibrating. However, its spatial and thermal resolution is usually too low for its successful use in smart structures. Furthermore, its expense restricts its penetration in some of the more obvious possible areas such as monitoring the setting procedures in concrete.

The only distributed sensing system to make any inroads in smart structures is the time domain reflectometry option of the microbend system which essentially combines the basic concept in Figure 6 with the sensor from Figure 3. Using an appropriately designed cable this can be used to monitor strain over quite large structures and a number of trial systems have been installed in the United States primarily championed through the activities of G2 Systems. [Ref. 7].

Finally the quest for the ideal distributed sensing system continues and Figure 9 shows one of the current research options involving the use of nonlinear phenomena as the means of transducing the physical measurand onto and optical carrier [Ref. 5]. Whether this will prove to be practical in the medium to long term remains to be seen.

5. FIBRE OPTIC SENSORS - SOME RESULTS

5.1 Sensor Techniques

The drive at the research end of optical fibre sensor activities is most definitely towards applications in fibre reinforced plastics with a particular bias towards the aerospace industry. Actual progress has been relatively modest and has highlighted a number of the problem areas which have already been alluded to. In contrast the civil engineering sector is beginning to accumulate field experience at a low but rapidly increasing rate. In this section we attempt to summarise the principal achievements which have been reported to date. Whilst such a summary can never be complete, it does represent a reasonably accurate picture. The discussion focuses upon measurands rather than applications sectors.

5.1.1 Distributed and Integrated Strain

Integrated dynamic strain is simple to measure. The problem is that interferometric sensors are too sensitive so that most strain sensitive systems for use in structural integrity monitoring will use a polarimetric sensing technique These systems are essentially of *distance* measurement devices rather than *strain* measurement devices and most polarimetric configurations can readily measure distance changes of a few microns. In an interferometric mode this sensitivity, for very simple detection schemes, is a few orders of magnitude higher. There have been demonstrations of integrated dynamic strain measurements in composites, though few have commented on the relative scale factors of the sensor in the embedded mode and in the free standing mode. None, within existing knowledge has related this to any modelling as the material interfaces.

Distributed dynamic strain is a different matter. The only demonstration of such a sensor is that undertaken under the OSTIC (Optical Sensing Techniques in Intelligent Composites) programme, a recently completed collaborative European project. The full experimental results have still to be reported but preliminary indications are that the necessary tens of micro-strains of sensitivity over a gauge length of 20 cm should be achievable with a sensor count of 6 or so. [Ref. 8].

Quasi-static strain measurements are an entirely different problem in that thermal changes and quasi-static strain changes produce the same signal (a change in optical delay or in the mode-mode case in differential optical delay). The only experimental results reported in detail on the temperature strain measurement are those again under the OSTIC programme which uses a combined mode:mode/ polarimetric system to make differentially sensitive temperature and strain measurement. The choice of fibre is critical in the success of the measurement technique. Temperature resolutions of the order of 1°C in the presence of strain resolutions corresponding to 20μm extensions can be individually separated. To date this has only been demonstrated on a single element (i.e. integrated) sensor but, provided that the delineation problem could be resolved, the concept could be extended to a distributed network.

One of the major difficulties with distributed strain measurement is the derivation of an adequately strong signal from a suitably simple optical network. The OSTIC work uses slightly twisted splices to provide coupling between the fast and slow modes of the birefringent fibre at pre-determined points. An alternative technique is to use crimp rings which have the same effect. Neither of these is entirely satisfactory since they involve tampering with the mechanical characteristics of the fibre (Fig. 7).

Many workers, most recently UTIAS (University of Toronto Institute of Aerospace Studies) and Bertin of France, have used the so-called "Hill" gratings in high germania core fibre to mark the ends of sections [Refs. 9&10]. This technique offers some promise but the relatively small index changes which can be achieved (of the order of 10^{-4}) mean that relatively long gratings are required to get decent reflectivity (at least 1000 periods). Consequently, the bandwidths of such gratings is 0.1%. When the gratings are strained through say 1%, then the operating frequency of the grating is significantly shifted. Of course, this shift can be used to measure the grating, an approach developed by UTRC (United Technologies Research Centre), [Ref. 11], but 1% tunability peak is beyond the range of simple tuning for most semiconductor sources. Whilst it is beyond the scope of the present discussion

to go into further details, the conclusion concerning Hill gratings is that they are very interesting devices but their potential applicability will require a more detailed investigation into the systems aspects offered by the fibre/grating/source/detector signal processing combination.

The strain measurement problem extends beyond the distributed requirements and in specific cases, the localised strain gauge could be an extremely useful device. The Fabry Perot rosette first investigated at the UTIAS appears to offer considerable possibilities in this context. They used Fabry Perot elements with gauge lengths in the order of mm as the sensors and achieved adequate sensitivities in the 10μstrain region. Temperature compensation is, of course, difficult though in principle the rosette is self balancing if isothermal, so again the concept is most readily applied to dynamic strain measurements [Ref. 12].

5.1.2 Cure Monitoring

This term usually refers to the observation of the curing processes of the resins in fibre reinforced plastics fabrication. Published work in this area is thin on the ground. The usual technique is to exploit the fact that the refractive index of the resin increases sharply during the cure transitions. Thus, if the resin is used as the cladding of a step index fibre, the fibre will guide until curing is completed provided that the core index is between the two extreme indices of the cladding.

The problem lies in finding a fibre with the correct core index, which must be around 1.6. Some years ago, workers at the University of Washington [Ref. 13], utilised the set resin itself as the core and showed that the light did indeed go out as the resin set. There is some - as yet unpublished - work being undertaken at Strathclyde using matched index glasses as the core. Again the light goes out with but the interpretation of the results needs further refinement.

An alternative generic approach to cure monitoring has been to observe the microbend signature as a function of the curing process in an conventional multimode fibre embedded within the material. The only work in this area of which the authors are aware, has been undertaken in the OSTIC programme and whilst reproducible "bend loss v. curing stage" signatures can be demonstrated, quite what these signatures mean is an entirely different matter. The signatures are, predictably, a function of the orientation of the optical fibre with respect to the reinforcing fibres in the material and even though the signatures thus far defied modelling, repeatability does indicate that they may prove to be useful. The fibre coating plays a central role in determining this signature.

A final approach which is closely related to the matched index fibre approach, is to arrange evanescently coupled spectroscopy of the chemical properties of the resin. Certainly evanescent wave spectroscopy offers some potential in this area though it is well known that the process is much better controlled if a single mode polarisation maintaining fibres are used as the excitation source. However, little work has been published in this area.

5.1.3 Temperature Distribution Measurements

There are two approaches. The phase/polarisation technique has already been mentioned in above. This has proven resolutions in the order of 1°C or better in gauge lengths of a fraction of a metre.

The alternative technique uses the Stokes : anti-Stokes ratio in the backscatter signal. Since, by definition, these signals are very small, the integration times of such measurements are long and the resolution in both temperature and distance is relatively modest. Resolutions of 1°C or so over distances of the order of a few metres are typical. The technique does, however, have the advantage of being "absolute" since the Stokes : anti-Stokes is unique function of temperature and of no other variable. There *may* be a role for such temperature measurements in large structures but such structures are extremely cost sensitive so that any potential role may therefore be limited.

5.1.4 Damage Detection

The essential conundrum with damage detection is that small area damage may have a very important effect on structural performance. Consequently, damage detection must generally be done inferentially since the probability of having a damage sensor in exactly the right place at exactly the right time is low. Therefore, only in situations where the damage location can be predicted with confidence can "tell-tale" monitors (i.e. those which break when the damage occurs) may be used with confidence.

The secondary effects of damage can be either changes in the resonant frequency spectrum of the structure, or acoustic emission during the onset of the damage.

Most of the reported work in this area has come from UTIAS [Ref. 9], who have looked at acoustic emission and have presented emission signatures. UTIAS has focused upon Kevlar epoxies which have the added benefit of being translucent, so they have also used suitably chosen back lighting and image processing to identify damage locations.

The simplest technique of all though is to rely upon cracks to interrupt the transmission through fibres in a matrix array. This technique was first demonstrated over ten years ago [Ref. 2].

5.2 Signal Processing

Processing of signals is an integral and essential part of any instrumentation system.

The sensor signal signatures obtained from most, if not all of the preceding systems are complex and usually cannot be repeated in detail. Therefore, what is really required is a broad signature analysis of these signals rather than a precise point by point measurement thereof.

The emergent technology of "neural networks" comes into play here and indeed any signal processing algorithm which is eventually adopted must respond to inexact criteria. Despite the fact that this observation is self evident, there has been little reported activity on the use of neural networks in sensor systems. Indeed the only papers on the topic are those coming from the Florida Institute of Technology Group though others are beginning to take the first tentative steps.

5.3 Materials Compatibility

The technical performance of the sensor technologies outlined in the previous section indicates the that the necessary measurands can be accessed with the required temporal and spatial resolution for a wide variety of the applications analysed in section 2. However, the materials compatibility is a key issue and the current status is briefly reviewed below.

In composite materials, the requirements are now well defined. The necessary coatings have been identified and, if these coatings are used with care, the mechanical integrity of the resulting material is insignificantly effected. The most successful coatings have been based upon hard polyimides and very successful mechanical results have been obtained with these coatings.

The position of the optical fibre within the lay-up of the composite is also fundamentally important. If the direction of the optical fibre is transverse to the reinforcing fibres then the resulting resin rich region produces both undesirable stress concentrations, and therefore potential weaknesses in the structure, and uncertainties in the temperature/strain transfer characteristic between the fibre and the overall sample.

This transfer characteristic is obviously essential to the understanding of the results obtained from fibre strain and temperature sensors within composites. Experimental data corroborated by finite element analysis has indicated that thin (5 micron or less) coatings produce very reliable strain/temperature transfer. The strain signal can be significantly diluted if a thick coating (greater than 50 microns) intercedes between the fibre and the composite itself. Whilst this reduction in strain transfer is predictable using finite element modelling and could be incorporated into a signal processing procedure there are obvious benefits in removing the interface so that thin hard coatings are desirable.

The thin hard coating is inevitably graced with a few problems. The most important of these introduces the potential for microbend losses in the embedded fibre and also introduces the potential for a strain dependent loss in the sensing system. With care and suitable calibration procedures these phenomena can be tuned out of the system.

All the reported experience with metal structures has involved attaching fibres to the outside of the structure. This inevitably requires environmentally resistant adhesives and little has been published on either the resin structures or the results derived from the monitoring procedures.

6. DISCUSSION

The evolutionary stages of the smart structure involve a number of parallel closely interacting avenues. Many of the control and instrumentation concepts can be demonstrated using current sensor technology, signal processing and novel modifications to established actuators. This approach has been put to good effect in work reported in Ref. 1. However the full benefit cannot be realised until fully integrated sensing comes on the scene and a new approach to actuation compatible with materials and systems requirements has been put in place.

The prime role for fibre optics appears to lie in the passive sensor system area, though there may be other avenues open both in developing communication networks and in the distribution of power to areas where hard wiring is prohibited.

There remain a number of major issues which must be resolved before fibre optics can become completely integrated with structural systems. Of these the most important (Figure 10) concerns interconnect between panels and the serviceability of smart panels. The mechanical tolerances on some optical fibres connectors are in the micron region, but there are known to be positional drifts during embedding of the order of fractions of a millimetre which prohibits the use of direct jointing. Solutions to this problem to date have been largely conceptual rather than real! However, the use of structural monitoring systems will undoubtedly have a great impact upon the design of the structure and the structural design will have to take into account the interconnection elements.

The other principal problem area is that of establishing the interface between the material and the fibre transmission properties unambiguously and reliably. This needs further investigations into mechanical and thermal properties and the stability thereof for a particular material system.

Taking a broader system view of the problem rapidly indicates that signal processing will have a vital role to play in fibre optics sensor networks. The response of the fibre network to complex measurand mixtures and the need to accurately identify fault conditions within the structure imply that neural network learning systems are an obvious step forward. Surprisingly little progress has been made on this particular front despite its obvious potential role.

Most of all, expanded field experience is essential to define the system requirements. The driving forces in smart structures technologies are very much culturally dependent. In the US the aerospace industry dominates with some interesting civil engineering. In Europe the response to date has been relatively unenthusiastic though overall interest is increasing rapidly and is, perhaps surprisingly, dominated by the civil rather than the aerospace sector. The Japanese are also interested but express the wish to short circuit the instrumented structure and put the entire effort into the technology of smart materials.

7. CONCLUSIONS

Fibre optic sensor systems have an obvious complementary role to play along with other sensor approaches in the definition of smart structures technologies.

Whilst there are a number of obvious gaps, for example the interconnection problems, in the current component set for fibre optic sensors in smart structures, much benefit could be obtained from substantially increased field experience with present sensing systems.

System integration is an essential feature of any future development programme and such integration should include not only the definition of technologies such as neural networks for signal processing but also the necessary technical critique to ensure that the correct approach using the hybrid options available is taken to define the optimum solution to a particular analysis problem.

The structure must be designed from inception with the smart system integrated into the design philosophy. The availability of smart structure concepts will radically modify established approaches to structural engineering since the effective material properties and structural dimensions will become responsive to variable applications imposed requirements.

A fully integrated smart structure has much to offer. Its role in twenty-first century technology has yet to be defined but we are sure it will be an important one.

8. ACKNOWLEDGEMENTS

The authors would like to acknowledge the contributions made by their friends and colleagues working under the EEC BRITE OSTIC programme and also the contributions from the Smart Structures Research Institute's international advisory panel.

9. REFERENCES

1. Muira, K. and Natori, M.C., "Aerospace Research Status on Adaptive Structures in Japan", *in* "Proceedings of Second Joint Japan - USA Conference on Adaptive Structures" (to be published), 1991.

2. Hale, K.F., Hockenhull, B.S. and Christodoulou, G., "The Application of Optical Fibres for Witness Devices for the Detection of Elastic Strain and Cracking", National Maritime Institute, January 1980.

3. Lee, C.E. et al, "Fibre Optic Fabry-Perot Sensors Embedded in Metal and a Composite", *in* "Proceedings of the 8th Optical Fibre Sensors Conference", IEEE Catalog #92CH3107-0, Monterey 1992.

4. Dakin, J. and Culshaw, B. "Optical Fibre Sensors: Principles and Components", Artech House, Boston & London 1988 (ISBN 0-89006-317-6(V.2)).

5. Rogers, A., "Distributed Optical Fibre Sensors", *in* "Volume of Invited Speakers: SPIE International Conference on Fibre Optic Sensors", (to be published), Wuhan, China, 1991.

6. Culshaw, B. "Fibre Optic Sensor Networks", *in* "Volume of Invited Speakers: SPIE International Conference on Fibre Optic Sensors", (to be published), Wuhan, China, 1991.

7. Griffiths, R.W., Rizkalla, M. and Colquhoun, I.R., "Developments in the Application of Fibre Optic Technology and Pipeline Structural Integrity Monitoring", Society of Petroleum Engineers, SPIE 22117, 1991.

8. Culshaw, B. and Michie, W.C. "Fibre Optic Strain and Temperature Measurement in Composite Material - a Review of the OSTIC Programme", *in* "Recent advances in Adaptive and Sensory Materials and their Applications", Technomic (to be published), April 1992.

9. Measures, R.M. "Fibre Optic Sensing for Smart Materials and Structures", *in* "Proceedings of 8th Optical Fibre Sensors Conference", IEEE Catalog #92CH3107-0, Monterey, 1992.

10. Vengsarkar, A.M., et al, "Grating Based, Two-mode Elliptical Core Optical Fibre Sensors", *in* "Proceedings of 8th Optical Fibre Sensors Conference" IEEE Catalog #92CH3107-0, Monterey, 1992.

11. Dunphy, J.R., Lamb, F.P. and Money, W.N., "Multi-function Distributed Optical Fibre Sensors for Composite Cure and Response", *in* "Fibre Optic Smart Structures and Skins III", SPIE Volume 1370, San Jose, 1990, page 116.

12. Valis T., "PhD Thesis", University of Toronto, Institute for Aerospace Studies, 1990.

13. Afromowicz, A.M. and Lamb, K.Y., "Optical Properties of Curing Epoxies and Applications to a Fibre Optic Composite Cure Sensor", *in* "Fibre Optic Smart Structures and Skins II", SPIE Volume 1170, Boston 1989, page 138.

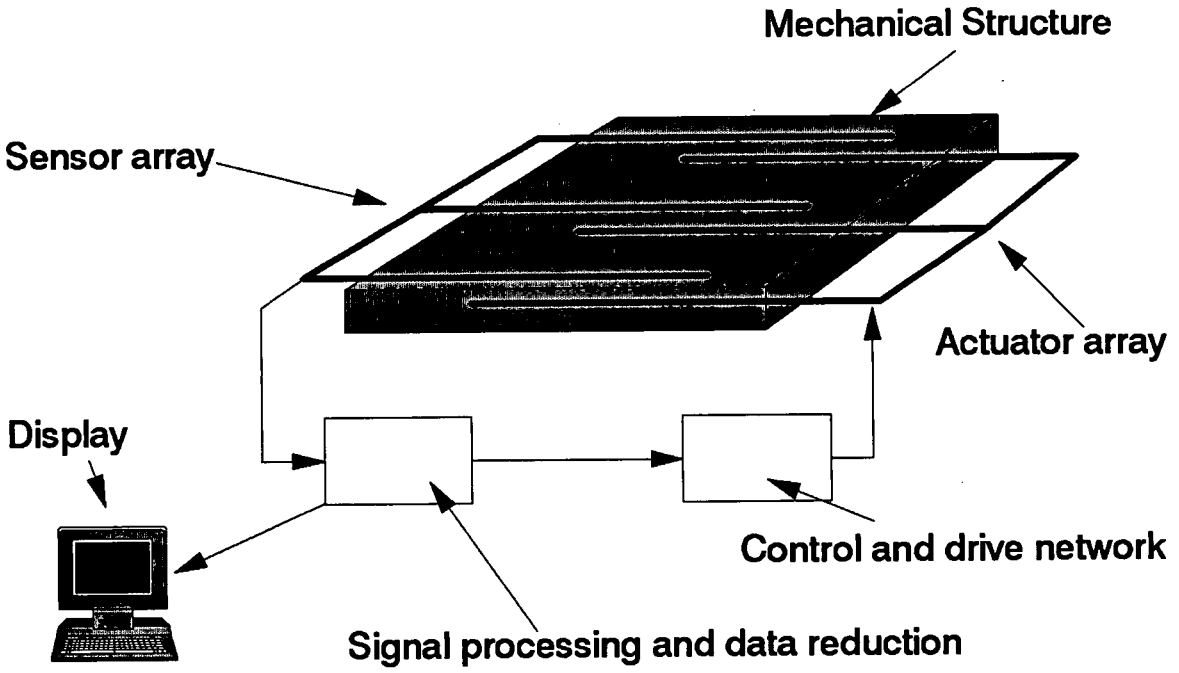

FIGURE 1

CONCEPTUAL DIAGRAM OF THE SMART STRUCTURE

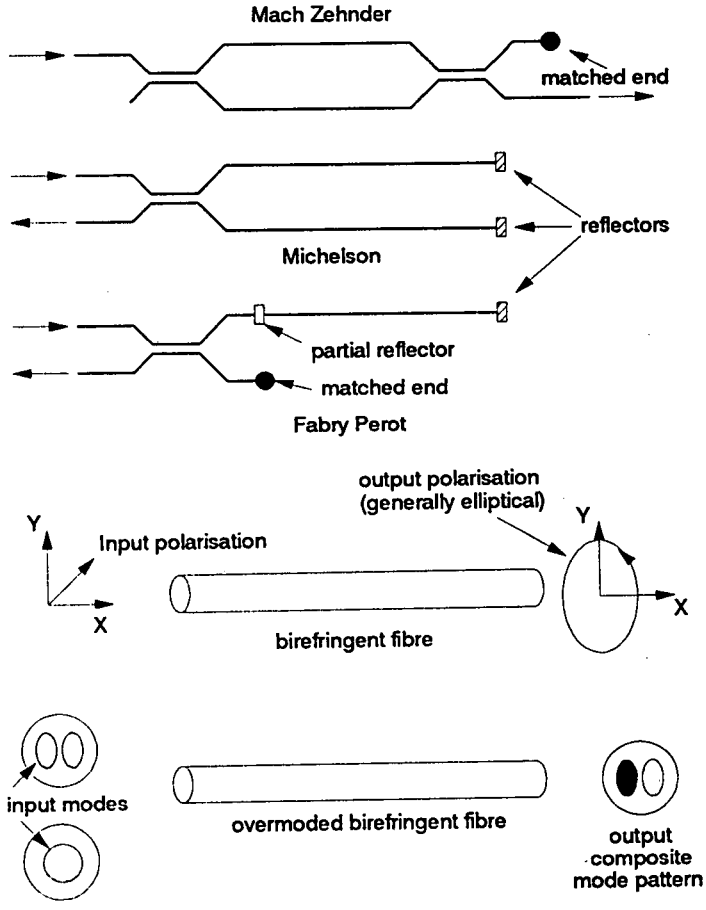

FIGURE 2

OPTICAL FIBRE INTERFEROMETERS, POLARIMETRIC AND MODE-MODE SENSORS

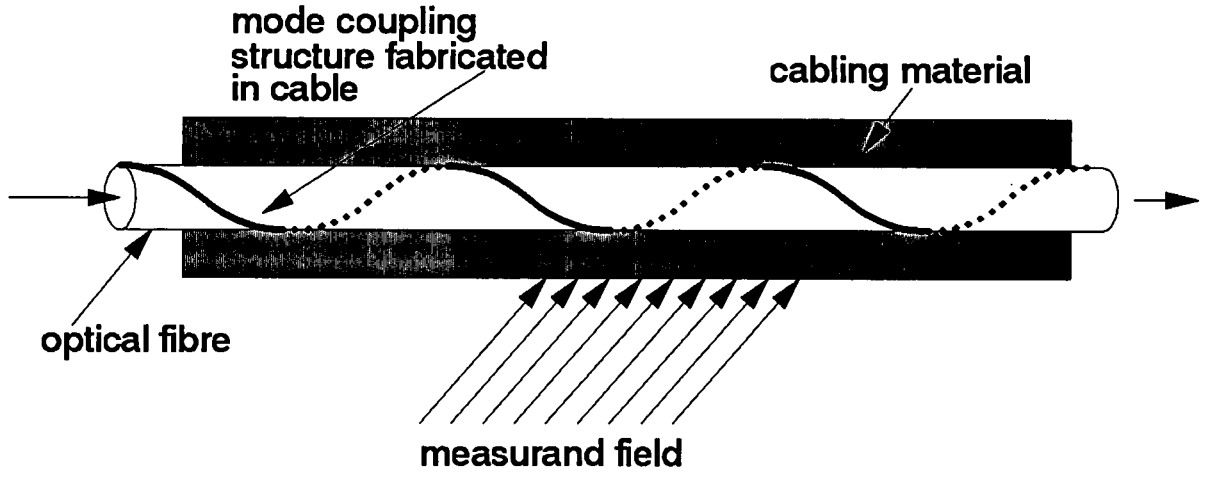

Deformations to the cabling material are transferred to microbending induced losses via the coupling structure

FIGURE 3

THE GENERAL PRINCIPLE OF MICROBEND CABLE SENSORS

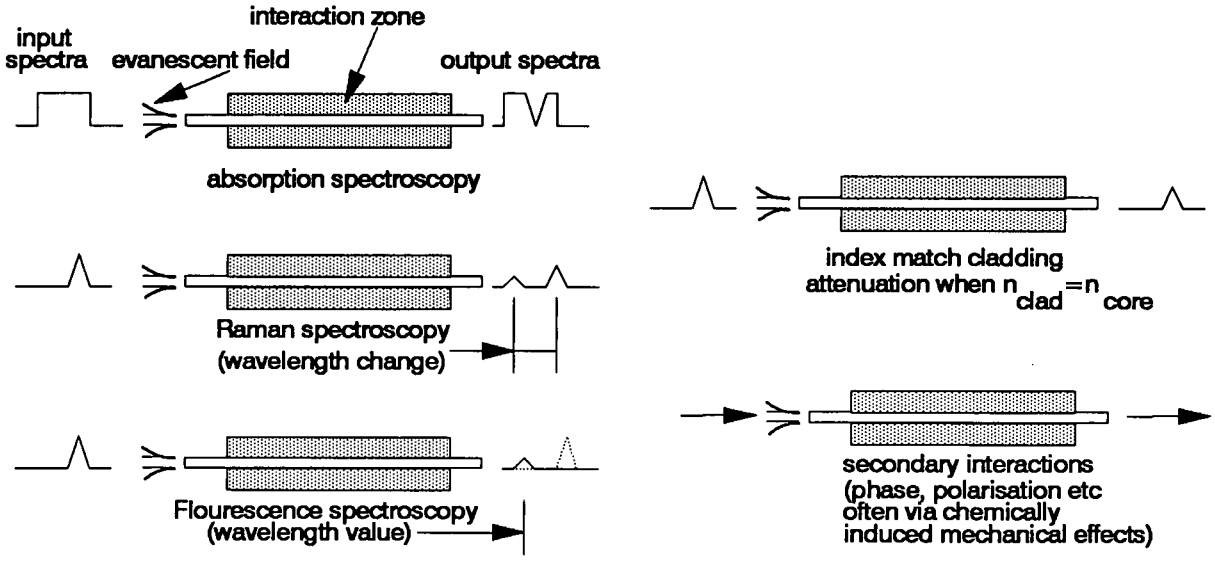

FIGURE 4

EVANESCENT APPROACHES TO CHEMICAL SENSING

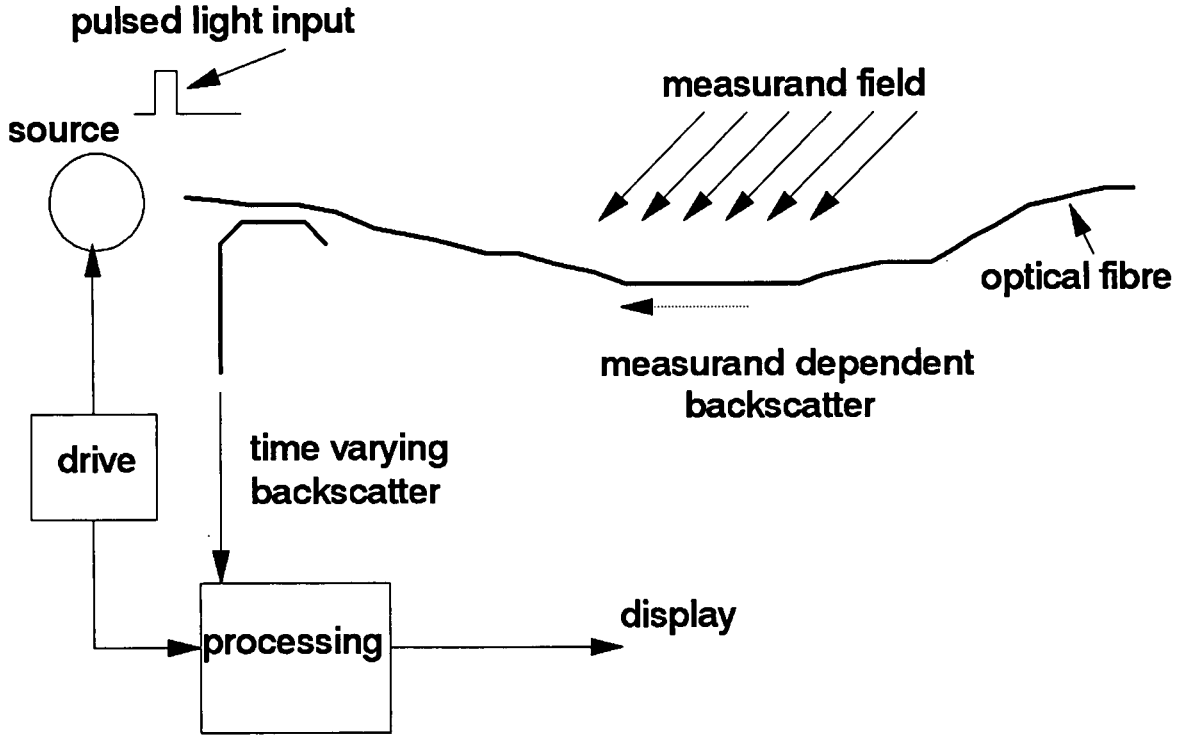

FIGURE 5

GENERIC REPRESENTATION OF DISTRIBUTED SENSING

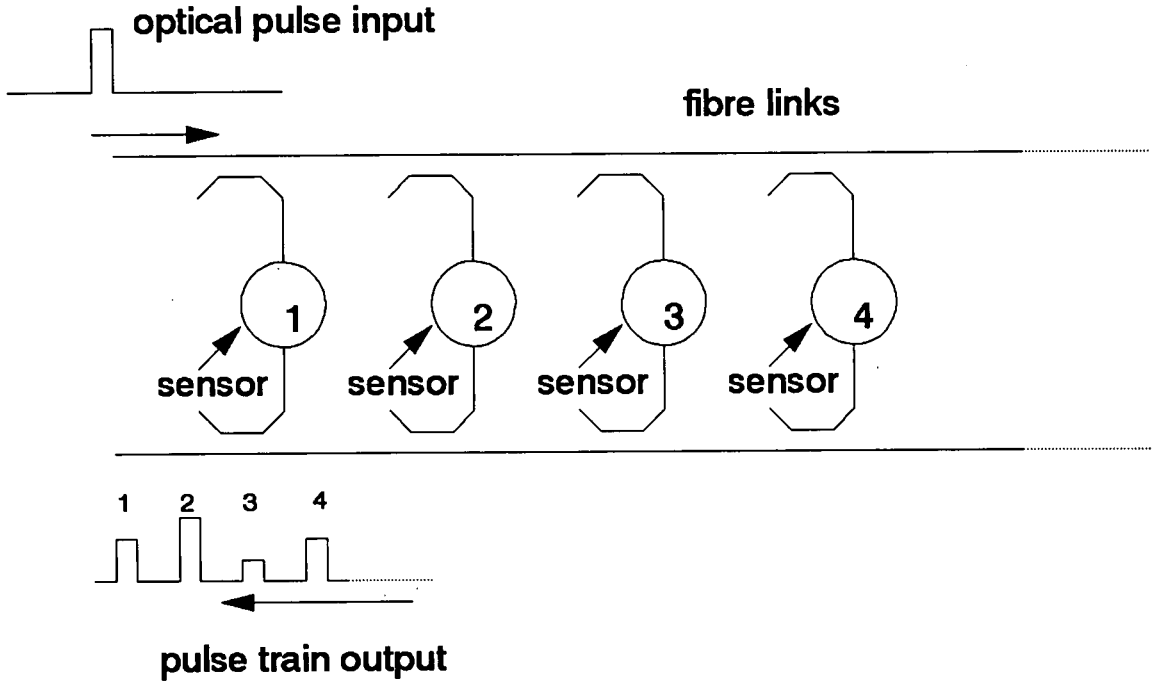

FIGURE 6

BASIC FEATURES OF A TDM FIBRE OPTIC SENSOR ARRAY

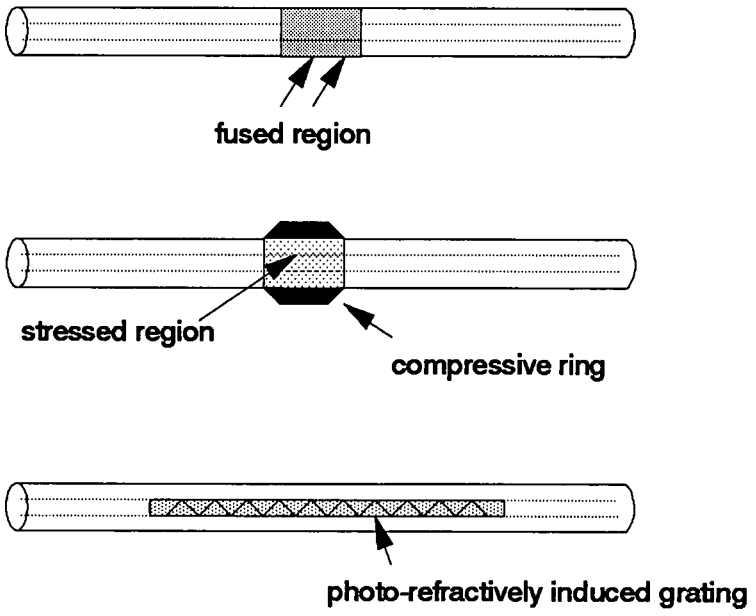

FIGURE 7

SOME TECHNIQUES FOR INDUCING COUPLING AT PREDETERMINED POINTS BETWEEN CO- OR COUNTER PROPAGATING MODES IN QUASI-DISTRIBUTED SENSOR NETWORKS

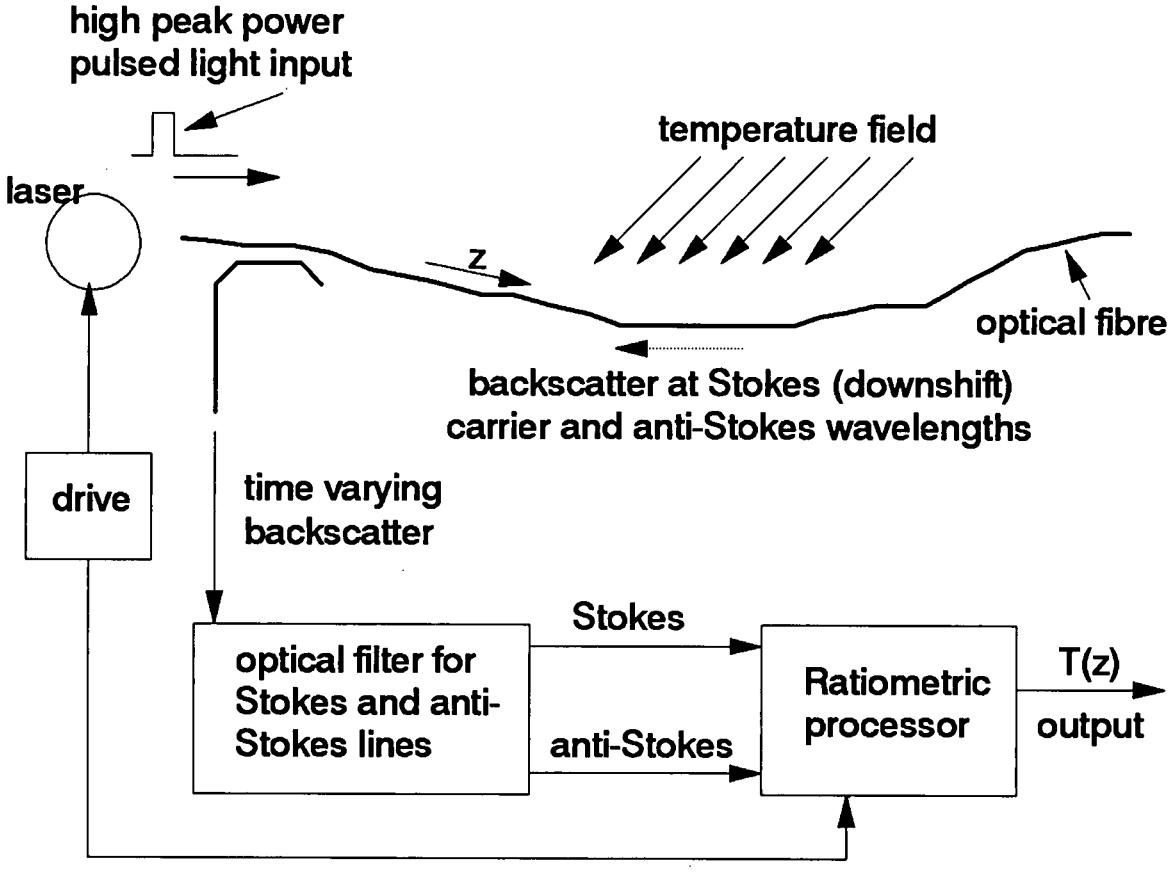

FIGURE 8

RAMAN (STOKES/ANTI-STOKES) DISTRIBUTED TEMPERATURE SENSING

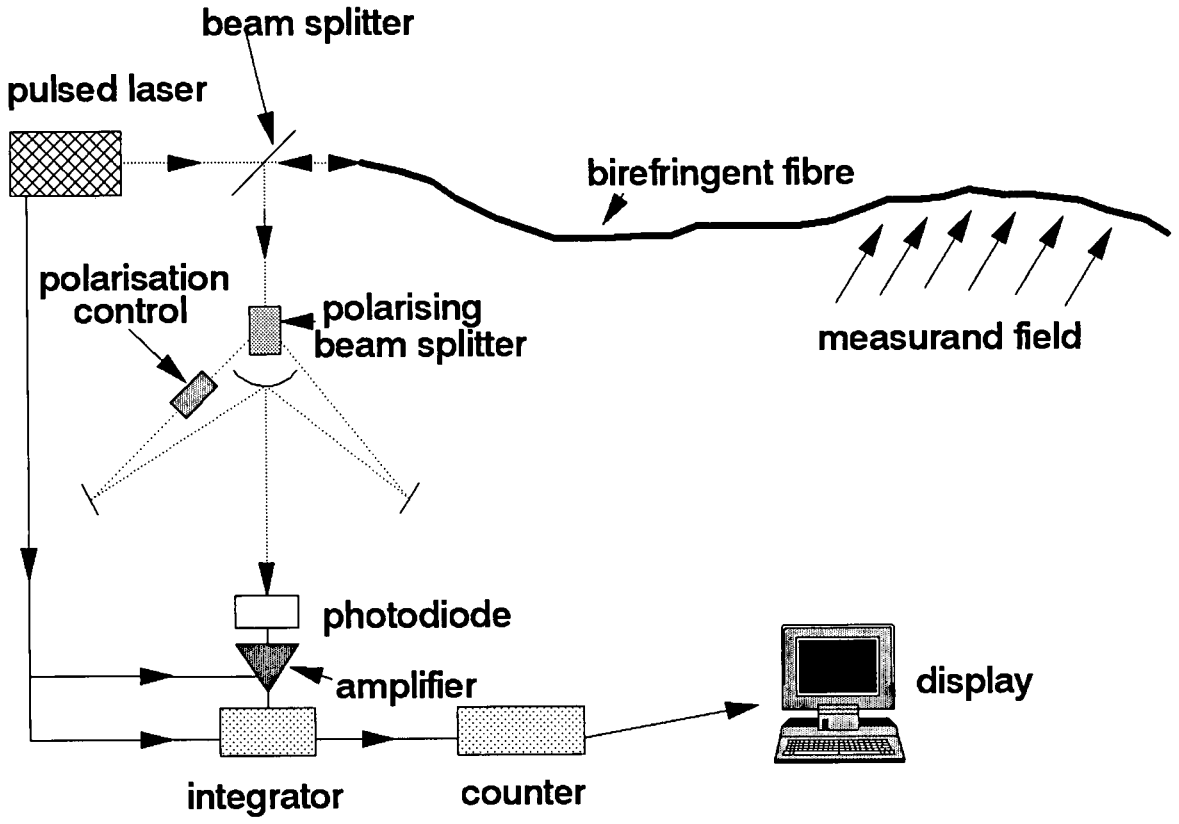

FIGURE 9

DISTRIBUTED BIREFRINGENCE MEASUREMENTS IN THE FREQUENCY DOMAIN
(after Alan Rogers)

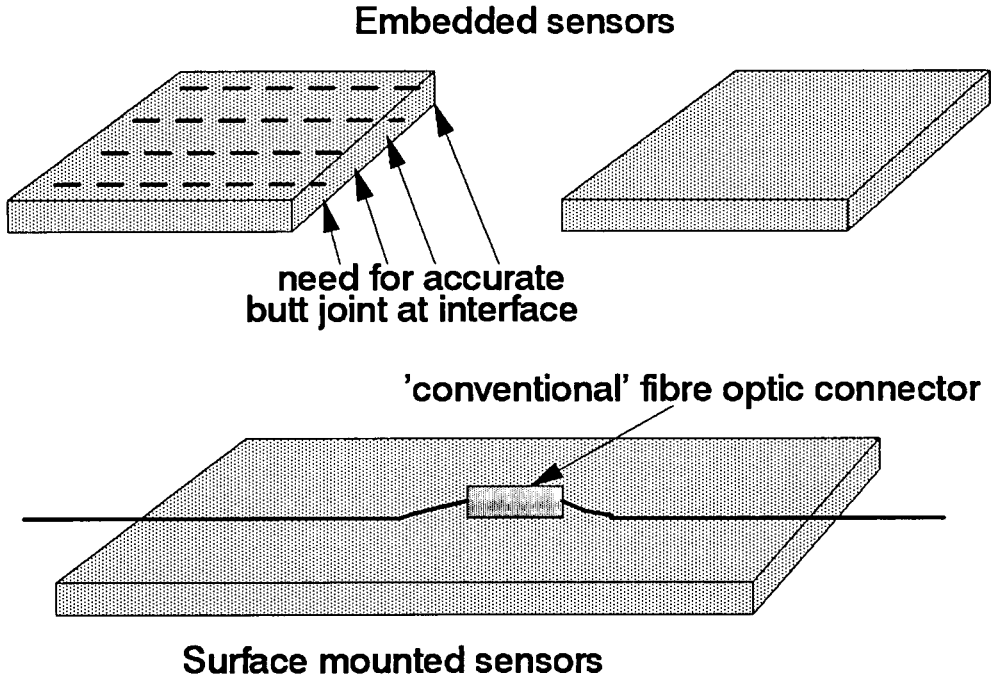

FIGURE 10

INTERFACING EMBEDDED AND SURFACE MOUNTED SENSORS

Fiber-Optic Gyroscope

Hervé C. Lefèvre and Hervé J. Arditty
PHOTONETICS
52, Avenue de l'Europe
78160 Marly-le-Roi - France

1- ABSTRACT

This paper reviews the technical evolution of the interferometric fiber gyroscope over the last fifteen years. Today a psychological barrier has been passed, and it is now accepted that this new technology will find many applications during the 90's.

2- INTRODUCTION

Over the last fifteen years, the interferometric fiber-optic gyroscope (I-FOG) research and development has evolved from an promising physics experiment [1] to a practical device that is now close to production [2]. This has been made possible by a refined analysis of the system architecture and of the possible signal processing schemes, but also by fundamental improvements of the various optoelectronic technologies, as, in particular, integrated optics, semiconductor sources, polarization preserving fibers, and in-line fiber components.

Today, a psychological barrier has been passed, and it is now accepted among inertial guidance and control specialists that this new technology will be a strong contender for many military and civilian applications of this decade. Most leading companies in the inertial guidance field are heavily involved in R & D programs on the fiber optic gyroscopes [2], and prototypes have been flight tested.

We are now going to describe the technical state-of-the-art and trends of present FOG R & D. We will also present the applications that are foreseen because of the specific advantages of the FOG due to its solid-state configuration : high dynamic range, high bandwidth, rapid start-up, ability to cope with a severe environment (in particular shocks and vibrations), and potential low cost.

3- BASIC ARCHITECTURE OF THE FIBER OPTIC GYROSCOPE

The interferometric fiber-optic gyroscope is a passive two-wave ring interferometer. The input light is split and propagates in opposite directions along a multiturn single mode fiber coil. Because of the Sagnac effect, the waves experience a phase difference when the whole system is rotated with respect to inertial space.This phase difference is proportional to the rotation rate component Ω parallel to the coil axis [3] :

$$\Delta\Phi_S = (2\pi\ L.D\ /\ \lambda.c).\ \Omega$$

where L is the length and D the diameter of the coil, λ is the source wavelength and c the light velocity in vacuo.

Practical fiber gyroscopes usually work over plus or minus half a fringe, i.e. $\pm\ \pi$ radian of phase difference. The theoretical sensitivity (limited by photon noise) is on the order of 10^{-6} radian or less of phase shift. Compared to the absolute phase accumulated by the waves when they propagate along the coil, this theoretical limit is extremely small, but reciprocity of light propagation in single-mode waveguides makes it detectable. This requires the use of the so-called minimum reciprocal configuration [4,5] [Figure 1], which is now universally employed. This architecture needs a single spatial mode and polarization filtering at the common input-output port of the interferometer and a biasing phase modulation at one end of the fiber coil that serves as a delay line. This brings a drastic enhancement to the ring interferometer stability by making both opposite paths identical in the absence of rotation. It is also accepted that to further improve noise and drift, it is important to use a broadband source (in particular a superluminescent diode or SLD) [6] and a polarization preserving fiber [7].

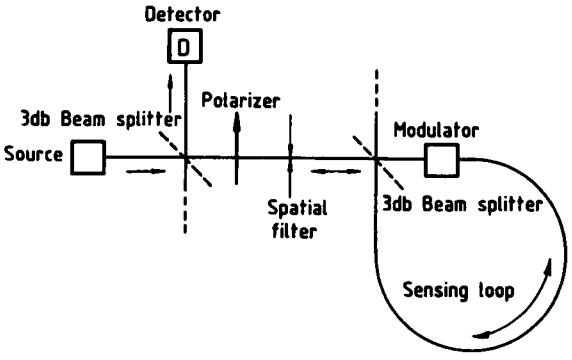

Figure 1
Minimum Configuration of the I-FOG

As a matter of fact the system comprises two primary waves sensitive to rotation but also a lot of parasitic waves (backreflected, backscattered or coupled in the crossed polarization) that yield secondary interferometers. The short coherence length of a broadband source suppresses the contrast of these spurious interferometers, and then limits their parasitic signals. The use of polarization preserving fibers is essential because such fibers are also birefringent by principle and one takes advantage of depolarization of cross-coupling with a broadband source [8,9]. This limits the required polarizer rejection to values that are compatible with present technology. Notice that white light interferometry has been found as a very powerful tool to carefully control the polarization and birefringence problems of the ring interferometer [Figure 2] [10], when one wants to get the best possible performances.

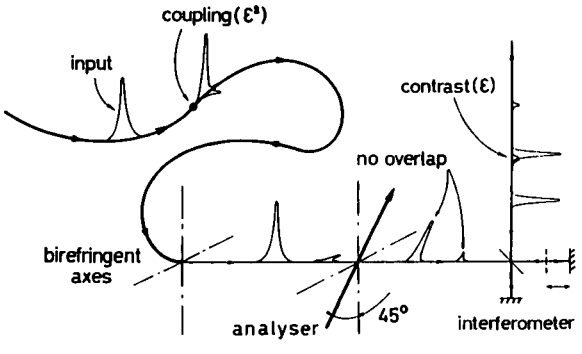

Figure 2
Test of polarization couplings
with white light interferometry

Another point of concensus is to use an all-guided technology for ruggedness. In particular it is possible to make an all-fiber gyroscope with in-line components [Figure 3] [11]. However, this approach has only been demonstrated with an open-loop signal processing which yields problems of linearity and stability of the scale factor. This can be good enough for certain applications, but most teams are now working on a closed-loop approach that allows one to linearize and stabilize the scale factor. This was first proposed with the use of bulk acousto-optic frequency shifters [12,13], but this approach yields an intrinsic source of bias unstability [14] and the general trend is now to use integrated optic modulators to implement specific closed-loop phase modulation schemes as serrodyne modulation (analog phase ramp) [15,16] or digital phase ramp [9,14,16]. Combined with a digital demodulation in an "all-digital" closed-loop processing scheme [17,18], this digital ramp feedback yields a very good scale factor linearity while preserving the good bias stability of the open-loop.

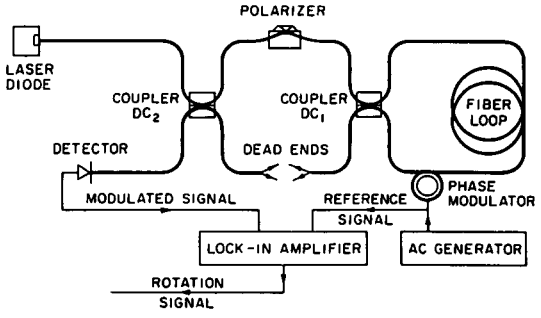

Figure 3
All-fiber gyroscope

Such schemes require a broad and flat modulation bandwidth of the phase modulator that is the main technical advantage of integrated optics. Notice that the digital phase ramp could simply look like a quantified analog ramp, but it is actually fundamentally better because the digital approach is synchronized with the modulation/demodulation biasing scheme. This solves automatically the problem of the finite fly-back of the ramping by synchronous gating and it eliminates the fiber index dependence in the scale factor [14].

Integrated optics is also a favored technology for implementing several functions on the same circuit for improving compactness and simplifying the connections. In particular the optimal simplicity is obtained with the so-called "Y-tap" or "Y-coupler"configuration [Figure 4] [9,14], which uses a three-function integrated optics composed circuit of a Y junction for wavesplitting, a polarizer on the common base trunk and two phase modulators on both branches.

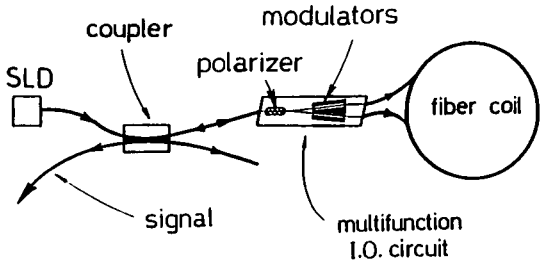

Figure 4
"Y-tap" or "Y-coupler" configuration

Such a circuit, now widely accepted and used as the " gyro circuit", has a parallelogram shape to avoid backreflections [9,14] induced by the index mismatch between the substrate and the fibers [Figure 5]. As it can be seen, the assembling of the components has a relative simplicity, requiring only a pigtailing of the source and three pigtailings on the I.O. circuit. These connections can be ruggedized to withstand a rough environment.

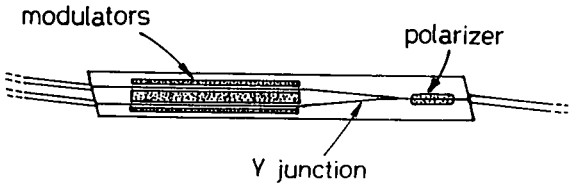

Figure 5
The "gyro circuit"

For sake of completeness, one should not forget two effects that are intrinsically non-reciprocal as the Sagnac effect : the magneto-optic Faraday effect [19] and the non-linear Kerr effect [20]. They could have been a drastic limitation to high performance because they cannot be distinguished from the Sagnac effect, but it was found that they can be eliminated very simply, and they are not a problem anymore. The use of a polarization preserving fiber eliminates the Faraday non-reciprocity if care is taken to avoid random twist in the fiber [21], and the use of a broadband source averages out the Kerr non-reciprocity [22,23]. We find here a very nice property of the interferometric FOG : there are not any parasitic effects that require incompatible solutions. On the contrary, the same solution solves nicely several different problems at the same time : polarization preserving fibers apply to the Faraday effect but also to birefringent non-reciprocity ; broadband sources eliminate backscattering and polarization coupling noise but also the Kerr non-reciprocity !

Finally thermal transients [24] and vibrations [25] can produce parasitic signals because reciprocity is strictly valid only for time invariant systems. Winding techniques must symmetrize the coil to get common mode rejection of the perturbations [24]. The so-called quadrupolar technique [26] looks like the most efficient method. Adequate potting is also necessary to define a stable pointing accuracy of the sensing coil.

4- PRESENT SUBJECTS OF CONCERN AND APPLICATIONS

FOG prototypes with very good performances have been reported by various R & D teams [2]. Their bias stability is in the 10 to 0.1 degree per hour range for compact devices (100 to 50 mm diameter) using 100 to 500 meters of polarization preserving fiber, and a superluminescent diode as a broadband source. Scale factor accuracy and linearity are in the 100 ppm range or less, for closed-loop FOG's using integrated optics and in the 1000 ppm range, for open-loop FOG's.

Present performances do fit tactical application requirements (0.1 to 10 °/h range) where they bring in addition a very high dynamic range (more than 1000 °/s) and a very large measurement bandwidth (several kHz) that cannot be reached with "classical" technologies. Interest is particularly strong for agile missiles for example. The good behaviour of FOG solid state technology under shocks and vibrations is also making it a strong candidate for smart ammunitions.

As an example we have recently reported [27] the realization of compact FOG 50 prototypes (50 mm diameter, 28 mm height) with state-of-the-art performances [Figure 6].

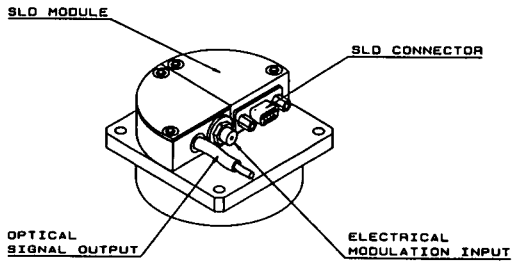

Figure 6
FOG 50 prototypes realized
by PHOTONETICS

The bias stability is 0.5 deg/h (σ value) and the scale factor linearity is in the 10 ppm range (σ value) [Figure 7] using an all-digital closed loop processing scheme over a dynamic range as high as ± 1300 deg/h.

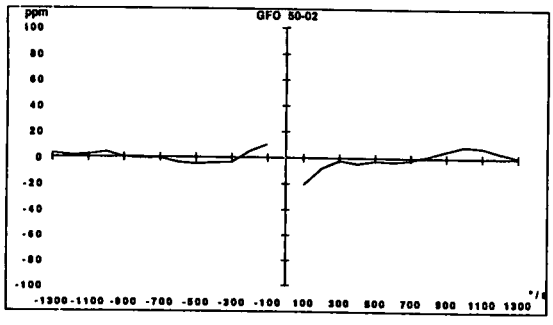

Figure 7
Typical scale factor linearity

Besides military applications, the FOG looks also very promising for use in a hybrid navigation, system with a GPS (Global Positioning System) receiver. For these applications, efforts are directed towards ruggedization and reduction of cost which is expected to be very competitive once the FOG enters production. Use in cars is even seriously envisaged in Japan [2].

Advanced reseach on components is still continuing for high performance applications. It concerns superfluorescent rare earth doped fiber sources [28] that will improve the wavelength stability of the broadband source, compared to semiconductor sources. This research field is very promising for many other applications, such as in particular telecommunications, and it should help to fulfil the ppm scale factor accuracy requirement of an inertial navigation grade FOG.

Another important topic is the improvement of the rejection of the integrated optic polarizer. The usual technique is Ti-indiffused waveguides on a lithium niobate substrate and polarization extinction is obtained with a metallic overlay. It is known however that proton exchange on a lithium niobate circuit yields single polarization waveguidance that gives a very high polarization extinction ratio (more than 60 dB). Great progress in the annealing technique of proton exchange has yielded gyro circuits with very attractive performances [29] that further improve the bias stability and get into the 0.01 °/h range of inertial grade navigation.

5- CONCLUSION

The fiber optic gyroscope is now widely accepted as the new gyro technology of the 90's and it will get a significant share of the market. Many companies, universities and governmental agencies are working on the subject : Litton, Honeywell, Smith Industries, Bendix, MIT, Stanford University, JPL and NRL, in the USA ; Mitsubishi, JAE, Hitachi and Tokyo University in Japan ; SEL, Litef, Teldix, AEG-Telefunken, British Aerospace, Ferranti, Sagem, University College, Strathclyde University and Photonetics in Europe. There is also an important effort on components.

Various demonstration prototypes have shown very good performances and several companies are close to production. The main advantage of the FOG compared to "classical" technologies is its solid-state configuration. This yields high dynamic range, high bandwidth, rapid start-up, good resistance to shocks and vibrations, which will extend the field of applications of inertial guidance techniques even further also because of its potential low cost.

6- ADDITIONAL COMMENT

This paper is dedicated to the evolution of the interferometric FOG, sometimes called IFOG. There is however another possible approach for making an optical fiber gyroscope by using a resonant fiber ring cavity instead of a two wave interferometer. This approach, known as RFOG (R standing for resonant) [30], has not reached the performances of IFOG so far and if it also has interesting prospects, technologically they seem much more

difficult to achieve. As a matter of fact the resonant approach requires the use of a very narrow band source which yields many sources of noise and drift whilst the I-FOG may work with a broadband source which eliminates these problems.

7- BIBLIOGRAPHY

- Most of the important publications about the fiber-optic gyroscope have been compiled in :
  "Selected Papers on Fiber-Optic Gyroscopes",
  Edited by R.B. Smith, SPIE Milestone Series, Vol. MS8, (1989).

- Two books on the fiber-optic gyroscope are going to be published by the end of 1992 :

  -*"Optical Fiber Rotation Sensing"*,
  Edited by W.K. Burns and to be published by Academic Press

  - *"The Fiber-Optic Gyroscope"*,
  by H.C. Lefèvre, to be published by Artech House.

8- REFERENCES

For references that can be found in the SPIE Milestone Series Compilation we have added : [MS 8, pages xx-yy].

[1] Vali V. and Shorthill R.W.,
"Fiber ring interferometer",
Applied Optics 15, 1099-1100, (1976), [MS 8, 134-136].

[2] Proceedings of *"Fiber Optic Gyro : 15th Anniversary Conference"*,
SPIE Proceedings, Vol. 1585, (1991).

[3] See for example : Arditty H.J. and Lefèvre H.C.,
"Sagnac effect in fiber gyroscopes",
Optics Letters, 6, 401-403, (1981), [MS 8, 105-107].

[4] Ulrich R.,
"Fiber optic rotation sensing with low drift",
Optics Letters, 5, 173-175, (1980), [MS 8, 170-172]

[5] Ezekiel S. and Arditty H.J.,
"Fiber-Optic Rotation Sensors : Tutorial Review",
Springer Verlag Series in Optical Sciences, Vol. 32, 2-26, (1981), [MS 8, 3-27]

[6] Böhm K. , Russer P. , Weidel E. and Ulbrich R.,
"Low drift fibre gyro using a superluminescent diode",
Electronics Letters, 17, 352-353, (1981), [MS 8, 181-182]

[7] Burns W.K., Moeller R.P., Villaruel C.A. and Abebe M.,
"Fiber-optic gyroscope with polarization holding fiber",
Optics Letters, 8, 540-542, (1983), [MS 8, 208-210]

[8] Fredericks R.J. and Ulrich R.,
"Phase error bounds of fibre gyro with imperfect polariser-depolariser",
Electronics Letters, 20, 330-332, (1984), [MS 8, 277-278]

[9] Lefèvre H.C., Bettini J.P., Vatoux S. and Papuchon M.,
"Progress in optical fiber gyroscopes using integrated optics",
NATO/AGARD Conference Proceedings, Vol. 383, 9A-1, 9A-13, (1985), [MS 8, 216-227]

[10] Lefèvre H.C.,
"Comments about fiber optic gyroscopes",
SPIE Proceedings, Vol. 838, 86-97, (1987), [MS 8, 56-67]

[11] Bergh R.A., Lefèvre H.C. and Shaw H.J.,
"All single mode fiber gyroscope with long term stability",
Optics Letters, 6, 502-504, (1981), [MS 8, 178-180]

[12] Davis J.L. and Ezekiel S.,
"Techniques for shot-noise-limited inertial rotation measurement using a multiturn fiber Sagnac interferometer",
SPIE Proceedings, Vol. 157, 131-136, (1978), [MS 8, 138-143]

[13] Cahill R.F. and Udd E.,
"Phase-nulling fiber-optic gyro",
Optics Letters, 4, 93-95, (1979), [MS 8, 152-154]

[14] Lefèvre H.C., Vatoux S., Papuchon M. and Puech C.,
"Integrated optics : a practical solution for the fiber-optic gyroscope",
SPIE Proceedings, Vol. 719, 101-112, (1986), [MS 8, 562-573]

[15] Kay C.J.,
"Serrodyne modulator in a fibre-optic gyroscope",
IEE Proceedings, Vol. 132, 259-264, (1985), [MS 8, 448-453]

[16] Lefèvre H.C., Graindorge Ph., Arditty H.J., Vatoux S. and Papuchon M.,
"Double closed-loop hybrid fiber gyroscope using digital phase ramp",
Proceedings of OFS-3 ' 85, Post deadline paper PSP 7, (1985), [MS 8, 444-447]

[17] Arditty H.J., Graindorge P., Lefèvre H.C., Martin P., Morisse J. and Simonpiétri P.,
"Fiber-Optic gyroscope with all-digital closed-loop processing",
Proceedings of OFS 6'89, Paris, 131-136, (1989)

[18] Lefèvre H.C., Martin P., Morisse J., Simonpiétri P., Vivenot P. and Arditty H.J.,
"High-dynamic range fiber gyro with all-digital signal processing",
SPIE Proceedings, Vol. 1367, 72-80, (1990)

[19] Böhm K., Petermann K. and Weidel E.,
"Sensitivity of a fiber-optic gyroscope to environmental magnetic fields",
Optics Letters, 7, 180-182, (1982), [MS 8, 328-330]

[20] Ezekiel S., Davis J.L. and Hellwarth R.W.,
"Intensity dependent nonreciprocal phase shift in a fiberoptic gyroscope",
Springer-Verlag Series in Optical Sciences, Vol. 32, 332-336, (1981), [MS 8, 308-312]

[21] Hotate K. and Tabe K.,
"Drift of an optical fiber gyroscope caused by the Faraday effect : influence of the earth's magnetic field",
Applied Optics, 25, 1086-1092, (1986), [MS 8, 331-337]

[22] Bergh R.A., Culshaw B., Cutler C.C., Lefèvre H.C. and Shaw H.J.,
"Source statistics and the Kerr effect in fiber-optic gyroscope",
Optics Letters, 7, 563-565, (1982), [MS 8, 313-315]

[23] Pertermann K.,
"Intensity-dependent non-reciprocal phase shift in fiber-optic gyroscopes for light sources with low coherence",
Optics Letters, 7, 623-625, (1982), [MS 8, 322-324]

[24] Schupe D.M.,
"Thermally induced non-reciprocity in the fiber-optic interferometer",
Applied Optics, 19, 654-655, (1980), [MS 8, 294-295]

[25] Lefèvre H.C., Bergh R.A., and Shaw H.J.,
"All-fiber gyroscope with inertial-navigation short-term sensitivity",
Optics Letters, 7, 454-456, (1982), [MS 8, 197-199]

[26] Frigo N.J.,
"Compensation of linear sources of non-reciprocity in Sagnac interferometers",
SPIE Proceedings, Vol. 412, 268-271, (1983), [MS 8, 302-305]

[27] Lefèvre H.C., Martin P., Morisse J., Simonpiétri P., Vivenot P. and Arditty H.J.,
"Fiber-Optic productization at Photonetics
SPIE Proceedings, Vol. 1585, (1991)

[28] Wysocki P.F., Fesler K., Liu K., Digonnet M.J.F., and Kim B.Y.,
"Spectrum thermal stability of Nd- and Er-doped fiber sources",
SPIE Proceedings, Vol. 1373, 234-245, (1990)

[29] Suchoski P.G., Findakly T.K. and Leonberger F.L.,
"$LiNbO_3$ integrated optical components for fiber optic gyroscopes",
SPIE Proceedings, Vol. 993, 240-244, (1988)

[30] See for example : Smith R.B., editor,
"Selected Papers on Fiber Optic Gyroscope",
SPIE Milestone Series, Vol. M.S.8, Section 7, 457-537, (1989)

FIBER OPTIC DATA BUSSES FOR AIRCRAFT

Norris E. Lewis
Litton Poly-Scientific
Blacksburg, Virginia USA

1. SUMMARY

A variety of fiber optic data busses are being developed for aircraft applications. This paper addresses five different data busses under consideration for both military and commercial aircraft. The impact of data bus protocol on component design, the effect of data bus topology on power budget and installation issues, and overall data bus performance are discussed.

2. INTRODUCTION

Fiber optic systems have been under consideration for aircraft applications for several years. As a means of reducing weight and improving aircraft performance, aircraft systems designers have been developing and implementing new systems for interconnecting avionics equipment. Sensors which in the past required dedicated wiring to a central processor will now be connected to a local processor, and the output data will be transmitted to other avionics equipment on a multiplexed data bus. At the same time that these developments are underway, non-metallic composite structures are being utilized to reduce weight. Composite structures provide less electrical shielding than the metallic structures they replace and, because of EMI associated with lightning, special consideration must be given to protect the integrity of the data transmitted throughout the aircraft. These developments are occurring at a time when the threat from high energy radio frequencies (HERF) and other manmade sources is increasing.

Fiber optic data busses and passive fiber optic sensors are being developed to allow system designers the option of using a medium that is inherently immune to EMI and is inherently capable of higher bandwidths. Studies are underway to find architectures that meet system requirements and are cost effective.

Several different fiber optic data busses are under consideration for future commercial and military aircraft applications. Data bus standards are being developed by Aeronautical Radio Incorporated (ARINC) for commercial aircraft. Relative to commercial aircraft, discussions in this presentation will be limited to ARINC 629 and ARINC Project 636. ARINC 629 is a multi-transmitter data bus that will interconnect avionic modules, actuators and other equipment. ARINC Project 636, also known as onboard local area network (OLAN), is based on the American National Standards Institute (ANSI) Fiber Distributed Data Interface (FDDI). Relative to military applications, this paper will focus on the following data busses for interconnecting avionic modules:

STANAG 3910
SAE AS4074.1 Linear Token Passing Bus (LTPB)
SAE AS4074.2 High Speed Ring Bus (HSRB)

3. BACKGROUND

3.1 ARINC 629

ARINC specification 629 governs a multiple transmitter data bus that has been designed for transmission of periodic and aperiodic data utilizing a deterministic protocol. ARINC 629 is classified as a broadcast bus that uses a carrier sense multiple access/collision avoidance protocol. This data bus was originally designed to utilize wire as a transmission medium. Now it is possible to use shielded or unshielded twisted pair in a current mode, shielded twisted pair in a voltage mode, or a fiber optic bus. Independent of the medium, the data bus must comply with the characteristics listed in Table I (Ref 1). Data presented in this paper will be limited to the fiber optic implementation of ARINC 629.

TABLE I
Each terminal should be able to "hear" every other terminal on the network.
The system should be suitable for operation with the terminal hardware described in ARINC Specification 629.
The serial data bit rate is specified to be 2.0 MBPS.
The bus cable including termination should support the reliability goal specified in ARINC Specification 629.
The installation should provide flexibility in a manner that reconfiguration (addition or removal of terminal stubs) should be possible with no reduction in bus reliability.
The installation should be economical, light weight and highly resistant to physical damage.
The system components should meet or exceed the pertinent RTCA DO160C environmental requirements.

The ARINC protocol requires that each terminal be heard by all other terminals as well as "hear" its own

signal when transmitting (Figure 1a)(Ref 2). This wrap-around between transmitter and receiver must occur within 500ns (Figure 1b). Terminals must be configured such that maximum terminal-to-terminal time delay is 600ns using consecutive time gaps (TG) or 1000ns using every other TG. The 500ns requirement includes both the electrical and optical delays. Electrical delays may be of the order of 150ns to 200ns. This means that the total wrap-around optical path between a transmitter and a receiver within a terminal can be no more than 70 meters if an electrical delay of 150ns is assumed and the optical propagation speed is 5ns/m.

The ARINC 629 data bus is a collision avoidance system with a minimum of 3.6875μs between each message string. Even so, a collision detection capability must be present in the terminal receiver because it is possible for more than one terminal to be transmitting simultaneously during bus initialization. A weak-after-strong condition exists when the strongest signal and the weakest signal arrive at a receiver within the minimum intermessage gap time. For most topologies, the wrap-around provides the strong signal and the most distant terminal the weak signal. Since each terminal must be able to hear every other terminal on the bus, the receiver optical dynamic range requirement is established by the maximum optical loss difference between any two terminals (Figure 1c). This requirement is less severe than that imposed by collision detection. Collision detection capability is best described as the receiver's ability to function over the required optical dynamic range in a time much shorter than the intermessage gap time. Collision detection time can be as short as 250ns. Figures 2a and 2b illustrate the collision detection requirement (Ref 3). When the collision detection requirement is met, the intermessage dynamic range capability is automatically satisfied.

3.2 ARINC Project 636

ANSI FDDI was developed for commercial applications where as many as 1000 terminals can be supported on a 200 Km ring (Ref 4). Distance between terminals can be up to 2 Km. The ANSI FDDI specification covers multiple logical and physical topologies and is based on a timed token rotation scheme. Reconfiguration around faults or cable breaks is an integral part of the standard (Ref 5). A simplified diagram of the counter rotating ring topology is illustrated in Figure 3a.

Each station on the ring must act as a repeater. In the event that a power failure or other failure mechanism such as a cable break occurs, a by-pass switch must be utilized at each station to route the signal to the next station to keep the ring from going down. Figure 3b illustrates a reconfigured ring using by-pass switches.

ANSI FDDI is based on a 4B/5B encoding method. This encoding scheme is used to insure data transitions. This encoding scheme requires an additional 25 percent increase in bandwidth whereas a 100 percent increase is incurred with Manchester II encoding. In order to accomplish a 100 Mb/s data throughput a data rate of 125 Mb/s is required.

The optical interface characteristics are given in Table II.

TABLE II. FDDI Optical Interface Characteristics

	Min.	Max.	Units
Output Center Wavelength	1270	1380	nm
Output Launch Power*	-20	-14	dBm avg.
Input Threshold**	-31	-14	dBm avg.
Power Budget**	11	--	dB
Output Risetime (10-90%)	0.6	3.5	ns
Output Falltime (90-10%)	0.6	3.5	ns
Input Risetime (10-90%)	0.6	5.0	ns
Input Falltime (90-10%)	0.6	5.0	ns
Random Jitter***	0	0.76	ns peak-peak
Duty Cycle Distortion	0	1.0	ns peak-peak
Output Data Dependent Jitter	0	0.6	ns peak-peak
Input Data Dependent Jitter	0	1.2	ns peak-peak
By-pass Switch Through Loss	0	2.5	dB

All measurements are at the station bulkhead connector.
* into precision 62.5/125 fiber.
** at 2.5×10^{-10} and 10^{-12} bit error rates using a specified test pattern.
*** specified for a probability of 2.5×10^{-10}

The specifications in Table II are based on a fiber diameter of 62.5/125 microns. Multi-mode diameters of 50/125, 82.5/125 and 100/140 microns and single mode fiber can be used. As mentioned before, ANSI FDDI has been directed toward commercial applications. As such the power budget provides only

a.

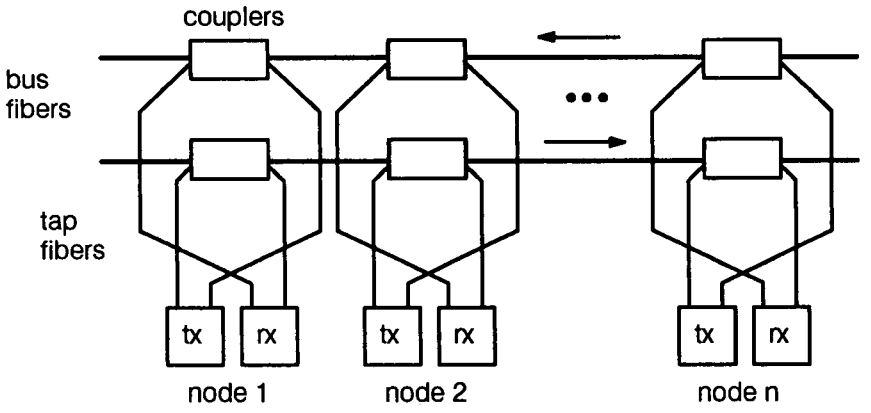

Broadcast bus requirement: All terminals must be able to "hear" each other and their own signal.

b.

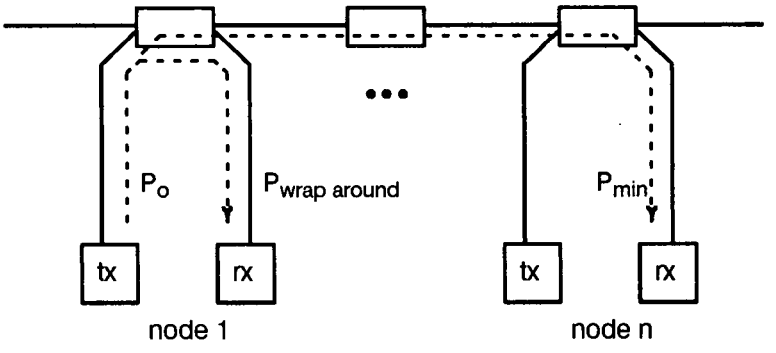

Dynamic range requirement = $P_{wrap\ around} - P_{min}$

c.

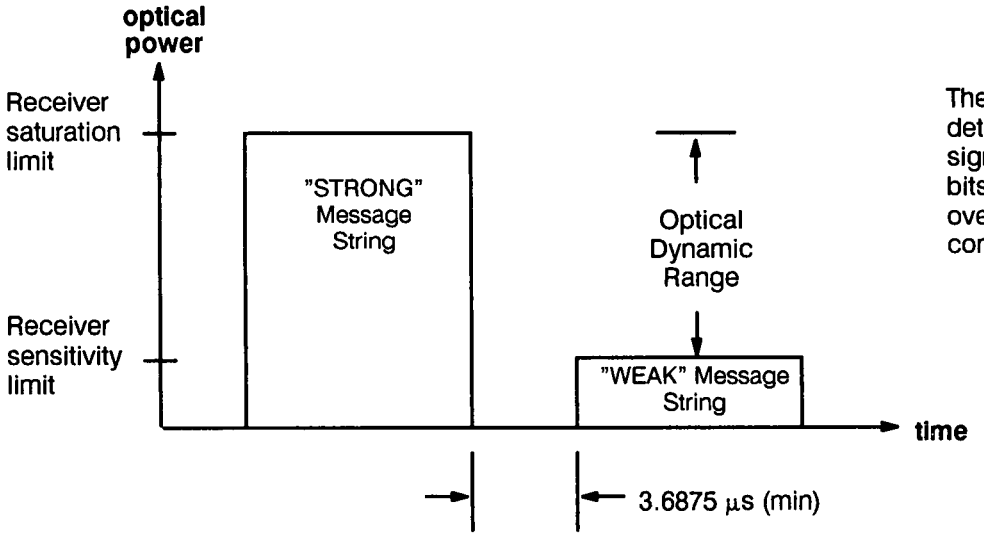

The receiver must also detect this scenario with no signal interruption, missed bits or degradation of BER over environmental conditions and lifetime.

Weak-After-Strong

FIGURE 1. Illustration of Some ARINC 629 Requirements Using a Linear Topology (Ref 2)

a.

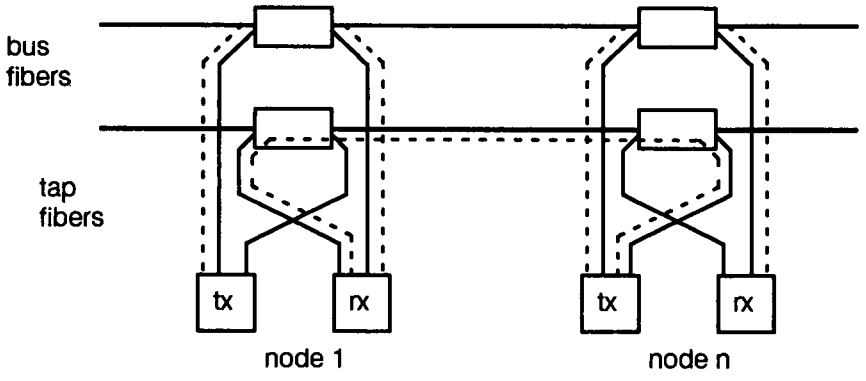

Collision detection requirement: The ability to detect a high level signal and a low level signal simultaneously.

b.

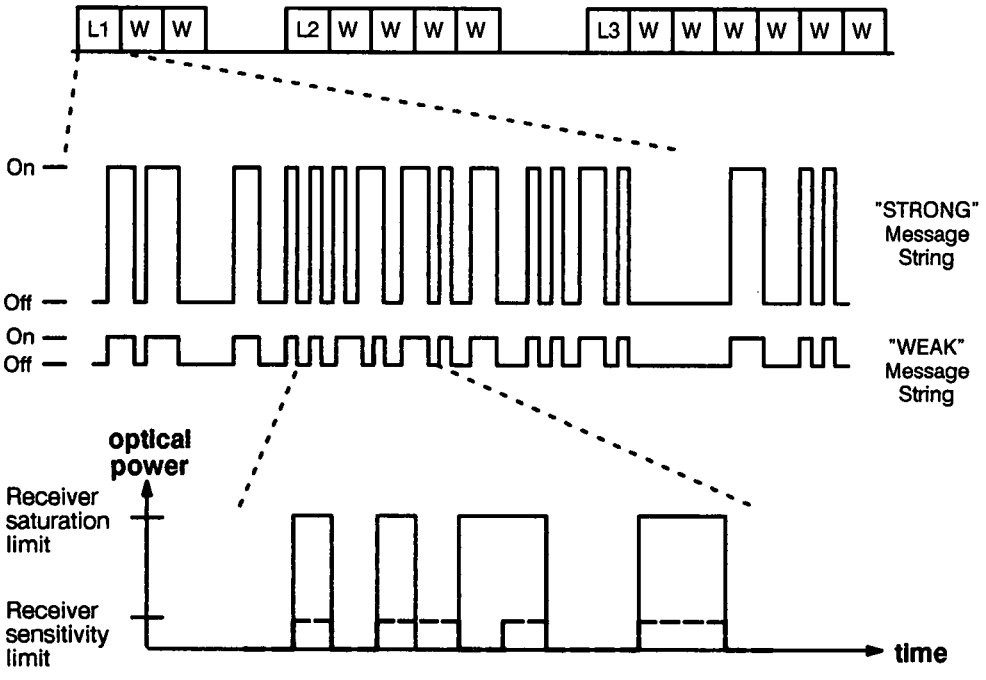

The receiver must "resolve" this scenario at least 90% of the time over full environmental conditions and lifetime.

"Resolve" is defined as outputting erroneous or out of tolerance signals RXI/RXN for at least the duration of the colliding bits.

FIGURE 2. Collision Detection (Example Using Optical Manchester Modulation) (Ref 3)

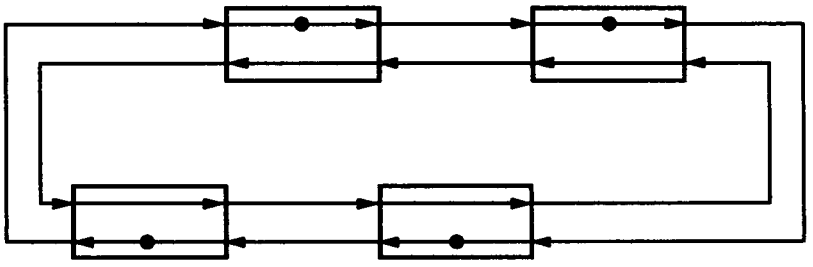

3a. Normal Mode

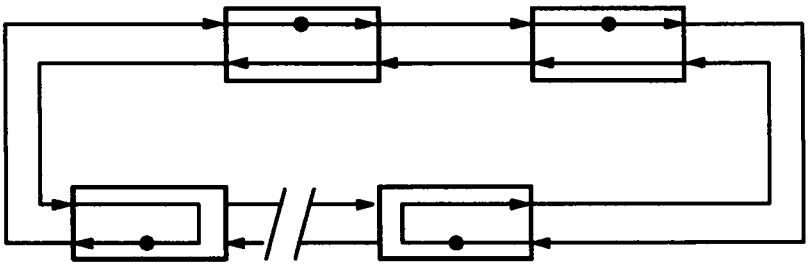

3b. By-Pass Mode

FIGURE 3. Counter Rotating Ring Topologies

enough power to survive the losses associated with four by-pass switches (Ref 6). When used for avionic applications, special consideration must be given to fiber, connectors, by-pass switches and transmitters and receivers.

One of the major goals of ANSI FDDI was to achieve interoperability between equipment from different vendors and to support ISO compatible network management to remotely monitor and configure stations (Ref 7). It is also the goal of ARINC Project 636 to provide the protocols to ensure that the OLAN FDDI LAN can be connected to, and interoperate with, other subnetworks (Ref 8).

3.3 STANAG 3910

STANAG 3910 is a real-time communications system based on proven MIL-STD-1553B (STANAG 3838) technology and as such represents a low risk solution for short and medium term avionics applications (Ref 9, 10). STANAG 3910 is a command/response data bus in which the high speed channel operates by commands from the low speed bus. The low speed data bus operates at 1 Mb/s over twin twisted wire. The increased data bus capacity is achieved by transmitting high speed data at 20 Mb/s over 200/280 micron fiber optic cable (Figure 4). Up to 32 terminals, the maximum that can be supported by STANAG 3838, can be implemented. The fiber optic network is broadcast and is passive.

Three data bus topologies are defined by STANAG 3910: a linear tee coupled bus, a transmissive star coupled bus, and a reflective star coupled bus. The Eurofighter implementation of STANAG 3910 will be based on a reflective star coupler. Because of power budget issues, there was concern that the linear tee coupled bus would not be able to support 32 nodes. The transmissive star represents a lower loss than the reflective star but could not be implemented because of installation and maintenance problems (Ref 11). A 32 node system would require 64 fiber optic cables and connectors to be located in a single area. The reflective star represents a more practical approach because the number of fiber optic cables and connectors are reduced by a factor of two. Figures 5 and 6 are block diagrams of dual redundant transmissive and reflective stars, respectively. Although the reflective star reduces the fiber and connector congestion at the star coupler, an additional component is added to the transceiver. To permit the transmit and receive function to be accomplished on the same fiber, a 50/50 optical coupler is located in the transceiver. This combination of electronics and fiber optics provides a packaging challenge.

The high speed chip set performs protocol, data handling, error checking and memory control functions. The high speed chip set transmits and receives 20 Mb/s Manchester II data in a burst mode format. The STANAG 3910 protocol allows the fiber optic receiver 40 bit times to achieve maximum sensitivity. This feature allows the receiver to be AC coupled as opposed to DC coupled and therefore the designer has more flexibility to achieve the required sensitivity. Fiber optic media interface characteristics are given in Table III.

TABLE III. STANAG 3910 (EFA Bus) Fiber Optic Media Interface Characteristics

Description	Units	Requirement
Common Characteristics		
Encoding Method		Manchester II
Data Rate	MBPS	20±0.01%
Nominal Bit Time	ns	50
Minimum Duration Between Transitions	ns	25
Minimum Intertransmission Gap	µs	2.2
Preamble Size	Bit Times	40
Optical Wavelength Lower	nM	770
Optical Wavelength Upper	nM	850
Spectral Bandwidth	nM	<60
Transmitter Characteristics		
Tx Optical Power (Signal High)	dBm	0.5±3.5
Tx Residual Power (Signal Low)	dBm	-14
Tx Maximum Risetime	ns	10
Tx Maximum Falltime	ns	10
Tx Maximum Pulse Width Distortion	ns	2.5
Receiver Characteristics		
Rx Operating Range	dB	25
Rx Intertransmission Dynamic Range	dB	23
Rx Minimum Optical Power Input	dBm	-37*
Rx Input Maximum Risetime	ns	12.5
Rx Input Maximum Falltime	ns	14.5
Rx Maximum Pulse Width Distortion	ns	5
Rx Maximum Bit Error Rate	–	10^{-10}

* Includes Optical Coupler and Connector

REFLECTIVE STAR

3.4 SAE AS4074.1

This standard defines a set of conditions whereby stations have distributed access control to a broadcast bus (Ref 12). Access to the bus is controlled by token passing and data exchange protocols. The token is

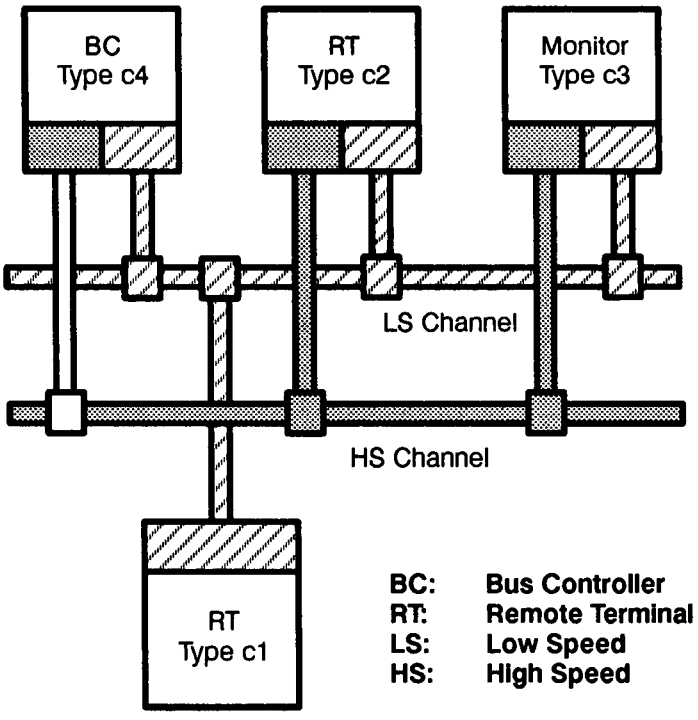

FIGURE 4. STANAG 3910 Block Diagram

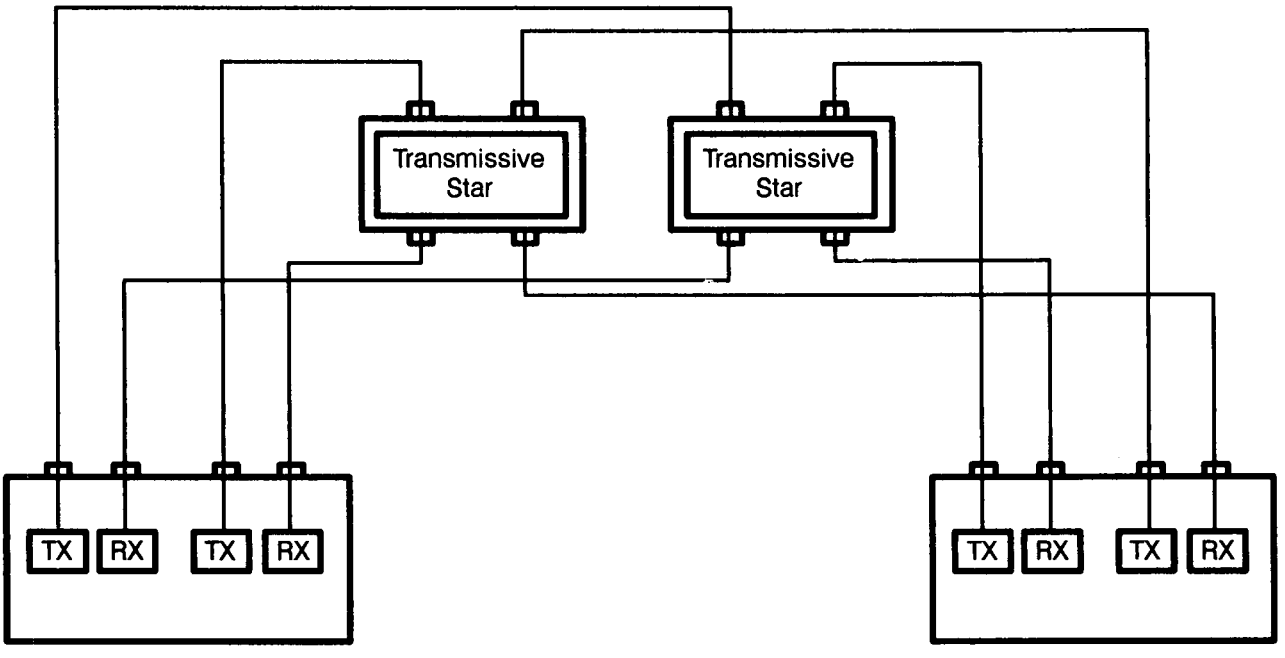

FIGURE 5. STANAG 3910 Dual Redundant Transmissive Star Coupled Bus

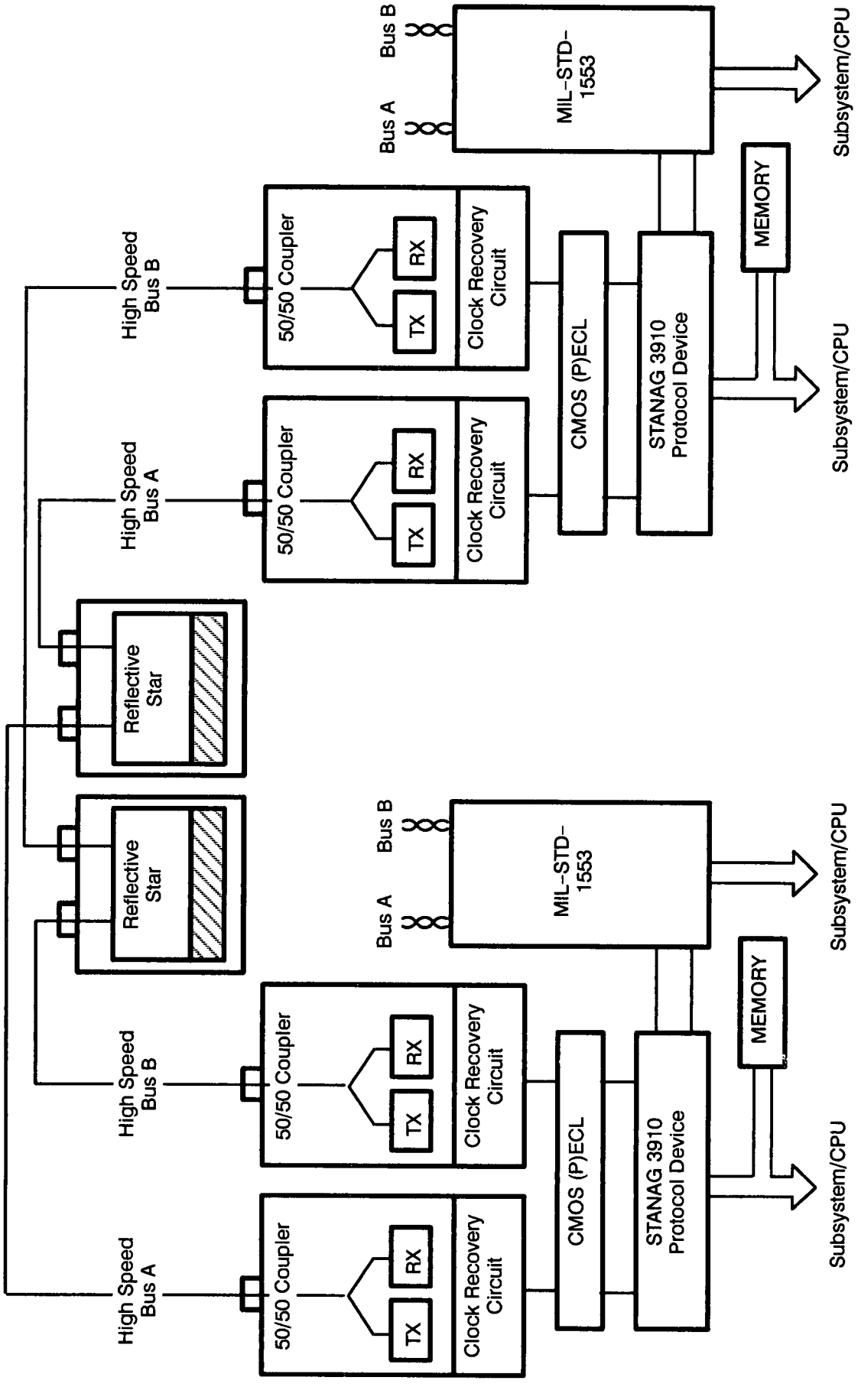

FIGURE 6. STANAG 3910 Dual Redundant Reflective Star Coupled Bus

continually passed around a logical ring superimposed in a linear bus (see Figure 7). A station receiving the token gains the right to use the medium for a time which is dependent upon the value of the Token Holding Timer (THT) as well as the residual value of the Token Rotation Timer (TRT). Several messages may be transmitted while the token is held. In order to assure a low latency for high priority messages when the bus is heavily loaded, message priority TRT's are used.

The LTPB specification permits redundant media when additional reliability is required. The redundant media is implemented so as to be transparent to the token passing protocol by using a "synchronous redundancy" scheme. "Synchronous redundancy" refers to hardware methods of implementing redundant physical paths where the transmitter, receiver, receive machine, and physical media are replicated with no effect on higher level protocol operations. Transmissions shall occur on both media simultaneously and shall be received by either, or both, receivers with the first valid data stream available being accepted. The receivers are capable of selecting frames in each physical media such that an error in one bus does not cause the loss of the complete message. One topology for implementation of the LTPB is a transmissive star coupler. A dual redundant transmissive star coupled bus has been shown in Figure 5. STANAG 3910 and LTPB are both broadcast systems that can be implemented using transmissive star couplers.

The LTPB stations transmit and receive 50 Mb/s Manchester II data in a burst format. The LTPB protocol allows the receiver a minimum preamble size of 16 bit times to achieve maximum sensitivity. As is the case with STANAG 3910, this preamble allows the receiver to be AC coupled and the required sensitivity can more readily be achieved. Fiber optic media interface characteristics are given in Table IV.

3.5 SAE AS4074.2

The SAE HSRB is a high speed bus which is being developed concurrently with the SAE LTPB (Ref 13). The HSRB is based on a physical ring architecture like ANSI FDDI (See Figure 8). Stations are connected in point-to-point links and are equipped with optical by-pass switches to circumvent ring failure if a station develops a fault. A token-passing technique is used to provide access to the bus. Only the station holding the token is allowed to transmit a message. All other stations in the point-to-point ring repeat the data. The station from which the message originates does not repeat the message. Since the stations repeat the message in a sequential fashion, there is no need for the token to be addressed. This is in contrast to the SAE AS4074.1 which is a broadcast network and therefore the protocol must provide an addressing mechanism to maintain a logical ring (Ref 14). The SAE HSRB sends the high priority messages before allowing lower priority messages to be sent.

TABLE IV. LTPB Type F-2 Fiber Optic Media Interface Characteristics

Description	Units	Requirement
Common Characteristics		
Encoding Method		Manchester II
Data Rate	MBPS	50±0.01%
Nominal Bit Time	ns	20
Minimum Duration Between Transitions	ns	10
System Minimum Intertransmission Gap	ns	280
Preamble Minimum Size	Bit Times	16
Optical Wavelength Lower	nM	800
Optical Wavelength Upper	nM	880
Spectral Bandwidth	nM	60
Transmitter Characteristics		
Tx Optical Power (Signal High)	dBm	-2.0±2.0
Tx Residual Power (Signal Low)	dBm	-15
Tx Maximum Risetime	ns	4
Tx Maximum Falltime	ns	6
Tx Nominal Bit Time	ns	20±10%
Receiver Characteristics		
Rx Operating Range	dB	21
Rx Intertransmission Dynamic Range	dB	15
Rx Minimum Optical Power Input	dBm	-32.5
Rx Input Maximum Risetime	ns	5
Rx Input Maximum Falltime	ns	7
Rx Nominal Bit Time	ns	20±10%
Rx Maximum Bit Error Rate	--	10exp[-10]

The SAE HSRB protocol is not data rate dependent. Currently the HSDB uses a 4B/5B encoding format which is the same as ANSI FDDI.

4.0 Discussion

4.1 Optical Bus Topologies

Topology trade-offs are not a major issue with electrical busses. A serial string allows the terminals to be connected with a minimum of wire. More emphasis is placed on the type of coupling (current or voltage), the need for shielding, stub length, termination,

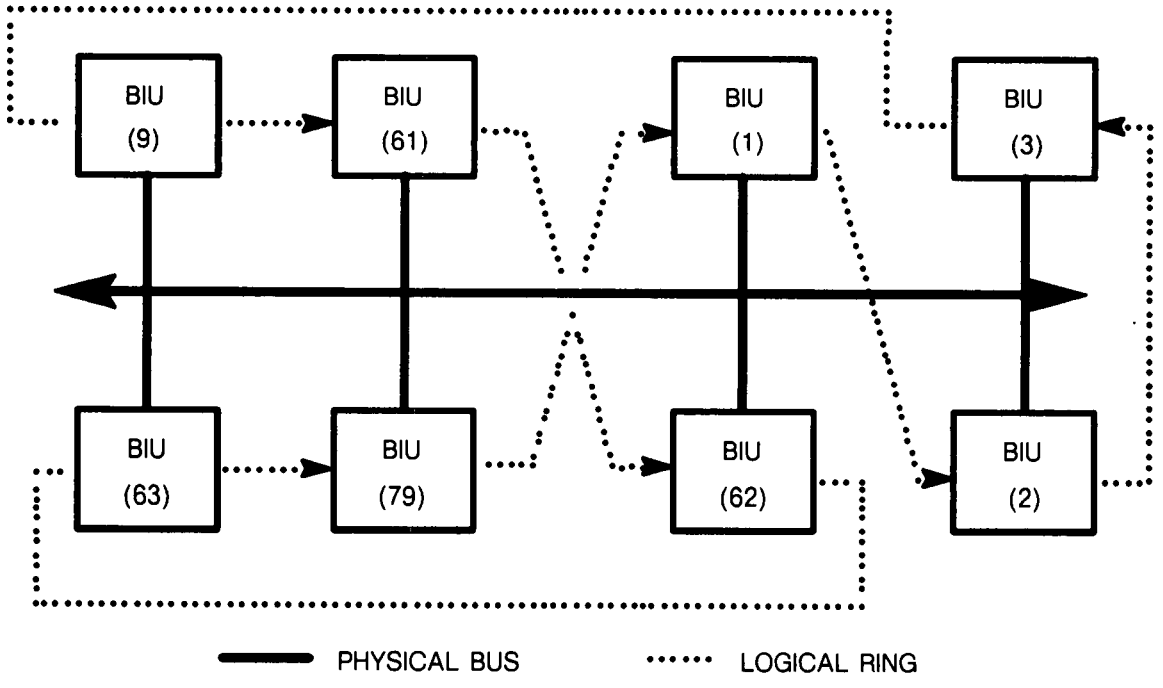

FIGURE 7.

grounding, reflections, etc. A large number of terminals can be interfaced on an electrical bus because coupling efficiencies are high.

Until recently, a linear optical bus supporting more than ten terminals has not been possible to implement because of coupler losses. More attention has been given to transmissive and reflective star coupled networks because a larger number of nodes could be configured for a given power budget. The development of low loss asymmetric couplers has allowed linear busses to be configured with a higher number of terminals than was possible using symmetric couplers. Figure 9 compares bus loss versus number of terminals for linear and star coupled networks.

Table V is a comparison of three different broadcast topologies relative to some of the aircraft data bus requirements. The requirements listed are those that place the most difficult constraints on the receiver design.

The data bus topologies used for this comparison are shown in Figures 1, 5 and 6. Distributed star networks can be designed that will reduce the concern for wrap-around paths that exceed the ARINC 629 limit. When star couplers are placed in series, the dynamic range and related parameters approach the requirement for a linear bus. In the final analysis, star coupled networks allow a larger number of nodes to be connected for a given power budget. A larger quantity of fiber than that used for a linear bus will be required. This difference may be significant for those busses that must be implemented with triple redundancy.

When using the reflective star topology, back reflections from the transceiver connector must be reduced below the receiver's sensitivity limit, otherwise collisions will occur with the data returning from the star. Thus, the topology choice for Eurofighter is not acceptable for ARINC 629.

TABLE V

Comparison of Linear and Star Coupled Topologies Relative to Some Aircraft Data Bus Requirements

Network Parameter	Topology		
	Linear	Reflective Star	Trans-missive Star
Number of nodes for a given power budget	Least	Intermediate	Most
Dynamic range required for a given number of nodes	Highest	Intermediate	Lowest
Wrap-around distance between terminal Tx and Rx	Least	Most	Most
		For ARINC 629, must be careful that wrap-around path does not exceed delay limit	
Weak-after-strong requirement for Rx	Most difficult	Intermediate level of difficulty	Least difficult
Collision detection requirement for Rx	Most difficult	Intermediate	Least difficult
Amount of fiber required to implement data bus	Least amount required. / Depends on configuration.		Largest amount required

4.2 Transmitter/Receiver Characteristics

Most electro-optic devices that are being targeted for aircraft applications operate in the short wavelength range. The short lengths of fiber between terminals do not merit the use of long wavelength devices. The FDDI (OLAN) data bus operates in the long wavelength range because it was originally designed to transmit data over long distances. Light emitting diodes rather than lasers are the sources of choice for transmitters because of cost, drive circuit simplicity, power consumption and extinction ratio. PIN photodiodes are more suitable for receivers than avalanche photodiodes because they offer stability over a broad temperature range, they can be biased with low voltage circuits, and they cost less.

Considerable attention must be given to the packaging of transmitters and receivers to meet the environmental conditions and the long term reliability requirements. Hybrid circuit technology is utilized to reduce component size and weight. Another level of complexity is added to the hybrid packing because of the fiber optic pigtails which must penetrate the package to be efficiently coupled to the active devices. Transceivers that are designed for reflective star coupled busses may include a 50/50 optical power splitter.

Transmitter Characteristics

Figure 10a illustrates the basic functionality of a transmitter designed for ARINC 629 data bus applications. Electrical data input to the transmitter is burst Manchester II. The converter circuit is utilized to

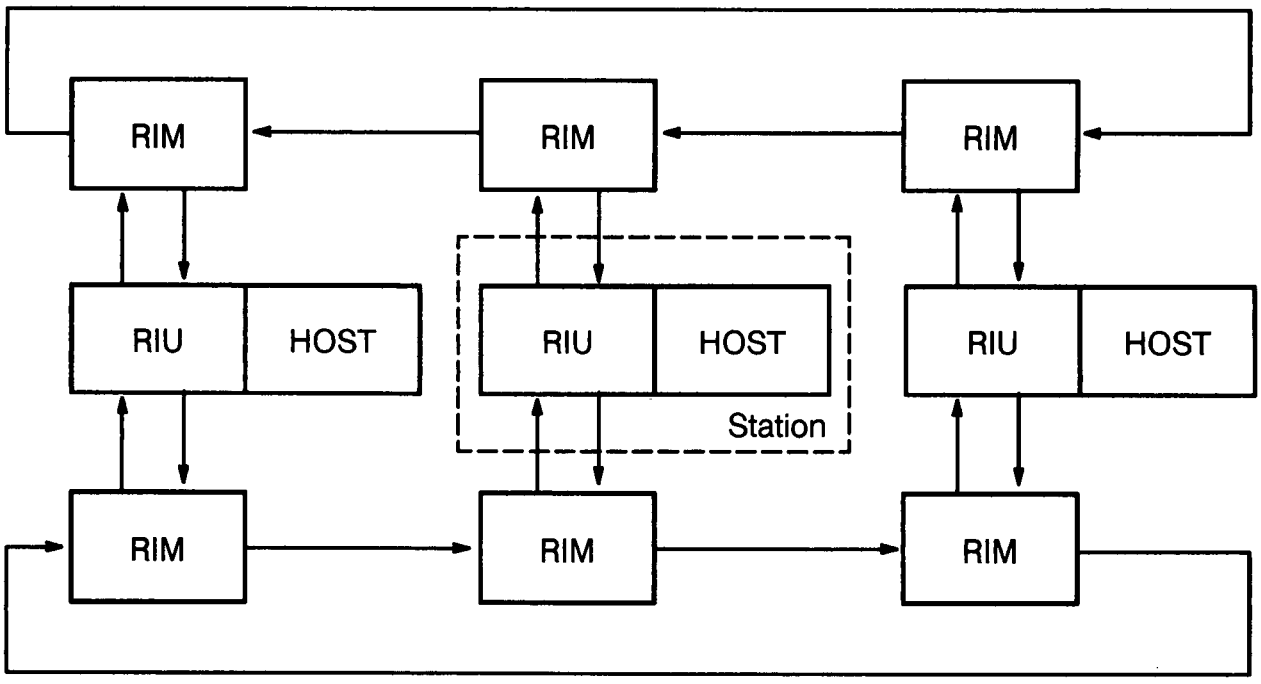

FIGURE 8. Counter-Rotating Ring Topology

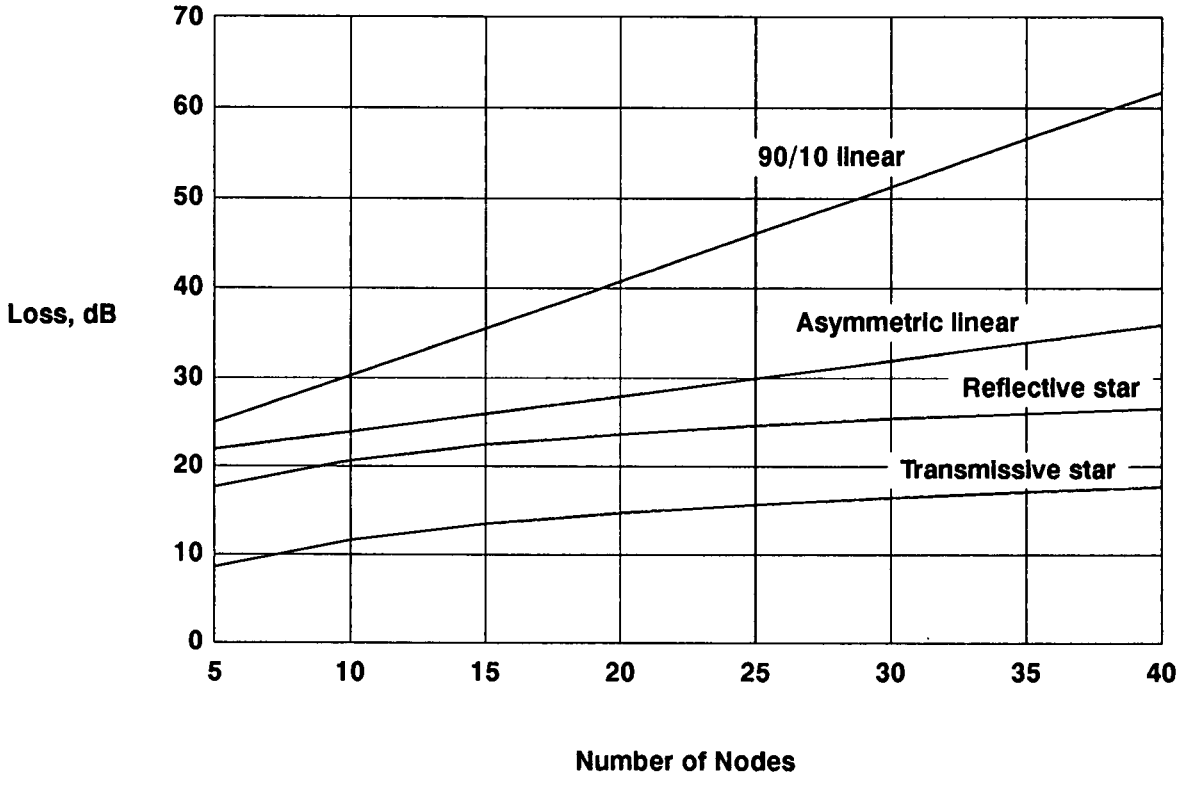

FIGURE 9. Data Bus Losses for Different Topologies

Transmitter

a.

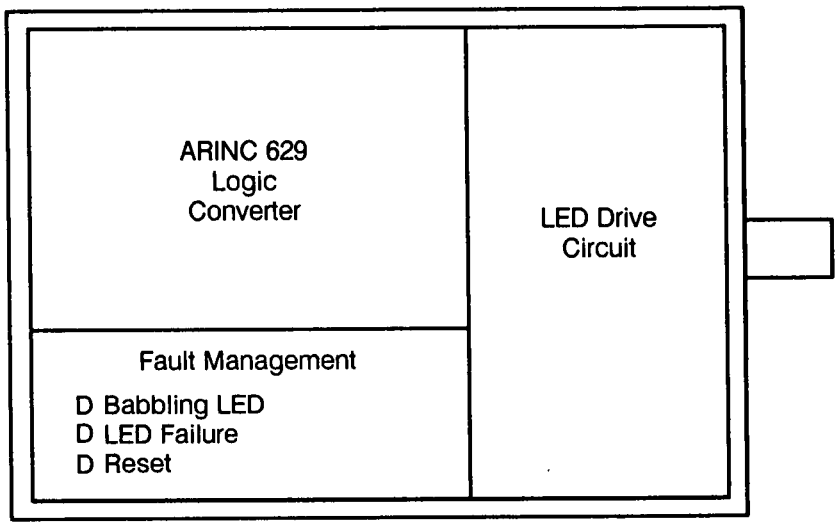

Receiver

b.

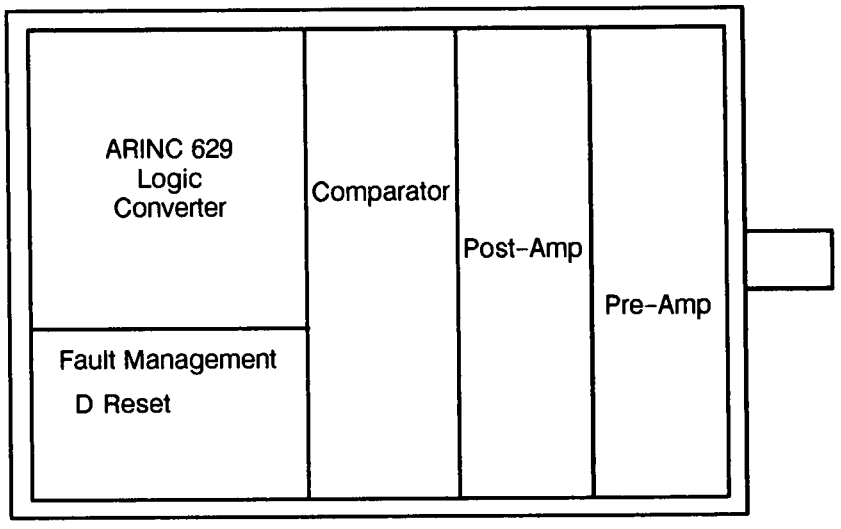

FIGURE 10. ARINC 629 Fiber Optic Transmitter/Receiver

convert this input electrical signal to the format of choice. The fault management circuit must detect two fault conditions:

1. The transmitter babbling condition whereby the transmitter is transmitting when not enabled.

2. The transmitter is not transmitting when enabled.

Transmitters designed for other data bus applications also require enables, fault management capability and LED drive circuitry.

The LED peak launch power for the three broadcast networks discussed in this paper, ARINC 629, STANAG 3910 and LTPB, all fall within the range of -4.0 to +3.0 dBm. This range of launch power is relatively narrow considering data rates range from 2 Mb/s to 50 Mb/s Manchester II. Some LRUs will be required to operate in the range of -55 to 85°C and others over the range of -55 to 125°C. The drive circuit must be capable of providing LED currents up to 150ma over the expected temperature range. Care must be exercised not to exceed critical junction temperatures to minimize LED failures.

Receiver Characteristics

Figure 10b illustrates the functionality of an ARINC 629 fiber optic receiver. The converter incorporates the necessary circuitry to interface to the ARINC 629 RXI and RXN signals. The fault management capability is limited to a reset line which provides a reset state with minimum delay.

Because bus idle conditions exist, the ARINC 629 receiver must be DC coupled. Also, because a preamble is not used with ARINC 629 message strings, the receiver must be capable of capturing the first bit of a data burst. Since the STANAG 3910 and the LTPB were designed to operate at higher data rates than ARINC 629, the protocols for these data busses provide a preamble to synchronize clocks. The preamble also allows an AC coupled receiver to "pump-up" to maximum sensitivity. AC coupled receivers require less bandwidth for a given data rate and therefore a higher sensitivity can be achieved than is the case for a DC coupled receiver. Additional circuitry is required to produce a DC coupled receiver which does not suffer from DC offset and drift problems over temperature.

The data in Table VI show that independent of data rate the broadcast data busses require a dynamic range of 21 to 25 dB. As the data rate increases, a broad dynamic range and a high sensitivity are increasingly difficult to achieve. A broadcast bus supporting a large number of terminals will require transceivers having a broad dynamic range and a high sensitivity independent of the topology used. For this reason high speed busses like ANSI FDDI and SAE HSRB are based on point-to-point links looped together to form a ring architecture. SAE HSRB has been designed to permit data rates into the gigabit range. In a point-to-point network, the variation in loss between terminals is limited to the length of fiber and number of connectors used. For avionic applications the receiver dynamic range and sensitivity will be established by the terminal-to-terminal losses and the anticipated number of terminal by-pass switches that will be placed in series as a result of multiple faults.

TABLE VI. Receiver Sensitivity and Dynamic Range Requirements for Different Data Bus Topologies

	Broadcast			Serial
	ARINC 629	STANAG 3910	LTPB	ARINC Project 636
Data rate	2 Mb/s	20 Mb/s	50 Mb/s	125 Mb/s
Sensitivity (dBm)*	-44	-37	-32.5	-28
Dynamic range	24	25	21	11
Receiver coupling	DC	AC	AC	AC

1. All sensitivities are reported as peak numbers.

2. This sensitivity includes the 50/50 optical splitter and connector that are a part of the EFA transceiver. The actual receiver sensitivity is -42 dBm.

3. This is a non-return to zero invert format (NRZI).

Data Bus Performance Criteria

Since ARINC 629 operates at a low data rate, this discussion will be limited to the high speed busses. Recent studies have been performed to compare the features of different data busses relative to future avionic requirements. In the work reported by H.S. McQuillan et al., the following conclusions were drawn (Ref 15):

1. STANAG 3910 has short to medium term application because it is based on proven MIL-STD-1553 technology. Because of a low overall data

throughput and a lack of priority ordering, it is less suitable for more advanced avionic architectures.

2. The SAE LTPB can give excellent performance provided the correct choice of timer settings has been selected. The SAE LTPB is more highly developed and thus could more readily be implemented than the HSRB.

3. When compared to STANAG 3910, SAE LTPB and ANSI FDDI, the SAE HSRB provides the best performance with regard to overall data throughput, separation of priorities and maintenance of low data latency.

DelCoco and Geyer concluded that the performance differences between the SAE HSRB and ANSI FDDI are a result of the differences in access methods and station delay (Ref 14). They also concluded that the overall throughput of the SAE HSDB is better than the ANSI FDDI. The high priority latency was also deemed to be considerably better.

5.0 Conclusions

A variety of data busses are being developed for aircraft applications. Certainly some are in more advanced stages than others. Hardware is being developed to meet the requirements of the different standards. Avionic companies and airframers are working together to solve installation, maintenance and operational problems. In some cases, focus is being placed upon the development or improvement of components that are impeding the progress of fiber optics into avionic applications. Significant growth of fiber optics into aircraft applications will occur in the next few years.

6.0 References

1. Draft 2 of Supplement 2 to ARINC Specification 629, "Multi-Transmitter Data Bus, Part 1 - Technical Description", Airlines Electronic Engineering Committee, April 30, 1991.

2. Ibid., pg 19.

3. Ibid., pg 17.

4. American National Standards Institute Fiber Distributed Data Interface (FDDI), ANSI X3.139, 1989.

5. Howard, A.J., "FDDI - The specification, Its Implementation and Its Military Applications", ERA Conference Proceedings, "Real-Time Data Communications for Military Applications", ERA Report 90-0301 Leatherhead, ERA Technology LTD, London, November 28-29, 1990.

6. Ibid., pg 3.3.8.

7. Ibid., pg 3.3.

8. "OLAN FDDI Strawman", Airlines Electronic Engineering Committee, May 8-10, 1991.

9. Turner, J., "The Air Force Perspective", ERA Conference Proceedings", "Real-Time Data Communications for Military Applications", ERA Report 90-0301, Leatherhead, ERA Technology LTD, London, November 28-29, 1990.

10. Windett, J.D., "Application of STANAG 3910 to the European Fighter Aircraft", ERA Conference Proceedings, "Real-Time Data Communications for Military Applications", ERA Report 90-0301, Leatherhead, ERA Technology LTD, London, November 28-29, 1990.

11. Ibid., pg 6.1.3.

12. Society of Automotive Engineers, SAE AS4074.1 Linear Token Passing Multiplex Data Bus, issued September 7, 1988.

13. Society of Automotive Engineers, SAE AS4074.2 High Speed Ring Bus, issued September 7, 1988.

14. DelCoco, R.J., and Geyer, M.A., "The SAE High Speed Bus Standards", ERA Conference Proceedings, "Real-Time Data Communications for Military Applications", ERA Report 90-0301, Leatherhead, ERA Technology LTD, London, November 28-29, 1990.

15. McQuillan, H.S., Conway, K.M., and Banner, M.G., "High Speed Databus Evaluation", ERA Conference Proceedings, "Real-Time Data Communications for Military Applications", ERA Report 90-0301, Leatherhead, ERA Technology LTD, London, November 28-29, 1990.

BIBLIOGRAPHY

This Bibliography was prepared by the Centre de Documentation de l'Armement (CEDOCAR), 00460 Armées, Paris, France in support of the Lecture Series.

To save space the field identifiers for each item have been omitted. This should cause little problem but to help understanding, a typical item is reprinted below with the identifiers in English and in French. Note that different types of document and documents from different sources do of course have somewhat different fields.

Accession Number/ NUMERO SIGNALEMENT	C-91-012741
French Title/ TITRE FRANCAIS	Section III.Systèmes de **guidage** et de pilotage à **gyroscope** optique.
English Title/ TITRE ANGLAIS	Part III.Optical **gyroscope** guidance and control systems.
Author(s)/ AUTEUR(S)	MARTIN G. J.; PAVLATH G. A.; WEBER D. J.; REMUZZI C. J.
Affiliation/ AFFILIATION	Litton Guidance and Control (US);Litton Guidance and Control (US);The Singer Company (US);Litton Systems INC (US)
Type of Document/ TYPE DE DOCUMENT	Publication en serie
Language Code/ CODE LANGUE	ENG
Country Code/ CODE PAYS D'ORIGINE	US
Periodical Title/ TITRE DU PERIODIQUE	Agardograph (FR)
Issue No., etc/ SOURCE	NO AG-314; 39 p.; 47 Ref.; 41 Fig.; 1 Tabl.; 4 Phot.; DP. 1990
CODEN/ CODEN	AGAGAS
ISSN/ ISSN	0365-2475
Location (in CEDOCAR)/ GISEMENT	02; AGARD-AG-314
Abstract/ RESUME	Les sujets suivants sont traités dans cette section III : - Principes et techniques du gyro laser.- Gyros à fibre de niveau inertiel.- Utilisation d'un Gyro laser monolithique trois-axes et d'un processeur de signaux dans un élément de capteur inertiel.- Systèmes de navigation inertielle à gyro laser pour la marine.
Origin of abstract/ SIGNATURE ANALYSTE	INFO/OK
Classification Code/ CODE CLASSIFICATION	17 07
Descriptors/ DESCRIPTEUR(S)	GUIDAGE INERTIE*;GYROSCOPE A LASER*;GUIDAGE LASER;APPLICATION DU LASER;NAVIGATION GUIDAGE;GUIDAGE INERTIE SANS PLATEFORME;GUIDAGE AERONEF;NAVIGATION ELECTROOPTIQUE;NAVIGATION MARITIME;CIRCUIT INTEGRE MONOLITHIQUE;FIBRE OPTIQUE
Identifiers/ IDENTIFICATEUR(S)	NAVIGATION INERTIE PAR LASER*;GUIDAGE OPTIQUE;PROCESSEUR OPTIQUE

NB The Classification Code uses the COSATI Field and Group Structure.

Words that are bracketed by ** and ** are the terms used for the search that produced this Bibliography.

C-92-001245
Contre-mesures sous marin contre **hélicoptère**.Un système d'auto défense de plateforme sous marine.
Helicoptere countermeasure for submarines.A self defence system.
UDT 1991 undersea defence technology.
Paris (FR)
1991/04/23-1991/04/25
WULFES C.
STN Systemtechnik Nord (DE)
Memoire Congres
ENG
DE
Microwave Exhibitions and Publishers Ltd Tunbridge Wells
pp. 167-171; DP. 1991
0-946-82132-1
05; M 3708/1991
Présentation d'un concept de défense du sous marin en plongée contre l'**hélicoptère** anti sous marin.Projet dans sa phase initiale.Début des études expérimentales par MBB et Aérospatiale à partir du **missile** à **guidage** par **fibre** **optique** polyphem développé pour l'armée de terre.Description du système.Composants principaux.Adaptation au lanceur sous marin.
INFO/BB
13 10; 15 03
SOUS MARIN*;ARME TACTIQUE*;DEFENSE ANTI HELICOPTERE*;MISSILE SURFACE AIR;MBB SOCIETE;AEROSPATIALE SOCIETE;GUIDAGE FIL;LANCEUR TORPILLE

C-91-016608
Acquisition, poursuite et pointage V.
Acquisition, tracking and pointing-V.
Orlando (US)
1991/04/03-1991/04/05
MASTEN M. K.; STOCKUM L. A.
SPIE (US)
Congres
ENG
US
SPIE (US)
SPIE (US)
VOL 1482; 504 p.; nb Ref.; nb Fig.; DP. 1991
SPIECJ
0-819-40591-4
1050-5784
05; Me 10628/1482
Congrès en 3 sessions regroupées sous les thèmes suivants : application au niveau des systèmes (poursuite à plusieurs degrés de liberté, système théodolite d'aire de lancement, poursuite laser, systèmes d'exploration embarqué, poursuite satellite, système de poursuite et de pointage GBL, poursuite vidéo), capteurs et systèmes de poursuite de cible (capteur IR de positionnement de cible, radar multitache et capteur optique, détecteur de cible, autopoursuite sur image pour des **missiles** guidés, poursuite multicible, algorithme de poursuite de haute précision), composants et sous-systèmes (erreur déterministe dans le pointage et la poursuite, **gyroscope** à **fibre** **optique** à faible dérive, système de vision de nuit pour le pilotage, profils de vitesses, systèmes de vision spatiale pour un explorateur laser, **guidage** 4D,...).
INFO/MA
17 11 '
ACQUISITION CIBLE*;POURSUITE CIBLE*;POINTAGE AUTOMATIQUE; RECONNAISSANCE CIBLE;DEGRE LIBERTE;POURSUITE LASER;EMBARQUE AERONEF;POURSUITE SATELLITE;CAPTEUR OPTIQUE;POURSUITE INFRAROUGE; RADAR POURSUITE EXPLORATION;ALGORITHME;DERIVE GYROSCOPE;FIBRE OPTIQUE
APPAREIL VISION NUIT;GUIDAGE

C-91-016097
Guides d'ondes lumineuses : Applications militaires.
Lichtwellenleiter fr militaerische anwendungen.
MAESSING W.
Publication en serie
GER
ZZ
Wehrtechnik (DE)
NO 8; pp. 60, 62; 2 Fig.; 2 Phot.; DP. 1991/08
WHTCAK
0043-2172
05; P 2045
Principes, structure, description, fonctionnement.1) des systèmes mobiles de transmissions par câble ou LWL - FERNFELD - KABEL 2) Systèmes de **guidage** pour véhicules terrestres robots, torpilles, **missiles**.
INFO/CH
20 06; 09 03
GUIDE ONDE OPTIQUE*;TRANSMISSION SIGNAL*;APPLICATION MILITAIRE*; SYSTEME COMMUNICATION DEFENSE;VEHICULE TELEGUIDE;FIBRE OPTIQUE; CABLE OPTIQUE

C-91-F03083
Système de transmissions d'ordres de **guidage** pour **missile** téléguidé en mode optoélectrique.
PAULET M.; PERES A.
Thomson-CSF (FR)
Brevet
FRE
FR
9 p.; 3 Fig.; DP. 1990/12/06
ERXX22
EP 0 437 126(A1)(90/12/06)
(FR)8 916 261 (89/12/08)
05; ME 1949/0437 126
Ce système comporte un détecteur optoélectronique recevant d'un poste de conduite de tir distant un signal de **guidage** transmis par un faisceau optique.Selon l'invention, il est prévu un porteur aérodynamique, non propulsé, relié au corps du **missile** par une liaison non rigide lui permettant d'être tracté par le **missile** pendant la phase de propulsion de celui-ci.L'ensemble est configuré de manière que, sous l'effet de cette traction, le porteur aérodynamique prenne une incidence lui permettant, en direction transversale, de s'écarter du corps du **missile** d'une distance supérieure à l'étendue de la zone dans laquelle la transmission du faisceau est essentiellement perturbée par la flamme du propulseur du **missile**.
17 07
GUIDAGE MISSILE*;DISPOSITIF ELECTROOPTIQUE*;TRANSMISSION SIGNAL; TRANSMISSION PAR FIBRE OPTIQUE
BRECL F42B 15 01;BRECL F41G 07 26

C-91-013616
Appareil pour le lancement de **missiles** filoguidés.
Apparatus for launching umbilical-guided **missiles**.
SCHOTTER K.
Hugues Aircraft (US)
Brevet
ENG
US
7 p.; 4 Fig.; DP. 1990/10/04
ERXX22
0 423 985 (A2)(90/10/04)
(US)423311 (89/10/18)
05; ME19490423985
Des **missiles** guidés qui trainent des fils de **guidage**, tels que desfibres optiques, sont lancés d'un réseau de tubes de lancement qui pointent dansla même direction.Un bras pivotant s'étend au dessus du réseau de tubes afin d e capter et déplacer les cordons ombilicaux des **missiles** précédemment lancés de la zone à partir de laquelle le prochain **missile** lancé, ceci afin d'éviter des interférences entre le **missile** lancé et les cordons.Lorsque chaque **missile** est lancé, le bras rotatif effectue un nouveau cycle de pivotement afin de capturer le cordon du **missile** lancé en dernier.
INFO/RO
22 04; 16 04
DISPOSITIF LANCEMENT*;LANCEMENT MISSILE*;GUIDAGE FIL;SYSTEME MECANIQUE;FIBRE OPTIQUE
PIVOTEMENT;BRECL F41F 03 055

C-91-013383
Dispensateur de filament amorti.
Damped filament dispenser.
CHESTER R. B.
Hughes Aircraft (US)
Brevet
ENG
US
6 p.; 4 Fig.; DP. 1990/10/26
ERXX22
0426 398 (A2)(90/10/26)
(US)430699 (89/11/01)
05; ME 1949 0426398
Un dévidoir de fil de liaison de données pour **missile** est logé dans un compartiment ayant une seule ouverture de petite taille à travers laquelle le fil se déroule après le lancement.Une quantité de matériau particulaire est transformé en un aérosol grâce au mouvement du filament.Cet aérosol agit comme un frein sur le filament et empêche la vitesse de distribution de dépasser une valeur maximale prédéterminée.
INFO/RO
16 04; 20 06
COMPOSANT MISSILE*;FIBRE OPTIQUE*;DISTRIBUTEUR*;GUIDAGE FIL; TRAINEE AERODYNAMIQUE;AEROSOL;GUIDAGE MISSILE
BRECL F42B 15 04;BRECL B65H 49 00

C-91-012741
Section III.Systèmes de **guidage** et de pilotage à **gyroscope** optique.
Part III.Optical **gyroscope** guidance and control systems.
MARTIN G. J.; PAVLATH G. A.; WEBER D. J.; REMUZZI C. J.
Litton Guidance and Control (US);Litton Guidance and Control (US);The Singer Company (US);Litton Systems INC (US)
Publication en serie
ENG
US
Agardograph (FR)
NO AG-314; 39 p.; 47 Ref.; 41 Fig.; 1 Tabl.; 4 Phot.; DP. 1990
AGAGAS
0365-2475
02; AGARD-AG-314
Les sujets suivants sont traités dans cette section III : - Principes et techniques du gyro laser.- Gyros à fibre de niveau inertiel.- Utilisation d'un Gyro laser monolithique trois-axes et d'un processeur de signaux dans un élément de capteur inertiel.- Systèmes de navigation inertielle à gyro laser pour la marine.

INFO/OK
17 07
GUIDAGE INERTIE*;GYROSCOPE A LASER*;GUIDAGE LASER;APPLICATION DU LASER;NAVIGATION GUIDAGE;GUIDAGE INERTIE SANS PLATEFORME;GUIDAGE AERONEF;NAVIGATION ELECTROOPTIQUE;NAVIGATION MARITIME;CIRCUIT INTEGRE MONOLITHIQUE;FIBRE OPTIQUE
NAVIGATION INERTIE PAR LASER*;GUIDAGE OPTIQUE;PROCESSEUR OPTIQUE

C-91-012144
Les méthodes d'analyse, de conception et de synthèse pour les systèmes de **guidage** et de pilotage.
Analyse, design and synthesis methods for guidance and control systems.
AGARD (FR)
Publication en serie
ENG
FR
AGARDOGRAPH (FR)
NO AG-314; 514 p.; nbr Ref.; nbr Fig.; DP. 1990
AGAGAS
0365-2475
02; AGARD-AG-314
L'arrivée de technologies nouvelles : circuits électroniques intégrés, calculateurs numériques embarqués, techniques de filtrage Kalman...- a permis de réhausser la capacité et les performances des systèmes de navigation et de **guidage** dans les années 60 et 70.Les années 80 ont vu apparaître d'autres innovations : gyrolaser annulaire, **gyroscope** à **fibre** **optique**, NAVSTAR/GPS.Les huit sections présentées font un tour d'horizon de ces technologies.
INFO/OK
17 07; 01 03
NAVIGATION GUIDAGE*;AVIONIQUE INTEGREE*;CALCULATEUR NAVIGATION*;GUIDAGE INERTIE;NAVIGATION TERRESTRE;CALCULATEUR AEROSPATIAL EMBARQUE;CHASSEUR;SYSTEME NAVIGATION;OMEGA SYSTEME NAVIGATION;SATELLITE NAVIGATION;EQUIPEMENT ELECTRONIQUE AERONEF;CONTROLE TRAFIC AERIEN;ETUDE CONCEPTION SYSTEME;AVION COMMERCIAL SURVIVABILITE MATERIEL;GPS SYSTEME NAVIGATION;GYROSCOPE A LASER;NAVSTAR SYSTEME NAVIGATION;SYSTEME COMMUNICATION INTEGRE

C-91-008840
Systèmes à **fibre** **optique** pour plateformes mobile III.
Fiber optics systems for mobile platforms III.
Boston (US)
1989/09/07-1989/09/08
SPIE (US)
Congres
ENG
US
Proceedings of the SPIE (US)
SPIE Bellingham
VOL 1173; 208 p.; nb Ref.; nb Fig.; nb Tabl.; nb Phot.; DP. 1990
PSISDG
0-819-40209-5
05; ME 10628/1173
Applications des systèmes à **fibre** **optique** aux navires (besoins généraux, applications militaires, système de contrôle, installation radar, expérience AEGIS) aux automobiles (panneau de contrôle optique, capteur à faible coût, réseau en étoile passive, capteur de pression pour combustion), aux aéronefs (capteur optique pour le système de propulsion, microphone, systèmes de vol à vue, unités de mesures inertielles), aux **missiles** et système de lancement (capteur à **fibre** **optique** à infra-rouge).
INFO/VR
20 06
FIBRE OPTIQUE*;DOMAINE AEROSPATIAL;AVIONIQUE;EMBARQUE NAVIRE;COUPLAGE OPTIQUE;RESEAU TELECOMMUNICATION LOCAL;TRANSMISSION PAR FIBRE OPTIQUE;APPLICATION MILITAIRE;CAPTEUR OPTIQUE;GUIDAGE MISSILE

C-91-F01826
Système de transmission d'images pour des **missiles** guidés par guides d'ondes lumineuses.
VON HOESSLE W.; KUCHLER H.
Messerschmitt-Bolkow-Blohm (DE)
Brevet
FRE
DE
14 p.; 2 Fig.; DP. 1990/08/23
FRXXAK
2 651 403 (A1)(90/08/23)
(DE)3928244 (89/08/26)
05; M 1372 / 2 654 403
L'invention concerne un système de transmission d'images à partir d'un **missile** guidé, qui est relié à une installation au sol par l'intermédiaire d'un guide d'ondes lumineuses, ce système étant conçu de façon que, sans accroître la largeur de bande de transmission du guide d'ondes lumineuses, on transmet deux images TV à l'installation de **guidage** au sol, des images fixes d'identification de l'objectif pouvant être demandées, en plus de l'image mobile servant à la navigation du **missile**, sans perturber le **guidage** assisté par image.
INFO/BC
17 02; 17 07
TRANSMISSION IMAGE*;GUIDAGE FIL*;GUIDAGE OPTIQUE*;GUIDAGE MISSILE;TRANSMISSION PAR FIBRE OPTIQUE
BRECL H04N 07 00;BRECL H04N 05 225;BRECL F41G 07 30;BRECL G05D 01 12

C-91-008070
La suppression du NLOS n'empêche pas la poursuite du programme FOG-M.
FOG-M lingering despite NLOS cancellation.
Rédaction revue
Publication en serie
ENG
ZZ
Defense Daily (US)
VOL 170; NO 9; p. 65; DP. 1991/01/15
DEDA23
0889-0404
05; P 2108
L'article analyse la manière dont l'armée de terre peut poursuivre son programme de **missile** à **guidage** par **fibre** **optique** FOG-M en utilisant une technologie moins sophistiquée que celle du Non-Line of Sight (NLOS) abandonnée sur ordre du Chef des Achats.
INFO/VZ
20 06; 17 07
FIBRE OPTIQUE*;GUIDAGE MISSILE*;ETUDE CONCEPTION MISSILE*;ETATS UNIS;ARMEE TERRE;PROGRAMME MILITAIRE
DIFFICULTE TECHNIQUE*

C-91-008068
Unité de mésure inertielle à **fibres** **optiques**.
Fiber optics based IMU.
Aerospace technology conference.
Long Beach, US
1990/10/01-1990/10/04
TAZARTES O.
Litton Systems, US
Memoire Congres
ENG
US
SAE Technical Paper series, US
NO 901826; 12 p.; 9 Fig.; 2 Tabl.; DP. 1990
STPSDN
0148-7191
05; Me 66/90 1826
Cet article décrit et montre les applications que l'on peut faire des gyros, à **fibre** **optique**.En effet, dans les années précédentes, les technologies d'optique intégrée et de **fibres** **optiques** ont suffisamment évoluées pour faire du gyro à **fibre** **optique** un candidat potentiel pour un bon nombre d'applications de dispositifs de mesure inertiels (IMU).Avec sa large bande passante, sa large plage dynamique, son faible poids et son coût moindre, cet article aboutit à la conclusion que le gyro à optique correspond de façon idéale à des petits dispositifs de mesure inertiels (IMU) de faible à moyenne précision applicables entre autre pour le contrôle en vol.
INFO/VR
20 06; 17 07
FIBRE OPTIQUE*;GYROSCOPE*;DETECTEUR OPTIQUE;FIBRE OPTIQUE;OPTIQUE INTEGREE;MODULATION PHASE;DISPOSITIF CONTROLE;GUIDAGE MISSILE;SYSTEME REFERENCE CAP AERONEF

C-91-004664
Système de **missile** guidé par radar à **fibre** **optique**.
Fiber optic radar guided **missile** system.
FRIENDENTHAL K.; DE LA CHAPELLE M.
Hughes Aircraft (US)
Brevet
ENG
US
15 p.; 1 Fig.; DP. 1989/11/06
ERXX22
EP 0 401 327(A1)(89/11/06)
(US)286 436 (88/12/19)
05; Me 1949 0 401 327
Ce système comprend un récepteur radar disposé dans un **missile** afin de recevoir les réflexions radar et fournir un premier signal optique en réponse à ces réflexions.Un récepteur optique est disposé au niveau du lanceur pour recevoir ce premier signal optique et pour fournir un ensemble de signaux électriques en réponse.Une liaison par **fibre** **optique** est assurée entre le **missile** et le lanceur afin de communiquer le premier signal optique du récepteur radar au récepteur optique.
INFO/RO
17 07; 20 06
GUIDAGE MISSILE*;FIBRE OPTIQUE*;AUTOGUIDAGE RADAR*;RECEPTEUR RADAR;EMETTEUR RADAR;RECEPTEUR OPTIQUE
RPV VEHICULE PILOTE DISTANCE;LIAISON OPTIQUE;BRECL F41G 07 32;BRECL F41G 07 22

C-91-F00117
Bobine de **fibre** **optique** de grande longueur utilisable sur un **missile** filoguide.
MAREE M.; MOREAU P.
Aérospatiale (FR)
Brevet
FRE
FR
9 p.; 5 Fig.; DP. 1990/03/20
ERXX22
0 389 360 (A1)(90/03/20)
(FR)8903752 (89/03/22)
05; Me 1949/0389 360

La bobine selon l'invention est de dimensions normales mais contient une grande longueur de **fibre** **optique**.Elle est constituée d'un support cylindrique principal autour duquel est enroulée une première partie de la **fibre** **optique** qui est destinée à être déroulée par traction.Elle est constituée d'un premier support cylindrique supplémentaire concentrique et placé à l'intérieur du support cylindrique principal, une deuxième partie de la **fibre** **optique** étant enroulée autour de ce premier support supplémentaire, la couche interne de la première partie de la **fibre** **optique** étant directement reliée à une couche externe de la deuxième partie de la **fibre** **optique**.Application aux **missiles** à très longue portée.
INFO/MS
17 07; 20 06
Guidage fil*;Fibre optique*;Guidage missile*;Grande distance
BRECL B65H 49 12

C-90-013011
Utilisation opérationnelle des **fibres** **optiques**.
Operational use of fibre-optics.
HEWISH M.
Publication en serie
ENG
ZZ
International Defense Review (CH)
VOL 23; NO 6/1990; pp. 707-710; 1 Fig.; 9 Phot.; DP. 1990/06
IDRVAL
0020-6512
05; P 1837
Les applications militaires possibles des **fibres** **optiques**, notamment dans les domaines suivants : communications;transmission de données;**gyroscopes** (Fiber-Optic Gyro ou Fog);sonars;**guidage**.
INFO/DH
20 06; 15 05
Fibre optique*;Application militaire*;Communication tactique; Transmission donnée;Gyroscope;Sonar;Guidage

C-90-011573
Applications des **fibres** **optiques**.
Fiber optics applications.
JACK W. B.; GAGNER W. P.; RAMSAY M. M.; GREY A. C.
ATT, US;SW ASSOC., US;STC, NEWPORT, GB;STC, NEWPORT, GB
Publication en serie
ENG
GB
Signal (US)
VOL 44; NO 7; pp. 57.69; 6 Ref.; 3 Fig.; 3 Phot.; DP. 1990/03
SGNAAZ
0037-4938
05; P 0835
Trois articles examinent les applications utilitaires potentielles de l'**optique** à **fibre**, en particulier dans les systèmes d'ordre , contrôle, transmission et renseignement (C3I) pour compléter les transmissions par satellites en exploitant les avantages des **fibres** **optiques** (sécurité, économie, capacité, facilité de planification et de réparation, absence de distorsion, rapidité, délais réduits) et dans diverses fonctions (observation sous marine, **guidage** de **missile**, détection de rayonnement, régulation de température, avionique, guerre électronique, communications tactiques).
INFO/CR
20 06; 15 05
Optique fibre*;Besoin militaire*;C3 ordre contrôle communication; Détecteur objet sous marin;Guidage missile;Communication tactique; Cable sous marin;Capteur optique
Télécommunication militaire;transmission par fibre optique; Avionique intégrée;Transmission armée

C-90-010451
Programmes d'applications des **fibres** **optiques**.
Optical fiber programs.
ROBINSON C. A.
Signal, Fairfax, US
Publication en serie
ENG
US
Signal (US)
VOL 44; NO 7; pp. 47-55; 3 Fig.; 5 Phot.; DP. 1990/03
SGNAAZ
0037-4938
05; P 0835
Présentation des recherches expérimentales de la firme "ATT Bell Laboratories" sur les calculateurs optiques numériques faisant appel aux dispositifs S-SEED ("Symetric self-induced electro-optic device") inventés par cette firme en 1987.Etude de l'extrapolation des transmissions par **fibres** **optiques** commerciales au **guidage** des **missiles** tactiques, de bombes planantes et de munitions à grande précision.Application de capteurs à **fibres** **optiques** à la surveillance sous-marine.Description de **gyroscopes** à **optique** à **fibre** et examen de ses applications possibles (remplacement des gysos mécaniques et à laser stabilisation d'antennes et d'armes, stabilisation et contrôle de munitions intelligentes, système anti-dérapage, robotique).
INFO/CR
20 06; 15 05
Optique fibre*;Besoin militaire*;Guidage missile;Munition guidée précision;Bombe guidée;Arme tactique;Océan surveillance; Communication sous marine;Gyroscope
Dispositif électrooptique*;Calculateur optique;Transmission par fibre optique;Walleye bombe;Détecteur sous marin

C-90-009891
L'Armée de terre américaine veut augmenter l'achat du NLOS dans le projet de programme.
Army seeks to up NLOS buy in program objective memoranum.
Rédaction Revue
Publication en serie
ENG
ZZ
Defense Daily (US)
VOL 167; NO 26; p. 210; DP. 1990/05/07
DEDA23
0889-0404
05; P 2108
Dans son projet de programme 1992- 1997, l'armée de terre américaine veut porter de 403 à 502 le nombre des unités de tir prévues de **missiles** guidé **fibre** **optique** FOG-M non-line of-sight NLOS.Le programme 403 comportait 285 versions lourdes et 118 légères.Le programme total prévoit 16.550 **missiles**.
INFO/VZ
16 04; 15 05
Missile sol air*;Fourniture force armée*;Etats Unis;Matériel armée terre;Programme militaire;Fibre optique;Guidage missile

C-90-008894
Gyroscope à **fibre** **optique**.
Fibre optical gyro.
JOHNSSON S.
AB Bofors (SE)
Brevet
ENG
SE
5 p.; 2 Fig.; DP. 1989/09/19
ERXX22
EP 0 362 172(A2)(89/09/19)
(SE)8803404 (88/09/27)
05; Me 1949 0 362 172
Gyroscope à **fibre** **optique** pour munitions telles que **missile** au projectile guidé en phase finale pour lesquelles le système de **guidage** a besoin d'informations sur l'orientation de la munition dans l'air.L'angle de rotation ou de lacet est déterminé à partir du déphasage de la lumière dans la ou les boucles de **fibre** **optique**.
INFO/BC
17 07
Gyroscope*;Fibre optique;Navigation guidage;Guidage final;Guidage missile
BRECL G01C 19 72

C-90-008165
Le **guidage** par **fibre** **optique** décolle.
Fibre-optic guidance takes off.
HEWISH M.; TURBE G.
Publication en série
ENG
ZZ
International Defense Review (CH)
VOL 23; NO 1/1990; p. 73; 2 Phot.; DP. 1990/01
IDRVAL
0020-6512
05; P1837
Le point sur le développements en cours, aux Etats Unis et en Europe, de systèmes de **guidage** par **fibre** **optique**, pour **missiles** destinés à attaquer les véhicules blindés et les **hélicoptères**.
INFO/DH
17 07; 20 06
Guidage missile*;Fibre optique*;Etats Unis;Europe ouest;Lutte antichar;Lutte anti aérienne
Lutte anti aérienne

C-90-007474
Les applications militaires de la technologie des véhicules à liaison ombilicale à **fibre** **optique**.
Military applications of fiber optic tethered vehicle technology.
Fiber Optic Systems for Mobile Platforms II.
Boston, (US)
1988/09/06-1988/09/07
CULVER W. H.
Optelecom Inc.Gaithersburg, (US)
Mémoire Congrès
ENG
US
Proceedings of the SPIE, (US)
SPIE, Bellingham, (US)
VOL 989; pp. 156-161; 5 Fig.; DP. 1988
PSISDG
05; Me 10628/989
L'article évoque les types de véhicules utilisant des liaisons **fibre** **optique** pour transmettre ou recevoir des informations : **missile** guidé, surveillance à distance, "launch and learn" **missile**, maintenance de réacteur nucléaire, lutte

incendie...Les techniques du dévidage sont mentionnées.
INFO/BR
20 06; 17 07
Fibre optique*;Guidage fil*;Véhicule spatial;Dévidoir câble;
Pilotage par fil;Guidage missile;Transmission par fibre optique
Application militaire*;Technologie sous marine;Robotique

C-90-007473
Le **missile** guidé par **fibre** **optique**.
The fiber optic guided **missile** (FOG-M).
Fiber Optic Systems for Mobile Platforms II.
Boston, (US)
1988/09/06-1989/09/07
JACOBS P. L.
US Army missile Command Redstone Arsenal, (US)
Mémoire Congrès
ENG
US
Proceedings of the SPIE, (US)
SPIE, Bellingham, (US)
VOL 989; pp. 178-182; DP. 1988
PSISDG
05; 10628/989
L'article décrit un système mis au point par le centre technique de recherche et développement de l'armée de terre américaine, pour démontrer la faisabilité d'un **missile** guidé par **fibre** **optique** contre des blindés.Il est actuellement monté sur véhicule à roues, à grande mobilités et mission multiple.Les questions d'enroulement et de dévidage de la **fibre** **optique** sont examinées plus spécialement.
INFO/BR
20 06; 17 07
Fibre optique*;Guidage missile*;Guidage fil;Transmission par fibre optique;Dévidoir cable
Système guidage

C-90-007276
Le plan de modernisation de l'armée de terre américaine met l'urgence sur l'amélioration des systèmes des défense aérienne.
Army modernization plan urges upgrades for air defense systems.
POLSKY D.
Publication en série
ENG
ZZ
Defense news (US)
VOL 5; NO 5; pp. 14,19; 1 Phot.; DP. 1990/01/29
DNEW2Z
0884-139X
05; P 2486
Le plan de l'armée de terre américaine de modernisation de la Défense Aérienne met l'accent sur l'amélioration des matériels existants plus que sur l'achat de nouveaux matériels ;soit 140 millions de dollars pour un nouveau logiciel du PATRIOT, doté d'un nouveau radar terrestre de désignation de cible ;un nouveau radar multirôle pour le HAWK, modernisation du SPARROW, abandon de la version lourde du NLOS à **guidage** par **fibre** **optique**.
INFO/VZ
15 05; 15 07
Matériel armée terre*;Programme militaire*;Modernisation*;Etats Unis;Défense militaire;Radar embarque aéronef;Désignateur cible radar;Missile sol air
Défense aérienne*;Sparrow missile

C-90-006599
Systèmes à **fibre** **optique** pour plateformes mobiles II.
Fiber Opitcs Systems for Mobile Platforms II.
Boston, (US)
1988/09/06-1988/09/07
Spie, (us)
Congrès
ENG
US
Proceedings of the Spie, (US)
SPIE, Bellingham
VOL 989; 214 p.; Nbx Ref.; Nbx Fig.; DP. 1989
PSISDG
0277-786X
05; Me 10628/989
Applications des systèmes à **fibre** **optique** aux aéronefs (capteurs, systèmes interférométriques, bus optiques, réseaux en anneau et en étoile de **fibre** **optique**, transducteur à **fibre** **optique**), aux bateaux (coupleur en étoile, systèmes de commande de moteur, réseau local), aux automobiles (capteur de pression pour combustion, coupleur en étoile à faible coût, système de transmission), aux spationefs, **missiles** et systèmes de lancement (**guidage** **missile**, réseaux de transmissions de données, commutateurs optiques).
INFO/BC
20 06
Fibre optique*;Domaine aerospatial;Avionique;Embarque navire;
Couplage optique;Reseau telecommunication local;Transmission par fibre optique;Application militaire;Guidage missile;Guidage fil;
Commutateur optique;Multiplexage optique;Capteur optique
Embarque spationef

C-90-005519
Des documents montrent qu'un **missile** à **fibres** **optiques** à détruit 8 de ses 16 objectifs.
Fiber-optic **missile** hits 8 of 16 targets, documents show.
BAKER C.
Publication en série
ENG
ZZ
Defense News (US)
VOL 5; NO 5; p. 36; DP. 1990/01/29
DNEW2Z
0884-139X
05; P 2486
Au cours des essais dans les conditions réelles du combat, terminés en décembre 1989, le **missile** antichar, antihélicoptère à **guidage** par **fibre** **optique** NLOS (Non-line-of sight) de l'armée de terre américaine a frappé 8 de ses 16 objectifs, constitués de chars en mouvement et d'**hélicoptères** stationnaires.
INFO/VZ
16 04; 20 06
Missile anti char*;Fibre optique*;Etude développement programme*;
Etats Unis;Matériel armée terre;Performance matériel

C-90-005507
L'armée de terre américaine pourrait abandonner le programme des **missiles** guidés lourds à **fibre** **optique**.
Army may drop heavy fiber-optic guided **missiles**.
BAKER C.
Publication en série
ENG
ZZ
Defense News (US)
VOL 5; NO 2; pp. 4, 37; 1 Fig.; DP. 1990/01/08
DNEW2Z
0884-139X
05; P 2486
Les réductions budgétaires et les restructurations entraînées par l'évolution stratégique en Europe de l'Est ont amené le Pentagone à retarder, voire supprimer le déploiement des premiers **missiles** NLOS, **missiles** lourds à **guidage** par **fibre** **optique**, dans les unités blindées d'Europe Centrale ou de Corée.La totalité des 403 unités de tir prévues équiperont les unités légères d'infanterie et les forces d'intervention rapide, basées aux Etats-Unis.Les 16.550 **missiles** seront tirés par les véhicules légers HMMWV pesant 4 tonnes.Initialement, 285 des 403 unités de tir devaient être portées et tirées par les lance-roquettes multiples MLRS de 22 tonnes.
INFO/VZ
16 04
MISSILE ANTI CHAR*;Fibre optique*;Force Armee Etats Unis;Programme militaire;Evaluation menace;Organisation militaire
Critere choix*;Deficit budgetaire*

C-90-004932
Navigation des véhicules aériens autonomes par senseurs passifs d'imageries.
Navigation of autonomeous air vehicles by passive imaging sensors.
Guidance and Control of Unmanned Air Vehicles.
Sans Francisco (US)
1988/10/04-1988/10/07
ZINNER H.; SCHMIDT R.; WOLF D.
MBB GmbH, Munich (DE);MBB GmbH, Munich (DE);MBB GmbH, Munich (DE)
Mémoire Congrès
ENG
DE
Agard Conference Proceedings (FR)
Agard, Neuilly
VOL 436; pp. 34.1-34.14; 12 Ref.; 7 Fig.; DP. 1989/08
AGCPAV
9-283-50523-9
0549-7191
02; AGARD CP 430
Les systèmes de navigation des véhicules autonomes doivent fournir : 1) des informations permettant le contrôle de vol;2) des informations sur l'environnement permettant de percevoir un paysage en 3 dimensions.Des senseurs passifs d'imageurs et les algorithmes convenables peuvent donner les deux informations.L'article présente un concept qui évalue le champ du défilement optique dans le plan d'image afin d'en déduire les données nécessaires pour le **guidage** et la commande du véhicule.La qualité du traitement des informations est améliorée en y incorporant la connaissance de l'environnement et de la dynamique du porteur.Le concept est appliqué à deux types de non pilotés : 1) sous munition autonome non propulsée qui doit détecter, classifier et poursuivre des véhicules terrestres;2) le **missile** guidé par **fibre** **optique** qui sert de plateforme d'essai en vue de systèmes à plus grande autonomie.
INFO/BR
01 03; 20 06
Véhicule sans pilote*;Image infrarouge*;Fibre optique*;Navigation guidage;Guidage missile;Guidage fil
RPV véhicule pilote distance*;Capteur image*;Sous munition

C-90-F01353
Procédé et appareil à **fibre** **optique**, comprenant un coupleur directionnel, pour la détection d'un taux de rotation.
BROCKETT W. S.; MARTIN J. M.
Martin Marietta Corporation (US)
Brevet

FRE
US
25 p.; 6 Fig.; DP. 1984/09/14
FRXXAK
2 633 713 (A1)(84/09/14)
(US)533180 (83/09/19)
05; M 1372 / 2 633 713
Détecteur de rotation à **fibre** **optique** particulièrement adapté pour le **guidage** à mi-distance et la stabilisation en rotation de **missiles**.Ce dispositif est basé sur l'effet SAGNAC et fournit une indication précise sur le taux et sur la direction de rotation angulaire.
INFO/BC
17 07; 20 06
Gyroscope*;Fibre optique*;Gyromètre;Angle rotation;Mesure angle; Guidage missile
BRECL G01C 19 72;BRECL G01B 11 26;BRECL G01P 09 00

C-90-F01195
Etude de **fibres** **optiques** spéciales pour filoguidage. Dixièmes journées nationales d'optique guidée.
JOUY-en-JOSAS (FR)
1989/08/28-1989/08/30
LE PESANT J. P.; TURPIN M.; GOMBERT J. C.; DESORMIERE B.
Thomson-CSF, LCR Corbeville (FR);Thomson-CSF, LCR Corbeville (FR);Thomson-CSF, LCR Corbeville (FR);Thomson-Sintra (FR)
Mémoire Congrès
FRE
FR
Société Française d'optique, Paris
p. 124-125.; 2 Fig.; DP. 1989
05; M5982/1989
Mise au point des **fibres** **optiques** spécifiques ayant une enduction hermétique métallique.Présentation d'essais de résistance mécanique.
INFO/BC
20 06
Fibre optique*;Guidage missile;Essai mécanique;Résistance mécanique;Guidage fil

C-90-003047
Etats Unis : **Missiles** a **guidage** **fibre** **optique**.
USA : Lenkweffen mit fiber-optscher lenkung (FOG-M).
Rédaction Revue
Publication en série
GER
ZZ
ASMZ (CH)
NO 10; p. 688; 1 Phot.; DP. 1989/10
ASMZAP
0002-5925
05; P1806
Etat d'avancement du développement du **missile** anti char et autre **hélicoptère** par les firmes US BOEING-MUGHES.Description, caractéristiques techniques.Emploi dans le cadre de la doctrine FOFA et AIR LAND BATTLE.
INFO/CM
16 04
Missile anti char*;Etats Unis;Etude développement programme; Spécification matériel
Défense anti hélicoptère*;US Army;Bataille aéroterrestre an 2000; FOFA concept

C-90-002518
Fiabilité des **fibres** **optiques** pour dévidoir de **missile**.
Reliability of optical fibers for **missile** payout.
Components for fiber optic applications III and coherent lightwave communications.
Boston (US)
1988/09/07-1988/09/09
WYSOCKI J.; BISWAS D.; FOX D.; HSU H. P.; REDFORD G.
Hughes Research Labs (US);ALCATEL Cable systems (US);FOX Technical Consultants (US);Hughes Aircraft Company Missile Systems Group (US);Hughes Aircraft Company Missile Systems Group (US)
Mémoire Congrès
ENG
US
Proceedings of the SPIE (US)
SPIE, Bellingham
VOL 988; pp. 157-162; 2 Ref.; 4 Fig.; DP. 1989
PSISDG
0277-786X
05; Me 10628 / 988
Essais mécaniques sur des câbles optiques en vue de leur utilisation sur des dévidoirs de **missiles** guidés par **fibres** **optiques**.
INFO/BC
20 06; 14 02
Câble optique*;Essai mécanique*;Dévidoir câble;Fibre optique; Composant missile;Guidage fil;Résistance mécanique

C-90-002427
Liaison pour communication entre deux objets mobiles.
Communication link between moving bodies.
PINSON G. T.
Boeing Compagny (US)
Brevet
ENG
US
16 p.; 14 Fig.; DP. 1989/04/04
ERXX22
EP 0 337 254(A2)(89/04/04)
(US)182025 (88/04/15)
05; Me 1949 0 337 254
Dispositif pour communication entre deux objets mobiles utilisant une liaison par **fibre** **optique**.Ce dispositif est utilisable dans le cas de **missiles** guidés et lancés à partir d'un **hélicoptère**.
INFO/BC
17 07; 20 06
Guidage missile*;Fibre optique*;Système guidage;Hélicoptère; Guidage fil;Armement aéronef
BRECL F41G 07 32;BRECL F42B 15 04

C-90-F00475
Installation de conditionnement et de lancement d'un **missile** filoguidé.
MAREE M.
Aérospatiale (FR)
Brevet
FRE
FR
10 p.; 4 Fig.; DP. 1989/04/12
ERXX22
0337880 (A1)(89/04/12)
(FR)8804951 (88/04/14)
05; ME 1949 / 0337880
Pour protéger, lors de la phase départ les premières spires du fil reliant un **missile** filoguidé à son conteneur de conditionnement et de lancement, notamment lorsque ce fil comprend une **fibre** **optique**, on place entre l'arrière du **missile** et le fond du conteneur un dispositif de protection tubulaire déformable.Ce dispositif, qui peut notamment être constitué par un manchon souple ou par des viroles rigides télescopiques, s'allonge lors de la mise à feu des propulseurs du **missile**, pour former un écran protégeant le fil des gaz chauds sortant des propulseurs, tant que ces derniers restent à l'intérieur du conteneur.Le dispositif se détache ensuite automatiquement du **missile**.
INFO/MS
16 04; 16 01
Composant missile*;Lancement missile*;Guidage fil*;Conditionnement; Protection thermique
BRECL F42B 15 04

C-89-015682
L'armée de terre américaine désigne un nouveau leader pour le programme de **missile** NLOS.
Army transfers leadership of mos **missile** program.
BAKER C.
Publication en série
ENG
ZZ
Defense news (US)
VOL 4; NO 32; p. 16;" 1 Phot.; DP. 1989/08/14
DNEW2Z
0884-139X
05; P 2486
L'armée de terre américaine vient de confier à son Centre Combiné d'Armements le rôle de leader pour le programme de **missile** à **guidage** par **fibre** **optique** NLOS (non-Light-Of-Sight) de 2,9 milliards de dollars, destiné à la lutte contre les **hélicoptères** et contre les chars.L'armée de terre prévoit d'ici 1993 l'achat de 406 units de tir et de 16.550 **missiles**.118 systèmes seront destinés aux forces légères, étant montés sur le véhicules HMMWV et 285 aux forces blindées, le tir s'effectuant à partir de MLRS.
INFO/VZ
16 04; 05 01
Missile anti char*;Etude développement programme*;Etats Unis; Programme militaire;Dépense militaire;Performance matériel; Matériel armée terre;Guidage;Fibre optique

C-89-013745
Le système Polyphem obtient un financement de recherche-développement sur les **fibres** **optiques**.
Polyphem gets exploratory funding for fibre-optics.
FOSS C. F.
Publication en série
ENG
ZZ
Jane's Defence Weekly (GB)
VOL 12; NO 3; pp. 126-127; 1 Phot.; DP. 1989/07/22
JADW25
0265-3818
05; P 2347
Euromissile s'est vu attribuer un financement jusqu'en 1993 pour un développement exploration du système Polyphem de **missile** guidé par **fibre** **optique**.Actuellement, les **fibres** **optiques** permettraient des portées **missiles** maximaées de 80 km.Euromissile proposerait toute une gamme de **missiles** Polyphem dont une version sous.marine destinée à être lancée par sous-marin contre **hélicoptère** en vol stationnaire sonar.
INFO/BR
20 06; 17 07
Fibre optique*;Guidage missile*;Missile sol air;Recherche

développement;Europe Ouest
Développement technologique*

C-89-012931
Consortium franco-allemand pour l'étude d'un **missile** antiaérien lancé par un sous-marin.
Firms study sub-launched antiaircraft **missile**.
DE BRIGANTI G.
Publication en série
ENG
ZZ
Defense News (US)
VOL 3; NO 44; p. 45; DP. 1988/10/31
DNEW2Z
0884-139X
05; P 2486
L'Aérospatiale et MBB étudient la faisabilité d'un **missile** antiaérien tiré à partir d'un sous-marin et qui grâce à son **guidage** par **fibres** **optiques** pourrait aussi être utilisé pour l'observation et la désignation d'objectifs.Le **missile** Polyphème SM, dérivé du Polyphème antichar Aérospatiale/MBB pourrait être tiré à partir d'un sous-marin en immersion périscopique et en plongée jusqu'à 300 m.Sa vitesse serait de 250 m/s.Description des spécifications et du fonctionnement.
INFO/VZ
16 04; 19 08
Missile antiaérien*;Armement sous marin*;Coopération internationale*;France;République Fédérale Allemande;Industrie armement;Etude faisabilité;Spécification matériel;Performance matériel;Fonctionnement;Fibre optique;Guidage missile

C-89-F03190
Engins antichars de deuxième génération améliorée et au-dela.
ALDER K.
Publication en série
FRE
ZZ
Armada international (CH)
VOL 13; NO 2; pp. 10-20; 9 Phot.; DP. 1989/04
ARIN2N
05; P 1804
Rappel des pécifications recherchées pour les **missiles** antichars de l'avenir.Résumé des solutions occidentales déjà adoptées ou à l'etude: Programmes d'amélioration / Engins de dernière génération / **Guidage** par **fibres** **optiques** / **Missiles** aéroportés / **Missiles** sol-sol à longue portée / Obus d'artillerie à **guidage** terminal / Rpv antichars / Systémes mixtes antichars et antiaériens.
INFO/CH
15 03
Arme antichar*;Etude développement programme;Modernisation;Missile sol sol;Missile anti char;Munition guidée précision;Matériel aéroporté;Lutte antichar
Production armement*;Occident

C-89-011734
La lente percée des **fibres** **optiques**.
Fibre optics catch on ...slowly.
STARR B.
Publication en série
ENG
ZZ
International defense review (GB)
NO 1; pp. 37-39; 3 Fig.; 3 Phot.; Informatique et electronique de defense; DP. 1989/03
IDRVAL
05; M 260-2 / no 47 p
Applications militaires des **fibres** **optiques** : **guidage** **missiles**...Industrialisation par les contractants du département de la defense (Corning...).Evolution et nature du marché (forte spécialisation nécessité de petites structures industrielles).
INFO/MZ
20 06; 15 03
Fibre optique*;Systeme arme*;Industrie armement*;Besoin militaire;Guidage missile;Etude marche;Etats Unis;Normalisation
Application militaire*

C-89-011600
Symposium : technologie des **gyroscopes** 1988.
Symposium : gyro technology 1988.
Symposium : gyro technology 1988.
Stuttgart (DE)
1988/09/20-1988/09/21
Universitaet Stuttgart.Deutsche gesellschaft fuer ortung und navigation (DGON)
Mémoire Congrès
ENG
ZZ
Universitaet Stuttgart
325 p.; DP. 1988
05; ME 10653
Le symposium comprend 17 exposés.Détection des pannes, isolement et reconfiguration dynamique des systèmes de réference inertiels.Logiciel des systèmes de **guidage** inertiel sans plate forme (strapdown).Filtre de kalman pour navigation et géodésie.Optimisation de la précision des systèmes strapdown.Gyro a cylindre vibrant.Gyro pour **guidage** des armes.Gyro chinois a cristal piézoélectrique.Servo accéléromètre miniature.Système aéroporté de cartographie.Technologie inertielle pour la géodésie et la surveillance.Essais comparatifs de gyro automatisés.Capteur optique de surveillance de précision.Réduction de données de calibrage de capteur.Mesures angulaires par gyrolaser à anneau.Gyro à **fibre** **optique**.Caractéristiques d'un gyro à **fibre** **optique**.
INFO/CD
17 07; 14 02
Gyroscope*;Accelerometre*;Gyroscope a laser;Guidage inertie;GUIDAGE INERTIE SANS PLATEFORME;Cristal piezoelectrique;Cartographie;Navigation inertie;Geodesie
Systeme reference inertiel*;Filtre kalman

C-89-011501
En gros, les programmes de défense aérienne et anti chars de l'armée de terre conservent leur budget.
Army air defense, anti tank systemes generally intoucheched.
Redaction revue
Publication en série
ENG
ZZ
Aerospace daily (US)
VOL 150; NO 18; p. 145; DP. 1989/04/26
ASDY24
05; P 2095
L'essentiel des programmes de défense aérienne et antichar de l'armée de etrre américaine n'est pas touché par les restrictions budgétaires de l'administration BUSH;notamment l'ADATS, le **missile** à **guidage** par **fibre** **optique**, le véhicule porteur de STINGER sur mât télescopique, le système d'arme tout temps de l'APACHE.
INFO/VZ
15 03
Defense antiaerienne*;Arme antichar*;Budget force armee*;Etats Unis;Materiel armee terre;Programme militaire;Defense militaire
Deficit budgetaire*;1989 annee
C-92-002146
Les structures deviennent intelligentes (2ème partie).
Structures get smart (part II).
STEVENS T.
Publication en serie
ENG
ZZ
Materials engineering (US)
VOL 108; NO 11; pp. 26-28; 3 Phot.; DP. 1991/11
MAENBO
0025-5319
05; P 0591
La performance des capteurs et actuateurs, encastrés dans des **structures** "**intelligentes**" dépend de la conductivité thermique, électrique et magnétique de ces structures.On présente la technologique et quelques applications des films piézoélectriques et alliages magnétostrictif tels que le Terfenol-D (contrôle de structures d'aéronefs et mesure de leurs vibrations en vol), céramiques électrostrictives (contrôle de miroirs optiques et lasers de systèmes spatiaux, contrôle de déplacements dans les machines-outils et machines tournantes, de mélanges gaz/air ...), et systèmes à fluides électrorhéologiques (amortissement de vibrations de rotors d'**hélicoptères** et de structures spatiales habitées).(Voir 1ère partie dans le No 10 de 10/91).
INFO/DS
14 02; 13 13
CONTROLE NON DESTRUCTIF*;VIBRATION STRUCTURE*;DEFORMATION STRUCTURE*;CAPTEUR PIEZOELECTRIQUE;ELECTROSTRICTION;NIOBATE;COMPOSE MAGNESIUM;MAGNETOSTRICTION;ALLIAGE TERBIUM;COMPOSE DYSPROSIUM;ALLIAGE CONTENANT FER;AMORTISSEMENT VIBRATION;MESURE VIBRATION;STRUCTURE AERONEF;STRUCTURE SPATIONEF
MATERIAU INTELLIGENT*;CONTROLE ACTIF*;ACTUATEUR;MESURE DEFORMATION;MESURE DEPLACEMENT;NIOBATE PLOMB;SYSTEME AEROSPATIAL;PROPRIETE DIELECTRIQUE;VISCOSITE

C-92-001280
Les structures deviennent inteligentes (1ère partie).
Structures get smart (part I).
STEVENS T.
Publication en serie
ENG
ZZ
Materials engineering (US)
VOL 108; NO 10; pp. 18-20; 1 Fig.; DP. 1991/10
MAENBO
0025-5319
05; P 0591
La performance des capteurs et actuateurs, encâstrés dans des **structures** "**intelligentes**" dépend de la conductivité thermique, électrique ou magnétique de ces structures.On présente, dans cette 1ère partie, la technologie et quelques applications des alliages à mémoire de forme et des capteurs piézocéramiques encâstrés (contrôle actif de forme et de vibrations de structures spatiales, sous-marines, pales d'**hélicoptères**...).
INFO/DS
13 13; 14 02
VIBRATION STRUCTURE*;CONTROLE NON DESTRUCTIF*;DEFORMATION

STRUCTURE*;ALLIAGE;PLASTIQUE EPOXY;CAPTEUR OPTIQUE;FIBRE OPTIQUE; CERAMIQUE PIEZOELECTRIQUE;STRUCTURE SPATIONEF;COQUE SOUS MARIN; SYSTEME AEROSPATIAL
MATERIAU INTELLIGENT*;CONTROLE ACTIF*;DETECTION FISSURE;ACTUATEUR; MESURE DEFORMATION;MEMOIRE FORME

C-91-016489
Chapitre 6 : matériaux techniques.Section A : **structures** **intelligentes**.
Chapter 6 : engineered materials.Section A : intelligent structures.
17th annual review of progress in quantitative nondestructive-evoluation.
LA JOLLA (US)
1990/07/15-1990/07/20
THOMPSON D. O.; CHIMENTI D. E.
Iowa state univ.(US);John Hopkins univ.(US)
Memoire Congres
ENG
US
Plenum press, New York (US)
VOL 10B; pp. 1231-1280; 44 Ref.; 46 Fig.; DP. 1991
0-306-43903-4
05; 459/10B
6 communications concernant : détection et mesures par fibre optique encastrée de déformations et températures élevées, dommages et déformations dans des composites (kevlar-époxy d'applications aéronautiques) : capteur FORRCS à fibre optique en cavité résonante haute fréquence, pour la mesure de déformations (de préimprégnés graphite-époxy);nouveau transducteur flexible à fibre optique (en serpentine) pour application à des **structures** **intelligentes**;contrôle du durcissement de composites (panneaux graphite-époxy AS4/3501-6 d'applications aéronautiques) par guide-ondes acoustiques multiples;le concept de détection de dommages dans le cas de **structures** **intelligentes** (d'aéronefs).
INFO/DS
14 02; 20 06
ESSAI NON DESTRUCTIF*;FIBRE OPTIQUE*;MESURE TEMPERATURE;CAVITE FABRY PEROT;CAVITE RESONNANTE;RESONATEUR OPTIQUE;COMPOSITE MATRICE EPOXY;PLASTIQUE RENFORCE GRAPHITE;STRUCTURE AERONEF;PANNEAU AVION; FATIGUE STRUCTURE;INTERFEROMETRE MICHELSON;GUIDE ONDE ACOUSTIQUE MATERIAU INTELLIGENT*;MESURE DEFORMATION;INTERFEROMETRE FABRY PEROT;INTERFEROMETRE LASER;ENDOMMAGEMENT MATERIAU;DELAMINAGE; KEVLAR MATERIAU;CONTROLE PROCESSUS;DETECTION FISSURE

C-91-003246
Structures **intelligentes** pour **hélicoptères**.
Smart **structures** for helicopters.
16 th european rotorcraft forum.
Glasgow, GB
1990/09/18-1990/09/20
HANAGUD S.; BABU G. L.; WON C. C.; OBAL M. B.
Georgia Inst.of Technol.(US);Georgia Inst.of Technol.(US);Georgia Inst.of Technol.(US);Georgia Inst.of Technol.(US)
Memoire Congres
ENG
US
Royal aeronautical society, Londres
VOL 1; pp. II-4-4-1-II-4-4-11; 59 Ref.; 11 Fig.; 2 Tabl.; DP. 1990
0-903-40969-0
05; M5938
On discute les applications de concepts de ce type de structures aux aéronefs à voilure tournante.Les définitions des **structures** **intelligentes**, adaptatives sont données et leur application à la suppressions des vibrations, le monitorage de la santé des structures et les possibles améliorations de leurs performances sont présentés.Les capteurs et les actuateurs disponibles et leur application à un problème spécifique de monitorage de santé et à un problème spécifique de contrôle de vibrations par utilisation du concept de structure adaptative sont présentés.
INFO/RO
01 03
HELICOPTERE*;EQUIPEMENT AERONEF*;STRUCTURE AERONEF*;AMORTISSEMENT VIBRATION;CAPTEUR MESURE;PERFORMANCE MATERIEL;CERAMIQUE PIEZOELECTRIQUE;ELECTROSTRICTION;MEMOIRE FORME
CONTROLE ACTIF*;COMMANDE ADAPTATIVE*;MONITORAGE;DETECTION FISSURE; ENTRETIEN MAINTENANCE AERONEF;INNOVATION TECHNOLOGIQUE;ACTUATEUR

C-90-010711
Les revêtements intelligents : une carte de leur développement.
Smart skins- A development roadmap.
Fiber Optic **Smart** **Structures** and Skins II.
Boston (US)
1989/09/05-1989/09/08
LOCHOCKI J. M.
Arvin/Calspan Advanced Technology Center-BUFFALO (US)
Memoire Congres
ENG
US
Proceedings of the Spie (US)
SPIE, Bellingham
VOL 1170; pp. 19-47; 22 Ref.; 4 Fig.; 1 Tabl.; DP. 1990
PSISDG
05; Me 10628/1170
Le présent article traite de l'initiative PT-16 (Revêtements intelligents) du projet FORECAST II de l'US Air Force.Il introduit brièvement le concept de revêtement intelligent en soulignant ses caractéristiques et avantages potentiels par rapport aux normes du conditionnement et de la maintenance de l'avionique, puis il décrit quelques uns des ingrédients principaux nécessaires à son développement.Les domaines à problèmes sont signalés ainsi que les compromis indispensables.Une exquisse de développement dans le temps est présentée qui propose une séquence de programmes de développement de cette technologie : premières mises en oeuvre fonctionnelles ponctuelles fin 1990, mises en oeuvre plus larges de 2000 à 2010, mise en oeuvre d'une structure intelligente intégrale d'**avion** après 2010.
INFO/BR
11 09; 01 02
Matériau intelligent*;Construction aéronautique*;Fibre optique; Avionique;Elément antenne;Réseau antenne;Semiconducteur

C-90-010710
Etude du concept des **structures** **intelligentes**.
Smart **structures** concept study.
Fiber Optic **Smart** **Structures** and Skins II.
Boston (US)
1989/09/05-1990/09/08
GARRET A.; SAFF C. R.
McDonnell Aircraft Cy St Louis (US);McDonnell Aircraft Cy St Louis (US)
Memoire Congres
ENG
US
Proceedings of the Spie (US)
SPIE, Belligham
VOL 1170; pp. 224-229; 4 Fig.; DP. 1990
PSISDG
05; Me 10628/1170
Application du concept de la structure intelligente à l'**avion** chasseur.La discussion traite des questions de survivabilité de la structure au cours du vol et du combat et de l'aptitude de l'**avion** à la maintenance en tant que système d'arme.Le concept de la structure intelligente est prometteur dans ces deux domaines.L'article fournit également des données qui résultent des recherches initiales sur les capteurs à fibres optiques intégrés dans les panneaux composites agglomérés à des éprouvettes d'aluminium.Les capteurs détectent les cas d'impact et mesurent les contraintes.
INFO/BER
11 09; 01 03
Matériau intelligent*;Avion combat*;Impact choc;Contrainte en vol; Fibre optique;Survivabilité matériel

C-90-010445
L'impact des fibres optiques (photonique) sur les **avions** de l'avenir.
The impact of fiber optics (phtonics) on future aircraft.
Fiber Optic **Smart** **Structures** and Skins II.
Boston (US)
1989/09/05-1989/09/08
REICH S.; RITTER C.
Grumman Aircraft Systems Div.BETHPAGE (US);Grumman Aircraft Systems Div.BETHPAGE (US)
Memoire Congres
ENG
US
Proceedings of the Spie (US)
SPIE, Bellingham
VOL 1170; pp. 77-89; 16 Fig.; DP. 1990
PSISDG
05; Me 10628/1170
La tendance moderne à développer une forte intégration entre les différents systèmes d'un aéronef fait apparaître de nouvelles spécifications pour les technologies émergentes, notamment pour la combinaison "photonique-optique intégrée et fibre optique".La méthode intégrée de développement de l'avionique, de ce qui n'est pas avionique et de la cellule de l'**avion** contribue à l'amélioration de l'efficacité de la mission de l'**avion** (grâce aux performances accrues de la fonction mission et des sensibilités associées à savoir fiabilité, disponibilité et capacité de survie).L'article évoque plus particulièrement le rôle de la photonique, de l'optique intégrée et des fibres optiques en matière d'avionique, d'équipement non électronique et de cellule sur les **avions** passés et futures.L'effet de ces nouvelles technologies optiques sur les programmes militaires faisant appel au revêtement intelligent est analysé.
INFO/BR
20 06; 01 03
Fibre optique*;Avionique*;Matériau intelligent;Avion combat Photonique*

C-90-009785
Développement d'un système à fibre optique de détection d'avarie de bord d'attaque d'aile d'**avion**.
Development of a fibre optic damage detection system for an aircraft leading edge.
Fiber Optic **Smart** **Structures** and Skins II.
Boston (US)
1989/09/05-1990/09/08
LE BLANC M.; DUBOIS S.; MCEWEN K.; HOGG D.; PARK B.
University of Toronto (CA);University of Toronto (CA);University of Toronto (CA);University of Toronto (CA);University of Toronto (CA)

Memoire Congres
ENG
CA
Proceedings of the Spie (US)
SPIE, Bellingham
VOL 1170; pp. 196-204; 5 Ref.; 11 Fig.; DP. 1990
PSISDG
05; Me 10628/1170
Le système est basé sur la détection d'une fracture de fibres optiques encastrés dans le bord d'attaque.La configuration du capteur a été déterminée à partir d'essais menés sur de petits éléments.L'article rend compte dela conception et de la construction récente d'un panneau équipé de bord d'attaque d'aile.Il expose les essais qui doivent être effectués en vue de l'évaluation.
INFO/BR
13 12; 20 04
Détection défaut*;Bord attaque*;Aile;Fibre optique;Matériau intelligent

C-90-003047
Etats Unis : Missiles a **guidage** **fibre** optique.
USA : Lenkweffen mit fiber-optischer lenkung (FOG-M).
Rédaction Revue
Publication en série
GER
ZZ
ASMZ (CH)
NO 10; p. 688; 1 Phot.; DP. 1989/10
ASMZAP
0002-5925
05; P1806
Etat d'avancement du développement du missile anti char et autre hélicoptère par les firmes US BOEING-MUGHES.Description, caractéristiques techniques.Emploi dans le cadre de la doctrine FOFA et AIR LAND BATTLE.
INFO/CM
16 04
Missile anti char*;Etats Unis;Etude développement programme; Spécification matériel
Défense anti hélicoptère*;US Army;Bataille aéroterrestre an 2000; FOFA concept

C-87-006047
Restructuration du programme de l'armée de terre américaine d'armes antiaériennes et antichar à technologie FOG-M, missile **guidage** **fibre** optique.
US army implements changes in FOG-M acquisition strategy.
DONNELLY T.
Publication en série
ENG
ZZ
Defense News (US)
VOL 2; NO 8; p. 25; DP. 1987/02/23
DNEW2Z
0884-139X
05; P 2486
Etude analytique de la restructuration du programme de l'armée de terre américaine d'armes antiaériennes et antichar à technologie FOG-M, missile à **guidage** **fibre** optique.
INFO/VZ
16 04
Missile sol air*;Guidage*;Fibre optique*;Missile anti char*; Programme militaire;Force armée Etats Unis;Armée terre
Etude analytique*

C-90-014791
Module de **guidage** miniaturisé basé sur le système GPS.
Miniature GPS-based guidance package.
Advances in techniques and technologies for air vehicle navigation and guidance.
Lisbonne, PT
1989/05/09-1989/05/12
SCOTTS L.; AEIN J.; DOHERTY N.
Darpa, Arlington, US;Rand, Washington, US;Mitre, Bedford, US
Memoire Congres
ENG
US
AGARD (Neuilly sur Seine)
NO CP 455; pp. 26.1-26.18; 10 Ref.; 16 Fig.; 6 Tabl.; DP. 1989/12
9-283-50535-2
02; AGARD-CP-455
Présentation de l'architecture fontionnelle, de la technologie et de l'état actuel de l'ensemble de microcircuits intégrés constituant un mini-récepteur GPS développé dans un programme DARPA.Examen des problèmes technologiques posés par le développement d'un **capteur** gyroscopique à **fibre** **optique**.Etude des problèmes de performances et d'intégration au niveau système (GPS et inertiel).
INFO/CR
17 07; 01 03
Navigation intégrée*;Avionique intégrée*;GPS système navigation; Navigation inertie;Filtre Kalman;Optique fibre;
Microminiaturisation électronique

C-90-014668
Une mise à jour sur le véhicule de neutralisation des mines Pinguin B3 et une vue sur les nouveaux véhicules télécommandés pour contremesures anti-mines.
An update on the Pinguin B3 mine disposal vehicle and outlook on new ROV's for MCM.
Warship' 89 - International symposium on mine warfare and vessels 2.
London, GB
1989/05/08-1989/05/10
GEHRKE P.; SCHOLZ H.
MBB Mar.and Spec.Prod.(DE);MBB Mar.and Spec.Prod.(DE)
RINA (GB)
Memoire Congres
ENG
DE
RINA, London
VOL 1; NO 14; 18 p.; 6 Fig.; 2 Phot.; Discussion vol. 3, pp. 33-34; DP. 1989
20; 90-150 STCAN/BIB
Description et caractéristiques de la version actuelle du véhicule de neutralisation des mines Pinguin B3, conçu et réalisé par le constructeur allemand MBB : structure du véhicule sous marin, système de propulsion, alimentation électrique, équipement électronique de **guidage**/commande/transmission de données, **senseurs** (caméra et sonar), liaison par **fibre** **optique**, charges de neutralisation, console de commande, ensemble portable de commande pour la mise à l'eau et la récupération, treuil, limiteur de mouvements, équipement de transport et manutention.En outre, vue générale sur les nouveaux véhicules sous marins télécommandés utilisables pour les contremesures anti-mines.
INFO/LV
13 10; 19 01
Véhicule sous marin*;Neutralisation mine*;Mine navale;Mine sous marine;Guerre mine navale;Chasse mine;République Fédérale Allemande
Véhicule téléguidé

C-90-003851
Interfaces sensorielles pour systèmes de télérobotique.
Sensory interfaces to telerobotic systems.
Sensor fusion : spatial reasoning and scene interpretation.
Cambridge, US
1988/11/07-1988/11/09
Spie (us)
Mémoire Congrès
ENG
US
Proceedings of SPIE (US)
SPIE (Bellingham)
NO 1003; pp. 386-430; 99 Ref.; 28 Fig.; 10 Phot.; 5 mémoires; DP. 1989
PSISDG
0-819-40038-6
05; Me 10628/1003
Présentation du concept de "fenêtre virtuelle" et de son application à la télécommande de robot.Etude de la modélisation et de la reconnaissance de terrain pour un véhicule terrestre autonome (contrat US-DACA76-85-C-0005).Description d'un système de diagnostic d'erreur et de défaillances dans les déplacements d'un robot autonome.Approche, par fusion de données, de la détection et de l'identification d'obstacle.Application de l'**optique** à **fibre** au développement de systèmes de **capteurs** pour robots intelligents.
INFO/CR
17 07; 06 04
Guidage par télécommande*;Intelligence artificielle*;Robot*; Intégration information;Optique fibre;Besoin militaire;Véhicule terrestre;Commande automatique machine outil;Capteur optique; Perception espace
Vision artificielle;Vision objet mobile;Capteur multiple;Autonomie matériel;Automatisme industriel

C-89-008985
Conception optomécanique et électro-optique de systèmes industriels.
Optomechanical and electro-optical design of industrial systems.
DEABORN (US)
1988/06/28-1988/06/29
Spie (us)
Congrès
ENG
US
Proceedings SPIE (US)
Spie, bellingham
VOL 959; 267 p.; NB Ref.; NB Fig.; 16 communications; DP. 1988
PSISDG
0-892-52994-6
05; ME 10628
Conception d'un instrument optique résistant.Montures compliantes pour éléments optiques à haute résolution.Mouvement de balayage : considération optomécaniques.**Capteurs** optiques pour environnements hostiles.**Capteurs** à **fibre** **optique**.Caméras pour le milieu industriel.La vision en environnement hostile.Système optique pour **guidage** de robot.Mesures répétitives de déplacement inférieur au micron sur les machines outil de précision par interférométrie laser.Système à balayage laser 3-D de haute précision.Etalonnage optique de haute précision.
INFO/BC
13 09; 20 06
Equipement industriel*;Systeme optique*;Instrument optique*; Support montage;Balayage mecanique;Capteur optique;Dispositif

charge couplee;Etalonnage
Environnement industriel;Environnement hostile;Camera video;Mesure deplacement;Robotique;Interferometrie laser

C-88-016554
Fibres acoustiques.
Acoustic fibers.
IEEE 1987 Ultrasonics Symposium.
Denver, Etats-Unis (US)
1987/10/14-1987/10/16
JEN C. K.
Ind.Mater.Res.Inst., Boucherville, CA
IEEE Ultrasonics Ferroelectric and Frequency Control Society (US)
Mémoire Congrès
ENG
CA
IEEE, New York
VOL 1; NO 87CH2492-7; pp. 443-454; 51 Ref.; 17 Fig.; 3 Tabl.; 15 Phot.; DP. 1987
05; ME 349-23
Les fibres acoustiques sont des candidats potentiels pour le développement des **senseurs** et des dispositifs de taitement de signal.Présentation de considérations relatives aux propriétés des matériaux, en particulier les verres à silice fondue, aux méthodes de caractérisation, à la polarisation des ondes acoustiques guidées, à la fabrication des fibres, aux transducteurs, aux techniques de couplage et aux géométries de **senseurs**.Vue sur la théories des fibres à **guidage** faible et les analogies entre fibres acoustiques et **fibres** **optiques**.
INFO/LV
20 01; 11 05
Matériel acoustique*;Fibre*;Traitement signal;Verre silice;Capteur Fibre acoustique*;Senseur;Ligne retard électrosonique

C-88-011211
Phénomènes de **guidage** d'ondes.
Guided wave phenomena.
Integrated optical circuit engineering V.
San Diego (US)
1987/08/17-1987/08/20
Spie (us)
Mémoire Congrès
ENG
US
Proceedings SPIE (US)
SPIE, Bellingham
VOL 835; pp. 18-38; nombr. Ref.; nombr. Fig.; 4 communications; DP. 1988
PSISDG
0-892-52870-2
05; Me 10628
Phénomènes de couplage et d'absorption dans les guides d'ondes optiques diélectriques enrobés de semiconducteur.Une nouvelle méthode de mesure, des pertes de propagation dans les guides d'ondes.Pertes de propagation dans les guides d'ondes films minces.Coupleurs pour **capteurs** à **fibres** **optiques**.
INFO/GD
20 06
Guide onde optique*;Mesure;Perte optique;Perte transmission;Couplage optique;Fibre optique;Film mince;Optique intégrée;Capteur optique
Guide onde diélectrique;Coupleur directif

C-86-F01590
Récentes percées technologiques et surestimation des armements.
LANGEREUX P.
Publication en série
FRE
ZZ
Air et Cosmos
NO 1080; pp. 38-39; DP. 1986/01/25
ACOSB5
0044-6971
05; P 0948
L'escalade technologique, les procédés spectaculaires en électronique, automatique et informatique tendent à masquer les progrés accomplis dans les matériaux composites, les **fibres** **optiques**, le spectre des fréquences accessibles aux **capteurs** de détection et de **guidage**, les gyromètres à laser, les munitions intelligentes.Mais on oublie le besoin de sommeil des combattants, les balbutiements dans la reconnaissance des formes, la difficulté à espérer le bon fonctionnement de systèmes d'armes complexes avec intégration et coordination en temps réel à des niveaux de commandement différents, dans les conditions dynamiques du combat ce sont les conclusions premières du colloque sur "les nouvelles technologies et la défense de l'Europe : une nouvelle conception du champ de bataille" tenu à Paris en janvier 1986 (CEPS, UEO, CHEAR).
INFO/VZ
19 04; 15 07
Armement matériel*;Stratégie militaire*;Tactique militaire*;International;Complexité;Intégration information;Reconnaissance forme;Facteur humain
Développement technologique*;Aptitude opérationnelle armée;Fonctionnement temps réel

C-85-002412
Alignement optique.
Optical alignment.
Arlington, US
1984/05/03-1984/05/04
RUDA M. C.
Talandic Res.Corp.(US)
The Soc.of Photooptical Instrum.Eng.(US)
Congrès
ENG
US
SPIE Conference Proceedings (US)
SPIE, Washington D.C.
VOL 483; NO 2; 140 p.; nombr. Ref.; nombr. Fig.; nombr. Tabl.; nombr. Phot.; DP. 1984
SPIECJ
0-892-52518-5
0361-0748
08; TLSE NO SPIE 483, MD(Me 10628)
TLSE NO 555
Recueil de 20 articles traitant principalement des grilles de diffraction, de l'alignement optique de trois longueurs d'onde dans le laser NOVA, de la fabrication des systèmes optiques, de la mesure de la déflexion d'un multidétecteur, des systèmes à alignement tels les télescopes à alignement infrarouge, de l'alignement actif, des **fibres** **optiques**, des composants en **guidage** optique ainsi que des techniques d'alignement dans les périscopes, les lentilles de précision et la technologie des **capteurs** LMSC.
TLSE/BML
20 06
Système optique*;Alignement*;Diffraction onde;Laser;Système optique infrarouge;Fibre optique;Guide onde optique;Périscope;Lentille;Télescope infrarouge
Fibre optique multimode;Guidage optique

C-82-F05578
Horizons de l'Optique 82.Comité français l'Optique.Grenoble 17-19 Mars 1982.
Institut National Polytechnique de Grenoble.
Congrès
FRE
ZZ
Institut National Polytechnique Grenoble (FR)
NO 82/1058 (03/1982), 73 P.; NBR réf. , NBR fig., NBR tabl., NBR phot. Grenoble 17-19 Mars 1982
05; M 5982
2006
L'optique des impulsions ultracourtes: transmission d'image, génération, interférométrie, réflectométrie.Surfaces asphériques: intérêt, usinage, utilisation.Optique infrarouge et U.V.Optique spatiale laser bifréquence et métrologie optique.Traitement du signal optique: **capteurs** à **fibres** **optiques**.Transmission d'images bidimentionnelles, optique non linéaire, **guidage** optique à la surface de substrats.
CNIT/CP
20 06
Système optique*;Lentille asphérique*;Traitement signal*;Congrès*;Transmission image;Interférométrie;Laser;Métrologie;Fibre optique;Capteur optique;Guide onde optique
Impulsion optique*;Impulsion ultra courte;Infrarouge;Optique non linéaire;Guidage optique;1982 année;Grenoble congrès

AD-A225 541/2/XAD
Proceedings of the 1989 Structural Integrity Program Conference Held in San Antonio, Texas on 5-7 December 1989.
COOPER T. D.; LINCOLN J. W.
Wright Research and Development Center, Wright-Patterson AFB, OH.
094951000; 420153
Report
ENG
US
WRDC-TR-90-4051
Final rept. 5 Dec-7 Dec 89; Availability: Document partially illegible; NP. 1033; DP. Apr 90.
U9024
NTIS Prices: PC A99/MF E09
2418
07
The purpose of this conference was to bring together technical personnel in DOD and the aerospace industry involved in the various turbine engines, airframes and other mechanical systems.It provided a forum to exchange ideas relating to the critical aspects of durability and damage tolerance technology for **aircraft** systems.Session topics included: Structural analysis;Structural analysis and testing;Materials and nondestructive evaluation;ENSIP;and Force management.
51 03; 81 04
Jet engines*;Jet aircraft*;Airframes*;Symposia*;Structural components*;Damage;Risk;Aircraft industry;Life expectancy Service life;Probability;Tolerances Mechanics;Structural analysis;Test methods;Nondestructive testing;Aging Materials;Aircraft equipment;Fatigue Mechanics;Cracks;Fatigue tests Mechanics;Repair;Finite element analysis;Jet transport aircraft;Jet bombers;Attack bombers;Jet training aircraft;Jet fighters;Jet engine nacelles;Wings;Spars Aluminum alloys*;Titanium alloys*;Meetings*;ENSIP Engine Structural Integrity Program;Damage tolerance;C 141 Aircraft;B 1 Aircraft;Smart structures;T 38 Aircraft;F 16 Aircraft;F 15 Aircraft;Durability;A 10 Aircraft;Tails Aircraft;Flight loads;

Structural integrity;Composite materials;Inspection;Reliability;
NTISDODXA

AD-A209 422/5/XAD
Hierarchical Damage Tolerant Controllers for **Smart**
Structures.
CAGLAYAN A. K.; ALLEN S. M.; EDWARDS S. J.
Charles River Analytics, Inc., Cambridge, MA.
Air Force Wright Aeronautical Labs., Wright-Patterson AFB, OH.
084097000; 398060
Report
ENG
US
Final rept. Jun-Dec 88; NP. 68; DP. Mar 89.
U8920
NTIS Prices: PC A04/MF A01
F33615-88-C-3212
3005
40
AFWAL-TR-89-3009
This report summarizes the research and development results of the SBIR Phase I study entitled Hierarchical Damage Tolerant Controllers for **Smart** **Structures** supported by U.S.Air Force under Contract No.F33615-88-C-3212.The major aim of this study is the investigation and definition of a baseline architecture for a smart aerospace structure which can detect and isolate structural damage in real-time and provide on-line reconfiguration of the structure's control system under the detected impairment conditions.In particular, we investigate how a smart aerospace structure can be implemented as a real-time knowledge based expert system by addressing issues involved with structural knowledge representation, structural damage detection and isolation strategies and real-time performance in an embedded environment.Keywords: Damage assessment;Damage control;Space vehicles;**Aircraft**;Flight controls;Sensors.(kt).
84 07; 84 02
Aerospacecraft*;Damage control*;Spacecraft*;Air Force;Aircraft; Architecture;Base lines;Computer programs;Control systems;Damage; Damage assessment;Detection;Detectors;Embedding;Environments; Flight control systems;Isolation;Real time;Strategy;Structures
Smart structures*;Damage tolerence*;NTISDODXA;NTISDODAF

AD-A241 728/5/XAD
Qualification Testing of a Diode-Laser Transmitter for Free-Space **Coherent** **Communications**.
PILLSBURY A. D.; TAYLOR J. A.
Massachusetts Inst.of Tech., Lexington.Lincoln Lab.
Electronic Systems Div., Hanscom AFB, MA.
009875001; 207650
Report
ENG
US
TR-922
Technical rept; NP. 27; DP. 23 Jul 91.
U9203
NTIS Prices: PC A03/MF A01
F19628-90-C-0002
ESD-TR-91-067
A diode-laser transmitter designed for space-based **coherent** **communications** has been successfully space qualified.Environmental testing, which consisted of random vibration at levels up to 16.2 g rms and thermal cycling over the range of -30 to 66 C, caused no significant degradation in the performance of the transmitter.Principal design issues and the qualification process of subassemblies and the complete transmitter are described.
45 03; 46 03; 46 04; 84 07
Coherence;Communication and radio systems;Cycles;Degradation; Environmental tests;Heating;Qualifications;Random vibration;Space based
Laser communications*;Communication satellites*;Gallium aluminum arsenide;Laser diodes;Laser transmitters;Lite project;NTISDODXA; NTISDODAF

AD-A227 942/0/XAD
1/F Frequency Noise Effects on Self-Heterodyne Linewidth Measurements for **Coherent** **Communications**.
MERCER L. B.
Massachusetts Inst.of Tech., Lexington.Lincoln Lab.
Electronic Systems Div., Hanscom AFB, MA.
009875001; 207650
Report
ENG
US
TR-881
Technical rept; NP. 32; DP. 31 Jul 90.
U9109
NTIS Prices: PC A03/MF A01
F19628-90-C-0002
ESD-TR-90-011
The effects of 1/f frequency noise on self-heterodyne detection are described and the results are applied to the problem of laser-diode-linewidth measurement.Laser diode linewidths determined by self-heterodyne methods are not adequate predictors of **coherent** **communications** system performance because the measurements often include significant broadening due to 1/f frequency noise.In this report, the autorcorrelation function and power spectrum of the detected self-heterodyne photocurrent are developed in terms of an arbitrary frequency noise.From numerical analysis, the power spectrum resulting from the 1/f frequency noise is shown to be approximately Gaussian and an empirical expression is given for its linewidth.These results are applied to the problem of self-heterodyne linewidth measurements for coherent optical communications, and the amount of broadening due to 1/f frequency noise is predicted.Two methods are then provided for estimating the portion of the measured self-heterodyne linewidth due to the white component of the frequency noise and the portion due to 1/f frequency noise.(rh).
45 03
Communication and radio systems*;Noise*;Optical communications*; Coherence;Diodes;Frequency;Lasers;Numerical analysis;Power spectra; Predictions
NTISDODXA;NTISDODAF

PB91-134106
Modulatable Narrow-Linewidth Semiconductor Lasers.
HOLLBERG L.; OHTSU M.
National Bureau of Standards (NML), Boulder, CO.Time and Frequency Div.
081416003
Report
ENG
US
Final rept; See also PB88-239470; Pub. in Applied Physics Letters 53, n11 p944-946 Sep 88; NP. 3; DP. 1988.
U9107
NTIS Prices: Not available NTIS
The authors found that using the technique of optical feedback locking, to narrow semiconductor linewidths, does not sacrifice the ability to modulate the laser's frequency via the injection current.The frequency of a laser is stabilized to a separate Fabry-Perot reference cavity using resonant optical feedback and can be modulated efficiently at frequencies related by rational fractions to the free-spectral range of the reference cavity.This system can provide an array of narrow-linewidth, frequency-stable laser lines and shows promise for applications in frequency-division-multiplexed **coherent** **communications**, as well as laser frequency control and precision measurement systems.Reprint: Modulatable Narrow-Linewidth Semiconductor Lasers.
46 03; 45 03
Semiconductor lasers*;Frequency control;Frequency stability;Line width;Optical communication;Reprints
Frequency division multiplexing;Line narrowing;NTISCOMNBS

N90-26306/2/XAD
Solid-State Lasers for Coherent Communication and Remote Sensing.
BYER R. L.
Stanford Univ., CA.
National Aeronautics and Space Administration, Washington, DC.
009225000; S0380476
Report
ENG
US
NAS 1.26:186634
Semiannual Progress Report, 1 Oct. 1989 - 31 Mar. 1990; NP. 54; DP. Jun 90.
S2820
NTIS Prices: PC A04/MF A01
NAGW-1760
NASA-CR-186634
Laser development, high efficiency, high power second harmonic generation, operation of optical parametric oscillators for wavelength diversity and tunability, and studies in **coherent** **communications** are reviewed.
46 03; 45 02; 49 05
Solid state lasers*;Communication;Parametric amplifiers;Remote sensing;Harmonic generations;Laser outputs
Optical communication;Second harmonic generation;Parametric oscillators;NTISNASA

AD-D014 479/0/XAD
Adaptive Polarization Diversity Detection Scheme for **Coherent** **Communications** and Interferometric Fiber Sensors.
KERSEY A. D.; MARRONE M. J.; DANDRIGE A.
Department of the Navy, Washington, DC.
001840000; 110050
Patent Application
ENG
US
Patent Application; This Government-owned invention available for U.S. licensing and, possibly, for foreign licensing. Copy of application available NTIS; NP. 32.
U9013
NTIS Prices: PC N03/MF A01
Filed 2 Feb 90;PAT-APPL-7-473 807
Mixing between a reference signal and a data signal is often necessary to extract information from an optical carrier.In communication, the mixing is typically between the received signal and a local oscillator signal at a different frequency.The result is an intermediate frequency (IF) that can be demodulated.In interferometric sensing, the mixing would be between a reference signal and a signal whose phase has been modified by the parameter being measured.The result is an interference signal.In both communication and interferometric sensing, amplitude of the mixed output is dependent upon efficiency of the mixing between the two input optical signals.A method and apparatus for overcoming polarization induced signal fading in both heterodyne

communication and interferometric sensing is disclosed.An adjustable birefringent element in series with a linear-polarization beam splitter forms an elliptical-polarization beam splitter.The birefringent element controllably evolves the states of polarization of two input signals thereby controlling the power contribution of each signal onto the orthogonal axes used by the linear beam splitter.When the states of polarization are evolved such that there are equal signals to reference power ratios on the beam splitter axes, subsequent detectors generate a constant, optimum amplitude signal without the need for weighting or decision circuits.Patent applications.(aw).
45 03; 46 08; 90 06
Patent applications*;Polarization*;Signal processing*; Interferometers*;Optical communications*;Amplitude;Axes;Beam splitting;Birefringence;Circuits;Data transmission systems; Decision making;Detection;Detectors;Efficiency;Fiber optics; Heterodyning;Input;Interference;Interferometry;Intermediate frequencies;Linear systems;Local oscillators;Mixing;Optical properties;Optimization;Orthogonality;Output;Power;Ratios;Coherent optical radiation
NTISGPN

NTN89-0626
Advanced Components for Fiber-Optical Systems: This concise review emphasizes highly birefringent fibers, couplers, and polarizers.
National Aeronautics and Space Administration, Washington, DC.
011249000
Report
ENG
US
NTIS Tech Note; FOR ADDITIONAL INFORMATION: Contact: NASA Technology Transfer Div., PO Box 8757 BWI Airport, MD 21240; (301) 621-0100 ext 241. Refer to NPO-17080/TN; NP. 1; DP. Aug 89.
D8922
NTIS Prices: Not Available NTIS
This citation summarizes a one-page announcement of technology available for utilization.A paper reviews the statuses of some advanced passive and active optical components for use with optical fibers.The emphasis is on highly birefringent components that control polarization, because the control of polarization is critical in such applications as fiber-optical gyroscopes, interferometric sensors, and **coherent** **communications**.The classes of passive components reviewed include highly birefringent fibers, coupler-based devices, and polarizers.Birefringent fibers have elliptical, stressed, cut, or otherwise non-circularly-symmetrical cores that maintain polarization.Such fibers are expensive (> $10/m) but perform well in that cross-coupling to the undesired polarization is typically less than .005 (km)-1.The coupler-based components include polished and fused single-mode couplers, special items that perform at several wave-lengths, arrays of high uniformity, and units made partly of highly birefringent fibers.Some of these devices couple both polarizations to the same degree, while others have been built to couple primarily one polarization, thus acting analogously to polarizing beam splitters.The active components of interest include piezoelectric transducers that indirectly produce optoelectronic or electro-optical effects to modulate phase, frequency, or polarization.Typically, a piezoelectric device surrounds a fiber and constricts it when an electrical signal is applied.The constriction gives rise to the birefringence that modulates the light traveling along the fiber.
49 05; 46 03; 45 03
Optical measuring instruments*;Fiber optics*
Optoelectronic devices*;Optical fibers*;NTISNTND

AD-A209 737/6/XAD
Theory of Multi-Frequency Modulation (MFM) Digital Communications.
MOOSE P. H.
Naval Postgraduate School, Monterey, CA.
019895000; 251450
Report
ENG
US
NPS-62-89-019
Interim rept. Oct 88-Mar 89; NP. 44; DP. 5 May 89.
U8921
NTIS Prices: PC A03/MF A01
Multi-frequency modulation (MFM) is a new digital signal processing (DSP) oriented communications signal developed at NPS specifically for computer-to-computer communications links and information exchange networks.MFM utilizes the hardware and software of the host computers to generate and to demodulate **coherent** **communications** discrete time signals.In this report, the theory behind MFM generation and reception is presented.Auto-correlation functions and power spectral densities of MFM signals are derived and examples presented for lowpass and bandpass white MFM sequences.The bit error rates are computed for three types of MFM: MFBPSK, MFQPSK and MF16-QAM.These modulation formats provide one, two and four bits per Hz of channel bandwidth respectively.Optimization arguments show that best system performance is obtained by using the maximum possible number of tones with the limit on the number of tones being set either by the packet length or the coherence time of the channel, whichever is shorter.(RH).
45 03; 46 08
Communications networks*;Digital communications*;Host computers*; Audio tones;Autocorrelation;Coherence;Communication and radio systems;Computer programs;Digital systems;Errors;Information exchange;Power spectra;Signal processing;Spectral energy distribution;Theory
Frequency modulation*;NTISDODXA

AD-D013 842/0/XAD
Method and Apparatus for Overcoming Polarization-Induced Signal Fading in Optical-Fiber **Coherent** **Communications**.
KERSEY A.
Department of the Navy, Washington, DC.
001840000; 110050
Patent Application
ENG
US
Patent Application; This Government-owned invention available for U.S. licensing and, possibly, for foreign licensing. Copy of application available NTIS; NP. 15.
U8824
NTIS Prices: PC A03/MF A01
Filed 31 May 88;PAT-APPL-7-200 267
A method and apparatus is disclosed for overcoming the polarization-induced signal fading problem in coherent heterodyne systems by mixing the incoming signal light with orthogonal local oscillator polarization modes which have been separated in the optical frequency domain to produce a composite beam, photodetecting the heterodyne mixing between this composite beam and the received signal light to produce first and second intermediate frequency signals, separately filtering and demodulating each of the first and second intermediate frequency signals to provide first and second demodulated signals, and combining the first and second demodulated signals to produce a non-fading output signal.
45 03; 90 06
Demodulation*;Patent applications*;Heterodyning;Light;Mixing; Signals
Optical communication*;Signal fading;Polarization;Optical fibers; NTISGPN

AD-A163 169/6/XAD
Optical Fiber Communication System Based on Coherent Modulation.Part 2.
JACOBSEN G.
Technical Univ.of Denmark, Lyngby.Inst.of Electromagnetics.
014560013; 397671
Report
ENG
DK
Final technical rept. Apr-Jul 85; See also Part 1, AD-A163 168; Availability: Microfiche copies only; NP. 109P; DP. Jun 85.
U8609
NTIS Prices: MF A01
DAJA37-82-C-0735
1T161102BH57
07
Contents: Phase Delay between Intensity and Frequency Modulation of a Semiconductor Laser (Including a New Measurement Method);Spectral Behaviour of a Directly Current-Modulated CSP Laser;A Theoretical and Experimental Analysis of Modulated Laser Fields and Power Spectra;Current/Frequency-Modulation Characteristics for Directly Optical Frequency-Modulated Injection Lasers at 830 nm and 1.3 micrometers;Optical Phase Modulation and Homodyne Detection using an Injection Locked Laser Transmitter;Frequency Stabilization of Singlemode Semiconductor Lasers at 830 nm and 1.3 micrometers;Light Intensity Pulsations in an Injection Locked Semiconductor Laser;The Influence of Asymmetric Locking Characteristics on the Coherent Modulation Behaviour of an Injection Locked Semiconductor Laser;New Approach towards Frequency Stabilisation of Linewidth-Narrowed Semiconductor Lasers;Locking Conditions and Stability Properties for a Semiconductor Laser with External Light Injection;Simple theory of Optical Dual-Filter Heterodyne FSK Receivers with Non-Negligible (Semiconductor) Laser Linewidths;Error-rate Floor in Optical ASK Heterodyne Systems Caused by Nonzero (Semiconductor) Laser Linewidth;Influence of (Semiconductor) Laser Linewidth on the Error-Rate Floor in Dual-Filter Optical FSK Receivers;Overview of **Coherent** **Communications** - Applications and Perspectives.
17 02; 45 03
Laser communications*;Semiconductor lasers;Heterodyning;Fiber optics transmission lines
Optical communications*;NTISDODXA;NTISFNDA

AD-A156 954/0/XAD
Performance of Coherent Multilevel Digital Communications Receivers in the Presence of Noise and Jamming.
VILA A. J. M.
Naval Postgraduate School, Monterey, CA.
019895000; 251450
Thesis
ENG
US
Master's thesis; NP. 56P; DP. Mar 85.
U8522
NTIS Prices: PC A04/MF A01
The effect of jamming waveforms on optimum multilevel digital **coherent** **communications** receivers designed to operate in a Gaussian noise only environment is analyzed and evaluated in terms of receiver performance.Near optimum jamming wave-forms (such as a

tone jammer and a weighted sum of signals jammer) are postulated in order to determine their effect on the performance of an M-ary Phase Shift Keying coherent receiver.Additionally, the optimum power constrained jamming waveform is derived and analyzed for an M-ary Amplitude Shift Keying coherent receiver.Graphical results of numerical analyses resulting from the evaluation of receiver performance are presented and interpreted in order to quantify the effectiveness of the jammers.Receiver Performance is measured in terms of word error probability as a function of signal-to-noise ratio.Keywords include: Effect of jamming waveforms on performance of optimum multilevel digital **coherent** **communications** receivers..
17 04; 09 04; 17 02; 63 02; 45 02; 45 07
Receivers*;Communication equipment*;Jamming*;Coherence;Digital systems;Functions;Signal to noise ratio;Waveforms;Optimization; Numerical analysis;Signals;Digital communications;Receivers; Environments;Noise;Power
NTISDODXA

EIM-91-034504
Fiber optics in liquid propellant rocket engine environments.
Fiber Optic Systems for Mobile Platforms IV
San Jose, CA, USA
1990 Sep 18
14623
DELCHER R.; DINNSEN D.; BARKHOUDARIAN S.
Rockwell Intl, Canoga Park, CA, USA
SPIE
ENG
US
Proceedings of SPIE - The International Society for Optical Engineering
Int Soc for Optical Engineering, Bellingham, WA, USA.
VOL. 1369; PP. 114-120; DP. 1991
9107
PSISDG
0277-786X
Fiber optics have recently been seen to offer several major benefits in liquid-fuel rocket engine applications.**Fiber**-**optic** **sensors** can provide measurements that cannot be made with conventional techniques.Fiber optics also can reduce harness weight, provide lightning immunity, and increase frequency response.This paper discusses the results of feasibility testing optical fibers in simulated liquid-fuel rocket engine environments.The environments included cryogenic and high temperatures, and high vibration levels.(Author abstract)
741; 654; 652
FIBER OPTICS*;Measurements*;Liquid Fuels;Rocket Engines ; Vibrations;Rockets And Missiles ;Cryogenic Equipment

EIM-91-033589
Fiber optic smart structures.Structures that see the light.
Optical Testing and Metrology III: Recent Advances in Industrial Optical Inspection
San Diego, CA, USA
1990 Jul 8-13
14586
MEASURES R. M.
Univ of Toronto Inst for Aerospace Studies, Downsview, Ont, Can
SPIE
ENG
CA
Proceedings of SPIE - The International Society for Optical Engineering
Int Soc for Optical Engineering, Bellingham, WA, USA.
VOL. 1332; PART. 1; PP. 377-398; DP. 1990
9107
PSISDG
0277-786X
The development of Fiber Optic Smart Structures Technology offers the promise of undertaking 'real-time' structural measurements with built-in sensor systems.This new technology could avoid many of the mechanical failures that today result in death, injury or environmental accidents.Eventually it could lead to radical new thinking in terms of engineering and structural integrity monitoring.An overview of this new field will be given with particular reference to our development and characterization of a number of **fiber** **optic** **sensors** for use as optical strain gauges.This includes: the development and testing of a fiber optic strain rosette for mapping two dimensional strain fields;the measurements of strain fields within composites, and the demonstration of damage detection within composites by means of embedded optical fiber sensors.The first results of impact damage detection by a multilayered fiber optic grid fabricated within an **aircraft** wing leading edge constructed of composite material, will also be revealed.(Author abstract)
741; 941
FIBER OPTICS*;Research*;Optical Systems ;Applications
Fiber optic smart structures technology;Structural integrity monitoring;Multilayered fiber optic grids;Fiber optic strain rosettes;Strain field measurements;Aircraft wing leading edges

EIM-91-029730
Application of analog fiber optic position sensors to flight control systems.
Fiber Optic and Laser Sensors VIII
San Jose, CA, USA
1990 Sep 17-19
14621
MILLER G. E.
Boeing Aerospace and Electronics High Technology Cent, Seattle, WA, USA
SPIE
ENG
US
Proceedings of SPIE - The International Society for Optical Engineering
Int Soc for Optical Engineering, Bellingham, WA, USA.
VOL. 1367; PP. 165-173; 23 Ref.; DP. 1991
9106
PSISDG
0277-786X
Sensors of one form or another are invariably required for interpreting pilot commands and for generating necessary servo position feedback information in the flight control systems of all high-performance **aircraft**, both military and commercial.Most of the recently-developed flight control systems have been designed around electrical analog principles, and have incorporated time-proven electrical analog position sensors such as the resolver and the LVDT.However, with fiber optics gaining maturity, and with confidence developing in that technology, it has become apparent that flight control systems could gain a much higher degree of EMI/EMP immunity if the electrical control wiring were replaced with glass fibers, and if the electrical sensors were replaced with electrically-passive optical sensors.These sensors could also offer the unique option of being inherently either analog or digital.The new technology has even made it possible for the first time to seriously consider flight control systems in which all control interconnects and sensors might be inherently digital and non-electrical.This paper addresses the relative advantages and disadvantages of both analog and digital **fiber** **optic** **sensors** as they apply to flight controls.It also describes a novel analog position sensor which corrects several of the deficiencies commonly associated with fiber optic analog sensors.(Author abstract)
741; 652; 632; 672; 943
SENSORS*;Applications*;Aircraft ;Control Equipment;Optical Fibers ; Applications;Mechanical Variables Measurement ;Position
Analog fiber optic position sensors;Flight control systems;In line monitoring

EIM-91-014960
Fiber **optic** **sensor** advances pertinent to smart structure development.
Fibre Optics '90
London, Engl
1990 Apr 24-26
13914
MEASURES R. M.
Univ of Toronto Inst for Aerospace Studies, Downsview, Ont, Can
Inst of Measurement Control (UK);Inst of Physics (UK);Optical Sensors Collaborative Assoc (UK)
ENG
CA
Proceedings of SPIE - The International Society for Optical Engineering
Int Soc for Optical Engineering, Bellingham, WA, USA.
VOL. 1314; PP. 255-261; 14 Ref.; DP. 1990
9104
PSISDG
0-8194-0365-2
0277-786X
Advances in structurally integrated **fiber** **optic** **sensor** technology both for damage assessment within composite materials and for strain mapping will be reported.This will include the results of work on a fiber optic test system imbedded within a full scale **aircraft** wing leading edge and the development of compact all-fibre optical strain rosettes for two dimensional strain mapping within composite structures.(Author abstract)
732; 741
SENSORS*;Materials*;Fiber Optics
Strain mapping;Damage assessment

EIM-91-007620
fly by light: fiber optics for **aircraft** communication, control, and sensing.
1990 Optical Fiber Communications Conference - OFC'90
San Francisco, CA, USA
1990 Jan 22-26
13972
LEONBERGER F. J.; GLOMB W. L.; DUNPHY J. R.
United Technol Res Center, East Hartford, CT, USA
IEEE Lasers and Electro-Optics Soc;Optical Soc of America
ENG
US
Technical Digest Series Opt Fiber Commun Conf OFC 90.
Optical Soc of America, Washington, DC, USA .
IEEE cat n 90CH2821-7; PP. 48-49; 7 Ref.; DP. 1990
9102
1-55752-112-3
A number of the architectural, system, and component technologies presently under development for fly-by-light **aircraft** systems are reviewed.Examples of flight test systems as well as research results are given.Of particular interest are flight and engine control architectures.Flight tests have been performed on individual components, including a variety of position

sensors.Component research has focused on both sensors and actuators.In the sensor area; a variety of temperature, pressure, and position sensors is under development.Considerable research is being conducted in the area of distributed **fiber**-**optic** **sensors**.These devices can, in principle, measure the parameter (e.g., temperature) distribution over a large mechanical part via a single fiber circuit.In addition to interferometric and other coherence multiplexing techniques, a recently developed embedded-grating sensor holds much promise for these applications.For a fully-fly-by-light system, it is important to develop an optical actuator.Another optically powered system under development is power by light.In this case, power from an array of high-power diode lasers has been fiber coupled to a set of custom GaAs solar cells to generate remotely approximately 1 W of electrical power.
652; 741; 731; 744; 717
AIRCRAFT COMMUNICATION*;Design*;Optical Fibers;Sensors;Control Systems;Multiplexing;Laser Beams ;Applications
Fly by light aircraft systems;Digest of paper

EIM-90-037434
Autoclave monitoring of composite resin chemistry in laminates with an in-situ fiber optic polymer reaction monitor.
35th International SAMPE Symposium and Exhibition - Advanced Materials: the Challenge for the Next Decade.Part 2
Anaheim, CA, USA
1990 Apr 2-5
13357
DRUY M. A.; ELANDJIAN L.; STEVENSON W. A.
Foster-Miller Inc, Waltham, MA, USA
ENG
US
National SAMPE Symposium and Exhibition (Proceedings) 2.
SAMPE, Covina, CA, USA.
VOL. 35; NO. Book; PP. 1517-1522; 4 Ref.; DP. 1990
9009
NSSED2
0147-9598
The real time in-situ monitoring of the chemical states of epoxy resins were investigated during cure in an autoclave using an embedded **fiber** **optic** **sensor** and a Fourier transform infrared spectrometer (FTIR).In this work a short length of sapphire fiber is used as sensor.The sapphire sensor is connected to infrared transmitting zirconium fluoride optical fiber cables which penetrate the wall of the autoclave and interface to the FTIR spectrometer.The results indicate that this equipment and sensor are suitable for monitoring the degree of cure of the laminate throughout the entire cure cycle.(Author abstract)
817; 815; 732; 415; 652; 802
COMPOSITE MATERIALS*;Processing*;Epoxy Resins ;Monitoring;Sensors ; Fiber Optic Chemical Sensors;Plastics Laminates ;Curing;Aircraft Materials ;Composite Materials;Autoclaves ;Monitoring
Zirconium fluoride;Autoclave monitoring;Composite resin chemistry; In situ fiber optic polymer reaction monitor;Sapphire fiber

EIM-90-020667
Sensor technology for smart structures.
Proceedings of the ISA/89 International Conference and Exhibition: Advances in Instrumentation and Control (Part 1 of 4)
Philadelphia, PA, USA
1989 Oct
13034
ROGOWSKI R. S.; HEYMAN J. S.; HOLBEN M. S.
NASA Langley Research Cent, Hampton, VA, USA
ENG
US
Proc ISA/89 Int Conf Exhib Adv Instrum Control.
ISA Services Inc, Research Triangle Pk, NC, USA.
PP. 27-33; 12 Ref.; DP. 1989
9005
The concept of 'Smart Structures' integrates **fiber** **optic** **sensor** technology with advanced composite materials.The optical fibers are embedded in a composite material and provide internal sensing capability for monitoring parameters which are important for the performance, safety and reliability of the material and the structure.
652; 732; 741; 655
AIRCRAFT*;Control Equipment*;Sensors ;Aerospace Applications;Fiber Optics;Composite Materials;Spacecraft ;Control Equipment
Smart structures;Fiber optic sensor

EIM-89-018451
Overview of nasa research in fiber optics for **aircraft** controls.
Proceedings of the ISA/88 International Conference and Exhibit
Houston, TX, USA
1988 Oct 16-21
12094
SENG G. T.
NASA Lewis Research Cent, Cleveland, OH, USA
ISA, Industries & Sciences Dep Div, Research Triangle Park, NC, USA;ISA, Technology Dep Div, Research Triangle Park, NC, USA;ISA, Education Dep, NC, USA
ENG
US
Advances in Instrumentation, Proceedings
ISA, Research Triangle Pk, NC, USA.
VOL. 43; PART. 2; PP. 855-861; 8 Ref.; DP. 1988
8906
AVINBP
1-55617-139-0
0065-2814
The challenge of those involved in **aircraft** control system hardware development is to accommodate an ever-increasing complexity in **aircraft** control, while limiting the size and weight of the components and improving system reliability.A technology that displays promise towards this end is fiber optics.The advantages of employing optical fibers, passive optical sensors and optically controlled actuators are weight/volume reduction, immunity from electromagnetic effects, high bandwidth capabilities and freedom from short circuits/sparking contacts.Since 1975, NASA/Lewis has been performing in-house, contract and grant research in **fiber** **optic** **sensors**, high temperature electro-optic switches and 'fly-by-light' control system architecture.Passive optical sensor development is a challenging area of work and has received much attention during this period.A major effort to develop fly-by-light control system technology, known as the 'Fiber Optic Control System Integration' (FOCSI) program was initiated in 1985 as a cooperative effort between NASA and the DOD.Phase I of FOCSI, completed in 1986, was aimed at the design of a fiber optic integrated propulsion/flight control system.Phase II will provide subcomponent and system development, and system testing.In addition to a summary of the benefits of fiber optics, the FOCSI program, sensor advances, and future directions in the NASA/Lewis program are discussed.(Edited author abstract)
652; 732; 741
AIRCRAFT*;Control*;Fiber Optics ;Space Applications;Actuators; Sensors;Optical Devices
Nasa research;Passive optical sensors;Optically controlled actuators;Fiber optic sensors;Fly by light control;Integrated propulsion flight control

EIM-89-006510
Fiber optics for **aircraft** engine controls.
Proceedings of the 1988 American Control Conference.
Atlanta, GA, USA
1988 Jun 15-17
11857
OVERSTREET M. A.; HOSKIN R. F.
Allison Gas Turbine Div, Indianapolis, IN, USA
American Automatic Control Council, Green Valley, AZ, USA
ENG
US
Proceedings of the American Control Conference.
American Automatic Control Council, Green Valley, AZ, USA..Available from IEEE Service Cent Piscataway, NJ, USA.
cat n 88CH2601-3; PP. 1819-1824; 1 Ref.; DP. 1988
8903
PRACEO
An examination is made of the fundamental physical characteristics of **fiber**-**optic** **sensor** technology, including EMI (electromagnetic interference) immunity, light weight and small size, high temperature and radiation tolerance, flexibility, stability and durability.Principles of operation for **fiber**-**optic** **sensors** and systems are discussed, including basic design principles, extrinsic vs.intrinsic sensing, and typical fiber-optic links.A discussion of the state of the art and application provides the status of development and outlook for various fiber sensor types (pressure, temperature, etc.) for the applications defined.
653; 741; 732
AIRCRAFT ENGINES*;Control Equipment*;Fiber Optics;Sensors
Fiber optics for aircraft engine controls;Fiber optic sensor technology;Extrinsic vs intrinsic sensing;Fiber optic links

EIM-89-002960
Fiber-optic circuits for **aircraft** engine controls.
Fiber Optic Systems for Mobile Platforms
San Diego, CA, USA
1987 Aug 20-21
11730
GLOMB W. L.
United Technologies Research Cent, East Hartford, CT, USA
SPIE, Bellingham, WA, USA;New Mexico State Univ, Las Cruces, NM, USA;Univ of Alabama in Huntsville, Huntsville, AL, USA;Rose-Hulman Inst of Technology, Terre Haute, IN, USA;Univ of Dayton, Dayton, OH, USA;et al
ENG
US
Proceedings of SPIE - The International Society for Optical Engineering
Int Soc for Optical Engineering, Bellingham, WA, USA.
VOL. 840; PP. 122-127; 19 Ref.; DP. 1987
8902
PSISDG
0277-786X
This paper describes environmental effects which impact the design of interfaces to **fiber**-**optic** **sensor** and data buses in **aircraft** engine controls.Emphasis is placed on selection of components and designs which maintain their performance and reliability in the harsh environment of an electronics enclosure mounted on a modern **aircraft** turbine engine.Particular attention is given to the effects of temperature on electro-optical component and system performance.The main conclusion is that electro-optical interfaces to a variety of fiber-optic systems can be installed in an engine-mounted control

if the designs and components are selected after careful analysis of the effects of the engine environment.(Author abstract)
741; 732; 714; 421; 653
FIBER OPTICS*;Electrooptical Devices ;Thermal Effects;Aircraft Engines Jet And Turbine ;Control Equipment;Sensors
Fiber optic sensors;Fiber optic data buses;Aircraft engine sensor interfaces;Aircraft fiber optics

EIM-88-061623
Performance of **fiber** **optic** **sensors** for **aircraft** applications.
IEEE 1988 National Aerospace and Electronics Conference - NAECON 1988.
Dayton, OH, USA
1988 May 23-27
11781
LEWIS N. E.; MILLER M. B.
Litton Systems Inc, USA
IEEE, Dayton Section, Dayton, OH, USA;IEEE, Aerospace and Electronics Systems Soc, USA
ENG
US
IEEE Proceedings of the National Aerospace and Electronics Conference.
IEEE, New York, NY, USA.Available from IEEE Service Cent , Piscataway, NJ, USA
cat n 88CH2596-5; PP. 162-167; 2 Ref.; DP. 1988
8812
NASEA9
Measured performance is presented for passive **fiber**-**optic** **sensors** including a rotary position sensor, a pressure sensor, and a temperature sensor.A linear position sensor derived from the principles of the rotary sensor is also presented.The use of a common sensing principle utilizing wavelength-division multiplexing is detailed.The requirements for the light source and receiver/decoder and the current status of development are discussed.Environmental performance data for the rotary sensor system are given.
652; 732; 741; 717
AIRCRAFT*;Sensors*;Fiber Optics;Applications;Light Sources; Multiplexing Equipment;Transducers
Passive fiber optic sensors;Wavelength division multiplexing; Rotary position sensor;Receiver decoder

A90087999; B90046958
Polarimetric fibre optic structural strain sensor characterisation
Fiber Optic **Smart** **Structures** and Skins II
Boston, MA, USA
5-8 Sept. 1989
HOGG W. D.; TURNER R. D.; MEASURES R. M.
Toronto Univ., Inst.for Aerosp.Studies, Downsview, Ont., Canada
SPIE
Conference paper
Application; Practical
ENG
CA
Proc.SPIE - Int.Soc.Opt.Eng.(USA);Proceedings of the SPIE - The International Society for Optical Engineering
VOL. 1170; PP. 542-50; 12 Ref.; DP. 1990
PSISDG
0277-786X
A polarimetric sensor using high birefringent **optic** **fibre** is used to measure strain on the surface of a cantilevered beam.Localization of the sensor is accomplished with either a dual 45 degrees splice or a single 45 degrees splice with mirrored endface.Quadrature signal recovery is obtained using a dual wavelength approach.The sensor's performance characteristics are compared with those of an equivalent fibre optic interferometer.Applications of the polarimetric sensor are discussed
A4281P; A4630R; A0760F; B7230E; B4125; B7320G
fibre optic sensors;mechanical birefringence;polarimetry;strain measurement
quadrature signal recovery;fibre optic structural strain sensor; cantilevered beam;splice;performance characteristics;polarimetric sensor

B83003163
Air-deployed, over-ocean, small, ruggedized optical fiber
Fiber Optics in Adverse Environments
San Diego, CA, USA
25-27 Aug. 1981
SEIPLE R. L.; FREEMAN R. S.
Environmental Sci.Dept., Naval Ocean Systems Center, Kailua, HI, USA
Los Alamos Nat.Lab.;Defense Nucl.Agency
Conference paper
Application; Practical; Experimental
ENG
US
Proc.SPIE Int.Soc.Opt.Eng.(USA)
VOL. 296; PP. 87-94; 8 Ref.; DP. 1981
PSISDG
The development of long distance optical fibers and electro-optical components have made new approaches for ocean-laid telemetry systems possible.One such approach being investigated at the Naval Ocean Systems Center (NOSC) is an air-deployed fiber optic system (ADFO) utilizing a small diameter, repeatered, fiber optic communication cable, 1600 kilometers in length.This paper addresses the problems associated with the development of such a cable system, designed to be deployed by an **aircraft** over deep oceans and provide a telemetry path for information data exchange.Rather than discuss electro-optical issues, this paper discusses the issues associated with deploying a cable;1 mm in diameter, and repeaters from an **aircraft** flying at 130-150 knots.Th simulation of high-speed cable deployment, including hardware descriptions of winding apparatus and pullout test equipment, are also presented.Problems associated with laying small, ruggedized **optic** **fiber** on the ocean floor and the design of a small, ruggedized optical cable for such ocean deployment are discussed
B6210J; B4130; B6260; B6240G
cable laying;optical communication equipment;optical fibres; submarine cables;telemetering systems
air deployed over ocean ruggedised optical fibre;electro optical components;ocean laid telemetry systems;fiber optic communication cable;cable system;telemetry path;information data exchange;high speed cable deployment;winding apparatus;pullout test equipment

A9203-4281P-002; B9202-7230E-049
Fiber optic sensors
HOTATE K.
RCAST, Tokyo Univ., Japan
Journal paper
General
JAP
JP
Rev.Laser Eng.(Japan);Review of Laser Engineering
VOL. 19; NO. 8; PP. 776-86; 44 Ref.; DP. Aug. 1991
REKEDA
0387-0200
Great progress in the practical application of fiber optic sensors is described.The first topic is a **fiber** **optic** **gyroscope**.Noise sources have been studied thoroughly for an interferometric sensor.High performance that can meet even specifications for aircraft navigation has already been realized.A resonator type has a possibility to shorten the length of a sensing fiber coil drastically.A fiber ring laser utilizing fiber Brillouin scattering is investigated as a new type of fiber gyroscope.A fiber optic interferometric sensor has also shown a high sensitivity as an acoustic sensor.A distributed temperature sensor based on temperature dependence of fiber Raman scattering has been developed and is used to monitor the distribution along a high voltage power transmission line.Brillouin scattering can also be applied to the measurement of temperature distribution
A4281P; A0760L; A4265C; A0720D; B7230E; B4125; B4340; B7320R
fibre optic sensors;gyroscopes;light interferometers;ring lasers; stimulated Brillouin scattering;stimulated Raman scattering; thermometers
noise sources;fibre coil length shortening;fiber optic sensors; fiber optic gyroscope;interferometric sensor;aircraft navigation; resonator type;sensing fiber coil;fiber ring laser;fiber Brillouin scattering;fiber optic interferometric sensor;high sensitivity; acoustic sensor;distributed temperature sensor;temperature dependence;fiber Raman scattering;high voltage power transmission line;temperature distribution

A9202-4281P-014; B9201-7230E-046
Triangular phase-modulation approach to an open-loop **fiber**-**optic** **gyroscope**
PIE YAU CHIEN; CI LING PAN; LIH WUU CHANG
Inst.of Electro-Opt.Eng., Nat.Chiao-Tung Univ., Hsinchu, Taiwan
Journal paper
New development; Practical; Experimental
ENG
TW
Opt.Lett.(USA);Optics Letters
VOL. 16; NO. 21; PP. 1701-3; 18 Ref.; DP. 1 Nov. 1991
OPLEDP
0146-9592
0146-9592/91/211701-03$5.00/0
A new approach to an open-loop, all-fiber gyroscope with a wide dynamic range and a linear scale factor is described.For signal processing, the Sagnac phase shift is converted into a phase shift in the low-frequency electrical signal by using a triangular phase-modulation waveform followed by gate switching.The basic principle of this technique and experimental results are reported
A4281P; B7230E; B4125
fibre optic sensors;gyroscopes;optical modulation;phase modulation optical switching;open loop fiber optic gyroscope;all fiber gyroscope;wide dynamic range;linear scale factor;signal processing; Sagnac phase shift;low frequency electrical signal;triangular phase modulation waveform;gate switching

A9201-4281P-002; B9201-7230E-002
Emerging technology in fiber optic sensors
Applications of Optical Engineering: Proceedings of OE/Midwest '90
Rosemont, IL, USA
27-28 Sept. 1990
DYOTT R. B.
Andrew Corp., Orland Park, IL, USA
SPIE
Conference paper
General
ENG
US
Proc.SPIE - Int.Soc.Opt.Eng.(USA);Proceedings of the SPIE - The

International Society for Optical Engineering
VOL. 1396; PP. 709-17; 11 Ref.; DP. 1991
PSISDG
0277-786X
0277-786X/91/$4.00
Interferometric fiber optic sensors are reviewed.General principles are outlined and types of sensors are described.Types of interferometer are considered including the Michelson, Mach-Zehnder, Fabry-Perot and Sagnac interferometers.Fiber technology and components are discussed including couplers and gratings.Sensor methods are described including polarimetric sensors, distributed sensors and the **fiber** **optic** **gyroscope**
A4281P; A0760L; A0130R; B7230E; B4125
fibre optic sensors;light interferometers;reviews
interferometric fiber optic sensors;Michelson interferometers; Fabry Perot interferometers;Mach Zehnder interferometers;fiber optic sensors;Sagnac interferometers;couplers;gratings; polarimetric sensors;distributed sensors;fiber optic gyroscope

A91126978; B91073108
Digital integrating **fiber**-**optic** **gyroscope** with electronic phase tracking
TOYAMA K.; FESLER K. A.; KIM B. Y.; SHAW H. J.
Edward L.Ginzton Lab., Stanford Univ., CA, USA
Journal paper
Theoretical mathematical; Experimental
ENG
US
Opt.Lett.(USA);Optics Letters
VOL. 16; NO. 15; PP. 1207-9; 8 Ref.; DP. 1 Aug. 1991
OPLEDP
0146-9592
0146-9592/91/151207-03$5.00/0
A novel demodulation scheme for interferometers with optical phase modulation is described.The optical phase shift is measured by mixing a train of square digital pulses with a photodetector current and adjusting the pulse spacing by using an electronic closed loop.The optical phase shift is tracked with deviation less than 0.007 rad, which can be easily corrected by using a look-up table.An experimental optically open-loop **fiber**-**optic** **gyroscope** that uses this demodulation shows a linear scale factor in good agreement with theory
A4281P; A0760L; B7230E; B4125; B6120
demodulation;fibre optic sensors;gyroscopes;light interferometers; optical modulation;phase modulation
integrating fiber optic gyroscope;electronic phase tracking; demodulation scheme;interferometers;optical phase modulation; optical phase shift;square digital pulses;photodetector current; pulse spacing;electronic closed loop;look up table;optically open loop fiber optic gyroscope;linear scale factor

A91133953; B91073131
Integrated optics for sensing
HARUNA M.; NISHIHARA H.
Dept.of Electron., Osaka Univ., Japan
Journal paper
Practical; Experimental
JAP
JP
Rev.Laser Eng.(Japan);Review of Laser Engineering
VOL. 19; NO. 4; PP. 363-71; 28 Ref.; DP. April 1991
REKEDA
0387-0200
A variety of integrated-optic sensors have been reported in the 1980s.Most integrated-optic sensors developed early belong to a so-called waveguide sensor type in which the waveguide itself is used as a transducer for sensing of temperature, pressure, humidity, and so on.The waveguide sensors, however, do not seem to have a technical advantage over existing fiber-optic sensors in practical use.On the other hand, very stable sensing becomes possible in freedom from an optical bench by integration of the whole interferometer optics on a chip, where an optical fiber, for instance, is used as a sensing probe.Replacement of a bulk-optic component by the waveguide counterpart also results in drastic improvement of the sensor performance.In most integrated-optic sensors reported so far, LiNbO3 was used as a waveguide material because it is relatively easy to make low-loss single-mode waveguides by Ti indiffusion into LiNbO3 without reduction of the electrooptic effect.This paper describes recent progress in integrated-optic sensors in LiNbO3.Particularly, integration of heterodyne interferometer optics used for the measurement of velocity and displacement are discussed in detail.The application of integrated optics to **fiber**-**optic** **gyroscopes** is also described
A4281P; A0760L; A4282; A0630C; A0630G; B7230E; B4125; B4270; B7320C; B7320E
displacement measurement;fibre optic sensors;gyroscopes;integrated optoelectronics;light interferometers;velocity measurement temperature measurement;pressure measurement;humidity measurement; velocity measurement;displacement measurement;integrated optic sensors;waveguide sensor;transducer;fiber optic sensors;stable sensing;interferometer optics;sensing probe;low loss single mode waveguides;fiber optic gyroscopes;LiNbO3;LiNbO3 Ti
LiNbO3Ti int; LiNbO3 int; NbO3 int; Li int; Nb int; O3 int; Ti int; O int; LiNbO3Ti ss; LiNbO3 ss; NbO3 ss; Li ss; Nb ss; O3 ss; Ti ss; O ss; Ti el; Ti dop; LiNbO3 ss; NbO3 ss; Li ss; Nb ss; O3 ss; O ss

A91131421; B91067306
Integrated Optics and Optoelectronics II
Integrated Optics and Optoelectronics II
San Jose, CA, USA
17-19 Sept. 1990
SPIE
Conference proceedings
ENG
ZZ
Proc.SPIE - Int.Soc.Opt.Eng.(USA);Proceedings of the SPIE - The International Society for Optical Engineering
VOL. 1374; DP. 1991
PSISDG
0277-786X
91/$4.00
The following topics were dealt with: proton- and ion-exchange technologies;radiation effects;advanced lightwave components and concepts;optical interconnects concepts;aircraft and engine control;IOCs for **fiber** **optic** **gyroscopes**;and commercial integrated optical devices
A0130C; A4282; A4281P; B0100; B4140; B4270; B7230E; B4125
fibre optic sensors;integrated optics;integrated optoelectronics; ion exchange;optical interconnections
integrated optics;integrated optoelectronics;fibre optic sensors; ion exchange technologies;radiation effects;advanced lightwave components;optical interconnects;engine control;fiber optic gyroscopes;commercial integrated optical devices

A91133654; B91070540
1.55 mu m broadband fiber sources pumped near 980 nm
Fiber Laser Sources and Amplifiers II
San Jose, CA, USA
18-19 Sept. 1990
WYSOCKI P. F.; KALMAN R. F.; DIGONNET M. J. F.; KIM B. Y.
Edward L.Ginzton Lab., Stanford Univ., CA, USA
SPIE
Conference paper
Experimental
ENG
US
Proc.SPIE - Int.Soc.Opt.Eng.(USA);Proceedings of the SPIE - The International Society for Optical Engineering
VOL. 1373; PP. 66-77; 15 Ref.; DP. 1991
PSISDG
0277-786X
0277-786X/91/$2.00
Stable, broadband, long-wavelength sources are required for accurate fiber sensors such as the **fiber**-**optic** **gyroscope**.The Er-doped superfluorescent fiber source and wavelength-swept fiber laser, which emit near 1.55 mu m and can be pumped near 980 nm, are excellent candidates for this application.The authors discuss the design of such sources, their efficiency, pump source requirements, and the spectra they produce.The spectrum sensitivity to environmental factors such as temperature is also briefly discussed
A4255R; A4281W; B4320G; B4125
erbium;fibre lasers;laser transitions;superradiance
stable broadband sources;long wavelength sources;fiber sensors; fiber optic gyroscope;Er doped superfluorescent fiber source; wavelength swept fiber laser;design;efficiency;pump source requirements;spectrum sensitivity;environmental factors; temperature;1 55 micron;980 nm
Er ss; Er el; Er dop
wavelength 1.55E-06 m; wavelength 9.8E-07 m

A91108161; B91059482
Deep phase-modulation approach to an open-loop **fiber** **optic** **gyroscope**
PIE YAU CHIEN; CI LING PAN
Inst.of Electr-Opt.Eng., Nat.Chiao-Tung Univ., Hsinchu, Taiwan
Journal paper
New development; Theoretical mathematical; Experimental
ENG
TW
IEEE Photonics Technol.Lett.(USA);IEEE Photonics Technology Letters
VOL. 3; NO. 3; PP. 284-6; 16 Ref.; DP. March 1991
IPTLEL
1041-1135
1041-1135/91/0300-0284$01.00
A new approach to an open-loop, all-fiber gyroscope with a wide dynamic range and linear scale factor is described.For signal processing, the Sagnac phase lift is converted into a phase shift in the low-frequency electrical signal by using a deep sinusoidal phase-modulation waveform followed by gate switching.With the duty cycle of the gating signal selected to be in the range between 20 and 70%, the scale factor is stable with respect to change in the amplitude of the phase modulation signal by as much as 15%.The basic principle of the technique and experimental results are reported
A4281P; B7230E; B4125
fibre optic sensors;gyroscopes;optical modulation;phase modulation modulation amplitude;open loop fiber optic gyroscope;wide dynamic range;linear scale factor;signal processing;Sagnac phase lift; phase shift;low frequency electrical signal;deep sinusoidal phase modulation waveform;gate switching;duty cycle;gating signal;scale factor

A91106183; B91059737
Measurements of nonreciprocal optical effects on magnetic and superconducting materials using a **fiber**-**optic** **gyroscope**
Thirty-Fifth IEEE Conference on Magnetism and Magnetic Materials
San Diego, CA, USA
29 Oct.-1 Nov. 1990
SPEILMAN S.; FESLER K.; EOM C. B.; GEBALLE T. H.; FEJER M. M.
KAPITULNIK A.
E.L.Ginzton Lab., Stanford Univ., CA, USA
AIP;IEEE;et al
Conference paper
Experimental
ENG
US
J.Appl.Phys.(USA);Journal of Applied Physics
VOL. 69; NO. 8; PART 2A; PP. 5117; 1 Ref.; DP. 15 April 1991
JAPIAU
0021-8979
0021-8979/91/085117-01$03.00
Summary form only given.The authors have modified a **fiber**-**optic** **gyroscope** based on the Sagnac interferometer to measure nonreciprocal phase shifts.The instrument has a sensitivity of better than 1 mu rad and is insensitive to any reciprocal phase shifts.Thin films of high-temperature superconductors (HTSC) have been measured in search for nonreciprocal effects below Tc due to 'anyon superconductivity' ground state.No nonreciprocal phase shift was observed in any of the measured samples.The Faraday effect in various magnetic thin films (e.g., EuO) have been measured using the instrument showing a great sensitivity to submonolayers of the materials
A0760L; A7570A; A7820L; A7475; A4281P; B7320P; B3220; B7230E; B3110
Faraday effect;fibre optic sensors;gyroscopes;high temperature superconductors;magnetic thin films;monolayers;phase measurement; superconducting thin films
thin film;magnetic thin films;high temperature superconductor; nonreciprocal optical effects;superconducting materials;fiber optic gyroscope;Sagnac interferometer;nonreciprocal phase shifts; high temperature superconductors;anyon superconductivity;Faraday effect;magnetic thin films;EuO;submonolayers;EuO
EuO bin; Eu bin; O bin

A91079387; B91045245
Excess noise in fiber gyroscope sources
Fiber Optic and Laser Sensors VIII
San Jose, CA, USA
17-19 Sept. 1990
BURNS W. K.; MOELLER R. P.; DANDRIDGE A.
Naval Res.Lab., Washington, DC, USA
SPIE
Conference paper
Experimental
ENG
US
Proc.SPIE - Int.Soc.Opt.Eng.(USA);Proceedings of the SPIE - The International Society for Optical Engineering
VOL. 1367; PP. 87-92; 9 Ref.; DP. 1991
PSISDG
0277-786X
0277-786X/91/$2.00
The issue of excess noise is of interest with respect to the broadband optical sources commonly used in interferometric **fiber** **optic** **gyroscopes** because it can limit the ultimate sensitivity of the device.In this letter the authors report measurements of excess noise in three potential fiber gyroscope sources, superluminescent diode, (SLD's) at 0.83 mu m and 1.3 mu m and a superfluorescent Nd doped fiber at 1.06 mu m.These noise measurements are shown to be in good agreement with the model of P.Morkel, see Electron.Lett., vol.26, p.96, 1990.The model for excess noise is used to calculate the random walk coefficient due to shot and excess noise in a interferometric fiber gyro to demonstrate the impact excess noise in these sources has on gyroscopes.They show that the gyros utilizing SLD sources are just barely impacted by excess noise due to their limited output power (1-3 mW in a single mode fiber).The fiber source at 1.06 mu m, with its higher potential output power, is limited by excess noise
A4272; A4281P; B4260D; B7260; B7230E; B4125
fibre optic sensors;fibre optics;gyroscopes;light emitting diodes; light sources;neodymium;noise;superradiance
fibre gyro sensitivity;shot noise;fiber gyroscope sources;excess noise;broadband optical sources;interferometric fiber optic gyroscopes;superluminescent diode;superfluorescent Nd doped fiber; noise measurements;random walk coefficient;limited output power; single mode fiber;0 83 micron;1 3 micron;1 06 micron;1 to 3 mW
SiO2 ss; Nd ss; O2 ss; Si ss; O ss; Nd el; Nd dop
wavelength 8.3E-07 m; wavelength 1.3E-06 m; wavelength 1.06E-06 m; power 1.0E-03 to 3.0E-03 W

A91073324; B91039443
1.55 mu m superluminescent diode for a **fiber** **optic** **gyroscope**
Components for Fiber Optic Applications V
San Jose, CA, USA
20-21 Sept. 1990
KASHIMA Y.; MATOBA A.; KOBAYASHI M.; TAKANO H.
Semicond.Technol.Lab., OKI Electr.Ind.Co.Ltd., Tokyo, Japan
SPIE
Conference paper
Practical; Experimental
ENG
JP
Proc.SPIE - Int.Soc.Opt.Eng.(USA);Proceedings of the SPIE - The International Society for Optical Engineering
VOL. 1365; PP. 102-7; 6 Ref.; DP. 1991
PSISDG
0277-786X
0277-786X/91/$2.00
The authors have developed a 1.55 mu m superluminescent diode using a revolutionary structure.A light diffusion surface is placed diagonally on the active layer within the device to suppress the lasing action, and V-groove structure is applied to achieve high coupling efficiency into a single-mode fiber.Superluminescent diode characteristics were achieved in the range from 0 to 50 degrees C, and the coupled power into a single-mode fiber reached 0.5 mW
A4281P; A4272; B4260D; B7230E; B4125
fibre optic sensors;gyroscopes;light emitting diodes;superradiance fiber optic gyroscope;superluminescent diode;light diffusion surface;single mode fiber;1 55 micron;0 to 50 degC;0 5 mW
wavelength 1.55E-06 m; temperature 2.73E+02 to 3.23E+02 K; power 5.0E-04 W

A91073317; B91041798
Phase-modulated **fiber** **optic** **gyroscope** with wide dynamic range and linear scale factor
ONO K.; NISHIURA Y.; NISHIKAWA M.
Inf.& Electron.Technol.Labs.1, Sumitomo Electr.Ind., Osaka, Japan
Journal paper
Theoretical mathematical; Experimental
ENG
JP
Appl.Opt.(USA);Applied Optics
VOL. 30; NO. 9; PP. 1070-3; 11 Ref.; DP. 20 March 1991
APOPAI
0003-6935
0003-6935/91/091070-04$05.00/0
An open-loop phase-modulated **fiber** **optic** **gyroscope** with a wide dynamic range and linear scale factor is described.The optical Sagnac phase shift is transposed into an electrical phase shift by introducing two phase sensitive detectors and two electronic amplitude modulators with independent carrier frequency from the optical phase modulation.Preliminary experiments show good linearity over a wide dynamic range up to 1000 degrees /s and verifies the theoretical prediction
A4281P; B7230E; B4125; B6120
fibre optic sensors;gyroscopes;optical modulation;phase modulation wide dynamic range;linear scale factor;open loop phase modulated fiber optic gyroscope;optical Sagnac phase shift;electrical phase shift;phase sensitive detectors;electronic amplitude modulators; independent carrier frequency;optical phase modulation

A91066635; B91034896
Scale-factor-stabilized **fiber**-**optic** **gyroscope** based on a spectrum-broadened laser-diode source
PIE YAU CHIEN; CI LING PAN
Inst.of Electro-Opt.Eng., Nat.Chiao-Tung Univ., Hsinchu, Taiwan
Journal paper
Experimental
ENG
TW
Opt.Lett.(USA);Optics Letters
VOL. 16; NO. 6; PP. 426-8; 6 Ref.; DP. 15 March 1991
OPLEDP
0146-9592
A spectrum-broadened laser-diode source that uses the optical feedback and current-modulation effects has been adopted as the light source of a **fiber**-**optic** **gyroscope** to reduce the inherent phase noise.The scale factor of the gyroscope has also been stabilized
A4281P; A4255P; A4260K; B7230E; B4125; B4320J; B4360
fibre optic sensors;gyroscopes;semiconductor junction lasers scale factor stabilized fiber optic gyroscope;spectrum broadened laser diode source;optical feedback;current modulation effects; inherent phase noise

A91059879; B91034891
Fiber-**optic** **gyroscopes** based on polarization scrambling
PIE YAU CHIEN; CI LING PAN
Inst.of Electro-Opt.Eng., Nat.Chiao-Tung Univ., Hsinchu, Taiwan
Journal paper
Experimental
ENG
TW
Opt.Lett.(USA);Optics Letters
VOL. 16; NO. 3; PP. 189-90; 9 Ref.; DP. 1 Feb. 1991
OPLEDP
0146-9592
0146-9592/91/030189-02$5.00/0
A novel **fiber**-**optic** **gyroscope** with a single-mode diode laser as the light source and two polarization scramblers as time-varying depolarizers is demonstrated.This arrangement reduces the nonreciprocal phase noise induced by the cross coupling between polarization modes in single-mode fibers.The experimental results show that a phase-noise reduction factor of 18 can be

achieved
A4281P; A4281F; B7230E; B4125
fibre optic sensors;gyroscopes;light polarisation;random noise
fiber optic gyroscope;single mode diode laser;light source;
polarization scramblers;time varying depolarizers;nonreciprocal
phase noise;cross coupling;polarization modes;single mode fibers;
phase noise reduction factor

A91047584; B91027838
Passive fibre optic gyroscope
TROMMER G. F.; POISEL H.; BUHLER W.; HARTL E.; MULLER R.
Messerschmitt-Bolkow-Blohm GmbH, Munich, West Germany
Journal paper
Practical; Theoretical mathematical
ENG
DE
Appl.Opt.(USA);Applied Optics
VOL. 29; NO. 36; PP. 5360-5; 12 Ref.; DP. 20 Dec. 1990
APOPAI
0003-6935
0003-6935/90/365360-06$02.00/0
A **fiber** **optic** **gyroscope** different from the standard concept is presented.A fused fiber 3*3 directional coupler provides a constant phase shift thus enabling the detection of rotation rate at the quadrature point without phase modulation.Bias errors due to birefringent coupling centers in the fiber coil are avoided by using an unpolarized light source.A contrast insensitive signal recovery scheme eliminates the influence of polarization fluctuations on the scale factor.First measurements with a prototype gyroscope (90 mm in diameter and 23 mm in height) show a bias stability of <4.7 degrees /h and scale factor accuracy of <0.1% in the range of +or-200 degrees /s
A4281P; A4281M; B7230E; B4125
directional couplers;fibre optic sensors;gyroscopes;optical couplers
rotation rate detection;passive gyroscopes;fiber optic gyroscope;
fused fiber 3*3 directional coupler;constant phase shift;
quadrature point;birefringent coupling centers;fiber coil;
unpolarized light source;contrast insensitive signal recovery
scheme;polarization fluctuations;bias stability;scale factor
accuracy

A91028066; B91020718
Linearity analysis of **fiber**-**optic** **gyroscope**
International Conference on Optoelectronic Science and Engineering '90
Beijing, China
22-25 Aug. 1990
SHANG CHANGHONG; FANG ZHENHE
Shanghai Inst.of Electron Phys., China
China Assoc.Sci.Technol.;Int.Comm.Optics;SPIE;IEEE;et al
Conference paper
Theoretical mathematical
ENG
CN
Proc.SPIE - Int.Soc.Opt.Eng.(USA);Proceedings of the SPIE - The International Society for Optical Engineering
VOL. 1230; PP. 513-15; 2 Ref.; DP. 1990
PSISDG
0277-786X
Fundamental principles of closed-loop **fiber**-**optic** **gyroscopes** are described.Based on the closed-loop condition, simulated by computer, the linearity of scale factor is analyzed.The result shows, that for a given gated time, it is possible to find the best amplitude ratio between the first and the second harmonics of the feedback signal so that the optimum linearity of scale factor for **fiber**-**optic** **gyroscope** can be achieved
A4281P; B7230E; B4125
fibre optic sensors;gyroscopes
scale factor linearity;closed loop fiber optic gyroscopes;closed loop condition;feedback signal

A91002250; B91005579
Compact fiber optic gyro
NISHIURA Y.; NISHIKAWA M.; OOKA A.; KOHSAKA Y.
Sumitomo Electr.Ind.Ltd., Osaka, Japan
Journal paper
Practical
ENG
JP
Sumitomo Electr.Tech.Rev.(Japan);Sumitomo Electric Technical Review
NO. 30; PP. 76-9; 6 Ref.; DP. June 1990
SETRAY
0376-1207
The authors have studied methods to miniaturize optics, fiber-coil and electronics for a compact **fiber** **optic** **gyroscope** (FOG).The optics were miniaturized by using small bulk optic parts, and hybrid integrated circuits were developed for the electronics of the FOG.To compensate for the reduction of the Sagnac phase shift, a small diametered polarization maintaining single-mode fiber (PMF) was developed, allowing long lengths of the fiber to be wound around a small sized coiling space.Using these components, a compact FOG with an outer diameter of 60 mm and height of 50 mm was developed.Sensitivity of 0.8 deg/hr and drift of 3.6 deg/hr/hr were observed
A4281P; B7230E; B4125
fibre optic sensors;gyroscopes
miniaturisation;sensitivity;optics;fiber coil;electronics;compact fiber optic gyroscope;small bulk optic parts;hybrid integrated circuits;Sagnac phase shift;small diametered polarization maintaining single mode fiber;60 mm;50 mm
size 6.0E-02 m; size 5.0E-02 m

A90152573; B90076915
Broad-spectrum, wavelength-swept, erbium-doped fiber laser at 1.55 mu m
WYSOCKI P. F.; DIGONNET M. J. F.; KIM B. Y.
Edward L.Ginzton Lab., Stanford Univ., CA, USA
Journal paper
Experimental
ENG
US
Opt.Lett.(USA);Optics Letters
VOL. 15; NO. 16; PP. 879-81; 7 Ref.; DP. 15 Aug. 1990
OPLEDP
0146-9592
0146-9592/90/160879-03$2.00/0
The authors describe an argon-ion-laser pumped erbium-doped fiber laser at 1.55 mu m that incorporates low-rate frequency modulation of an intracavity acousto-optic modulator to provide repeated, continuous tuning of the output spectrum.The spectral width of this wavelength-swept fiber laser is as large as 20 nm with 9 mW of output power, even though erbium in silica has a mostly homogeneously broadened gain.The time-averaged visibility curve for a 14-nm-wide source indicates a short (160- mu m) coherence length, which is of interest for **fiber**-**optic** **gyroscopes** that operate with long integration times and short-coherence-length sources
A4260F; A4260B; A4255R; A4281W; A4260D; B4320G; B4125; B4320L; B4170; B4320M
acousto optical devices;erbium;fibre optics;laser accessories; laser cavity resonators;optical modulation;optical pumping;solid lasers;spectral line breadth
Er fibre laser;Ar ion laser pumping;broad spectrum laser;low rate frequency modulation;intracavity acousto optic modulator; continuous tuning;spectral width;wavelength swept fiber laser; homogeneously broadened gain;time averaged visibility curve; coherence length;fiber optic gyroscopes;long integration times; short coherence length sources;1 55 micron;9 mW;160 micron
SiO2 ss; Er ss; O2 ss; Si ss; O ss; Er el; Er dop
wavelength 1.55E-06 m; power 9.0E-03 W; wavelength 1.6E-04 m

B90072409; C90062585
Interferometric **fiber**-**optic** **gyroscopes**: a summary of progress
IEEE PLANS '90: Position Location and Navigation Symposium Record.'The 1990's - A Decade of Excellence in the Navigation Sciences' (Cat.No.90CH2811-8)
Las Vegas, NV, USA
20-23 March 1990
LIU R. Y.; ADAMS G. W.
Honeywell Syst.& Center, Phoenix, AZ, USA
IEEE
Conference paper
Practical
ENG
US
IEEE;New York, NY, USA
NP. xii+655; PP. 31-5; 5 Ref.; DP. 1990
CH2811-8/90/0000-0031$01.00
An overview of both open-loop and closed-loop IFOG (interferometric **fiber**-**optic** **gyroscope**) technologies is presented.Error sources associated with short-term random noise and long-term bias stability have been identified and properly controlled.Current research activities are focused on improving both the dynamic range and the scale factor performance for inertial navigation applications.For low- and medium-performance requirements, IFOG technology is close to the production stage.Cost and packing issues are being addressed to bring the IFOG from a laboratory instrument to a product.Progress on an attitude and heading reference system (AHRS) open-loop IFOG and an inertial-grade, closed-loop IFOG is presented, and the prospects and applications of these newly emerging technologies are discussed
B7230E; B7630; C3360L; C3240F
closed loop systems;fibre optic sensors;gyroscopes;inertial navigation;light interferometry;stability
attitude control;Sagnac effect;aircraft instrumentation;open loop; closed loop;interferometric fiber optic gyroscope;short term random noise;long term bias stability;inertial navigation;heading reference system

B90072408; C90062584
Phase modulation control for an interferometric **fiber** **optic** **gyroscope**
IEEE PLANS '90: Position Location and Navigation Symposium Record.'The 1990's - A Decade of Excellence in the Navigation Sciences' (Cat.No.90CH2811-8)
Las Vegas, NV, USA
20-23 March 1990
LAVIOLETTE K. D.; BOSSLER F. B.
Bell Aerosp.Textron, Buffalo, NY, USA
IEEE
Conference paper

Application; Theoretical mathematical
ENG
US
IEEE;New York, NY, USA
NP. xii+655; PP. 29-30; 3 Ref.; DP. 1990
CH2811-8/90/0000-0029$01.00
A FOG (**fiber**-**optic** **gyroscope**) scale factor control has been developed by implementing a second-phase modulation producing an error function.This error function is used to drive the first original modulation depth, forcing J0(M) to zero.A reduction factor of 100 in scale factor error is accomplished with a 0.1% loss in the SNR (signal-to-noise ratio) of the rate signal.The implementation of this control loop can be applied in a straightforward manner to a phase-modulated FOG.Therefore, an open-loop FOG can be used for more stringent applications such as attitude and reference
B7230E; C3360L; C3240F
aerospace control;fibre optic sensors;gyroscopes;light interferometry;phase modulation;stability
interferometric fiber optic gyroscope;scale factor control;second phase modulation;error function;modulation depth;SNR;control loop; attitude;reference

A81096097; B81046560
Air Force applied research on fiber optic couplers
Proceedings of the 31st Electronic Components Conference 1981
Atlanta, GA, USA
11-13 May 1981
NICHOLS E. R.
AFWAL, AADO-2, Wright-Patterson AFB, OH, USA
IEEE;Electron.Ind.Assoc
Conference paper
New development; Experimental
ENG
US
IEEE;New York, USA
NP. xii+522; PP. 387-92; 3 Ref.; DP. 1981
Fabrication techniques and the development of passive fiber optic couplers from single strand, multimode, plastic-clad fused silica fibers are presented.Performance data and test results under environmental influences of shock, vibration, and humidity are described for directional, T and transmissive star couplers.Preliminary evaluations of **active** **fiber** optic coupler techniques are given
A4280M; A4280L; B4130; B7630
aircraft instrumentation;environmental testing;optical couplers; optical fibres
test results;shock;vibration;humidity;transmissive star couplers; fabrication;optical fibre couplers;plastic clad fused SiO2 fibres; performance;environmental testing;directional couplers;T couplers; passive couplers;active couplers;airborne optical fibre communications

B88068575; C88060179
Cockpit displays for a knowledge-based system: the intelligent air attack system
Proceedings of the IEEE 1988 National Aerospace and Electronics Conference: NAECON 1988 (Cat.No.88CH2596-5)
Dayton, OH, USA
23-27 May 1988
LIND J. H.
US Naval Weapons Center, China Lake, CA, USA
IEEE;Aerosp.& Electron.Syst.Soc
Conference paper
Practical
ENG
US
IEEE;New York, NY, USA
NP. 4 vol. 1597; PP. 918-25 vol.3; 7 Ref.; DP. 1988
The author describes the intelligent air-attack system (IAAS), a prototype integrated-avionics system in the advanced development phase, which is intended for integration into attack aircraft in the early 1990s.The prototype IAAS will serve as an assistant to the crew by helping with three critical tasks: (1) classification of ship targets at long range;(2) detection, identification, and countering or evasion of in-the-air missile threats;and (3) on-the-fly strike management and strike-plan modification.IAAS will extract and correlate sensor data from **aircraft** **data** **bus** signals, and fuse it into a 'best-picture-of-the-world' database.After using a knowledge-based program to determine the specific information needed for current tasks, the system will format this information into intuitively-recognizable pictorial displays for rapid, accurate aircrew understanding and response
B7630; B7990; C7460; C7410H; C7150; C6170
aerospace computing;aircraft instrumentation;computerised instrumentation;expert systems;military computing;military systems
missile threat detection;ship target classification;computerised instrumentation;knowledge based system;intelligent air attack system;integrated avionics system;aircraft;long range;in the air missile threats;on the fly strike management;strike plan modification;sensor data;data bus signals;pictorial displays

B87050514
Avionics standard communications bus, its implementation and usage
Proceedings of the IEEE/AIAA 7th Digital Avionics Systems Conference (Cat.No.86CH2359-8)
Fort Worth, TX, USA
13-16 Oct. 1986
JENNINGS R. G.
Sperry Corp., Glendale, AZ, USA
IEEE;AIAA
Conference paper
Practical
ENG
US
IEEE;New York, USA
NP. 803; PP. 250-4; 3 Ref.; DP. 1986
CH2359-8/86/0000-0250$01.00
A description is given of the Avionics Standard Communications Bus (ASCB), which was developed to meet the needs of digital avionic system communications in today's aircraft.ASCB is a high-speed (2/3-MHz), bidirectional bus that uses the HDLC industry standard protocol and components to link all the avionic and aircraft subsystems.ASCB utilizes a number of features in both software and hardware to provide the safety and redundancy that is required for **aircraft** **data** **bus** networking.ASCB is presently certified in a number of business jets and commuter turboprop airplane applications
B7630; B6210Z
aircraft communication;data communication equipment;local area networks;protocols;redundancy;safety;standards
aircraft communication;Avionics Standard Communications Bus; digital avionic system communications;bidirectional bus;HDLC industry standard protocol;safety;redundancy;aircraft data bus networking;business jets;commuter turboprop airplane;2 to 3 MHz frequency 2.0E+06 to 3.0E+06 Hz

B75042949; C75028439
Fibre optic star coupler for **aircraft** **data** **bus**
Journal paper
New development
ENG
ZZ
Electron.Engineering (GB)
VOL. 47; NO. 571; PP. 23; 0 Ref.; DP. Sept. 1975
ELCEA9
Describes a coupler which allows a multimode optical waveguide system to perform the same function as a tapped trunk or data bus in an electrical network.It allows each terminal to transmit and receive information from any or all of the other terminals.A bundle from each terminal is brought to the star coupler.The coupler consists of a cylindrical housing containing a glass mixer rod with a mirror endface
B3584; B3282; B3290; C8849; C9610; B4740
aerospace applications of computers;aircraft instrumentation;data communication equipment;fibre optics;optical waveguides;waveguide couplers
star coupler;aircraft data bus;multimode optical waveguide;glass mixer rod;mirror endface;fibre optic coupler;fibre optics

A9203-4280S-007; B9202-6260-327
Novel photonic device using nonlinear corner-bend structure
CHANG W. C.; LIU S. F.; WANG W. S.
Dept.of Electr.Eng., Nat.Taiwan Univ., Taipei, Taiwan
Journal paper
New development; Practical; Theoretical mathematical; Experimental
ENG
TW
Electron.Lett.(UK);Electronics Letters
VOL. 27; NO. 23; PP. 2190-2; 7 Ref.; DP. 7 Nov. 1991
ELLEAK
0013-5194
0013-5194/91/$3.00+0.00
A novel photonic device is proposed for optical switching by using a corner-bend waveguide structure with a Kerr-like nonlinear dielectric interface.For certain specific input signal power, the device proposed can also function as a power divider.The switching characteristics and spatial **soliton** **propagation** in the structure are discussed
A4280S; A4280L; A4265P; A4265G; B6260; B4130; B4340
directional couplers;nonlinear optics;optical couplers;optical switches;solitons
all optical switching devices;optical communications equipment; nonlinear corner bend structure;optical switching;corner bend waveguide structure;Kerr like nonlinear dielectric interface;power divider;switching characteristics;spatial soliton propagation

B91072589
Optoelectronics: from concept to application
NOBLANC J. P.
CNET, Issy-les-Moulineaux, France
Journal paper
General
FRE
FR
Echo Rech.(France);L'Echo des Recherches
NO. 143; PP. 5-14; 24 Ref.; DP. 1991
ECRCAF
0012-9283
The performance of optical land-based and underwater transmission networks has increased with respect to both link distance and data rate.The optoelectronic components which have allowed this progress to be made well illustrate the driving forces behind the emerging technology.Some examples are given, like quantum wells which radically modify the properties of semiconductor lasers and

enable optical-flip-flops to be produced at ambient temperature.The way is opened for totally optical processing, or even nonlinear effects during transmission like **soliton** **propagation** or quantum noise reduction.One characteristic of this continually evolving work is the rapid move from the design stage to the application stage
B6260; B4320J
optical communication equipment;optoelectronic devices; semiconductor junction lasers
optical communications technology;optoelectronic components; quantum wells;semiconductor lasers;optical flip flops;optical processing;nonlinear effects;soliton propagation;quantum noise reduction

A91079426; B91045095
Analysis of soliton pulse propagation in a birefringent optical fiber using the finite-element method
EGUCHI M.; HAYATA K.; KOSHIBA M.
Fac.of Eng., Hokkaido Univ., Sapporo, Japan
Journal paper
Theoretical mathematical; Experimental
ENG
JP
Electron.Commun.Jpn.2, Electron.(USA);Electronics and Communications in Japan, Part 2 (Electronics)
VOL. 73; NO. 11; PP. 50-9; 12 Ref.; DP. Nov. 1990
ECJEEJ
8756-663X
8756-663X/90/0011-0050$7.50/0
Since the problem of waveform distortion in optical **communications** can be overcome by optical soliton, very wide band transmission becomes possible.It is foreseen that **soliton** **propagation** is the candidate for future optical systems.The soliton behavior can be expressed by coupled nonlinear Schrodinger equations.In this equation, taking the nonlinear oscillatory or loss terms due to the mutual parametric effects of each polarization component into account, the analysis will become very complicated.Concerning this point, in most analytical procedures, such oscillatory terms are neglected.However, the contribution of these terms are large in optical fibers of low birefringence and they cannot be neglected.In the case of subpicosecond pulse transmission in optical fibers of low birefringence, it is shown that the contribution of these terms is quite remarkable
A4281D; A4280S; A4281F; B4125; B6260; B5240D; B0290F
birefringence;finite element analysis;optical communication; optical fibres;optical waveguide theory;solitons
pulse compression;soliton propagation;optical solitons;soliton pulse propagation;birefringent optical fiber;finite element method; optical communications;optical soliton;very wide band transmission; soliton propagation;soliton behavior;coupled nonlinear Schrodinger equations;mutual parametric effects;oscillatory terms; subpicosecond pulse transmission;optical fibers of low birefringence

A89069924; B89038214
Soliton **propagation** in optical waveguides: a review
Proceedings of the XVIth Workshop on Interdisciplinary Study of Inverse Problems: Some Topics on Inverse Problems
Montpellier, France
30 Nov.-4 Dec. 1987
LAKSHMANASAMY S.; JORDAN A. K.; MITRA S. S.; SABATIER P. C.(Ed.)
Dept.of Electr.Eng., Rhode Island Univ., Kingston, RI, USA
Conference paper
Theoretical mathematical
ENG
US
World Scientific;Singapore
NP. xii+420; PP. 391-403; 35 Ref.; DP. 1988
Recent developments in **soliton** **propagation** in optical waveguides are reviewed and applications to long-distance **communications** are discussed.The effects of loss, dispersion and nonlinearity are analyzed.The importance of studying the effects of the continuous spectrum on propagating solitons is indicated
A4281D; A0340K; A4220G; A4281F; A4280S; A0130R; B4125; B6260
inverse problems;light propagation;nonlinear optics;optical communication equipment;optical dispersion;optical fibres;optical losses;reviews;solitons
inverse problems;optical fibres;optical waveguides;soliton propagation;long distance communications;loss;dispersion; nonlinearity;continuous spectrum

A87123251; B87068130
Stability of solitons in birefringent optical fibers.I.Equal propagation amplitudes
MENYUK C. R.
Sci.Appl.Int.Corp., McLean, VA, USA
Journal paper
Theoretical mathematical
ENG
US
Opt.Lett.(USA)
VOL. 12; NO. 8; PP. 614-16; 13 Ref.; DP. Aug. 1987
OPLEDP
0146-9592
0146-9592/87/080614-03$2.00/0
The effect of birefringence on **soliton** **propagation** in single-mode optical fibers is considered.Emphasis is on solitons with multipicosecond widths that are appropriate for **communications** applications.It is shown that while linear birefringence will lead to a substantial splitting of the two polarizations over 20 km, this effect can be eliminated by use of the Kerr nonlinearity.Above a certain amplitude threshold, the central frequency of each polarization shifts just enough to lock the two polarizations together
A4280M; A4210Q; A4210N; A4265J; B4130; B4340
birefringence;guided light propagation;light polarisation;optical fibres;optical Kerr effect;solitons
birefringence;soliton propagation;single mode optical fibers; communications;Kerr nonlinearity;amplitude threshold;polarizations; 20 km
distance 2.0E+04 m

A86075192; B86042260
Soliton **propagation** in long fibers with periodically compensated loss
MOLLENAUER L. F.; GORDON J. P.; ISLAM M. N.
AT&T Bell Labs., Holmdel, NJ, USA
Journal paper
Practical; Theoretical mathematical
ENG
US
IEEE J.Quantum Electron.(USA)
VOL. QE-22; NO. 1; PP. 157-73; 18 Ref.; DP. Jan. 1986
IEJQA7
0018-9197
0018-9197/86/0100-0157$01.00
With computer simulation, **soliton** **propagation** in an all-optical, long-distance **communications** system where fiber loss is periodically compensated by Raman gain is discussed.It is found that distortion of the transmitted pulses from true solitons show a peak near z0=L/8, where L and z0 are the amplification and soliton periods, respectively.An optimal system design based on the exceptional pulse stability and low soliton powers obtained in the region z0>>L/8 is described.Typical amplification periods are in the range 30-50 km, pump powers are less than 100 mW;and for bit rates in the 10 GHz range, time average signal powers are at most a few milliwatts.The single-channel rate-length product for error rate less than 10 sup -9 is approximately 29000 GHz-km.Finally, it is shown that in the gain-compensated system with wavelength multiplexing, soliton-soliton collisions produce random modulation of individual pulse velocities.Nevertheless, multiplexing can yield rate-length products greater than 300000 GHz-km
A4280M; A4265; B4130; B4340
digital simulation;optical fibres;optical losses;solitons
all optical long distance communications system;amplification period;long fibers;periodically compensated loss;computer simulation;soliton propagation;fiber loss;Raman gain;distortion; transmitted pulses;optimal system design;pulse stability;low soliton powers;pump powers;bit rates;time average signal powers; single channel rate length product;error rate;gain compensated system;wavelength multiplexing;soliton soliton collisions;random modulation;pulse velocities;rate length products

B85052370
Through the future's looking glass (optical **communications**)
BOIRAT R.
Journal paper
General
ENG
ZZ
Telecommunications (USA)
VOL. 19; NO. 5; PP. 73, 97, 101; 0 Ref.; DP. May 1985
TLCOAY
0040-2494
Discusses developments in optical fibres, light emitters, monolithic integration of optical receivers, direct detection link regenerators, and heterodyne techniques.Other types of optical links may be devised.These links would be based on different optical fibre properties, such as Raman amplification or **Soliton** **propagation**.Another possibility is to work with materials that have IR absorption bounds at longer wavelengths
B6260
optical communication;technological forecasting
technological forecasting;optical fibres;light emitters;monolithic integration;optical receivers;direct detection link regenerators; heterodyne techniques;optical links;Raman amplification;Soliton propagation;IR absorption

A85016276; B85008443
Optical fiber **communications**-present and future.III
MIDWINTER J. E.
Dept.of Electr.Eng., Univ.Coll., London, England
Journal paper
General
ENG
GB
Telephony (USA)
VOL. 207; NO. 18; PP. 56-62; 18 Ref.; DP. 22 Oct. 1984
TLPNAS
0040-2656
For pt.II see ibid., vol.207, no.14, p.64 (1984).Discusses some of the properties, characteristics, phenomena and research considerations of this mode of communication.Studies of dispersion

in graded index fibres showed the presence of pulse compression effects.These effects have been proposed as a way of generating extremely short pulses in fibres to overcome linear dispersion on a long link.Stimulated Brillouin scattering has been shown to be a potentially serious power limiting mechanism in monomode fibre.One way around this problem is to use PSK, with a zero disparity code
A4280M; B6260; B4130
optical cables;optical fibres;optical links
nonlinear attenuation;optical soliton propagation;dispersion;
graded index fibres;pulse compression;Brillouin scattering;PSK

A82097206; B82053039
Solitons in optical fibers
MOLLENAUER L. F.; STOLEN R. H.
Bell Labs., Holmdel, NJ, USA
Journal paper
Theoretical mathematical; Experimental
ENG
US
Laser Focus (USA)
VOL. 18; NO. 4; PP. 193-8; 17 Ref.; DP. April 1982
LAFOAK
Data transmission rates of tens of gigabits per second and extreme compression of picosecond pulses result when nonlinearity and dispersion are made to work together
A4280M; A4280S; B4130; B6260
optical fibres;optical links;solitons
optical fibres;pulse narrowing;soliton propagation;communications applications;extreme compression;picosecond pulses;nonlinearity; dispersion

REPORT DOCUMENTATION PAGE

1. Recipient's Reference	2. Originator's Reference	3. Further Reference	4. Security Classification of Document
	AGARD-LS-184	ISBN 92-835-0673-1	UNCLASSIFIED

5. Originator Advisory Group for Aerospace Research and Development
North Atlantic Treaty Organization
7 Rue Ancelle, 92200 Neuilly sur Seine, France

6. Title
ADVANCES IN FIBRE-OPTIC TECHNOLOGY IN COMMUNICATIONS AND FOR GUIDANCE AND CONTROL

7. Presented on 18th—19th May 1992 in Rome, Italy, 21st—22nd May 1992 in Leiden, The Netherlands and 26th—27th May 1992 in Monterey, United States.

8. Author(s)/Editor(s)	9. Date
Various	May 1992
10. Author's/Editor's Address	**11. Pages**
Various	174

12. Distribution Statement This document is distributed in accordance with AGARD policies and regulations, which are outlined on the back covers of all AGARD publications.

13. Keywords/Descriptors

Guidance and control
Fiber optics
Military communication
Missiles
Aircraft
Optical communication
Optical fibers

14. Abstract

Fibre-optics is progressively changing from the research stage to the field of application. However, new possibilities are emerging, which will probably bring a new revolution in the field of telecommunications, such as coherent transmission, new transmission material transparent to mid-infrared radiation, active fibres and soliton propagation.

Fibre-optics is gaining increasing importance in tactical missile and aircraft guidance and control. This has been driven by the commercial development of fibre optic cable and related components over the last ten years. The requirements for military guidance and control applications are highly demanding for the characteristics of the fibres and the necessary related components (transmitters, receivers, connectors etc.).

The Lecture Series will bring together a group of speakers with both theoretical and practical experience in the areas of communications and guidance and control. The Lecture Series will introduce fibre optics technology to scientists and engineers who are now in the field as well as enhance the knowledge of those already working in the area.

This Lecture Series, sponsored jointly by the Electromagnetic Wave Propagation Panel and the Guidance and Control Panel of AGARD, has been implemented by the Consultant and Exchange Programme.

AGARD Lecture Series 184 Advisory Group for Aerospace Research and Development, NATO ADVANCES IN FIBRE-OPTIC TECHNOLOGY IN COMMUNICATIONS AND FOR GUIDANCE AND CONTROL Published May 1992 174 pages Fibre-optics is progressively changing from the research stage to the field of application. However, new possibilities are emerging, which will probably bring a new revolution in the field of telecommunications, such as coherent transmission, new transmission material transparent to mid-infrared radiation, active fibres and soliton propagation. P.T.O.	AGARD-LS-184 Guidance and control Fiber optics Military communication Missiles Aircraft Optical communication Optical fibers	AGARD Lecture Series 184 Advisory Group for Aerospace Research and Development, NATO ADVANCES IN FIBRE-OPTIC TECHNOLOGY IN COMMUNICATIONS AND FOR GUIDANCE AND CONTROL Published May 1992 174 pages Fibre-optics is progressively changing from the research stage to the field of application. However, new possibilities are emerging, which will probably bring a new revolution in the field of telecommunications, such as coherent transmission, new transmission material transparent to mid-infrared radiation, active fibres and soliton propagation. P.T.O.	AGARD-LS-184 Guidance and control Fiber optics Military communication Missiles Aircraft Optical communication Optical fibers
AGARD Lecture Series 184 Advisory Group for Aerospace Research and Development, NATO ADVANCES IN FIBRE-OPTIC TECHNOLOGY IN COMMUNICATIONS AND FOR GUIDANCE AND CONTROL Published May 1992 174 pages Fibre-optics is progressively changing from the research stage to the field of application. However, new possibilities are emerging, which will probably bring a new revolution in the field of telecommunications, such as coherent transmission, new transmission material transparent to mid-infrared radiation, active fibres and soliton propagation. P.T.O.	AGARD-LS-184 Guidance and control Fiber optics Military communication Missiles Aircraft Optical communication Optical fibers	AGARD Lecture Series 184 Advisory Group for Aerospace Research and Development, NATO ADVANCES IN FIBRE-OPTIC TECHNOLOGY IN COMMUNICATIONS AND FOR GUIDANCE AND CONTROL Published May 1992 174 pages Fibre-optics is progressively changing from the research stage to the field of application. However, new possibilities are emerging, which will probably bring a new revolution in the field of telecommunications, such as coherent transmission, new transmission material transparent to mid-infrared radiation, active fibres and soliton propagation. P.T.O.	AGARD-LS-184 Guidance and control Fiber optics Military communication Missiles Aircraft Optical communication Optical fibers

Fibre-optics gaining increasing importance in tactical missile and aircraft guidance and control. This has been driven by the commercial development of fibre optic cable and related components over the last ten years. The requirements for military guidance and control applicagtions are highly demanding for the characteristics of the fibres and the necessary related components (transmitters, receivers, connectors etc.).

The Lecture Series will bring together a group of speakers with both theoretical and practical experience in the areas of communications and guidance and control. The Lecture Series will introduce fibre optics technology to scientists and engineers who are now in the field as well as enhance the knowledge of those already working in the area.

This Lecture Series, sponsored jointly by the Electromagnetic Wave Propagation Panel and the Guidance and Control Panel of AGARD, has been implemented by the Consultant and Exchange Programme of AGARD presented on 18th—19th May 1992 in Rome, Italy, 21st—22nd May 1992 in Leiden, The Netherlands and 26th—27th May 1992 in Monterey, United States.

ISBN 92-835-0673-1

Fibre-optics gaining increasing importance in tactical missile and aircraft guidance and control. This has been driven by the commercial development of fibre optic cable and related components over the last ten years. The requirements for military guidance and control applicagtions are highly demanding for the characteristics of the fibres and the necessary related components (transmitters, receivers, connectors etc.).

The Lecture Series will bring together a group of speakers with both theoretical and practical experience in the areas of communications and guidance and control. The Lecture Series will introduce fibre optics technology to scientists and engineers who are now in the field as well as enhance the knowledge of those already working in the area.

This Lecture Series, sponsored jointly by the Electromagnetic Wave Propagation Panel and the Guidance and Control Panel of AGARD, has been implemented by the Consultant and Exchange Programme of AGARD presented on 18th—19th May 1992 in Rome, Italy, 21st—22nd May 1992 in Leiden, The Netherlands and 26th—27th May 1992 in Monterey, United States.

ISBN 92-835-0673-1

Fibre-optics gaining increasing importance in tactical missile and aircraft guidance and control. This has been driven by the commercial development of fibre optic cable and related components over the last ten years. The requirements for military guidance and control applicagtions are highly demanding for the characteristics of the fibres and the necessary related components (transmitters, receivers, connectors etc.).

The Lecture Series will bring together a group of speakers with both theoretical and practical experience in the areas of communications and guidance and control. The Lecture Series will introduce fibre optics technology to scientists and engineers who are now in the field as well as enhance the knowledge of those already working in the area.

This Lecture Series, sponsored jointly by the Electromagnetic Wave Propagation Panel and the Guidance and Control Panel of AGARD, has been implemented by the Consultant and Exchange Programme of AGARD presented on 18th—19th May 1992 in Rome, Italy, 21st—22nd May 1992 in Leiden, The Netherlands and 26th—27th May 1992 in Monterey, United States.

ISBN 92-835-0673-1

Fibre-optics gaining increasing importance in tactical missile and aircraft guidance and control. This has been driven by the commercial development of fibre optic cable and related components over the last ten years. The requirements for military guidance and control applicagtions are highly demanding for the characteristics of the fibres and the necessary related components (transmitters, receivers, connectors etc.).

The Lecture Series will bring together a group of speakers with both theoretical and practical experience in the areas of communications and guidance and control. The Lecture Series will introduce fibre optics technology to scientists and engineers who are now in the field as well as enhance the knowledge of those already working in the area.

This Lecture Series, sponsored jointly by the Electromagnetic Wave Propagation Panel and the Guidance and Control Panel of AGARD, has been implemented by the Consultant and Exchange Programme of AGARD presented on 18th—19th May 1992 in Rome, Italy, 21st—22nd May 1992 in Leiden, The Netherlands and 26th—27th May 1992 in Monterey, United States.

ISBN 92-835-0673-1

AGARD

NATO OTAN

7 RUE ANCELLE · 92200 NEUILLY-SUR-SEINE

FRANCE

Téléphone (1)47.38.57.00 · Télex 610 176
Télécopie (1)47.38.57.99

DIFFUSION DES PUBLICATIONS
AGARD NON CLASSIFIEES

L'AGARD ne détient pas de stocks de ses publications, dans un but de distribution générale à l'adresse ci-dessus. La diffusion initiale des publications de l'AGARD est effectuée auprès des pays membres de cette organisation par l'intermédiaire des Centres Nationaux de Distribution suivants. A l'exception des Etats-Unis, ces centres disposent parfois d'exemplaires additionnels; dans les cas contraire, on peut se procurer ces exemplaires sous forme de microfiches ou de microcopies auprès des Agences de Vente dont la liste suite.

CENTRES DE DIFFUSION NATIONAUX

ALLEMAGNE
Fachinformationszentrum,
Karlsruhe
D-7514 Eggenstein-Leopoldshafen 2

BELGIQUE
Coordonnateur AGARD-VSL
Etat-Major de la Force Aérienne
Quartier Reine Elisabeth
Rue d'Evere, 1140 Bruxelles

CANADA
Directeur du Service des Renseignements Scientifiques
Ministère de la Défense Nationale
Ottawa, Ontario K1A 0K2

DANEMARK
Danish Defence Research Board
Ved Idraetsparken 4
2100 Copenhagen Ø

ESPAGNE
INTA (AGARD Publications)
Pintor Rosales 34
28008 Madrid

ETATS-UNIS
National Aeronautics and Space Administration
Langley Research Center
M/S 180
Hampton, Virginia 23665

FRANCE
O.N.E.R.A. (Direction)
29, Avenue de la Division Leclerc
92322 Châtillon Cedex

GRECE
Hellenic Air Force
Air War College
Scientific and Technical Library
Dekelia Air Force Base
Dekelia, Athens TGA 1010

ISLANDE
Director of Aviation
c/o Flugrad
Reykjavik

ITALIE
Aeronautica Militare
Ufficio del Delegato Nazionale all'AGARD
Aeroporto Pratica di Mare
00040 Pomezia (Roma)

LUXEMBOURG
Voir Belgique

NORVEGE
Norwegian Defence Research Establishment
Attn: Biblioteket
P.O. Box 25
N-2007 Kjeller

PAYS-BAS
Netherlands Delegation to AGARD
National Aerospace Laboratory NLR
Kluyverweg 1
2629 HS Delft

PORTUGAL
Portuguese National Coordinator to AGARD
Gabinete de Estudos e Programas
CLAFA
Base de Alfragide
Alfragide
2700 Amadora

ROYAUME UNI
Defence Research Information Centre
Kentigern House
65 Brown Street
Glasgow G2 8EX

TURQUIE
Millî Savunma Başkanlığı (MSB)
ARGE Daire Başkanlığı (ARGE)
Ankara

LE CENTRE NATIONAL DE DISTRIBUTION DES ETATS-UNIS (NASA) NE DETIENT PAS DE STOCKS DES PUBLICATIONS AGARD ET LES DEMANDES D'EXEMPLAIRES DOIVENT ETRE ADRESSEES DIRECTEMENT AU SERVICE NATIONAL TECHNIQUE DE L'INFORMATION (NTIS) DONT L'ADRESSE SUIT.

AGENCES DE VENTE

National Technical Information Service
(NTIS)
5285 Port Royal Road
Springfield, Virginia 22161
Etats-Unis

ESA/Information Retrieval Service
European Space Agency
10, rue Mario Nikis
75015 Paris
France

The British Library
Document Supply Division
Boston Spa, Wetherby
West Yorkshire LS23 7BQ
Royaume Uni

Les demandes de microfiches ou de photocopies de documents AGARD (y compris les demandes faites auprès du NTIS) doivent comporter la dénomination AGARD, ainsi que le numéro de série de l'AGARD (par exemple AGARD-AG-315). Des informations analogues, telles que le titre et la date de publication sont souhaitables. Veuiller noter qu'il y a lieu de spécifier AGARD-R-nnn et AGARD-AR-nnn lors de la commande de rapports AGARD et des rapports consultatifs AGARD respectivement. Des références bibliographiques complètes ainsi que des résumés des publications AGARD figurent dans les journaux suivants:

Scientifique and Technical Aerospace Reports (STAR)
publié par la NASA Scientific and Technical
Information Division
NASA Headquarters (NTT)
Washington D.C. 20546
Etats-Unis

Government Reports Announcements and Index (GRA&I)
publié par le National Technical Information Service
Springfield
Virginia 22161
Etats-Unis

(accessible également en mode interactif dans la base de données bibliographiques en ligne du NTIS, et sur CD-ROM)

Imprimé par Specialised Printing Services Limited
40 Chigwell Lane, Loughton, Essex IG10 3TZ

AGARD
NATO OTAN
7 RUE ANCELLE · 92200 NEUILLY-SUR-SEINE
FRANCE
Telephone (1)47.38.57.00 · Telex 610 176
Telefax (1)47.38.57.99

DISTRIBUTION OF UNCLASSIFIED AGARD PUBLICATIONS

AGARD does NOT hold stocks of AGARD publications at the above address for general distribution. Initial distribution of AGARD publications is made to AGARD Member Nations through the following National Distribution Centres. Further copies are sometimes available from these Centres (except in the United States), but if not may be purchased in Microfiche or Photocopy form from the Sales Agencies listed below.

NATIONAL DISTRIBUTION CENTRES

BELGIUM
Coordonnateur AGARD — VSL
Etat-Major de la Force Aérienne
Quartier Reine Elisabeth
Rue d'Evere, 1140 Bruxelles

CANADA
Director Scientific Information Services
Dept of National Defence
Ottawa, Ontario K1A 0K2

DENMARK
Danish Defence Research Board
Ved Idraetsparken 4
2100 Copenhagen Ø

FRANCE
O.N.E.R.A. (Direction)
29 Avenue de la Division Leclerc
92322 Châtillon Cedex

GERMANY
Fachinformationszentrum
Karlsruhe
D-7514 Eggenstein-Leopoldshafen 2

GREECE
Hellenic Air Force
Air War College
Scientific and Technical Library
Dekelia Air Force Base
Dekelia, Athens TGA 1010

ICELAND
Director of Aviation
c/o Flugrad
Reykjavik

ITALY
Aeronautica Militare
Ufficio del Delegato Nazionale all'AGARD
Aeroporto Pratica di Mare
00040 Pomezia (Roma)

LUXEMBOURG
See Belgium

NETHERLANDS
Netherlands Delegation to AGARD
National Aerospace Laboratory, NLR
Kluyverweg 1
2629 HS Delft

NORWAY
Norwegian Defence Research Establishment
Attn: Biblioteket
P.O. Box 25
N-2007 Kjeller

PORTUGAL
Portuguese National Coordinator to AGARD
Gabinete de Estudos e Programas
CLAFA
Base de Alfragide
Alfragide
2700 Amadora

SPAIN
INTA (AGARD Publications)
Pintor Rosales 34
28008 Madrid

TURKEY
Milli Savunma Başkanlığı (MSB)
ARGE Daire Başkanlığı (ARGE)
Ankara

UNITED KINGDOM
Defence Research Information Centre
Kentigern House
65 Brown Street
Glasgow G2 8EX

UNITED STATES
National Aeronautics and Space Administration (NASA)
Langley Research Center
M/S 180
Hampton, Virginia 23665

THE UNITED STATES NATIONAL DISTRIBUTION CENTRE (NASA) DOES NOT HOLD STOCKS OF AGARD PUBLICATIONS, AND APPLICATIONS FOR COPIES SHOULD BE MADE DIRECT TO THE NATIONAL TECHNICAL INFORMATION SERVICE (NTIS) AT THE ADDRESS BELOW.

SALES AGENCIES

National Technical
Information Service (NTIS)
5285 Port Royal Road
Springfield, Virginia 22161
United States

ESA/Information Retrieval Service
European Space Agency
10, rue Mario Nikis
75015 Paris
France

The British Library
Document Supply Centre
Boston Spa, Wetherby
West Yorkshire LS23 7BQ
United Kingdom

Requests for microfiches or photocopies of AGARD documents (including requests to NTIS) should include the word 'AGARD' and the AGARD serial number (for example AGARD-AG-315). Collateral information such as title and publication date is desirable. Note that AGARD Reports and Advisory Reports should be specified as AGARD-R-nnn and AGARD-AR-nnn, respectively. Full bibliographical references and abstracts of AGARD publications are given in the following journals:

Scientific and Technical Aerospace Reports (STAR)
published by NASA Scientific and Technical
Information Division
NASA Headquarters (NTT)
Washington D.C. 20546
United States

Government Reports Announcements and Index (GRA&I)
published by the National Technical Information Service
Springfield
Virginia 22161
United States
(also available online in the NTIS Bibliographic Database or on CD-ROM)

Printed by Specialised Printing Services Limited
40 Chigwell Lane, Loughton, Essex IG10 3TZ

ISBN 92-835-0673-1